

Are Bering Sea canyons unique habitats within the eastern Bering Sea?

Michael F. Sigler, Christopher N. Rooper, Gerald R. Hoff, Robert P. Stone, Robert A. McConnaughey and Thomas K. Wilderbuer

Abstract

Some of the largest submarine canyons in the world incise the eastern Bering Sea shelf break, including Bering, Pribilof, Zhemchug, Pervenets and Navarin canyons. In 2012, the North Pacific Fishery Management Council (NPFMC) received testimony from environmental organizations to protect coral, sponge and other benthic habitat of fish and crab species in two of these canyons (Pribilof and Zhemchug). In response to this testimony, the NPFMC requested that the NOAA Alaska Fisheries Science Center analyze the distribution of fishes and benthic invertebrates and the vulnerability of their habitat to fishing activities. We compiled data from the eastern Bering Sea that included trawl survey data on fish and invertebrate distributions and observations of ocean conditions and benthic habitat. These data were analyzed using multivariate techniques to determine if the two canyons are distinguishable from the adjacent continental slope. The potential for fishing effects on coral and sponge was assessed with spatial modeling of historical fishing effort, coral and sponge distributions and an index of their vulnerability to physical damage. Pribilof and Zhemchug canyons do show some distinguishing physical characteristics from the adjacent slope such as lower oxygen and pH and higher turbidity, but none based on biological characteristics (i.e., fish, coral and sponge distributions). These analyses imply that Pribilof and Zhemchug canyons are not biologically unique. Instead the major variables structuring the communities of fish and invertebrates on the eastern Bering Sea slope appear to be depth and latitude rather than submarine canyons. Corals were predicted to occur predominantly along the eastern Bering Sea slope, whereas sea whips were predicted to occur predominantly along the outer continental shelf. Sponges were mixed, with about two-

thirds of their habitat predicted for the outer shelf and the remainder for the slope. One unique feature of the focal canyons is that about one third of the coral habitat predicted for the eastern Bering Sea slope occurs in Pribilof Canyon, an area that comprises only about 10% of the total slope area. Although apparently concentrated there, the average density of coral for Pribilof Canyon ($0.28 \text{ colonies m}^{-2}$) is much less than the density for the Aleutian Islands ($1.23 \text{ colonies m}^{-2}$). The physical and biological characteristics of Zhemchug and Pribilof canyons are spatially heterogeneous; coral habitat was more common in some sections of Pribilof Canyon. Higher vulnerability indices were found both within and between canyons and were not unique to Pribilof and Zhemchug canyons. Pelagic trawl, longline and pot gear but not bottom trawl gear overlapped some coral and sponge habitats of the slope including canyons. Substantial overlap does not explain whether effects of fishing were light, medium or high, just that effects likely were greater in overlap areas compared to other areas. Further, the effect for the pelagic trawl fishery will depend on how often and where fishing occurs on bottom.

Introduction

In 2012, the North Pacific Fishery Management Council (NPFMC) received testimony from environmental organizations for management measures to provide Essential Fish Habitat (EFH) protection to coral, sponge and other benthic habitat of fish and crab species for two of the largest eastern Bering Sea canyons (Pribilof and Zhemchug). Earlier testimony prompted a review of scientific information in 2006 (McConnaughey et al. 2006), which found that canyons are unique geological features but insufficient information was available to judge their importance as EFH. In this paper, we address a 2012 request by the NPFMC to the NOAA Alaska Fisheries Science Center to determine whether these two canyons (Pribilof and Zhemchug) provide unique coral and sponge habitats for managed fish species.

Some of the largest submarine canyons in the world incise the eastern Bering Sea shelf break (Karl et al. 1996, Normarck and Carlson 2003) including Bering, Pribilof, Zhemchug, Pervenets and Navarin canyons (Figure 1). All five canyons are large but their seafloor gradients and shapes differ. Navarin (total volume = $5,400 \text{ km}^3$), Pervenets ($1,700 \text{ km}^3$) and Bering ($4,300 \text{ km}^3$) canyons have lower seafloor gradients than Pribilof ($1,300 \text{ km}^3$) and Zhemchug ($5,800 \text{ km}^3$) canyons (Karl et al. 1996). Navarin and Pervenets canyons resemble gently sloping

amphitheaters; Zhemchug and Pribilof canyons are very elongate parallel to the shelf edge, rugged and steeper; Bering Canyon is V-shaped and gradually widens downslope (Karl et al. 1996). Two other large canyons, St. Matthew (740 km³) and Middle (1,800 km³), lie along the eastern Bering Sea outer shelf, but barely indent the shelf break (Karl et al. 1996). Roughly 20% of the shelf edge between Alaska and the Equator is interrupted by steep, narrow and abrupt submarine canyons (Hickey 1995). An estimated 290 submarine canyons are found along the western coast of North America and are spaced an average of 30-35 km apart (Harris and Whiteway 2011).

An along-slope current, the Bering Slope Current, flows northwest along the slope of the eastern Bering Sea (Stabeno et al. 1999) with moderate flow (2 to 18 cm sec⁻¹) following the bathymetry and existing primarily in the upper 300 m (Schumacher and Reed 1992). Eddies ranging in size from 40 to 150 km may be imbedded in the flow (Stabeno et al. 1999). Depending on their size and shape, canyons that indent the shelf break can interrupt along-slope currents and thus may create unique physical environments in canyons compared to the adjacent slope. Results from a model of Bering Sea physical oceanography indicate that deep-basin water is moved northward onto the eastern Bering Sea shelf by mesoscale processes along the shelf break; canyons along the shelf break appear to be more prone to eddy activity and, therefore, are associated with higher rates of on-shelf transport (Clement Kinney et al. 2009). Onshelf transport may occur virtually anywhere along the shelf break and preferential transport onto the shelf has been observed at Bering Canyon and west of the Pribilof Islands (Stabeno et al. 1999). The latter occurs as the outer shelf narrows south of St. George Island, accelerating the flow, which then turns northward, becomes shallower and parallels the 100-m contour west of the Pribilof Islands; some weak, northward transport also may occur east of the Pribilof Islands (Stabeno et al. 2008). Tidal motion and topography interact in the Pribilof Canyon where observations show enhancement of the diurnal tidal currents (Kowalik and Stabeno 1999). Other detailed physical oceanography studies of Bering Sea canyons are lacking, in part because measurements in submarine canyons are difficult to make (Hickey 1995); their availability for some other Pacific Coast canyons provide insights into processes that also may occur for Bering Sea canyons. In steep-sided (up to 45 degrees seafloor gradient) and narrow Astoria Canyon, estimated vertical velocities were as great as 50 m d⁻¹ (upward) during upwelling and 90 m d⁻¹ (downward) during wind relaxation following upwelling events; at depths up to 100 m above the canyon, a cyclonic

86 circulation pattern occurred, but above that the flow field was undisturbed by canyon topography
87 (Hickey 1997). Sediment deposition rates were high ($\sim 60 \text{ g m}^{-2} \text{ d}^{-1}$) in the head of Quinault
88 Canyon but were low ($3\text{-}6 \text{ g m}^{-2} \text{ d}^{-1}$) elsewhere in the canyon and on the open slope (Baker and
89 Hickey 1986).

90 Enhanced production often occurs at continental shelf margins like the eastern Bering Sea
91 slope and outer shelf, which have been previously identified as an area of enhanced primary and
92 secondary productivity (the “Bering Sea Greenbelt”) (Springer et al. 1996). More recent
93 oceanographic observations (Rho and Whitledge 2007) and estimates derived from satellite
94 observations (Brown et al. 2011) imply that this area of enhanced primary production also
95 includes the middle shelf in addition to the outer shelf and slope. Areas of further concentration
96 may occur in the Bering Sea that are related to eddies. Earlier research found that these eddies
97 transit parallel to the continental slope and are not tied to the canyons (Schumacher and Staben
98 1994). However recent research found that eddy activity in eastern Bering Sea is particularly
99 strong near the major shelf-break canyons during the spring months, likely influencing the spring
100 bloom, and in situ data from an eddy sampled near Pribilof Canyon in 1997 suggest that these
101 eddies can carry water from the outer shelf into the basin (Ladd et al. 2012). Nevertheless
102 enhanced production may occur in canyons under some circumstances. In Kaikoura Canyon,
103 New Zealand, the physical setting appears suitable for trapping particulate organic matter
104 derived from pelagic production and coastal detrital export; benthic biomass and infauna were
105 elevated and fish abundance was higher in the canyon than the adjacent slope (De Leo et al.
106 2010). The head of Scripps Canyon lies immediately adjacent to the California coast and
107 longshore transport delivers substantial quantities of macrophyte detritus from macroalgae which
108 strong tidal and gravity currents distribute through much of the canyon system (Vetter and
109 Dayton 1999).

110 Our analysis addresses five questions posed by the NPFMC, which we simplified as: 1)
111 Are the canyons unique habitats?; 2) Are the canyons homogeneous habitats?; 3) What are the
112 fish associations with habitat features?; 4) What is the vulnerability of the canyons?; 5) Are
113 benthic habitats vulnerable? Our paper is organized into three topics: 1) Physical habitat
114 characteristics (questions 1 and 2); 2) Fish, crab, coral and sponge distributions and associations
115 (question 3); and 3) Overlap of fishing and vulnerable habitats (questions 4 and 5). All of the
116 questions are addressed within the context of the eastern Bering Sea geographic area. The terms

habitat and benthic habitat often are used interchangeably and can include both physical (e.g., sediment) and biological (e.g., coral) structure. In this paper, we distinguish physical and biological habitats and for the overlap analysis, focus on the overlap of fishing with coral and sponge habitats.

Methods

Data

Available information that describes eastern Bering Sea seafloor and ocean habitat includes bathymetry (depth and seafloor gradient), sediment (grain size and sorting) and oceanographic information such as temperature, current speed and productivity. The bathymetry information covers the eastern Bering Sea shelf and slope and has been assembled from National Ocean Service “smooth sheets” based on digitized soundings collected from historical surveys by hydrographic ships (S. Lewis, Alaska Regional Office-NMFS, personal communication). A smooth sheet is the final, neatly drafted, accurate plot of a hydrographic survey using verified or corrected data. These data are mostly from historical mapping efforts and have better coverage in shallow waters of the eastern Bering Sea shelf and slope. We transformed the depth data to a continuous coverage on a fine scale (100 m x 100 m) grid of the eastern Bering Sea shelf and slope using inverse distance weighting implemented in ArcGIS software (ESRI 2009). The Spatial Analyst package in ArcGIS was then used to compute maximum seafloor gradient at each grid point (maximum gradient among adjacent eight grid cells, expressed as rise divided by the run multiplied by 100 and expressed as a percentage. The seafloor gradient and bathymetry information were then aggregated into a regular 1 x 1 km grid for further analysis.

Two measurements of sediment type were used in these analyses, grain size and sediment sorting. The sediment information is stored in the Eastern Bering Sea Sediment Database (EBSSD) (McConnaughey and Smith 2000) and was supplemented with data from the National Geophysical Data Center Sea Floor Sediment Grain Size database (<http://ngdc.noaa.gov/geosamples/metadata.jsp?g=G00127>). The sediment information describes grain size and sorting for the top-most 10 cm of seafloor. Mean grain size is expressed as “phi” which is a negative log₂-transform of grain size in millimeters (e.g., large “phi” indicates fine

grains). Because the usual sampling tools are bottom grabs and corers, the sediment information does not distinguish boulder or bedrock habitat and as a result, this habitat type is implicitly excluded from our analysis. Sediment sorting is defined as the standard deviation of phi in each sediment sample. The grain size and sorting values from the sediment data were kriged into a continuous coverage on a 1 x 1 km grid of the eastern Bering Sea shelf and slope using ordinary kriging (Venables and Ripley 2002). For kriging this data set, an exponential model was the best fit to the semi-variogram of both grain size and sorting values and was used for interpolation.

Measurements of bottom temperature have been collected routinely since 1996 during standard bottom trawl surveys for fish and crab of the eastern Bering Sea shelf and slope (Hoff and Britt 2011, Lauth 2011). Standard surveys of the continental shelf have been conducted annually during June-July 1982-2012. Shelf survey stations are located at the mid-point of 37 x 37-km grid cells for depths of 30-200 m. Standard surveys of the upper continental slope were conducted during June-July 2002, 2004, 2008, 2010 and 2012. Each year, the slope survey was conducted by randomly sampling 200 stations from approximately 350 possible stations. The slope survey covers depths of 200-1,200 m and the latter marks the depth limit of our analyses. The bottom temperature data from all survey years were kriged using a spherical semi-variance model to create an interpolated surface of bottom temperatures that represent the long-term average of summer conditions in the eastern Bering Sea. Additional types of oceanographic measurements, including oxygen, turbidity, pH and light were collected only during the 2012 slope survey. Bottom salinity was collected on both the eastern Bering Sea shelf and slope during 2012 surveys.

Two other sources of oceanographic information (ocean currents and ocean productivity) were included in our analysis. A model-based reconstruction of ocean currents from 1975 to 2010 is available for the eastern Bering Sea from the Northeast Pacific (NEP) “Regional Ocean Modeling System” (ROMS) (e.g., Danielson et al. 2011). Major eastern Bering Sea currents are the Bering Slope Current which follows the shelf break and the Alaska Coastal Current which follows the Alaska coastline; mid-shelf currents are sluggish. Currents vary both in time (e.g., shelf circulation and transport across the shelf break are influenced by seasonal patterns in wind direction (Danielson et al. 2012)) and space (e.g., stronger currents occur south of St. George Island where the shelf narrows (Stabeno et al. 2008)). For our analysis, the values were averaged because long-term current patterns likely influence spatial patterns of long-lived benthic species

including deepwater coral and sponge. The long-term average current data were available on a regular grid (10 x 10 km) and were transformed to a 1 x 1 km grid using inverse distance weighting because there was no indication of non-random spatial structure in semi-variogram plots.

Satellite-based measurements of ocean productivity (ocean color) from 2003 to 2011 are available for the eastern Bering Sea from the Sea-viewing Wide Field-of-view Sensor (SeaWiFS) Project (Behrenfeld and Falkowski 1997). The monthly average data for May to September of each year on a regular grid (11.9 x 18.5 km) was downloaded from Oregon State University's Ocean Productivity website (<http://www.science.oregonstate.edu/ocean.productivity/>) for the years 2003-2011. For each grid cell, these data were averaged across months within each year and then averaged across all years. We averaged over all years rather than taking annual values because months often were poorly sampled or sampled not at all due to cloud cover. There was no indication of non-linear spatial structure in the regularly spaced data points, so average productivity was interpolated using inverse distance weighting into a continuous coverage on a 1 km x 1 km grid.

The standard bottom trawl surveys of the eastern Bering Sea shelf and slope (Hoff and Britt 2011, Lauth 2011) also describe fish and invertebrate (e.g., coral) distributions and are the primary source of data for these taxa in our study (http://www.afsc.noaa.gov/RACE/groundfish/survey_data/default.htm). We analyzed data for both the shelf and slope surveys from 2002, 2004, 2008, 2010 and 2012, which are the years standard slope surveys have been conducted. For these analyses, records were only used if trawl performance was satisfactory and if the distance fished, geographic position, average depth and water temperature profile were recorded. Trawl tows were deemed satisfactory if the net opening was within a predetermined normal range, the gear maintained contact with the seafloor, and the net suffered little or no damage during the tow. Data from a total of 2,696 bottom-trawl tows were used (1,777 from the shelf survey and 919 from the slope survey). All fish and invertebrates captured during a survey tow were sorted to the lowest taxonomic level practical, typically species, and the total weight in the catch was determined. Catch per unit effort (CPUE, number ha^{-1}) for each taxonomic group was calculated using the area swept computed from the net width for each tow multiplied by the distance towed recorded with GPS. In addition, longline surveys cover the eastern Bering Sea slope (http://www.afsc.noaa.gov/abl/mesa/mesa_sfs_lsd.htm).

Fourteen stations are sampled every other year. Data from a total of 84 longline sets for the years 2001, 2003, 2005, 2007, 2009 and 2011 were available. All fish and invertebrates captured during a longline set were sorted to the lowest taxonomic level practical and the total weight in the catch was determined. Catch per unit effort (CPUE, number hook⁻¹) for each taxonomic group was calculated.

Other data sets were considered but not used in our analysis. Small areas of the seabed and associated fauna have been observed visually (Brodeur 2001, Busby et al. 2005, Hoff 2010, Rooper et al. 2010, Miller et al. 2012) and tabular data of habitat classification are available from these studies. However these samples are limited mostly to canyon habitat. Measures of habitat type derived from acoustic backscatter ('Q-values') have been reported for the Bering Sea shelf (McConnaughey and Syrjala 2009) but not for the slope. The lack of comparative values for either of these data sources prevents their use in our overall habitat analyses, though we complete some analysis of the visual observations. Coral and sponge data are collected by observers in fisheries observer programs; however identification has not been a high priority historically and only limited training has been provided for that purpose. The spatial resolution is variable, depending on gear type, fishing practices and haul duration. The data may be useful for presence validation but not absence validation, unless significant data filtering based on assumptions about sampling and operations, is done. Other surveys using acoustics and surface trawls sample pelagic but not benthic habitat and so were not analyzed.

Analyses of physical habitat characteristics

We distinguish three major physical habitats in our analysis: shelf, canyon and non-canyon slope. The shelf is further divided into three oceanographic domains based on the usual location of oceanic fronts during summer (inner < 50 m, middle 50-100 m, outer 100-180 m) (Coachman 1986). We made one change in these boundaries that affected the seaward, oceanographic boundary of the outer shelf. We substituted the geological boundary between the continental shelf and slope, the shelf break, which is defined as a prominent change in seafloor gradient from low to steeper (pers. comm., David W. Scholl, USGS emeritus). This boundary was chosen using the following approach. Contours were placed on the seafloor gradient map at 0.5, 1, 2, 3 and 5 percent. The contours for 1, 2 and 3 percent generally were close together, indicating that the seafloor gradient is changing rapidly there. In contrast, the contours for 0.5 percent were

237 distinctly separated from 1, 2 and 3 percent. The contours for 5 percent often were discontinuous
238 and irregular. We chose the 1 percent contour as the shelf-slope boundary because this was the
239 shoreward contour where a prominent change in seafloor gradient occurred (i.e., the distinct
240 separation of 0.5 from 1, 2 and 3 percent). The resultant shelf-slope boundary typically lies at
241 about 200 m except for the northern edge of Bering Canyon and the adjacent slope where the
242 boundary lies at about 500 m. The lateral boundary of a canyon is defined as the intersection of
243 the canyon opening with the continental slope; the canyon lateral boundaries were located at the
244 closest ridge crest on either side of the canyon axis (pers. comm., H. Gary Greene, Moss Landing
245 Marine Laboratories). These two measures were then used to define the boundaries of each
246 canyon in our analysis.

247 We distinguish five large canyons that intersect the eastern Bering Sea shelf break
248 including three lower seafloor gradient canyons (Navarin, Pervenets and Bering) and two higher
249 seafloor gradient canyons (Pribilof and Zhemchug) (Karl et al. 1996). We do not distinguish two
250 other canyons, St. Matthew and Middle canyons, because they barely indent the shelf break and
251 have only minor morphological expression on the shelf (Karl et al. 1996).

252 Multivariate analyses were applied to determine whether physical habitat characteristics
253 differ among the five large canyons, the four slope areas lying between the canyons and the three
254 oceanographic domains of the continental shelf (a total of 12 areas). These analyses were
255 completed using data on depth collected annually during trawl surveys, data on salinity, oxygen,
256 turbidity, pH and light collected only during the 2012 trawl survey and other habitat information
257 including seafloor gradient, current, long-term average temperature, productivity and grain size
258 and sorting that were not associated with a specific trawl haul, but potentially are useful in
259 defining habitats. We completed the multivariate analyses using three data groupings (Table 1)
260 because more measurement types were collected in 2012 and also to determine if separately
261 analyzing the slope data affected the results. These three data groupings were Case A: all years
262 (2002, 2004, 2006, 2008, 2010, 2012) data - from both shelf and slope surveys when both
263 surveys occurred; Case B: all years data - from slope survey only; and Case C: 2012 data - from
264 slope survey only (when additional types of oceanographic measurements were collected).

265 As described in the data section, the seafloor gradient, current, long-term temperature,
266 productivity and grain size and sorting information was compiled on a 1 x 1 km grid. For each
267 trawl survey station, this 1 x 1 km grid (e.g., seafloor gradient in the grid cell where the bottom

trawl tow occurred) was associated with the information collected during the trawl survey (e.g., depth) and then the habitat data were analyzed. For each trawl survey station, there were measurements of depth for all years and measurements of salinity, oxygen, turbidity, pH and light for 2012 only. For the corresponding 1 x 1 km grid cell, there were values of seafloor gradient, temperature, current, productivity and grain size and sorting. Data were normalized (to mean = 0 and SD = 1) by subtracting the mean and dividing by the standard deviation to remove the effect of scale differences among variables.

These habitat variables were used in a principal component analysis (PCA) of the trawl survey stations using the MASS package implemented in R statistical software (Venables and Ripley 2002). Patterns in the PCA were examined graphically to determine if the 12 habitat areas were easily distinguishable and if so, what factors were associated with these differences. The PCA also indicated the habitat variables that contributed the most to the variability of the habitat data set and indicated where strong or weak covariation among habitat variables was apparent.

Each station was located in one of the 12 areas and this classification was tested using quadratic discriminant function analysis (DFA) with the normalized data using the MASS package implemented in R statistical software (Venables and Ripley 2002). The quadratic DFA measures how well group membership is predicted for each habitat area using an optimal combination of quadratic functions. Station groupings were determined using leave-one-out cross-validation of the data. The percentage agreement between the observed classifications and the predicted classifications indicated the degree to which the areas could be discriminated from each other using the habitat variables. Lastly an analysis of similarity (ANOSIM) was completed to test for statistically significant differences among habitat areas using the MASS package implemented in R statistical software (Venables and Ripley 2002). This analysis compares the rank order of dissimilarity values between two or more groups. In this case the groupings were the 12 areas and the dissimilarity matrix was computed from the habitat variables. ANOSIM produces an R-value, which is a test statistic that varies between -1 and 1, and a probability based on random permutation of the groupings. An R-value of 0 indicates random assignment of the data into groups, while an R-value of 1 indicates perfect discrimination between groups was obtained. Statistical significance can be determined by $p < 0.05$, but with large sample sizes such as ours, the probability must be viewed in light of the R-value. An R-value close to zero can indicate that the relationship is not meaningful, even if $p < 0.05$.

Analyses of fish, crab, coral and sponge distributions

Our approach was to examine ecologically important fish and crab species with importance based on density (kg ha^{-1}). We selected the top 10 fish and crab species from each survey (shelf trawl survey, slope trawl survey, longline survey) and created a combined list of species to analyze. The combined list consisted of 20 fish and crab species (Table 2) and totaled less than 30 species because some species were on more than one top 10 list. We used the longline survey data only to compile the list, but not for analysis, because only 14 longline survey stations were sampled every other year and the sample years differed for the longline and slope trawl surveys. For coral and sponges, we initially selected several major taxa and also differentiated some notable taxa like *Primnoa* spp. Based on preliminary analyses however we had to pool the taxa further because sample sizes for some taxa were too low for reliable analysis. The resultant three groups were coral (all corals except sea whips and sea pens), sea whip (this group name includes one species of sea whip (*Halipteris willemoesi*) and sea pens, which were uncommon), and sponge (Table 3). All catch data were log (+ constant) transformed prior to analysis. The constant used for each species was one-half of the minimum positive catch (> 0) for that species. Data were normalized (to mean = 0 and SD = 1) by subtracting the mean and dividing by the standard deviation to remove the effect of scale differences among variables for multivariate analyses.

We applied a similar multivariate analysis approach (i.e., PCA, DFA, ANOSIM) to the biota information as we applied to the habitat information except that only slope and outer shelf data were analyzed (Figure 1). We excluded the inner and middle shelf from the analysis because of their consistent difference from the other areas. For the biota analysis, unlike the physical habitat analysis, there was no need to group data and distinguish Cases A, B and C (Table 1) because the same biota information was collected for all survey years. Multivariate analysis (DFA) was applied to determine how well group membership could be predicted for the focal canyons (Zhemchug and Pribilof canyons) and the slope areas lying between the canyons.

In addition to the multivariate analyses, we also used the bottom trawl survey data to test for relationships between physical habitat and biota. We used generalized additive modeling (GAM, Hastie and Tibshirani 1990) fit using the mgcv package in R (Wood 2006) to construct relationships between habitat variables (location, depth, temperature, gradient, current speed, ocean productivity, grain size and sediment sorting) and the density of the top 20 fish and crab

species. A parallel method was used to individually predict the presence or absence of coral, sponge and sea whips. Presence-absence was used in the GAMs for corals and sponges instead of density (CPUE) because the combination of a large number of zero catches and high variability in positive catches where they occurred were difficult to model an appropriate error distribution. Our approach was similar but not identical to other recent predictive modeling of coral distribution (Woodby et al. 2009, Ross and Howell 2013).

The GAMs were constructed for each fish and crab species using the log-transformed catch per unit of effort (LCPUE in kg ha^{-1}). A factorial analysis was used to determine the best-fitting model for each species or taxa group, where the full model containing all variables was fit to the data, and then the least significant variable was eliminated and the model refit. LCPUE models were compared using the generalized cross-validation (GCV) criterion (Wood 2006). The elimination of the least significant variable was repeated until no further gain in GCV was attained. This model was then determined to be the best-fitting model for the species. Overfitting of the models was reduced using the ad-hoc method of increasing the penalty on effective degrees of freedom by 1.4 for each degree of freedom used by the smoothing function (Kim and Gu 2004). For LCPUE data, a normal distribution was used in the fitting, while for presence-absence data, a binomial distribution was used. Presence models were compared using the unbiased risk estimator (UBRE) criterion (Wood 2006). For LCPUE data the scale parameter was estimated from the data and for presence-absence data the scale was one. When the best-fitting model was determined for each fish species, the LCPUE was predicted for each 1 x 1 km block in the eastern Bering Sea outer shelf and slope. For the invertebrate groupings, predictions were made for the probability of presence. Summaries of these prediction layers are presented graphically.

To judge the accuracy of the LCPUE models, the model predictions were correlated to the observations using the squared Pearson correlation coefficient. Two methods were used to judge the accuracy of the presence-absence models. For the first method, the area under the curve (AUC) was computed which calculates the probability that a randomly chosen presence observation would have a higher probability of presence than a randomly chosen absence observation using rank data. We used the scale of Hosmer and Lemeshow (2005), where AUC value > 0.5 is estimated to be better than chance, a value > 0.7 is estimated to be acceptable, and values > 0.8 and 0.9 are excellent and outstanding, respectively. The coral, sea whip and sponge

361 presence-absence models predicted the probability of each group being present, a continuous
362 variable. This was then translated into a prediction of presence-absence using a threshold value
363 for the probability. Since the data set contained many more absences than presences, the
364 resulting models could be biased towards absence (Hosmer and Lemeshow 2005). Thresholds
365 were chosen empirically for translating the probabilities to presence-absence that balanced the
366 number of false positives and false negatives in the predictions. The empirically derived
367 thresholds were about 0.3 and varied slightly depending on data set. This presence-absence
368 information was then used to calculate a contingency matrix and Cohen's Kappa (Fielding and
369 Bell 1997), which is the second method used to judge the accuracy of the predictions.

370 We used visual survey data for coral and sponge to evaluate their numerical abundances
371 in Pribilof and Zhemchug canyons. In analysis of visual survey data, the term coral includes sea
372 whips and sea pens unlike the analyses of trawl survey data which distinguish sea whips and sea
373 pens from other coral taxa. Data are available from surveys conducted in 2007 (Miller et al.
374 2012) and 2012 (pers. comm., J. Hocevar, Greenpeace). A total of 23 dives were completed;
375 7,209 frames were available that covered a total of 30,132 square meters. Transects were located
376 to cover the geographical extent of the canyons, as well as the slope nearby, and were located
377 approximately equidistantly, although a few dives were close together to cover a broader depth
378 range at a location. These video frames were a subset of the entire dive; non-overlapping frames
379 were extracted from each video transect at a constant rate of 1 frame per 30 seconds (Miller et al.
380 2012). We applied the same method to compute numerical density as Stone (2006) in order to
381 compare Bering canyon densities to those for the Aleutian Islands. In this method, the total
382 number of coral and sponge colonies counted is divided by the total area surveyed (e.g., divide a
383 count of 1,000 colonies by an area surveyed of 2,000 m² with a result of 0.5 colonies m⁻²).
384 Confidence intervals for these values were estimated by the bootstrap method (Efron and
385 Tibshirani 1993). In our application of the bootstrap method, dives were sampled with
386 replacement within canyon, a density (the bootstrap replicate) was computed and the 95%
387 confidence intervals determined from a distribution of 1,000 bootstrap replicates which was
388 corrected for bias if necessary (bias-corrected percentile method).

Spatial overlap of fishing and vulnerable habitats

We examined the spatial overlap of fishing and vulnerable habitats by combining the probability of coral, sea whip and sponge presence, fishing effort distributions and an index of susceptibility to damage by fishing. The probability of coral, sea whip, and sponge presence was based on the predictive maps produced by the GAM modeling. Intensive fisheries observer programs for groundfish (National Marine Fisheries Service, Seattle WA, North Pacific Groundfish Observer Program database), and crab (Alaska Department of Fish and Game, Division of Commercial Fisheries, Kodiak, Bering Sea/Aleutian Islands crab observer database) monitor fishing effort in the eastern Bering Sea. Set location and gear type (bottom trawl, pelagic trawl, longline (hook and line), pot) are among the data types recorded. We compiled the number of observed sets during 2002-2011 by gear type on the recorded 1 minute latitude x 1 minute longitude grid and then interpolated (linear) these totals onto the 1 km x 1 km grid used for our other data types.

For the susceptibility index, each coral and sponge taxon was scored for vulnerability to damage from fishing based on visual observations of damage rates from the central Aleutian Islands and the height and rigidity of the specimens (Stone and Alcorn, in press) (Table 3). Large, upright rigid taxa such as Antipatharians and bamboo corals were damaged more often (Stone and Alcorn, in press) so we assigned a score of 3, whereas small, flexible taxa such as plexaurid (*Swiftia pacifica*) and acanthogorgiid gorgonians (*Calciorgia* spp.) were damaged less often (Stone and Alcorn, in press) so we assigned a score of 1. Primnoid gorgonians (*Plumarella aleutiana*) are of similar size to the plexaurids and acanthogorgiids but generally have a more rigid skeleton and appear to have intermediate vulnerability to disturbance (Stone and Alcorn, in press) so we assigned a score of 2. Sea whips were assigned an intermediate score of two since they are upright and rigid but vary greatly in size from < 5 cm to > 1 m. These scores consider vulnerability to physical damage only and do not consider differences in recovery rates once damage occurs. Only limited information on recovery rates is available to incorporate into our analyses. Coldwater coral and sponge generally are long-lived (decades or centuries) and slow-growing (typically < 2 cm per year), so that any damage likely will have long-lasting effects. The susceptibility scores for each of the three coral and sponge groups were based on the catch-weighted average of the group members' scores, which were 2.93 for coral, 2.93 for sea whip/pen and 2.14 for sponge.

Vulnerability indices were computed for each 1 km x 1 km grid cell by multiplying probability of occurrence of coral, sea whip and sponge presence by the corresponding susceptibility scores and summing across the three coral and sponge groups. The maximum possible value of the vulnerability index is about eight which occurs when the probability of presence is one for all three taxa ($1 \times 2.93 + 1 \times 2.93 + 1 \times 2.14$). The vulnerability indices were mapped and then summarized for 10 areas (five canyons, four inter-canyon areas and outer shelf). Overlap indices were computed for each 1 km x 1 km grid cell by multiplying these vulnerability indices by the corresponding number of observed fishery sets by gear type. The overlap indices were mapped by gear type and then summarized for the 10 areas. Overlap indices were segregated by gear type because gear effects on benthic invertebrates differ by gear type. Because reliable, quantitative estimates of these differences are not available, we did not compute a single set of overlap indices that combined fishing gears.

Results

Habitat characteristics

The eastern Bering Sea is characterized by a broad, flat shelf. The adjacent slope is shallow-gradient seafloor; most (90%) is 10% gradient or less. Most (90%) seafloor gradient of Pervenets, Navarin and Bering canyons is 5% or less and most seafloor gradient of Pribilof and Zhemchug canyons is 10% or less. The maximum seafloor gradients of any 1 x 1 km grid cell in Zhemchug and Pribilof canyons are 45% and 50% respectively. Most (90%) seafloor gradients of the intercanion areas are 7% or less (Bering-Pribilof), 16% or less (Pribilof-Zhemchug) or 11% or less (Zhemchug-Pervenets, Pervenets-Navarin). The maximum seafloor gradient of any 1 x 1 km grid cell on the slope is 67% for the Pribilof-Zhemchug intercanion area.

We computed the seafloor area of individual canyons and non-canyon slope based on the canyon definitions described in the methods. Compared to the total seafloor area of the eastern Bering Sea slope, canyons comprise almost half (43%) of the total area (Bering 11%, Pribilof 10%, Zhemchug 10%, Pervenets 5% and Navarin 7%). The relative volumes (Navarin (total volume = 5,400 km³), Pervenets (1,700 km³), Bering (4,300 km³), Pribilof (1,300 km³) and Zhemchug (5,800 km³) canyons (Karl et al. 1996)) often differ from the relative areas due to

morphological differences. For example, the areas of Pribilof and Zhemchug canyons are similar but the volume of Zhemchug Canyon is larger because of the larger opening of this canyon. In addition, our study excludes seafloor depths below 1,200 m (the depth limit of the bottom trawl surveys) and Zhemchug Canyon has more habitat below this depth than Pribilof Canyon. The total seafloor areas of the intercanion areas comprise over half (57%) of the total slope area (Bering-Pribilof 18%, Pribilof-Zhemchug 20%, Zhemchug-Pervenets 14%, Pervenets-Navarin 4%).

Broad-scale patterns were apparent in the physical characteristics of the eastern Bering Sea. Focusing on the outer shelf and slope, bottom temperature and ocean color were higher southward (Supplement (S) 1, S2). Current speed was lower for the southeastern shelf compared to the slope and the shelf farther north, especially Navarin Canyon (S3). Grain size generally was coarser and more sorted shoreward (S4-5). Oxygen and pH were lower and turbidity higher in Pribilof and Zhemchug canyons (S6-7). Salinity was higher on the slope than outer shelf (S8).

These broad-scale patterns in physical characteristics distinguished the shelf from the slope and the canyons from the adjacent slope areas. The Case A (for case definitions, see Table 1) PCA distinguished inner shelf from middle and outer shelf based on grain size, sediment sorting, temperature and ocean color and distinguished shelf from slope based on depth, seafloor gradient and current (Figure 2). The related DFA indicated that group membership was medium to highly predictable for inner shelf (97% of stations were grouped correctly), middle shelf (90% of stations were grouped correctly), outer shelf (80% of stations were grouped correctly), canyon (79% of stations were grouped correctly) and inter-canyon slope (78% of stations were grouped correctly) (Table 4). Quadratic discriminants of deeper depths, larger seafloor gradients and higher current speeds were characteristics that defined canyons and inter-canyon slope areas from the shelf areas of the eastern Bering Sea. ANOSIM indicated that there were significant differences among the 12 areas of the eastern Bering Sea ($R = 0.557$, $p = 0.001$).

A division segregates the left and right-hand sides of the Case B plot of PCA components 1 and 2 with Pribilof Canyon to the left and Zhemchug Canyon to the right which are distinguished by grain size, sediment sorting and ocean color (Pribilof Canyon) and seafloor gradient and current (Zhemchug Canyon) (Figure 3a). The Case B plot of PCA components 1 and 3 distinguished Pribilof Canyon based on depth and sediment sorting (Figure 3b). Of the two focal canyons, Pribilof and Zhemchug, the related DFA indicated that group membership was

highly predictable for Pribilof Canyon compared to adjacent slope areas where 98% of canyon stations were grouped correctly and all the adjacent slope stations were predicted correctly. Zhemchug Canyon and its surrounding areas were also highly predictable, as 99% of Zhemchug Canyon were predicted correctly and 98% of adjacent slope stations were predicted correctly (Table 5). Sediment sorting distinguished Pribilof Canyon from the rest of the slope and grain size distinguished the two canyons and the intercanyon areas. Zhemchug Canyon also was less productive (lower ocean color) than other slope areas including Pribilof canyon. Depth and temperature were not very useful in discriminating among canyon and inter-canyon slope areas. ANOSIM also indicated there were significant differences among canyons and inter-canyon areas ($R = 0.54$, $p = 0.001$). The R -value was approximately the same as for the slope and shelf combined analysis, indicating strong differences among slope areas.

A division segregates the upper and lower sections of the Case C PCA plot with Pribilof Canyon below and Zhemchug Canyon above which are distinguished by grain size, sediment sorting, color, temperature and turbidity (Pribilof Canyon) and seafloor gradient and current (Zhemchug Canyon). Of the two focal canyons, Pribilof and Zhemchug, the related DFA indicated that group membership was highly predictable (for Pribilof Canyon stations (100% correct) compared to adjacent slope areas and highly predictable (91% and 71% correct) for adjacent slope areas and Zhemchug Canyon respectively. The results were very similar to the results from Case B although the addition of the physical variables collected in 2012 resulted in slightly worse discrimination of Zhemchug Canyon from the adjacent intercanyon areas. Sample sizes within each grouping in 2012 did not allow for quadratic DFA, so linear DFA was used instead. The distinguishing features of the linear discriminants for the 2012 slope data were sediment characteristics (grain size and sorting), ocean color and bottom temperature. ANOSIM also indicated there were significant differences among canyons and inter-canyon areas ($R = 0.36$, $p = 0.001$). The smaller R -value compared to $R = 0.56$ and $R = 0.54$ for all years data (above) likely occurred because sample sizes were reduced by including only 2012 data.

Coral, sponge and sea whip distributions

The analysis of coral, sponge and sea whip presence-absence did not distinguish the canyons from the adjacent slope areas (Table 6). The DFA indicated that group membership was poorly predicted for Pribilof Canyon stations where 78% of stations were grouped with the adjacent

slope stations. No bottom trawl survey tows in Pribilof Canyon captured sea pens or whips, so this variable could not be used in the DFA. For Zhemchug Canyon, groupings were also inaccurate, as 84% of Zhemchug stations were grouped with stations from adjacent slope areas. Although the ANOSIM results were significant ($p = 0.001$), the R-value (0.052) indicated that there was very little dissimilarity among the different slope areas in coral, sponge and sea whip presence-absence.

The best-fitting GAMs of coral, sea whip and sponge explained 31-39% of deviance in presence-absence data (Table 7, S9-11). The significant explanatory variables were current (coral, sea whip, sponge), depth (sea whip, sponge), grain size (sponge), seafloor gradient (coral, sea whip, sponge), ocean color (sea whip, sponge) and location (coral, sea whip, sponge). Using threshold probabilities of 0.30 and 0.28, the models accurately predicted coral and sea pen presence-absence as they were correct 93% and 90% of the time (Table 8). Using a threshold probability of 0.53, sponge presence-absence was correctly predicted 77% of the time. The AUC and the Kappa statistics indicated an acceptable predictive ability for these models.

Coral (Figure 4a), sponge (Figure 4b) and sea whip (Figure 4c) are predicted to occur both inside and outside canyons. Predicted coral distribution is limited to sections of the slope, both within and between canyons. In contrast, predicted sea whip distribution includes sections of the outer shelf and is shallower than coral. Predicted sponge distribution occurred for sections of the slope, both within and between canyons, as well as outer shelf. Within Pribilof Canyon, there is some tendency for more coral presence inside or adjacent to the lateral wings of these two canyons. Sea whips are predicted to occur adjacent to Zhemchug but not Pribilof Canyon.

More coral habitat was predicted for slope areas (61%) than for the outer shelf (39%) (Table 9). Within slope areas, the highest amount of coral habitat was predicted to be in Pribilof Canyon (33%). Only 1% of coral habitat for slope areas was predicted for Zhemchug Canyon and the rest was primarily in the Pribilof-Zhemchug inter-canyon area (29%), in the Zhemchug-Pervenets inter-canyon area (18%) and in Navarin Canyon (13%).

One unique feature of the focal canyons is that one third (33%) of the coral habitat predicted for the eastern Bering Sea slope occurs in Pribilof Canyon, an area that comprises only about 10% of the total slope area. The area of predicted coral habitat in Pribilof Canyon extends into the Pribilof-Zhemchug intercanion area (Figure 4a). In contrast, about two-thirds of sponge (64%) and most sea whip (91%) habitat was predicted to occur on the outer shelf, an area that

comprises about 82% of the total area of the slope and outer shelf. In the combined slope areas, Pribilof and Zhemchug canyons contained about 28% of the predicted total sponge habitat. For sea whip there is no predicted occurrence in Pribilof Canyon and only 14% of the total slope sea whip habitat occurs in Zhemchug Canyon.

Coral and sponge are less common on the Bering Sea slope compared to the Aleutian Islands. The average densities of coral were 0.28 colonies m⁻² (Pribilof Canyon) and 0.15 (Zhemchug Canyon), much less than the average density for the Aleutian Islands (1.23) (Stone 2006) (Figure 5a). The average densities of sponge were 0.10 (Pribilof Canyon) and 0.21 (Zhemchug Canyon), again much less than the average density for the Aleutian Islands (5.25) (Stone and Alcorn, in press). From trawl surveys, coral frequency of occurrence was highest for the Aleutian Islands (0.54) and about five times that for the Bering Sea slope and Gulf of Alaska (both ~0.1) (Figure 5b). Sponge frequency of occurrence was more similar among these three regions (0.57-0.95) but still highest for the Aleutian Islands (0.95). Common taxa from the visual surveys of Pribilof and Zhemchug canyons were the gorgonian coral *Plumarella aleutiana*, the sponges *Aphrocallistes vastus*, *Heterchone calyx*, *Acanthascus vastus* and *Acanthascus* spp. and the sea pen *Halipteris willemoesi*.

Fish and crab distributions

Like the analysis of coral and sponge, the analysis of fish and crab did not reliably distinguish the canyons from the adjacent slope areas. The DFA indicated that group membership was not very predictable, as only 30% of stations in Pribilof Canyon were classified correctly (Table 6). For Zhemchug Canyon, only 51% of stations were classified correctly as being from Zhemchug Canyon. The ANOSIM indicated statistical differences among slope data ($p = 0.001$), but the dissimilarity among groups was not great, as indicated by the low R-value (0.127).

Generalized additive modeling explained 31-91% of deviance in fish and crab spatial distributions (Table 10, S12-28). Latitude, longitude and depth were significant explanatory variables for all species. All of the variables considered were significant in at least seven of the models. Sediment characteristics were important for all of the species. Predictions were reasonable; observations and predictions generally followed a 1:1 line. The predicted catches occurred in areas with observed catch to a large extent and the areas with little or no positive catches did not have predicted high abundance. Less variability was explained for Pacific

halibut, roughey/blackspotted rockfish and shortraker rockfish. The two rockfish taxa were caught in only a small proportion of the bottom trawl hauls.

Habitat associations generally were reasonably predicted and stereotypical habitats were correctly assigned for a shelf species, arrowtooth flounder (Figure 6a), a shelf break species, Pacific ocean perch (Figure 6b) and a slope species, sablefish (Figure 6c). By modeling the entire data set without regards to year, interannual variability in catches or overall trends in abundance were not considered. Within one year of the survey, Pacific ocean perch often exhibit a patchy distribution in trawl survey catches, even though their depth distribution is well defined. By combining trawl survey years for analysis, predicted Pacific ocean perch abundance occurred as a band of high abundance within a well-defined depth range (Figure 6b), which over the years, matches the observations of positive catches reasonably well for the slope and less so for the outer shelf.

Are the canyons homogeneous?

The canyons are not homogeneous. For example, coral habitat is predicted to be concentrated in the western wing of Pribilof Canyon (Figure 4a) and sponge habitat is predicted to be concentrated in central Zhemchug Canyon (Figure 4b). In addition, fish typically exhibit depth preferences and so are concentrated in a depth band within a canyon (e.g., sablefish, Figure 6c). However these patterns of patchiness and depth preference are not limited to canyons and occur for other sections of the slope as well.

Overlap of fishing and vulnerable habitats

Average habitat vulnerability indices were higher for Pribilof Canyon than other areas but not markedly greater than averages for Pribilof-Zhemchug or Zhemchug Canyon. Higher vulnerability indices were found both within and between canyons and were not unique to Pribilof and Zhemchug canyons (Figure 7). Higher vulnerability indices also were found in sections of the outer shelf. The average vulnerability range was 2.5-6 (Figure 8). The highest index was for Pribilof Canyon (6), then Bering Canyon (5) which was closely followed by Pribilof-Zhemchug, Zhemchug Canyon, Pervenets Canyon and Navarin Canyon (all >4).

Bottom trawl (fishing) effort and pot effort were more concentrated spatially than pelagic trawl effort and longline effort (Figure 9). For the outer shelf and slope, bottom trawl effort was

concentrated in Bering Canyon and relatively low elsewhere; pot effort was concentrated in sections of Bering and Pribilof canyons and the outer shelf between Pribilof and Zhemchug canyons (Figure 9). In contrast pelagic trawl effort and longline effort extended the entire length of the Bering slope and outer shelf. The highest concentrations of pelagic trawl effort occurred in Bering and Pribilof canyons and the outer shelf. The highest concentrations of longline effort occurred in Pribilof and Zhemchug canyons, the Pribilof-Zhemchug, Zhemchug-Pervenets and Pervenets-Navarin intercanion areas and the outer shelf.

Overlap indices were computed from the fishing effort information and the habitat vulnerability indices (Figure 10). The maximum value was about 40 (about 1.6 on the log-scale plots in Figure 10). For the slope including canyons, overlap indices were greater than ten (1.0 on log-scale) for the southeastern wing of Pribilof Canyon (pelagic trawl), northwestern wing of Pribilof Canyon (pot) and the central section of Zhemchug Canyon and some of the slope habitat between Zhemchug and Pribilof canyons (longline). The overlap indices were less than ten for bottom trawl for all of the slope including canyons.

Average overlap indices were low for bottom trawl (Figure 11) because this fishery largely concentrates in areas outside our study area (i.e., inner and middle shelf). The average overlap indices for pot gear were still low but somewhat higher in Bering and Pribilof canyons than other areas. In contrast, the overlap indices were higher for longline and pelagic trawl than the other fishing gears. For longline, the overlap indices were higher for Pribilof and Zhemchug canyons, Pribilof-Zhemchug and Zhemchug-Pervenets intercanion areas. For pelagic trawl, the overlap indices were higher for Bering and Pribilof canyons.

Discussion

The five questions

In this paper, we address a request by the NPFMC in 2012 to determine whether Pribilof and Zhemchug canyons provide unique coral and sponge habitats for managed fish species. Our analyses address five questions from the NPFMC; our answers are summarized here:

1. Are the canyons unique habitats? Zhemchug and Pribilof canyons have distinct physical characteristics including sediment characteristics, ocean color and seafloor gradient that distinguish them from the rest of the Bering Sea slope. These physical differences are more tied to latitude than characteristics unique to these two canyons; for example, both ocean color and temperature decrease northward. These two canyons cannot be distinguished based on biological characteristics because coral and sponge presence and fish and crab densities are similar in canyons and the adjacent slope. One unique feature of the focal canyons is that about one third of the coral habitat predicted for the eastern Bering Sea slope occurs in Pribilof Canyon, an area that comprises only about 10% of the total slope area. Although concentrated there, the average density of coral for Pribilof Canyon ($0.28 \text{ colonies m}^{-2}$) is much less than the density for the Aleutian Islands ($1.23 \text{ colonies m}^{-2}$).
2. Are the canyons homogeneous habitats? The physical and biological characteristics of Zhemchug and Pribilof canyons are not spatially homogeneous. Turbidity and oxygen concentrations varied within these two canyons. Coral habitat was more common in some areas of Pribilof Canyon than others. Each fish species generally occupied a distinct depth zone.
3. What are the fish associations with habitat features? Coral, sponge, fish and crab distributions were associated with specific physical habitat characteristics. The presence of coral and sponge could be predicted based on location, depth, current speed and sediment characteristics. The abundance of fish and crab could be predicted based on location, depth and sediment characteristics.
4. What is the vulnerability of the canyons? Average habitat vulnerability indices were higher for Pribilof Canyon than other areas but not markedly greater than averages for Pribilof-Zhemchug or Zhemchug Canyon.
5. Are benthic habitats vulnerable? Concentrated fishing effort overlapped areas of Pribilof and Zhemchug canyons with higher vulnerability indices for two of the four fishing

gears. Longline fishing overlapped areas of the Bering slope with higher vulnerability indices including both Pribilof and Zhemchug canyons and adjacent slope. Pelagic trawling overlapped sections of Pribilof Canyon with higher vulnerability indices but not Zhemchug Canyon. Most bottom trawling and pot fishing occurred in less vulnerable areas except perhaps Bering and Pribilof canyons for pot fishing. These vulnerability and overlap indices provide relative values but are not absolute measures of fishing effects.

Validation of results

Our estimates of coral and sponge densities based on visual survey information differed from Miller et al. (2012) in part because we used a different approach to estimate density; we followed the approach of Stone (2006). We estimated coral densities of 0.28 colonies m^{-2} (Pribilof Canyon) and 0.15 (Zhemchug Canyon), compared to 0.97 and 0.18, respectively (Miller et al. 2012); we estimated sponge densities of 0.10 colonies m^{-2} (Pribilof Canyon) and 0.21 (Zhemchug Canyon), compared to 0.41 and 0.02, respectively (Miller et al. 2012). In our approach, density was computed for each canyon by dividing total count by total area surveyed, whereas Miller et al. (2012): 1) computed density by video frame; 2) computed the mean density for each transect; 3) computed the mean density for each canyon. One way to think of this difference is that in our approach, density is weighted by sample effort (frame size and transect length) whereas Miller et al. 2012 treated each video frame and transect equally regardless of sample effort. One other difference is that Miller et al. (2012) analyzed only the 2007 data (all that was available at the time) whereas we also analyzed the new data collected in 2012.

We compared visual survey information to our predictions based on trawl survey information in order to understand the reliability of these predictions. The limited visual survey data generally supports our predictions of coral and sponge distributions but indicates some mismatch with our predictions of sea whip distributions. We predicted coral (Figure 4a) primarily for slope habitat of Pribilof and Zhemchug canyons, which matches Miller et al. (2012) who found most coral were present at depth 200-400 m (slope) and were absent at depth 150-200 m (outer shelf). We predicted sponge (Figure 4b) in both slope and outer shelf habitat of these two canyons; Miller et al. (2012) found most sponge at depth 200-400 m (slope) but absent from outer shelf habitat (150-200 m). However, Miller et al. (2012) may have missed sponges in outer shelf habitat because their sample size was only 77 video frames. We predicted sea whip habitat

687 primarily for outer shelf habitat adjacent to Zhemchug but not Pribilof Canyon (Figure 4c).
688 Miller et al. (2012) found more sea whips in Pribilof (0.07 m^{-2}) than Zhemchug (0.001 m^{-2})
689 canyon at depth 254-488 m (slope).

690 Brodeur (2001) found sea whips in the western wing of Pribilof Canyon but we predicted
691 none there (Figure 4a). In 5 of 7 ROV deployments there, Brodeur (2001) reported areas
692 containing dense aggregations of 1-2 m high sea whips (*Halipteris willemoesi*) evenly spaced
693 about 2 m apart over the depth interval of 185-240 m (i.e., outer shelf and slope habitat). The
694 absence of sea whips in the prediction for the outer shelf likely occurred because trawl survey
695 effort is minimal there. Slope survey effort covers the depth range of 200-1,200 m and shelf
696 survey effort covers the depth range of 20-200 m, but is reduced below depth of 165 m because
697 few standard 37 km x 37 km grid cells occur there. As a result, sampling effort by depth was
698 65.6% for depths <165 m and 33.9% (>205 m) but only 0.5% (165-205 m) ($n = 2,696$).

699 The frequency of occurrence of coral in trawl surveys but not sponge was similar to their
700 frequency of occurrence in visual surveys. Miller et al. (2012) reported that corals are patchy in
701 the canyons and separated by large areas of open silt/sand habitat, such that only 15% of frames
702 contained coral for their 2007 data. For both 2007 and 2012 visual data, we found that 10% of
703 frames contained coral, the same frequency as the 10% of tows that caught coral during slope
704 surveys (Figure 5b). Miller et al. (2012) did not report the frequency of occurrence of sponge,
705 but we found that for both 2007 and 2012 visual data, 13% of frames contained sponge, much
706 less than the frequency of occurrence of sponge from 2002 to 2012 Bering slope trawl surveys of
707 nearly 60%. Given that the area sampled by a trawl is much larger than that sampled in a video
708 frame, this difference in occurrence implies that sponge are ubiquitous but sparse.

709 Most of our study area was available to the trawl survey gear and major areas of the slope
710 missed by our analyses were few. Major areas that were untrawlable totaled about 5% of slope
711 habitat and were found in Pribilof-Zhemchug (intercanyon area) (13% of this area was
712 untrawlable), Zhemchug Canyon (17%), Zhemchug-Pervenets (1%) and Pervenets-Navarin (8%)
713 (S29). In general, survey scientists characterized these untrawlable areas as “too steep and
714 bumpy” to trawl. Of the two focal canyons, one area of Zhemchug Canyon was untrawlable and
715 covered a linear length of about 25 km of the southeast wall of this canyon; no large area of
716 Pribilof Canyon was considered untrawlable. A statistical analysis comparing habitat
717 characteristics derived from a multibeam map of Pribilof Canyon to locations of successful trawl

tows also indicated that Pribilof Canyon within the surveyed depths (< 1,200 m) is available to the trawl survey gear.

Overlap of fishing and vulnerable habitats

The potential for fishing effects on benthic habitat depends on the benthic community composition, gear type and the spatial overlap of fishing and vulnerable habitats. Stable communities of low-mobility, long-lived species are more vulnerable to acute and chronic physical disturbance than are short-lived species in dynamic environments (NRC 2002). Structurally complex habitats (e.g., biogenic reefs) and those that are relatively undisturbed by natural perturbations (e.g., deep-water mud substrata) are more adversely affected by fishing than unconsolidated sediment habitats that occur in shallow coastal waters (Kaiser et al. 2002). In the context of the Bering Sea, these findings imply that the inner shelf that is frequently impacted by winter storms is less vulnerable than the deeper and more stable outer shelf and slope. Nevertheless, trawling effects on benthic invertebrates have been documented for the inner shelf, including both positive and negative changes in biomass of individual taxa, as well as reduced species diversity, niche breadth, and mean body sizes (McConnaughey et al. 2000, Brown et al. 2005, McConnaughey et al. 2005). In some cases, these effects were small relative to natural variability in the surrounding area (McConnaughey et al. 2005).

Pelagic trawls used in the pollock fishery are not designed to be fished on the seafloor, however some contact occurs when larger, more valuable pollock aggregate near the seafloor. A measure of this occurrence is the catch of crabs which are strictly benthic. Crab bycatch in the pollock fishery averaged 15,955 crabs during 2007-2011 (Ianelli et al. 2012). The overlap index identifies areas where fishing effects on coral and sponge habitat may occur. For the pelagic trawl fishery, the actual effect will depend on how often and in what areas bottom contact commonly occurs.

Within the classification of bottom trawls, rock-hopper otter trawls disturb the seabed most intensively, whereas for lighter gears such as smaller otter trawls, disturbance is largely restricted to the trawl boards except when erect benthic invertebrates such as sponge are present and the warps and footrope of either otter trawl can detach individuals from the seafloor (Kaiser et al. 2002). Trawl effects studies in Alaska have found that large epifaunal invertebrates were removed or damaged by a single trawl pass (Freese et al. 1999), sponges were slow to recover

748 from trawling effects (Freese 2001), and chronic bottom trawling affected the abundance and
749 diversity of epibenthos (Stone et al. 2005). Trawl effects can be reduced by gear modifications
750 that reduce seafloor contact (Rose et al. 2010).

751 Fishing effort tends to be patchy and the same grounds are fished year after year (Kaiser
752 et al. 2002). For most habitats that are vulnerable to fishing, a consistently patchy distribution of
753 a given level of trawling effort from year to year is likely to have lower environmental impacts
754 than if the same trawling effort were distributed evenly because the initial effect usually is
755 greater than recurrent effects (Kaiser et al. 2002). For this reason, tabulation of fishing effort
756 should account for overlap in assessing effects of fishing which can be challenging (Rose and
757 Jorgensen 2005). It is also important to consider the consequences of redistributed effort if new
758 closures are implemented (Fujioka 2006).

759 The computation of the vulnerability index implies that an area is highly vulnerable
760 where, for example, upright corals or sponges are common. The computation of the overlap
761 index implies that there is higher potential for a fishing effect if fishing effort is intense there.
762 However the vulnerability and overlap indices are relative values and are not absolute measures
763 of fishing effects. While an index value of 3 implies more effect than a value of 1, the effect is
764 not 3 times greater for the former than the latter. Further a relatively high value does not explain
765 whether effects were light, medium or high (i.e., not scaled to actual damage), just that effects
766 likely were greater compared to other areas. An alternate approach to defining vulnerability is to
767 define an organism as vulnerable if it is rare. We did not follow this population-based approach
768 and instead focused on identifying areas where higher coral and sponge densities overlapped
769 higher fishing effort.

770 **Other ecological considerations related to coral and sponge**

771 Coral and sponge densities were much less in the Bering Canyons compared to the Aleutian
772 Islands. Compared to Aleutian Islands average coral density of 1.23 colonies m⁻² (Stone 2006),
773 using the same computational method we found that Pribilof Canyon average coral density (0.28)
774 was 23% of the Aleutians value and that Zhemchug Canyon average coral density (0.15) was
775 12% of the Aleutian value. The frequency of occurrence of coral from trawl surveys was about
776 10% for the eastern Bering Sea slope and like the numeric densities, much less than the
777 frequency of occurrence for the Aleutian Islands (~50%). Compared to Aleutian Islands average

sponge density of 5.25 colonies m⁻² (Stone and Alcorn in press), we found that Pribilof Canyon average sponge density (0.10) was 2% of the Aleutians value and that Zhemchug Canyon average coral density (0.21) was 4% of the Aleutian value. The frequency of occurrence of sponge from trawl surveys was nearly 60% for the eastern Bering Sea slope and unlike the numeric densities, only somewhat less than the frequency of occurrence for the Aleutian Islands (nearly 100%).

No coral taxa, with one possible exception, are known to be endemic to the eastern Bering Sea (Stone et al. in preparation). Reviews of the biogeographical distribution of corals in Alaskan waters indicate that there are 19 taxa found throughout the eastern Bering Sea (Stone et al. in preparation). A single recently described demosponge *Aaptos kanuxx* (Lehnert et al. 2008) is known only from Pribilof Canyon so may be endemic to that region. Reviews of the biogeographical distribution of sponges in Alaskan waters indicate that there are 67 taxa found throughout the Bering Sea (Stone et al. 2011).

Our analysis of the 2002-2012 trawl surveys of the eastern Bering Sea slope found 17 coral, 25 sponge and 10 sea whip and sea pen taxa. Whenever two or more specimens of a taxon were caught, at least one specimen was found in both canyon and non-canyon slope areas. Sometimes only one specimen was caught. However this commonly happened in both canyons and non-canyon slope, indicating that this occurred due to chance rather than endemism in canyons. Of taxa only caught once, 13% occurred in canyons and 27% occurred in non-canyons. Comparing 2002-2012 trawl survey data for eastern Bering Sea slope to other regions of Alaska, we found only three taxa that occurred only on the eastern Bering Sea slope. These three taxa were *Calcigorgia beringi*, Isididae unidentified (an unidentified bamboo coral) and *Antipatheria* unidentified (an unidentified black coral). However *Calcigorgia beringi* ranges from the eastern Bering Sea south to Washington State (Stone et al. in preparation). Additionally, at least one species of bamboo coral (*Keratoisis* sp. A) and one species of black coral (*Lillipathes wingi*) are known from the eastern Bering Sea and broadly distributed throughout Alaskan waters (Stone et al. in preparation).

Recovery rates from disturbance of cold-water corals and sponges depend on several factors including growth rate, recruitment rate, and reproductive ecology. Alaskan corals, including *Keratoisis* sp. A (Andrews et al. 2009) and *Primnoa pacifica* (Andrews et al. 2002), are slow-growing and consequently long-lived given the maximum sizes observed for these taxa.

The stylasterid corals in the Aleutian Islands (Brooke and Stone, 2007) and *Primnoa pacifica* in the Gulf of Alaska (Waller et al. in preparation) are gonochoristic brooders with limited potential to provide sources of recruits to disjunct disturbed habitats. Limited biological information for sponges indicates that they too are very susceptible to physical disturbance with long recovery periods from disturbance (Stone et al. 2011).

Other ecological considerations related to fish, seabirds and marine mammals

There are consistent seasonal patterns of pollock spawning locations in the eastern Bering Sea, but these patterns are not uniquely associated with any eastern Bering Sea canyon; seasonally, Bacheler et al. (2012) showed that peak spawning occurs early in the year (March) in the Bogoslof and Islands of Four Mountains regions and progresses toward the slope area and around the Pribilof Islands by May. The latter concentration is found around and slightly east of the Pribilof Islands (Bacheler et al. 2010) and not limited to Pribilof Canyon.

Skates (Rajidae) deposit their large leathery egg cases in specific areas often found in eastern Bering Sea canyons. To date 14 skate nursery sites have been identified in the eastern Bering Sea. Ten of the 14 sites are at the heads of large canyons (Navarin 1, Pervenets 3, Zhemchug 2, Pribilof 2, Bering 2) with the additional 4 sites at the heads of smaller deeper canyons. Nursery sites occur on relatively flat sandy to muddy bottom with little relief or bottom structure (Hoff 2010), which is the most common eastern Bering Sea bottom type. The reason for the strong association with undersea canyons is believed to be correlated with oceanographic conditions such as bottom currents, oxygen content and productivity, but a clear understanding of site location is still being investigated (G. Hoff, pers. comm.). Recent action by the NPFMC recognized six skate nursery sites in the eastern Bering Sea as Habitat Areas of Particular Concern (HAPC) and recommended additional research into habitat and oceanographic conditions driving site selection and into impacts of disturbances on these important skate nursery areas.

Some marine mammal and seabird species commonly are found along the outer shelf and slope, sometimes associated with Bering Sea canyons. In marine mammal surveys during 1999-2004 (Friday et al. 2012), only fin whales and Dall's porpoise consistently occupied the outer and middle shelf; there was no concentration of fin whales related to Zhemchug or Pribilof canyons, whereas Dall's porpoise was concentrated in Pribilof Canyon in one of three survey

years. Both female (Call et al. 2008) and juvenile male (Sterling and Ream 2004) fur seal forage widely away from the Pribilof Islands and while sometimes located in Pribilof Canyon, show no concentration there. In seabird surveys during the 1960s, seabirds often were concentrated along the continental slope and outer shelf but not limited to canyons (Shuntov 1993). Foraging seabirds tied to a colony often forage nearby but even black-legged kittiwakes on St. George Island near Pribilof Canyon may forage farther away and not at the nearby canyon (Paredes et al. 2012). Some seabird species near the Pribilof Islands showed spatial preferences (e.g. thick-billed murres south and west of the islands) and others did not (e.g. short-tailed shearwaters showed no preference relative to the islands); no species concentrated over Pribilof Canyon (Jahncke et al. 2008). In contrast, short-tailed albatross were more common along the slope northwest of the Pribilof Islands and may concentrate in Zhemchug and Pervenets canyons (Piatt et al. 2006).

Acknowledgments

We thank Al Hermann, NOAA's Pacific Marine Environmental Laboratory, for providing the model-based estimates of ocean currents; Carla J. Moore, NOAA's National Geophysical Data Center, for providing the sediment data; and John Hocevar, Greenpeace, for providing visual survey data of Pribilof and Zhemchug canyons. We thank Gary Greene, Moss Landing Marine Laboratory, and Dave Scholl, US Geological Survey, for advice on canyon definitions. We also thank Jon Heifetz, Carol Ladd, Bob Lauth, Ivan Mateo and Paul Spencer for their reviews and useful comments.

References

- Andrews AH, Cordes EE, Mahoney MM, Munk K, Coale KH, Cailliet GM, Heifetz J. 2002. Age, growth and radiometric age validation of a deep-sea, habitat-forming gorgonian (*Primnoa resedaeformis*) from the Gulf of Alaska. *Hydrobiologia* 471: 101-110.
- Andrews AH, Stone RP, Lundstrom CC, DeVogelaere AP. 2009. Growth rate and age determination of bamboo corals from the northeastern Pacific Ocean using refined ^{210}Pb dating. *Marine Ecology Progress Series* 397: 173-185.

866
867 Bacher NM, Ciannelli L, Bailey KM, Duffy-Anderson JT. 2010. Spatial and temporal patterns
868 of walleye pollock (*Theragra chalcogramma*) spawning in the eastern Bering Sea inferred from
869 egg and larval distributions. Fisheries Oceanography 19: 107-120.
870
871 Bacher NM, Ciannelli L, Bailey KM, Bartolino V. 2012. Do walleye pollock exhibit flexibility
872 in where or when they spawn based on variability in water temperature? Deep-Sea Research Part
873 II: Topical Studies in Oceanography.
874
875 Baker ET, Hickey BM. 1986. Contemporary sedimentation processes in and around an active
876 west coast submarine canyon. Marine Geology 71: 15-34.
877
878 Behrenfeld MJ, Falkowski PG. 1997. Photosynthetic rates derived from satellite-based
879 chlorophyll concentration. Limnology and Oceanography 42: 1-20.
880
881 Brooke S, Stone R. 2007. Reproduction of deep-water hydrocorals (family Stylasteridae) from
882 the Aleutian Islands, Alaska. Bulletin of Marine Science 81: 519-532.
883
884 Brodeur RD. 2001. Habitat-specific distribution of Pacific ocean perch (*Sebastes alutus*) in
885 Pribilof Canyon, Bering Sea. Continental Shelf Research 21: 207-224.
886
887 Brown EJ, Finney B, Hills S, Dommissie M. 2005. Effects of commercial otter trawling on
888 benthic communities in the southeastern Bering Sea. In Barnes PW, Thomas JP (editors).
889 Benthic habitats and the effects of fishing. American Fisheries Society Symposium 41, Bethesda,
890 Maryland.
891
892 Brown ZW, van Dijken GL, Arrigo KR. 2011. A reassessment of primary production and
893 environmental change in the Bering Sea. Journal of Geophysical Research 116, C08014,
894 doi:[10.1029/2010JC006766](https://doi.org/10.1029/2010JC006766).
895

- 896 Busby MS, Mier KL, Brodeur RD. 2005. Habitat associations of demersal fishes and crabs in the
897 Pribilof Islands regions of the Bering Sea. Fisheries Research 75: 15-28.
898
- 899 Call KA, Ream RR, Johnson D, Sterling JT, Towell RG. 2008. Foraging route tactics and site
900 fidelity of adult female northern fur seal (*Callorhinus ursinus*) around the Pribilof Islands. Deep-
901 Sea Research Part II: Topical Studies in Oceanography 55: 1883-1896.
902
- 903 Clement Kinney J, Maslowski W, Okkonen S. 2009. On the processes controlling shelf-basin
904 exchange and outer shelf dynamics in the Bering Sea. Deep-Sea Research Part II: Topical
905 Studies in Oceanography 56: 1351-1362.
906
- 907 Coachman LK. 1986. Circulation, water masses and fluxes on the southeastern Bering Sea shelf.
908 Continental Shelf. Research 5: 23-108.
909
- 910 Danielson S, Curchitser E, Hedstrom K, Weingartner T, Stabeno P. 2011. On ocean and sea ice
911 modes of variability in the Bering Sea, Journal of Geophysical Research 116, C12034,
912 doi:10.1029/2011JC007389.
913
- 914 Danielson S, Hedstrom K, Aagaard K, Weingartner T, Curchitser E. 2012. Wind-induced
915 reorganization of the Bering shelf circulation. Geophysical Research Letters 39,
916 doi:10.1029/2012GL051231
917
- 918 De Leo FC, Smith CR, Rowden AA, Bowden DA, Clark MR. 2010. Submarine canyons:
919 hotspots of benthic biomass and productivity in the deep sea. Proceedings Royal Society B 277:
920 2783-2792.
921
- 922 Efron B, Tibshirani R. 1993. An introduction to the bootstrap. Chapman & Hall/CRC. 437 p.
923
- 924 ESRI 2009. ArcGIS Desktop: Release 9. Redlands, CA: Environmental Systems Research
925 Institute.
926

- 927 Fielding AH, Bell JF. 1997. A review of methods for the assessment of prediction errors in
928 conservation presence/absence models. *Environmental Conservation* 24: 38-49.
929
- 930 Freese L, Auster PJ, Heifetz J, Wing BL. 1999. Effects of trawling on seafloor habitat and
931 associated invertebrate taxa in the Gulf of Alaska. *Marine Ecology Progress Series* 182: 119-126.
932
- 933 Freese JL. 2001. Trawl-induced damage to sponges observed from a research submersible.
934 *Marine Fisheries Review* 63(3): 7-13.
935
- 936 Friday NA, Waite JM, Zerbini AN, Moore SE. 2012. Cetacean distribution and abundance in
937 relation to oceanographic domains on the eastern Bering Sea shelf: 1999–2004. *Deep-Sea*
938 *Research Part II: Topical Studies in Oceanography*.
939
- 940 Fujioka JT. 2006. A model for evaluating fishing impacts on habitat and comparing fishing
941 closure strategies. *Canadian Journal of Fisheries and Aquatic Sciences*, 63: 2330-2342.
942
- 943 Harris PT, Whiteway T. 2011. Global distribution of large submarine canyons: Geomorphic
944 differences between active and passive continental margins. *Marine Geology* 285: 69-86.
945
- 946 Hastie T, Tibshirani R. 1990. Generalized additive models. Chapman & Hall/CRC. 335 p.
947
- 948 Hickey BM. 1995. Coastal submarine canyons. Topographic effects in the ocean. SOEST Special
949 publications, 95-110.
950
- 951 Hickey BM. 1997. The response of a steep-sided, narrow canyon to time-variable wind forcing.
952 *Journal of Physical Oceanography* 27: 697-726.
953
- 954 Hoff GR. 2010. Identification of skate nursery habitat in the eastern Bering Sea. *Marine Ecology*
955 *Progress Series* 403: 243-254.
956

- 957 Hoff GR, Britt LL. 2011. Results of the 2010 eastern Bering Sea upper continental slope survey
958 of groundfish and invertebrate resources. U.S. Department Commerce, NOAA Technical
959 Memorandum NMFS-AFSC-224, 300 p.
960
- 961 Hosmer DW, Lemeshow S. 2005. Multiple logistic regression. Applied Logistic Regression,
962 Second Edition, 31-46.
963
- 964 Ianelli JN, Honkalehto T, Barbeau S, Kotwicki S, Aydin K, Williamson N. 2012. Assessment of
965 the walleye pollock stock in the Eastern Bering Sea. In Stock assessment and fishery evaluation
966 report for the groundfish resources of the Bering Sea/Aleutian Islands regions. North Pacific
967 Fishery Management Council, Anchorage, Alaska.
968
- 969 Jahncke J, Vlietstra LS, Decker MB, Hunt GL. 2008. Marine bird abundance around the Pribilof
970 Islands: a multi-year comparison. Deep-Sea Research Part II: Topical Studies in Oceanography,
971 55: 1809-1826.
972
- 973 Kaiser MJ, Collie JS, Hall SJ, Jennings S, Poiner IR. 2002. Modification of marine habitats by
974 trawling activities: prognosis and solutions. Fish and Fisheries 3(2), 114-136.
975
- 976 Karl HA, Carlson PR, Gardner JV. 1996. Aleutian Basin of the Bering Sea: Styles of
977 sedimentation and canyon development. In Gardner JF, Field ME, Twichell DC. Geology of the
978 United States seafloor: the view from GLORIA. Press Syndicate of the University of Chicago.
979
- 980 Kim YJ, Gu C. 2004. Smoothing spline Gaussian regression: more scalable computation via
981 efficient approximation. Journal of the Royal Statistical Society: Series B (Statistical
982 Methodology) 66: 337-356.
983
- 984 Kowalik Z, Staben P. 1999. Trapped motion around the Pribilof Islands in the Bering
985 Sea. Journal Geophysical Research, 104(C11), 25667–25684, doi:[10.1029/1999JC900209](https://doi.org/10.1029/1999JC900209).
986

Ladd C, Stabeno PJ, O'Hern JE. 2012. Observations of a Pribilof eddy. Deep-Sea Research Part I: Oceanographic Research Papers 66: 67-76.

Lauth RR. 2011. Results of the 2010 eastern and northern Bering Sea continental shelf bottom trawl survey of groundfish and invertebrate fauna. U.S. Dep. Commerce, NOAA Technical Memorandum NMFS-AFSC-227, 256 p.

Lehnert H, Hocevar J, Stone RP. 2008. A new species of *Aaptos* (Porifera, Hadromerida, Suberitidae) from Pribilof Canyon, Bering Sea, Alaska. Zootaxa 1939: 65–68.

McConnaughey RA, Smith KR. 2000. Associations between flatfish abundance and surficial sediments in the eastern Bering Sea. Canadian Journal of Fisheries and Aquatic Science 56: 2410-2419.

McConnaughey, R. A., Mier, K., and Dew, C. B. 2000. An examination of chronic trawling effects on soft-bottom benthos of the eastern Bering Sea. ICES Journal of Marine Science 57: 1377-1388.

McConnaughey R, Syrjala SE, Dew CB. 2005. Effects of chronic bottom trawling on the size structure of soft-bottom benthic invertebrates. In Barnes PW, Thomas JP (editors). Benthic habitats and the effects of fishing. American Fisheries Society Symposium 41, Bethesda, Maryland. Pages 425-437.

McConnaughey RA, Amend M, Berger J, Busby M, Campbell G, Hoff J, Ito D, Lang G, Lunsford C, Nichol D, Rodgveller C, Rose C, Shotwell K, Smith K, Stone R. 2006. A review of scientific information related to Bering Sea canyons and skate nursery areas. Available North Pacific Fisheries Management Council, 605 West 4th, Suite 306, Anchorage, Alaska 99501-2252.

- McConnaughey RA, Syrjala SE. 2009. Statistical relationships between the distributions of groundfish and crabs in the eastern Bering Sea and processed returns from a single-beam echosounder. *ICES Journal of Marine Science* 66:1425-1432.
- Miller RJ, Hocevar J, Stone RP, Fedorov DV. 2012. Structure-forming corals and sponges and their use as fish habitat in Bering Sea submarine canyons. *PLoS ONE* 7(3): e33885.doi:10.1371/journal.pone.0033885.
- NRC (National Research Council). 2002. Effects of trawling and dredging on seafloor habitat. National Academy Press, Washington, D.C.
- Normarck WR, Carlson PR. 2003. Giant submarine canyons: Is size any clue to their importance in the rock record? *Geological Society America, Special Paper* 370.
- Paredes R, Harding A, Irons DB, Roby DD, Suryan RM, Orben RA, Renner H, Young R, Kitaysky A. 2012. Proximity to multiple foraging habitats enhances seabirds' resilience to local food shortages. *Marine Ecology Progress Series* 471: 253-269.
- Piatt JF, Wetzel J, Bell K, DeGange AR, Balogh GR, Drew GS, Geernaert T, Ladd C, Byrd GV. 2006. Predictable hotspots and foraging habitat of the endangered short-tailed albatross (*Phoebastria albatrus*) in the North Pacific: Implications for conservation. *Deep-Sea Research Part II: Topical Studies in Oceanography* 53: 387-398.
- Rho T, Whitledge TE. 2007. Characteristics of seasonal and spatial variations of primary production over the southeastern Bering Sea shelf. *Continental Shelf Research* 27: 2556-2569.
- Rooper CN, Hoff GR, De Robertis A. 2010. Assessing habitat utilization and rockfish (*Sebastes* sp.) biomass in an isolated rocky ridge using acoustics and stereo image analysis. *Can. J. Fish. Aquat. Sci.* 67: 1658-1670.

Rose CS, Jorgensen EM. 2005. Spatial and temporal distributions of bottom trawling off Alaska: consideration of overlapping effort when evaluating the effects of fishing on habitat. In Barnes PW, Thomas JP (editors). Benthic habitats and the effects of fishing. American Fisheries Society Symposium 41, Bethesda, Maryland.

Rose CS, Gauvin JR, Hammond CF. 2010. Effective herding of flatfish by cables with minimal seafloor contact. Fishery Bulletin, U.S. 108: 136-144.

Ross RE, Howell KL. 2013. Use of predictive habitat modelling to assess the distribution and extent of the current protection of 'listed' deep-sea habitats. Diversity and Distributions 19: 433-445.

Schumacher JD, Reed RK. 1992. Characteristics of currents over the continental slope of the eastern Bering Sea. Journal of Geophysical Research 97(C6), 9423-9433.

Schumacher JD, Stabenho PJ. 1994. Ubiquitous eddies of the eastern Bering Sea and their coincidence with concentrations of larval pollock. Fisheries Oceanography 3: 182-190.

Shuntov VP. 1993. Biological and physical determinants of marine bird distribution in the Bering Sea. In: The status, ecology, and conservation of marine birds of the North Pacific, Editors Vermeer K, Briggs KT, Morgan KH, Siegel-Causey D.

Smith KR, McConnaughey RA. 1999. Surficial sediments of the eastern Bering Sea continental shelf: EBSED database documentation. U.S. Department Commerce, NOAA Tech. Memo. NMFS-AFSC-104, 41 p.

Springer AM, McRoy CP, Flint MV. 1996. The Bering Sea Green Belt: shelf-edge processes and ecosystem production. Fisheries Oceanography, 5: 205–223. doi: 10.1111/j.1365-2419.1996.tb00118.x

- 1076 Stabeno PJ, Schumacher JD, Ohtani K. 1999. The physical oceanography of the Bering Sea. In:
1077 Loughlin, T.R., Ohtani, K. (Eds.), Dynamics of the Bering Sea: A Summary of Physical,
1078 Chemical, and Biological Characteristics, and a Synopsis of Research on the Bering Sea, North
1079 Pacific Marine Science Organization (PICES), University of Alaska Sea Grant, AK-SG-99-03,
1080 Fairbanks, Alaska, USA, pp. 1–28.
1081
- 1082 Stabeno PJ, Kachel N, Mordy C, Righi D, Salo S. 2008. An examination of the physical
1083 variability around the Pribilof Islands in 2004. Deep-Sea Res. II 55: 1701-1716.
1084
- 1085 Sterling JT, Ream RR. 2004. At-sea behavior of juvenile male northern fur seals (*Callorhinus*
1086 *ursinus*). Canadian Journal of Zoology, 82: 1621-1637.
1087
- 1088 Stone RP, Masuda MM, Malecha PW. 2005. Effects of bottom trawling on soft-sediment
1089 epibenthic communities in the Gulf of Alaska. In American Fisheries Society Symposium (Vol.
1090 41, p. 461). American Fisheries Society.
1091
- 1092 Stone RP. 2006. Coral habitat in the Aleutian Islands of Alaska: depth distribution, fine-scale
1093 species associations, and fisheries interactions. Coral Reefs 25: 229-238.
1094
- 1095 Stone RP, Alcorn D. In press. The ecology of deep-sea coral and sponge habitats of the central
1096 Aleutian Islands of Alaska.
1097
- 1098 Stone RP, Lehnert H, Reiswig H. 2011. A guide to the deep-water sponges of the Aleutian Island
1099 Archipelago. U.S. Department of Commerce, NOAA Professional Paper NMFS 12, 187 p.
1100
- 1101 Stone R, Guinotte J, Cohen A, Cairns SD. In preparation. Calcium carbonate mineralogy of
1102 Alaskan corals. NOAA Technical Memorandum.
1103
- 1104 Venables WN, Ripley BD. 2002. Modern Applied Statistics With S. Springer New York, 2002.
1105 495 p.
1106

- 1107 Vetter EW, Dayton PK. 1999. Organic enrichment by macrophyte detritus, and abundance
1108 patterns of megafaunal populations in submarine canyons. Marine Ecology Progress Series 186,
1109 137–148.
1110
- 1111 Waller RG, Stone R, Johnstone J, Mondragon J. In preparation. Sexual reproduction and
1112 seasonality of the Alaskan red tree coral *Primnoa pacifica*.
1113
- 1114 Wood SN. 2006. Generalized additive models: an introduction with R (Vol. 66). Chapman &
1115 Hall.
1116
- 1117 Woodby D, Carlile D, Hulbert L. 2009. Predictive modeling of coral distribution in the Central
1118 Aleutian Islands, USA. Marine Ecology Progress Series 397: 227-240.
1119

Table 1. Data groupings for multivariate analyses of habitat data. Case A: all years when both surveys occurred (2002, 2004, 2008, 2010 and 2012) using data from both surveys; Case B: data from the same 5 years, slope survey only; Case C: 2012 slope survey data only (when additional types of oceanographic measurements were collected).

	Case A	Case B	Case C
Variable	all years, shelf and slope	all years, slope	2012
depth	X	X	X
slope	X	X	X
grain size	X	X	X
ocean color	X	X	X
sediment sorting	X	X	X
current	X	X	X
temperature	X	X	X
salinity			X
oxygen			X
turbidity			X
pH			X

1127 Table 2. Top 10 fish and crab species by survey (longline, shelf trawl, slope trawl) during 2002-
 1128 2012.
 1129

Common name	longline	shelf trawl	slope trawl
Alaska skate		X	
Aleutian skate	X		X
arrowtooth flounder	X	X	X
Kamchatka flounder			X
Greenland turbot	X		X
Pacific halibut	X	X	
flathead sole		X	X
yellowfin sole		X	
northern rock sole		X	
Alaska plaice		X	
sablefish	X		
giant grenadier	X		X
Pacific grenadier			X
Pacific cod	X	X	
walleye pollock	X	X	X
shortspine thornyhead	X		X
shortraker rockfish	X		
rougheye or blackspotted rockfish	X		
Pacific ocean perch			X
snow crab		X	

1130 Table 3. Data groupings for coral, sponge and sea whip/sea pen data. For each taxa, the number
 1131 and weight caught and their higher-level groupings (e.g. hard corals) used in the statistical
 1132 analyses are shown. In addition, scores for susceptibility to physical damage by taxa are shown.
 1133

High-level grouping	Mid-level grouping	Taxon	Number caught	Weight (kg) caught	Susceptibility score
Corals	Paragorgiidae	<i>Paragorgia</i> sp.	7	1.68	3
Corals	Paragorgiidae	<i>Paragorgia arborea</i>	30	55.41	3
Corals	Primnoidae	<i>Amphilaphis</i> sp. (<i>Plumarella</i> spp.)	23	3.78	2
Corals	Primnoidae	<i>Primnoa willeyi</i>	3	0.70	3
Corals	Primnoidae	<i>Plumarella</i> sp.	7	0.36	2
Corals	Primnoidae	<i>Primnoa</i> sp.	4	2.10	3
Corals	Primnoidae	<i>Plumarella</i> sp. 1 (Bayer)	1	0.02	2
Corals	Antipatharia	Antipatharia	5	0.24	3
Corals	Antipatharia	<i>Lillipathes</i> sp. B	2	0.20	3
Corals	Antipatharia	<i>Crysopathes speciosa</i>	1	0.20	3
Corals	Plexauridae	<i>Swiftia</i> sp.	13	0.74	1
Corals	Plexauridae	<i>Swiftia pacifica</i>	1	0.00	1
Corals	Plexauridae	<i>Swiftia</i> cf. <i>beringi</i>	4	0.07	1
Corals	Plexauridae	Muriceides cf. cylindrical (<i>Calciorgia beringi</i>)	1	0.02	1
Corals	Isididae	<i>Isidella</i> sp.	26	11.73	3
Corals	Isididae	<i>Keratoisis</i> sp.	3	1.41	3
Corals	Isididae	Isididae (unidentified)	1	4.57	3
Sea whips	Pennatulacea	Pennatulacea	41	31.59	3
Sea whips	Pennatulacea	<i>Virgularia</i> sp. (<i>Halipteris</i> sp. A)	16	32.46	3
Sea whips	Pennatulacea	Virgulariidae (<i>Halipteris</i> sp. A)	63	119.95	3
Sea whips	Pennatulacea	<i>Stylatula</i> sp.	11	0.22	2
Sea whips	Pennatulacea	<i>Halipteris</i> sp.	11	0.65	3
Sea whips	Pennatulacea	<i>Halipteris willemoesi</i>	20	1.34	3
Sea whips	Pennatulacea	<i>Halipteris californica</i>	1	0.00	3
Sea whips	Pennatulacea	<i>Ombellula</i> sp.	1	0.00	1
Sea whips	Pennatulacea	<i>Anthoptilum murrayi</i> (<i>Halipteris</i> sp. B)	5	13.45	2
Sponges	Hexactinellid	<i>Aphrocallistes vastus</i>	119	120.26	3
Sponges	Porifera	Sponge unidentified	405	789.83	2
Sponges	Porifera	Vase sponge	11	32.52	3
Sponges	Demosponge	<i>Suberites</i> sp.	6	24.84	1
Sponges	Demosponge	<i>Suberites ficus</i>	6	0.02	1

Sponges	Demosponge	<i>Mycale</i> sp.	2	0.75	2
Sponges	Demosponge	<i>Mycale loveni</i>	18	6.59	3
Sponges	Demosponge	<i>Halichondria</i> sp.	1	0.32	2
Sponges	Demosponge	<i>Halichondria panicea</i>	2	11.33	2
Sponges	Demosponge	<i>Stelodoryx oxeata</i> (scapula)	4	0.60	2
Sponges	Demosponge	cf. <i>Myxilla lacunosa</i>	1	0.10	2
Sponges	Demosponge	<i>Isodictya quatsinoensis</i>	2	0.03	2
Sponges	Demosponge	<i>Axinella blanca</i>	4	0.33	3
Sponges	Demosponge	<i>Polymastia</i> sp.	3	0.86	1
Sponges	Demosponge	<i>Halichondria</i> cf. <i>sitiens</i>	1	0.01	2
Sponges	Demosponge	<i>Stelletta</i> sp.	1	0.15	2
Sponges	Hexactinellid	<i>Rhabdocalyptus</i> sp.	9	8.44	2
Sponges	Hexactinellid	<i>Staurocalyptus</i> sp.	2	23.67	2

1134

1135

1136 Table 4. Results of quadratic discriminant function analysis, where the model predicts group
 1137 membership for the shelf and slope survey data from 2002, 2004, 2008, 2010, and 2012.
 1138 Discrimination was performed using physical habitat variables.
 1139

Observed classification	Total stations	Predicted classification				Canyon
		EBS Inner Shelf	EBS Middle Shelf	EBS Outer Shelf	Inter- canyon Slope	
EBS Inner Shelf	444	0.97	0.03			
EBS Middle Shelf	871	0.06	0.90	0.04		
EBS Outer Shelf	616		0.12	0.80	0.04	0.04
Inter-canyon Slope	439			0.04	0.78	0.18
Canyon	326			0.11	0.10	0.79

1140

1141 Table 5. Results of quadratic discriminant function analysis, where the model predicts group
 1142 membership for the eastern Bering Sea slope data as either a canyon or not a canyon from 2002,
 1143 2004, 2008, 2010, and 2012. Discrimination was performed using physical habitat variables.

1144

Observed classification	Total stations	Predicted classification	
		Inter- canyon Slope	Canyon
Inter-canyon Slope	326	0.89	0.11
Canyon	439	0.19	0.81

1145

1146 Results of quadratic discriminant function analysis, where the model predicts group membership
 1147 for Pribilof canyon and its surrounding slope areas from 2002, 2004, 2008, 2010, and 2012.
 1148 Discrimination was performed using the physical habitat variables.

1149

Predicted classification			
Total stations		NOT	PC
NOT	300	1.00	0.00
PC	60	0.02	0.98

1150

1151 Results of quadratic discriminant function analysis, where the model predicts group membership
 1152 for Zhemchug canyon and its surrounding slope areas from 2002, 2004, 2008, 2010, and 2012.
 1153 Discrimination was performed using the physical habitat variables.

1154

Predicted classification			
Total stations		NOT	ZC
NOT	236	0.98	0.02
ZC	76	0.01	0.99

1155

1156

Table 6. Results of quadratic discriminant function analysis, where the model predicts group membership for Pribilof canyon and its surrounding slope areas from 2002, 2004, 2008, 2010, and 2012. Discrimination was performed using the log-transformed CPUE of invertebrate species groups.

Predicted classification			
	Total stations	NOT	PC
NOT	300	0.95	0.05
PC	60	0.78	0.22

Results of quadratic discriminant function analysis, where the model predicts group membership for Zhemchug canyon and its surrounding slope areas from 2002, 2004, 2008, 2010, and 2012. Discrimination was performed using the log-transformed CPUE of invertebrate species groups.

Predicted classification			
	Total stations	NOT	ZC
NOT	236	0.89	0.11
ZC	76	0.84	0.16

Results of quadratic discriminant function analysis, where the model predicts group membership for Pribilof canyon and its surrounding slope areas from 2002, 2004, 2008, 2010, and 2012. Discrimination was performed using the CPUE of the top 20 fish species.

Predicted classification			
	Total stations	NOT	PC
NOT	300	0.97	0.03
PC	60	0.70	0.30

Results of quadratic discriminant function analysis, where the model predicts group membership for Zhemchug canyon and its surrounding slope areas from 2002, 2004, 2008, 2010, and 2012. Discrimination was performed using the CPUE of the top 20 fish species.

Predicted classification			
	Total stations	NOT	ZC
NOT	236	0.92	0.08
ZC	76	0.49	0.51

1177 Table 7. Generalized additive model results for coral, sponge and sea whip data (n = 1,361) for
 1178 Bering slope and outer shelf habitats and statistically significant variables, unbiased risk
 1179 estimator (UBRE) score and deviance explained.
 1180

Taxon	Significant variables (p < 0.05)	UBRE score	Deviance explained
Coral	Long*Lat, Seafloor gradient, Current speed	-0.638	0.393
Sea whip	Long*Lat, Depth, Seafloor gradient, Bottom temperature, Current speed, Ocean color	-0.472	0.362
Sponge	Long*Lat, Depth, Seafloor gradient, Bottom temperature, Current speed, Ocean color, Grain size, Sediment sorting	0.0550	0.312

1181

Table 8. Generalized additive model results for classification of coral, sponge and sea whip data for Bering slope and outer shelf habitats. The abbreviations are Cohen's Kappa (Fielding and Bell 1997) and area under the curve (AUC).

			Predicted				
Taxon	Threshold	Observed	Absent	Present	Percent correct	Kappa (sd)	AUC (sd)
Coral	0.30	Absent	1251	44	93%	0.44 (0.05)	0.92 (0.01)
		Present	46	40			
Sea whip	0.28	Absent	1145	67	90%	0.51 (0.04)	0.90 (0.01)
		Present	65	84			
Sponge	0.53	Absent	548	158	77%	0.54 (0.02)	0.85 (0.01)
		Present	157	498			

1188 Table 9. The predicted presence of each taxon expressed as the percentage of total area within a
 1189 habitat, as a percentage of the total area of the slope and as a percentage of the total area within
 1190 the slope and outer shelf habitats combined.

Taxa	Area	Absent (km ²)	Present (km ²)	Within area (%)	Within slope (%)	Within slope and outer shelf (%)
Coral	Bering Canyon	3294	17	1%	1%	0%
	Bering-Pribilof	5330	38	1%	1%	1%
	Pribilof Canyon	1888	982	34%	33%	20%
	Pribilof-Zhemchug	4493	850	16%	29%	17%
	Zhemchug Canyon	2976	28	1%	1%	1%
	Zhemchug-Pervenets	3222	523	14%	18%	11%
	Pervenets Canyon	1317	153	10%	5%	3%
	Pervenets-Navarin	1188	0	0%	0%	0%
	Navarin Canyon	1530	387	20%	13%	8%
	Outer shelf	133163	1888	1%	na	39%
Sea whip	Bering Canyon	3174	137	4%	5%	0%
	Bering-Pribilof	5003	365	7%	14%	1%
	Pribilof Canyon	2870	0	0%	0%	0%
	Pribilof-Zhemchug	4309	1034	19%	38%	4%
	Zhemchug Canyon	2619	385	13%	14%	1%
	Zhemchug-Pervenets	3354	391	10%	15%	1%
	Pervenets Canyon	1430	40	3%	1%	0%
	Pervenets-Navarin	1026	162	14%	6%	1%
	Navarin Canyon	1744	173	9%	6%	1%
	Outer shelf	108827	26224	19%	na	91%
Sponge	Bering Canyon	471	2840	86%	17%	6%
	Bering-Pribilof	2706	2662	50%	16%	6%
	Pribilof Canyon	210	2660	93%	16%	6%
	Pribilof-Zhemchug	2240	3103	58%	18%	7%
	Zhemchug Canyon	1032	1972	66%	12%	4%
	Zhemchug-Pervenets	2418	1327	35%	8%	3%
	Pervenets Canyon	500	970	66%	6%	2%
	Pervenets-Navarin	984	204	17%	1%	0%
	Navarin Canyon	814	1103	58%	7%	2%
	Outer shelf	105164	29887	22%	na	64%

1191

1192 Table 10. General additive model results for fish and crab data (n = 1,361) for outer shelf and
 1193 slope data and statistically significant variables, generalized cross-validation (GCV) score and
 1194 deviance explained. Alaska plaice and yellowfin sole were dropped from this analysis because
 1195 they are only found in the inner and middle shelf.

Common name	Significant variables (p < 0.05)	GCV score	Deviance explained
Alaska skate	Long*Lat, Depth, Bottom temperature, Ocean color	4.235	0.682
Aleutian skate	Long*Lat, Depth, Current speed, Ocean color, Grain size, Sediment sorting	5.322	0.578
Arrowtooth flounder	Long*Lat, Depth, Bottom temperature, Current speed, Ocean color, Grain size	1.619	0.826
Flathead sole	Long*Lat, Depth, Bottom temperature, Current speed, Ocean color, Grain size, Sediment sorting	2.475	0.796
Giant grenadier	Long*Lat, Depth, Bottom temperature, Current speed, Ocean color, Grain size, Sediment sorting	1.038	0.905
Greenland turbot	Long*Lat, Depth, Seafloor gradient, Bottom temperature, Ocean color, Grain size	5.965	0.652
Kamchatka flounder	Long*Lat, Depth, Bottom temperature, Current speed, Grain size	2.865	0.536
Northern rock sole	Long*Lat, Depth, Bottom temperature, Ocean color, Grain size, Sediment sorting	1.844	0.681
Pacific cod	Long*Lat, Depth, Bottom temperature, Current speed, Ocean color, Grain size, Sediment sorting	1.308	0.838
Pacific grenadier	Long*Lat, Depth, Seafloor gradient, Current speed, Ocean color, Grain size, Sediment sorting	1.519	0.792
Pacific halibut	Long*Lat, Depth, Grain size, Sediment	3.508	0.313

	sorting		
Pacific ocean perch	Long*Lat, Depth, Current speed, Ocean color, Grain size	4.486	0.742
Pollock	Long*Lat, Depth, Bottom temperature, Current speed, Grain size, Sediment sorting	7.902	0.704
Rougheye/black spotted rockfish	Long*Lat, Depth, Seafloor gradient, Bottom temperature, Ocean color, Grain size, Sediment sorting	2.877	0.446
Sablefish	Long*Lat, Depth, Seafloor gradient, Current speed, Ocean color, Sediment sorting	0.983	0.719
Shortraker rockfish	Long*Lat, Depth, Seafloor gradient, Current speed, Ocean color, Sediment sorting	1.971	0.484
Shortspine thornyhead	Long*Lat, Depth, Seafloor gradient, Bottom temperature, Current speed, Ocean color, Grain size, Sediment sorting	4.694	0.833
Snow crab	Long*Lat, Depth, Seafloor gradient, Bottom temperature, Grain size, Sediment sorting	4.907	0.752

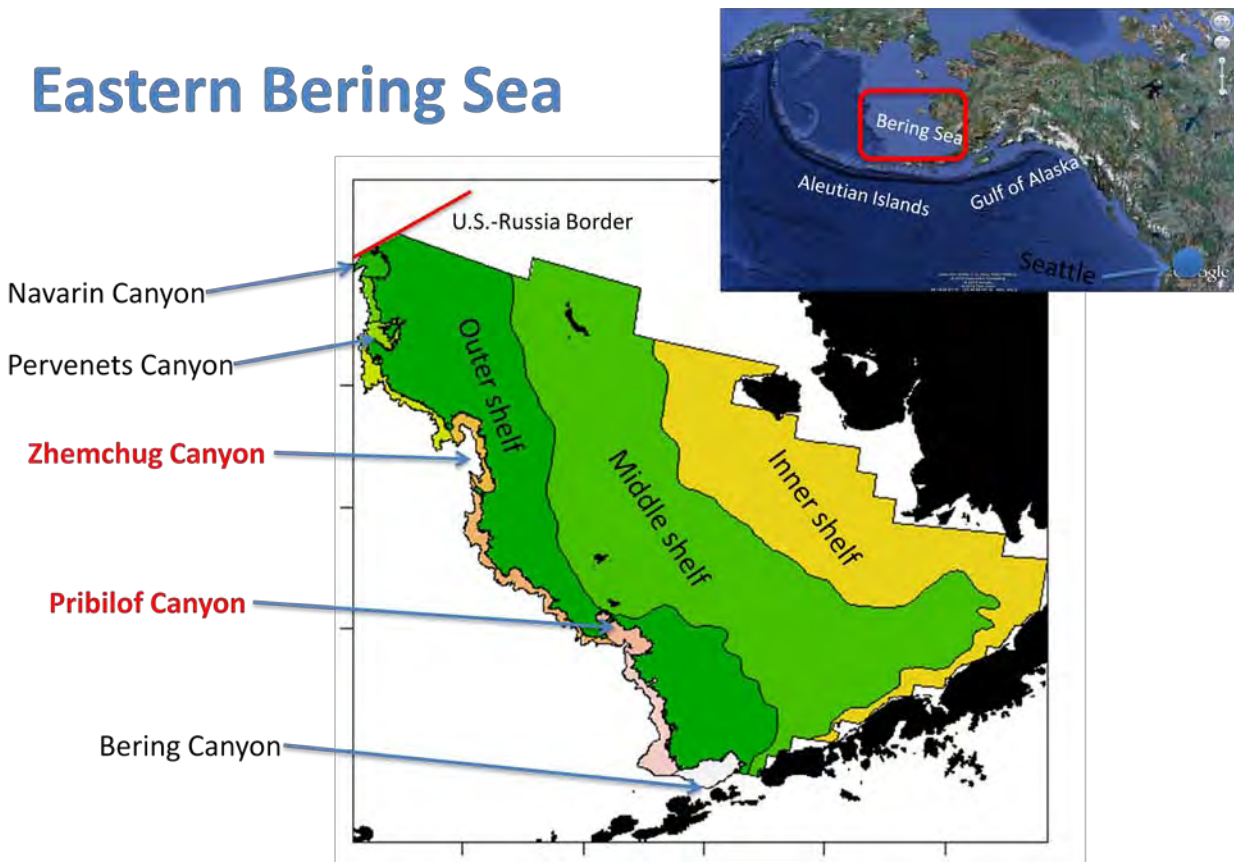
1196

1197

1198 Figure 1. Some of the largest submarine canyons in the world incise the eastern Bering Sea shelf
1199 break including Bering, Pribilof, Zhemchug, Pervenets and Navarin canyons.

1200

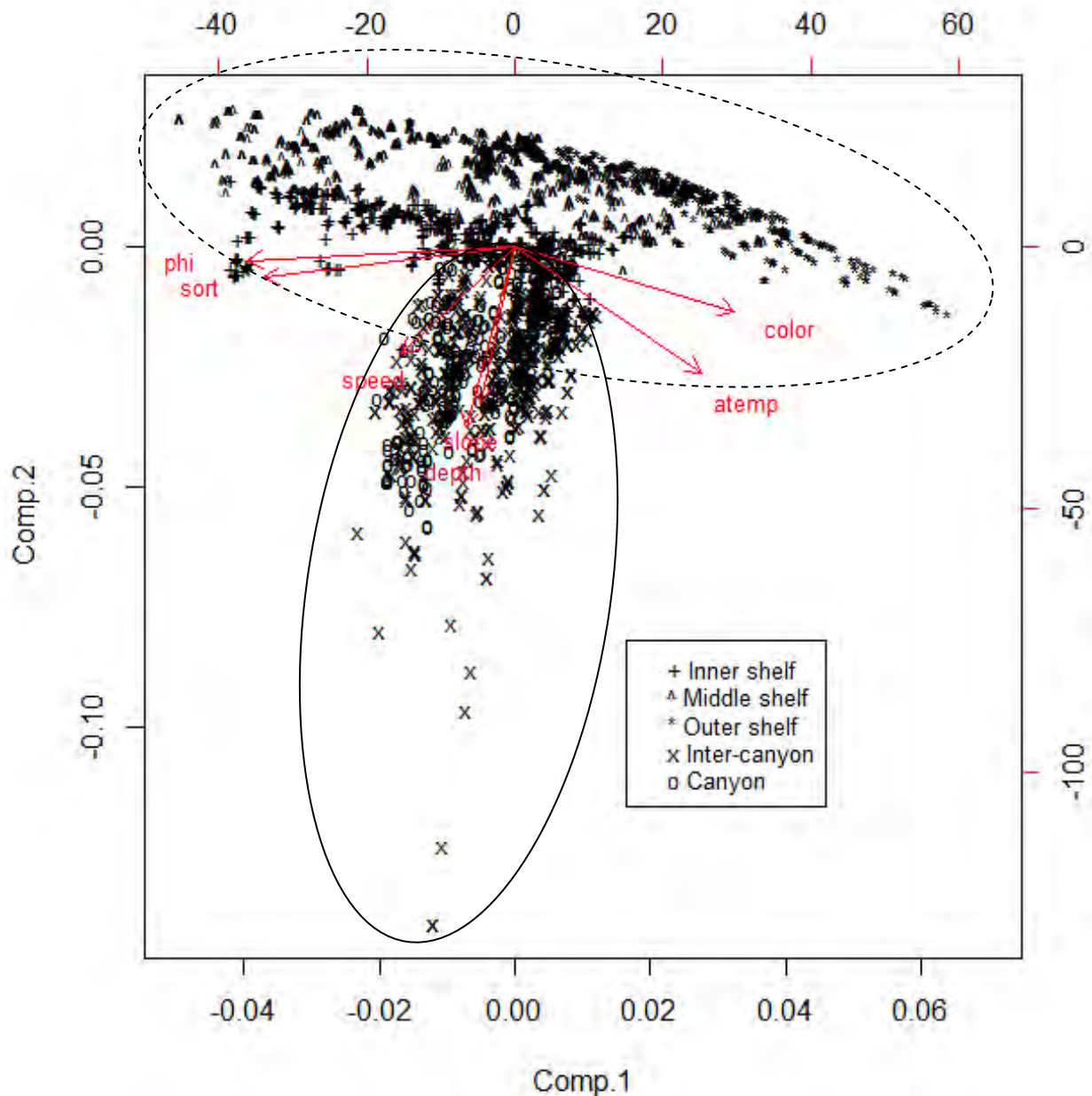
Eastern Bering Sea



1201

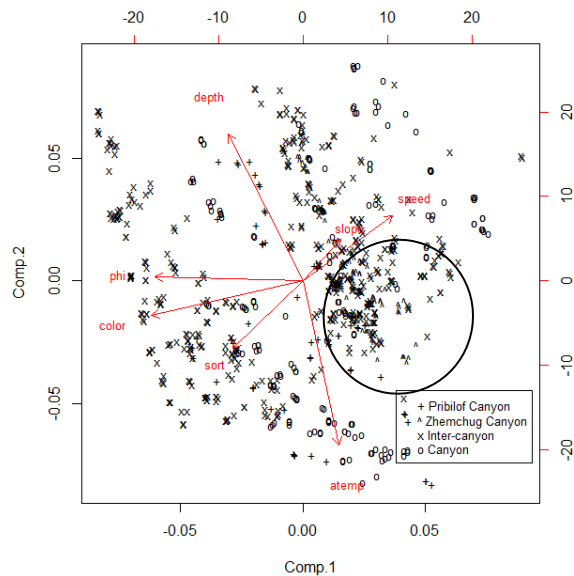
1202

Figure 2. Biplot of principal components 1 and 2 of all years and areas of eastern Bering Sea survey data showing individual bottom trawl hauls labeled by their area classification (5 canyons, 5 intercanyon areas and outer shelf stations). The physical habitat variables are from data collected with the bottom trawl survey tow (depth), data interpolated from survey data (long term average temperature) and inferred from other sources (slope, color, speed, and phi). Survey tow locations from 2002, 2004, 2008, 2010 and 2012 are used (Case A). The continuous line oval indicates slope stations and the dashed line oval indicates shelf stations; for the latter, inner shelf stations are leftward, outer shelf stations are rightward and middle shelf stations are in between.

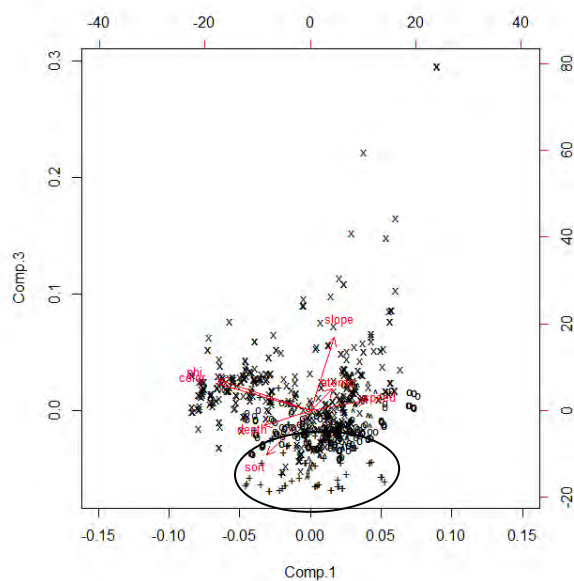


1212

Figure 3. Biplots of principal components 1 to 3 of all years and areas of slope data showing individual bottom trawl hauls labeled by their area classification. The physical habitat variables are from data collected with the bottom trawl survey tow (depth), data interpolated from survey data (long-term average temperature) and inferred from other sources (slope, color, speed, and phi). Survey tow locations from 2002, 2004, 2008, 2010 and 2012 are used (Case B). The oval in the upper biplot (Figure 3a) indicates stations in Zhemchug Canyon. The oval in the lower biplot (Figure 3b) indicates stations in Pribilof Canyon.

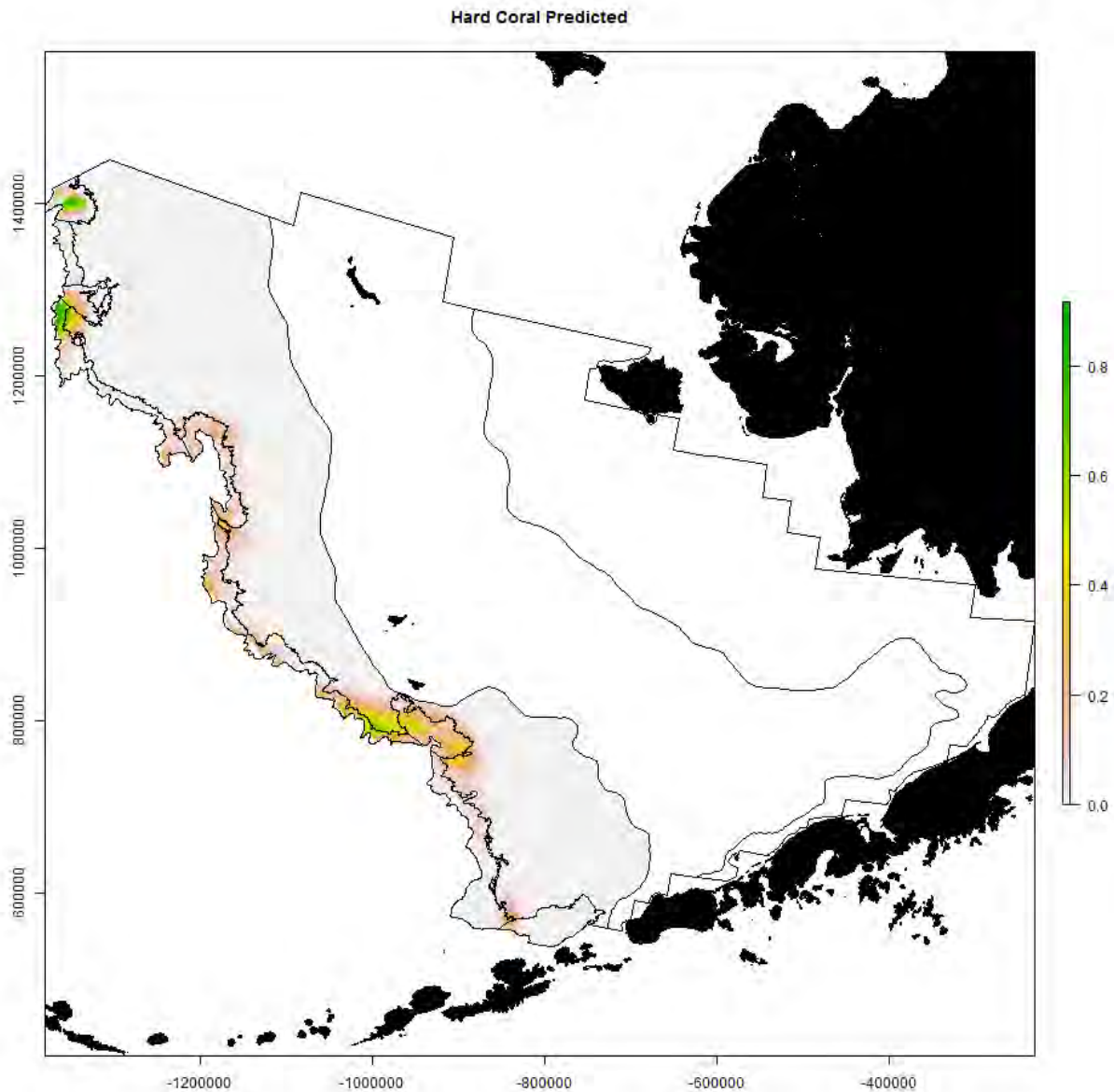


1220



1221

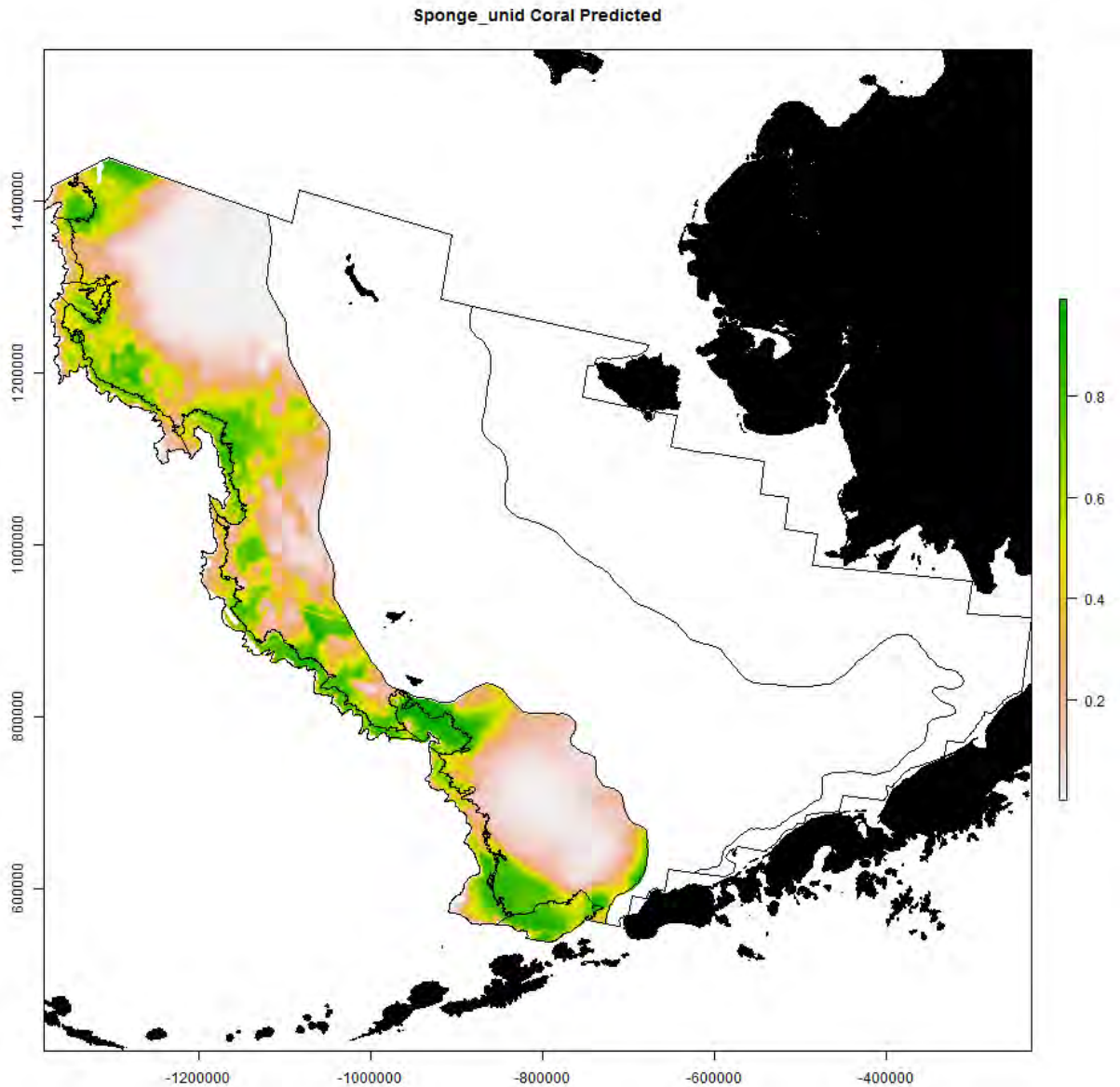
1222 Figure 4a. Probability that coral is present by 1 x 1 km grid cell for the eastern Bering Sea shelf
1223 and outer slope based on generalized additive modeling. The x-axis label is easting and the y-
1224 axis label is northing and the unit is meters (Alaska Albers Equal Area Conic projection with
1225 center latitude = 50° N and center longitude = 154° W).



1226

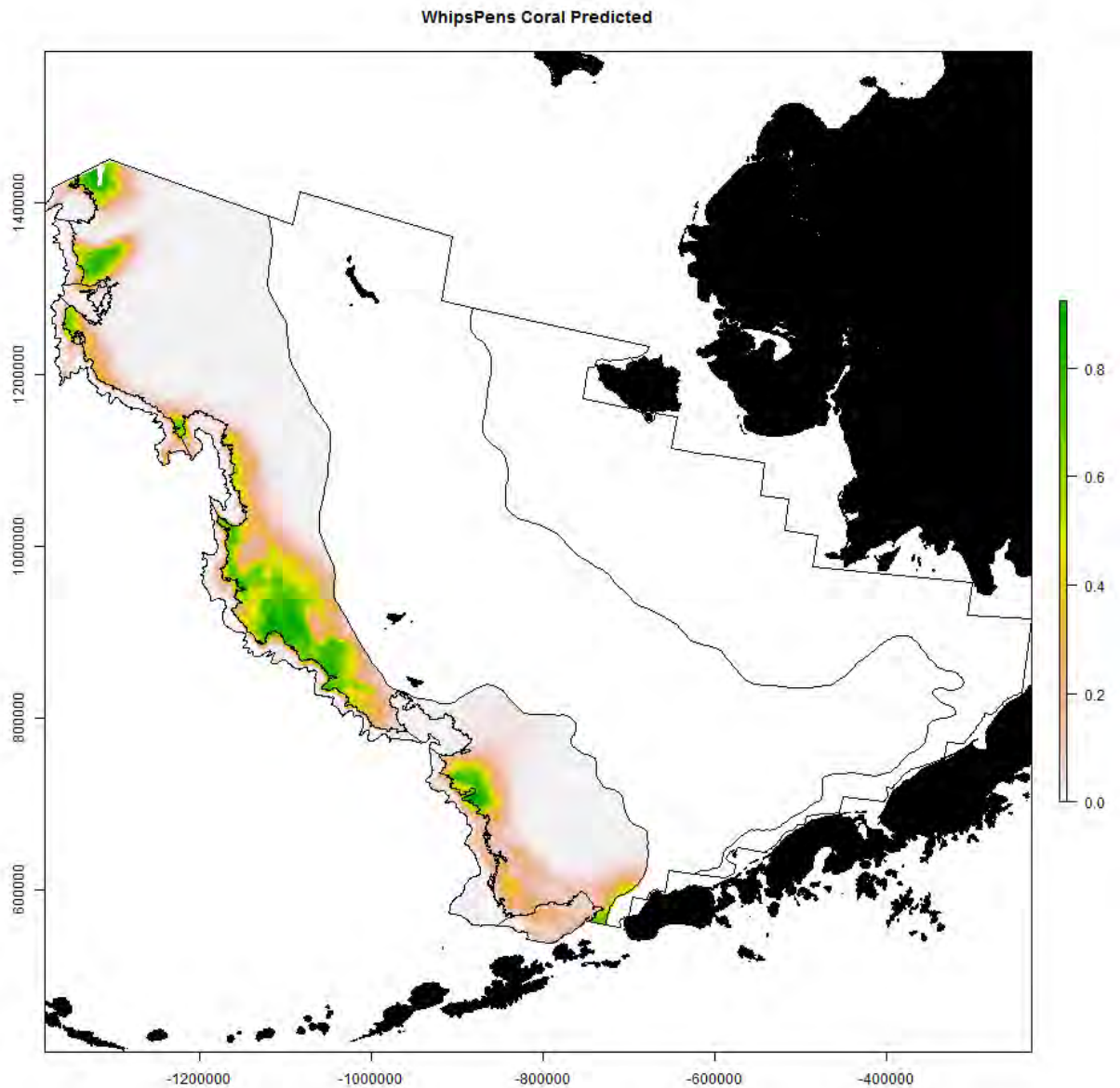
1227

1228 Figure 4b. Probability that sponge is present by 1 x 1 km grid cell for the eastern Bering Sea
1229 shelf and outer slope based on generalized additive modeling. The x-axis label is easting and the
1230 y-axis label is northing and the unit is meters (Alaska Albers Equal Area Conic projection with
1231 center latitude = 50° N and center longitude = 154° W).



1232
1233

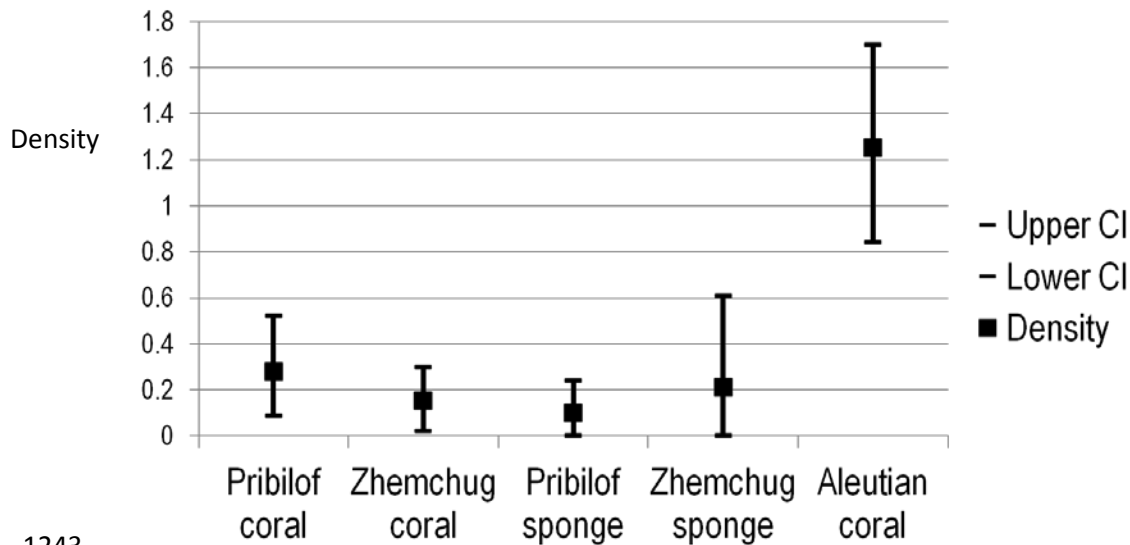
1234 Figure 4c. Probability that sea whip is present by 1 x 1 km grid cell for the eastern Bering Sea
1235 shelf and outer slope based on generalized additive modeling. The x-axis label is easting and the
1236 y-axis label is northing and the unit is meters (Alaska Albers Equal Area Conic projection with
1237 center latitude = 50° N and center longitude = 154° W).



1238

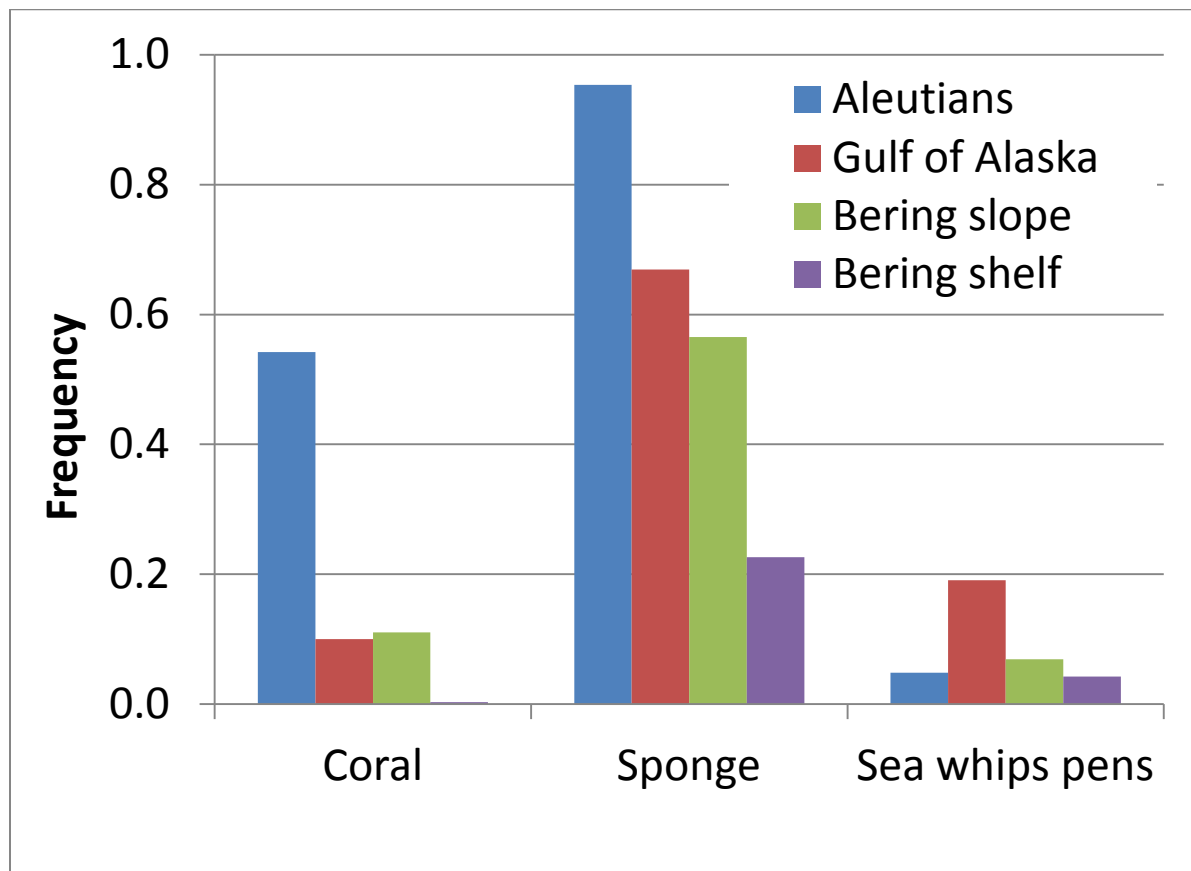
1239

1240 Figure 5a. Numerical densities (colonies m^{-2}) of coral and sponge from visual surveys. Pribilof
 1241 and Zhemchug canyons data courtesy of John Hocevar, Greenpeace (do not cite without
 1242 permission of J. Hocevar). Aleutian data from Stone (2006).



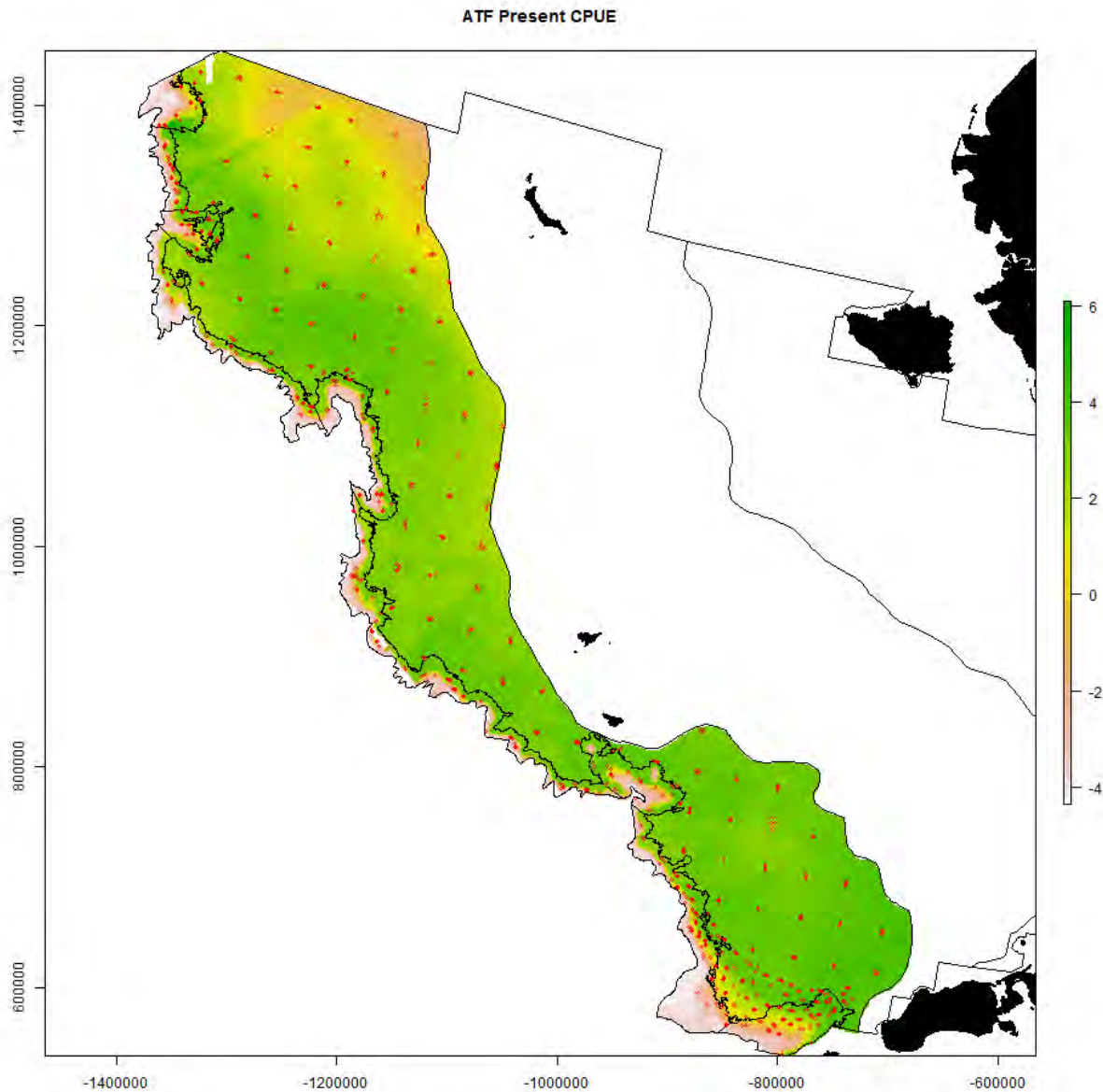
1243

1244 Figure 5b. Frequency of occurrence of coral, sponge and sea whip during trawl surveys in
 1245 Alaska.



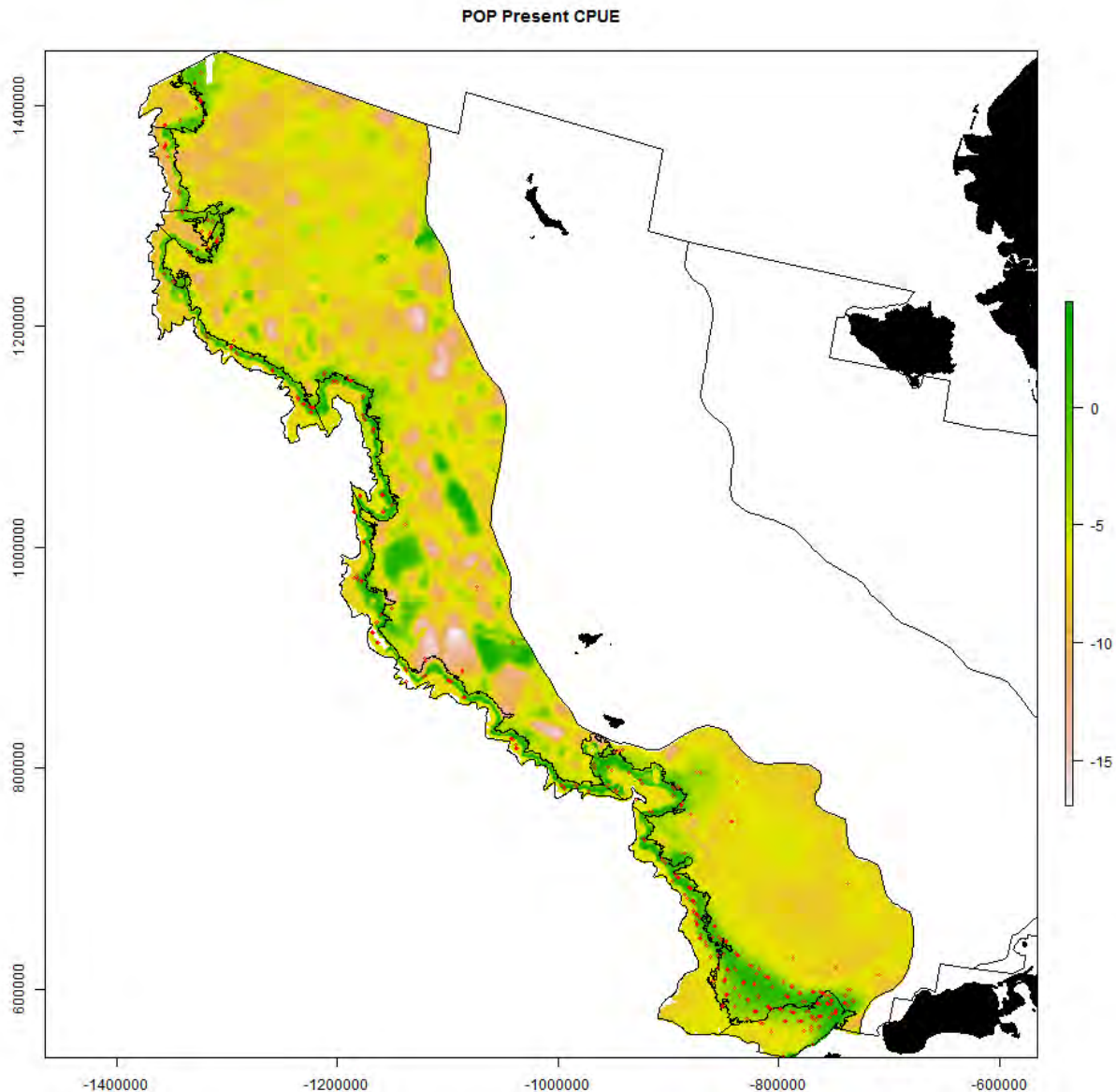
1246

1247 Figure 6a. Predicted LCPUE of arrowtooth flounder, a shelf species, by 1 x 1 km grid cell for the
1248 eastern Bering Sea shelf and outer slope based on generalized additive modeling. Red crosses
1249 indicate survey tow locations from 2002, 2004, 2008, 2010 and 2012 where arrowtooth flounder
1250 was observed. The x-axis label is easting and the y-axis label is northing and the unit is meters
1251 (Alaska Albers Equal Area Conic projection with center latitude = 50° N and center longitude =
1252 154° W).



1253
1254

1255 Figure 6b. Predicted LCPUE of Pacific ocean perch, a shelf break species, by 1 x 1 km grid cell
1256 for the eastern Bering Sea shelf and outer slope based on generalized additive modeling. Red
1257 crosses indicate survey tow locations from 2002, 2004, 2008, 2010 and 2012 where Pacific
1258 ocean perch was observed. The x-axis label is easting and the y-axis label is northing and the unit
1259 is meters (Alaska Albers Equal Area Conic projection with center latitude = 50° N and center
1260 longitude = 154° W).

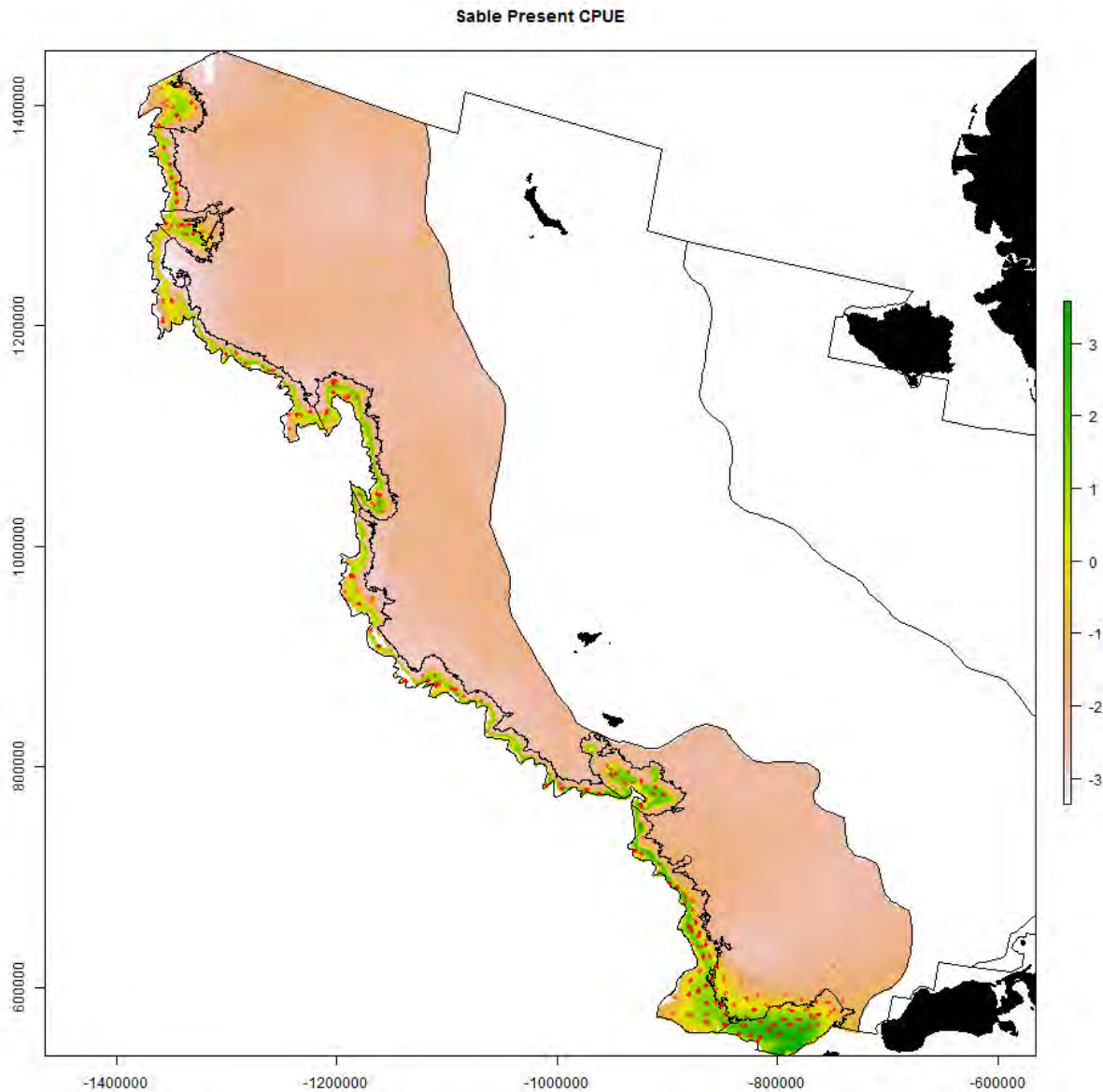


1261

1262

1263

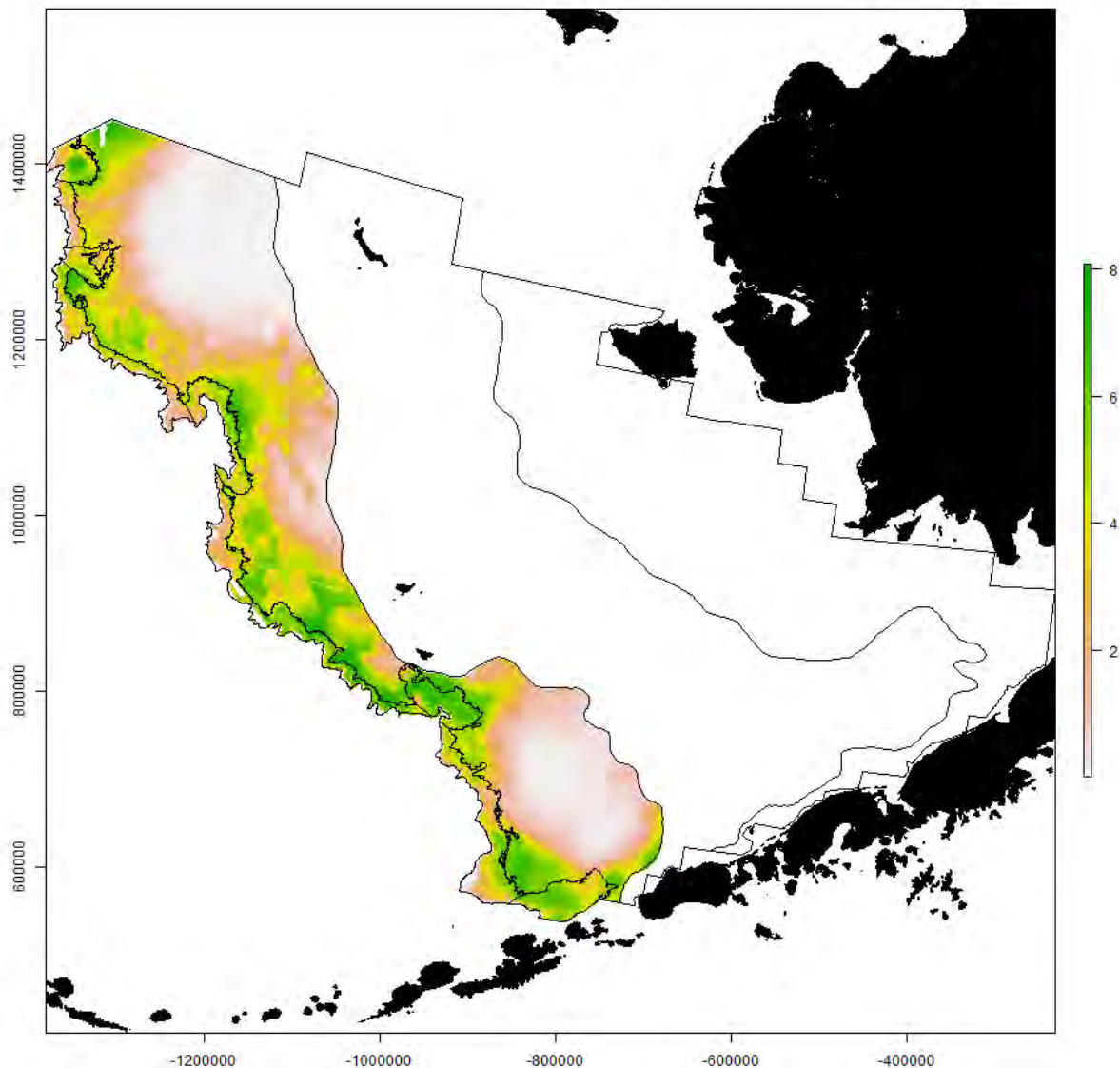
1264 Figure 6c. Predicted LCPUE of sablefish, a slope species, by 1 x 1 km grid cell for the eastern
1265 Bering Sea shelf and outer slope based on generalized additive modeling. Red crosses indicate
1266 survey tow locations from 2002, 2004, 2008, 2010 and 2012 where sablefish was observed. The
1267 x-axis label is easting and the y-axis label is northing and the unit is meters (Alaska Albers Equal
1268 Area Conic projection with center latitude = 50° N and center longitude = 154° W).



1269

1270

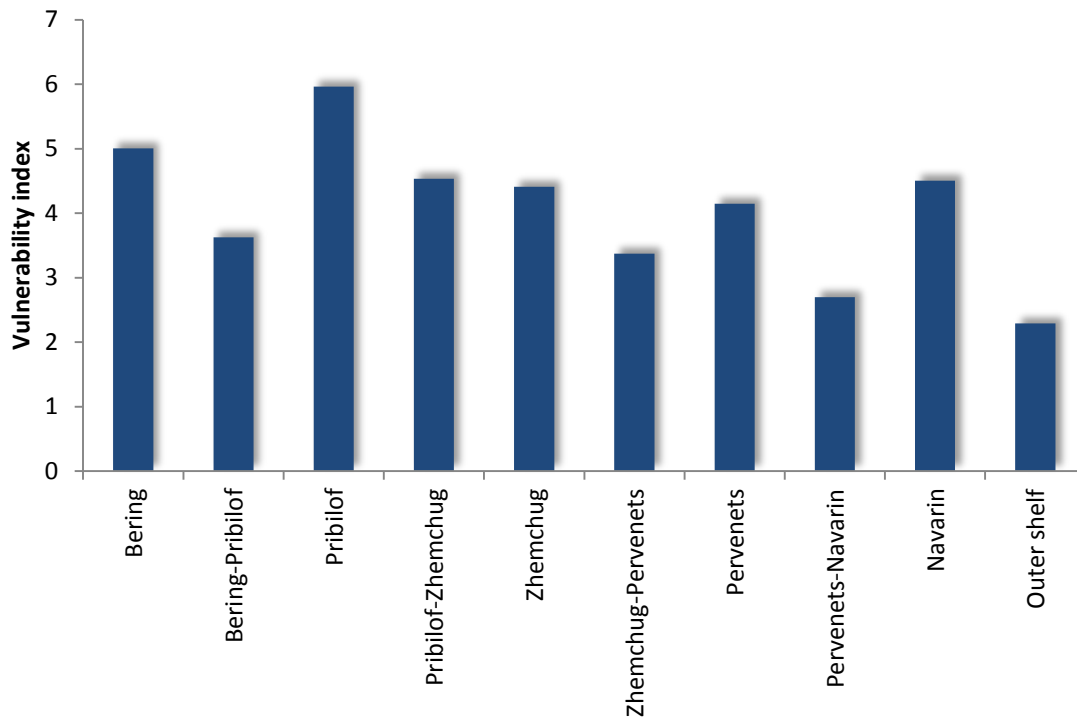
1271 Figure 7. Habitat vulnerability indices by 1 x 1 km grid cell for the eastern Bering Sea shelf and
1272 outer slope based on generalized additive modeling. The x-axis label is easting and the y-axis
1273 label is northing and the unit is meters (Alaska Albers Equal Area Conic projection with center
1274 latitude = 50° N and center longitude = 154° W).



1275

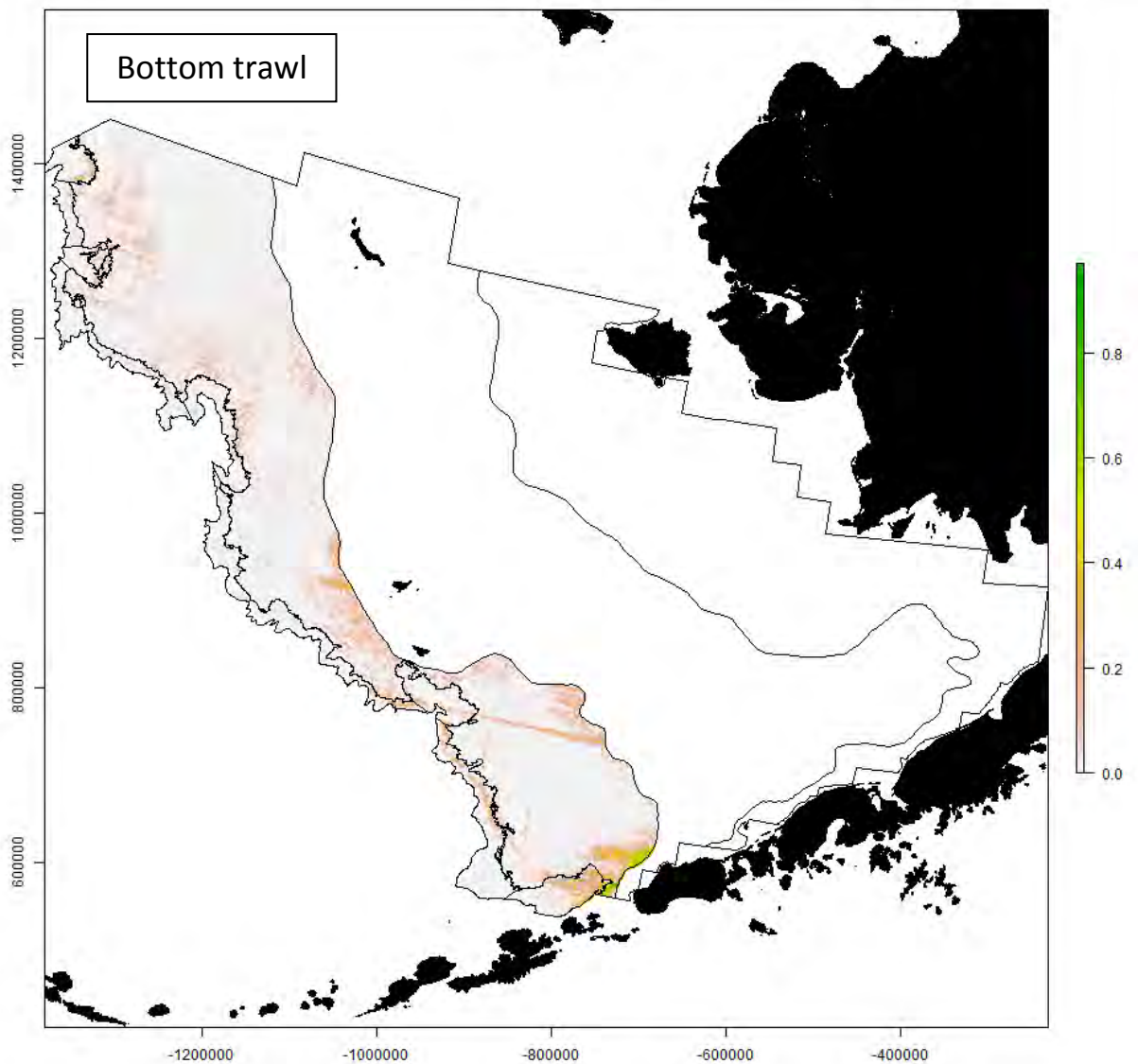
1276

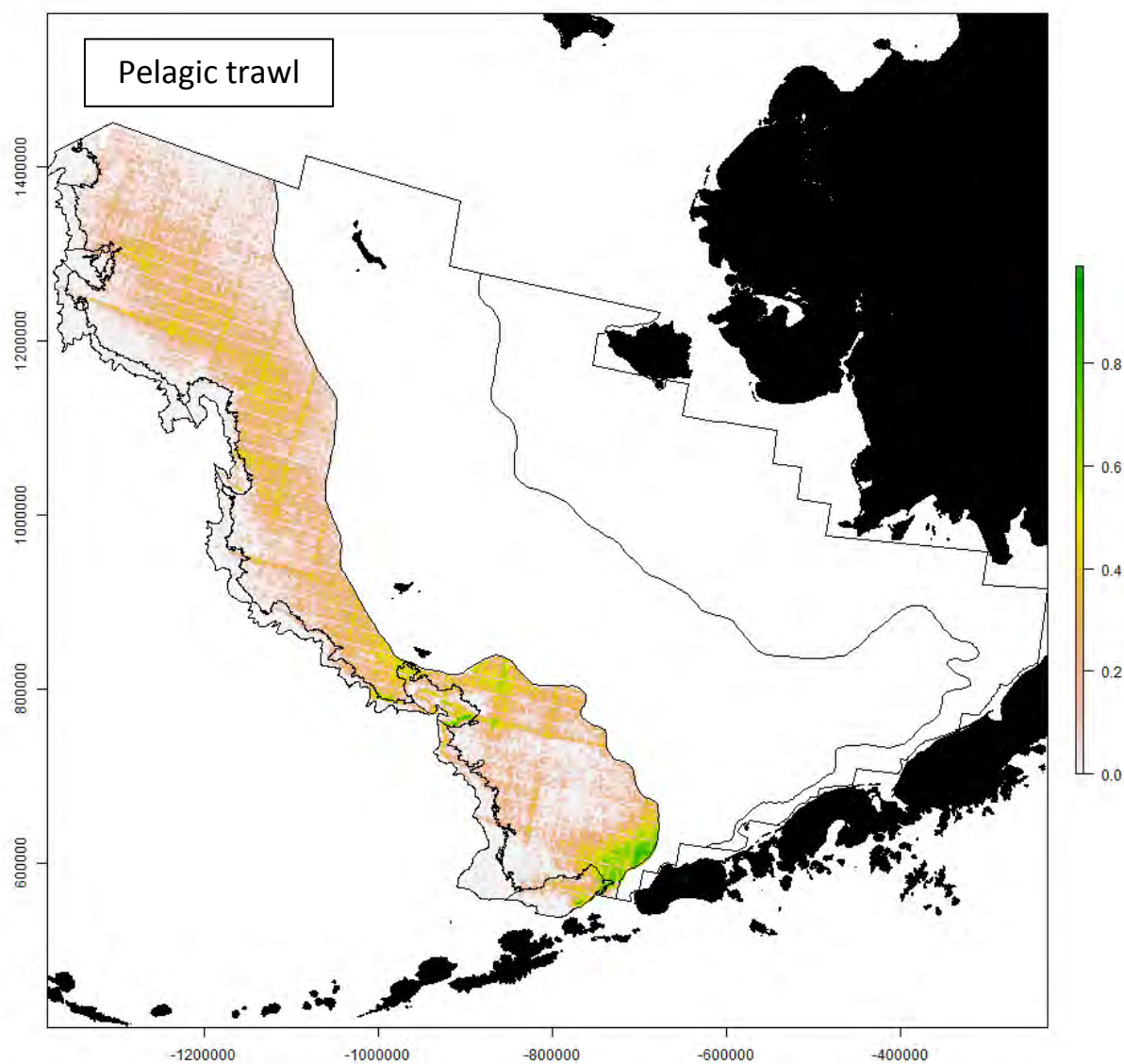
1277 Figure 8. Average vulnerability indices by area for the eastern Bering Sea slope and outer shelf.



1278

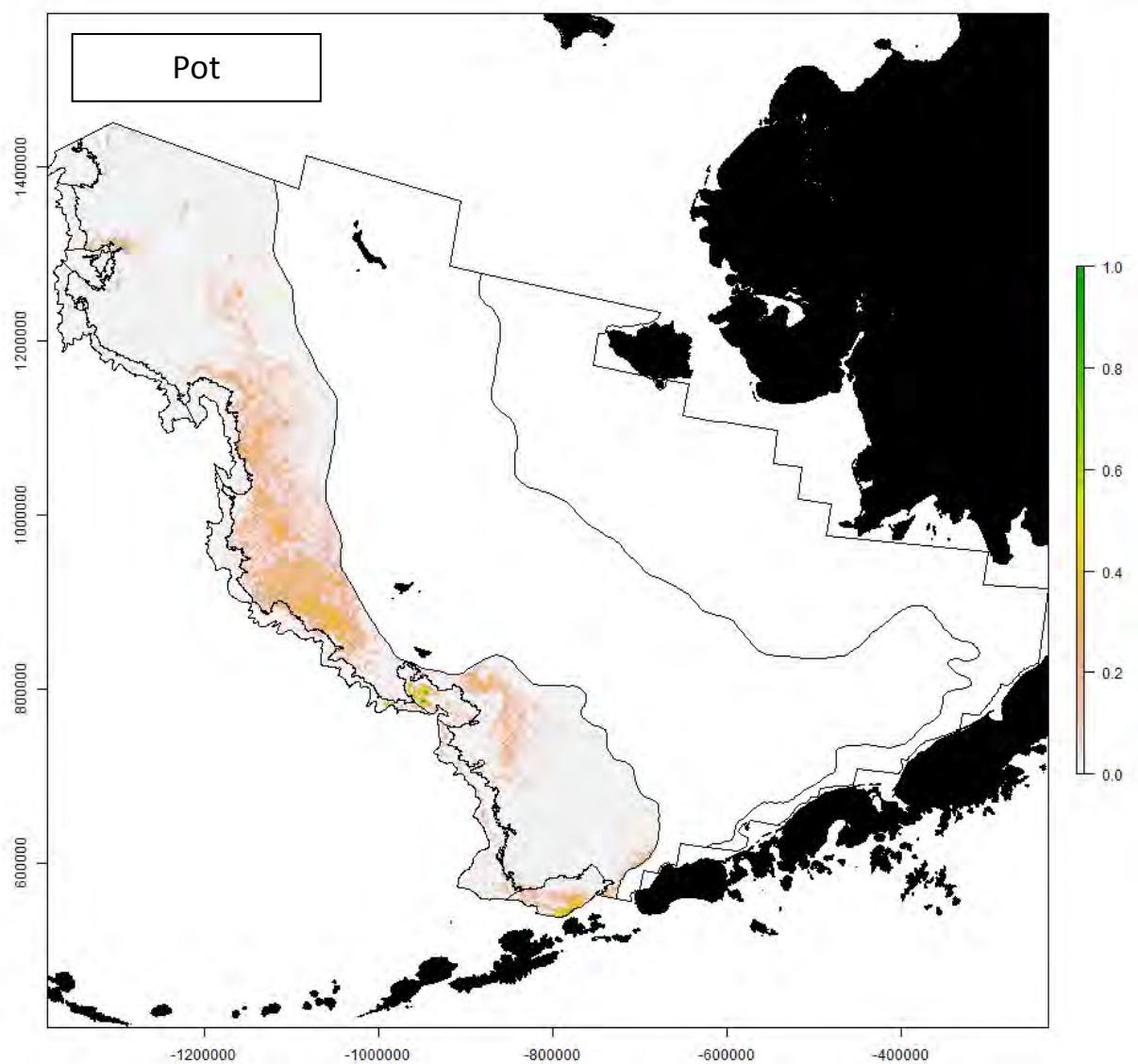
Figure 9. Fishing effort by gear type including bottom trawl, pelagic trawl, pot and longline for the eastern Bering Sea slope and outer shelf. Fishing effort is expressed as the number of sets per 1 x 1 km grid cell during 2002-2011 and then log-transformed in the maps for display. The x-axis label is easting and the y-axis label is northing and the unit is meters (Alaska Albers Equal Area Conic projection with center latitude = 50° N and center longitude = 154° W).





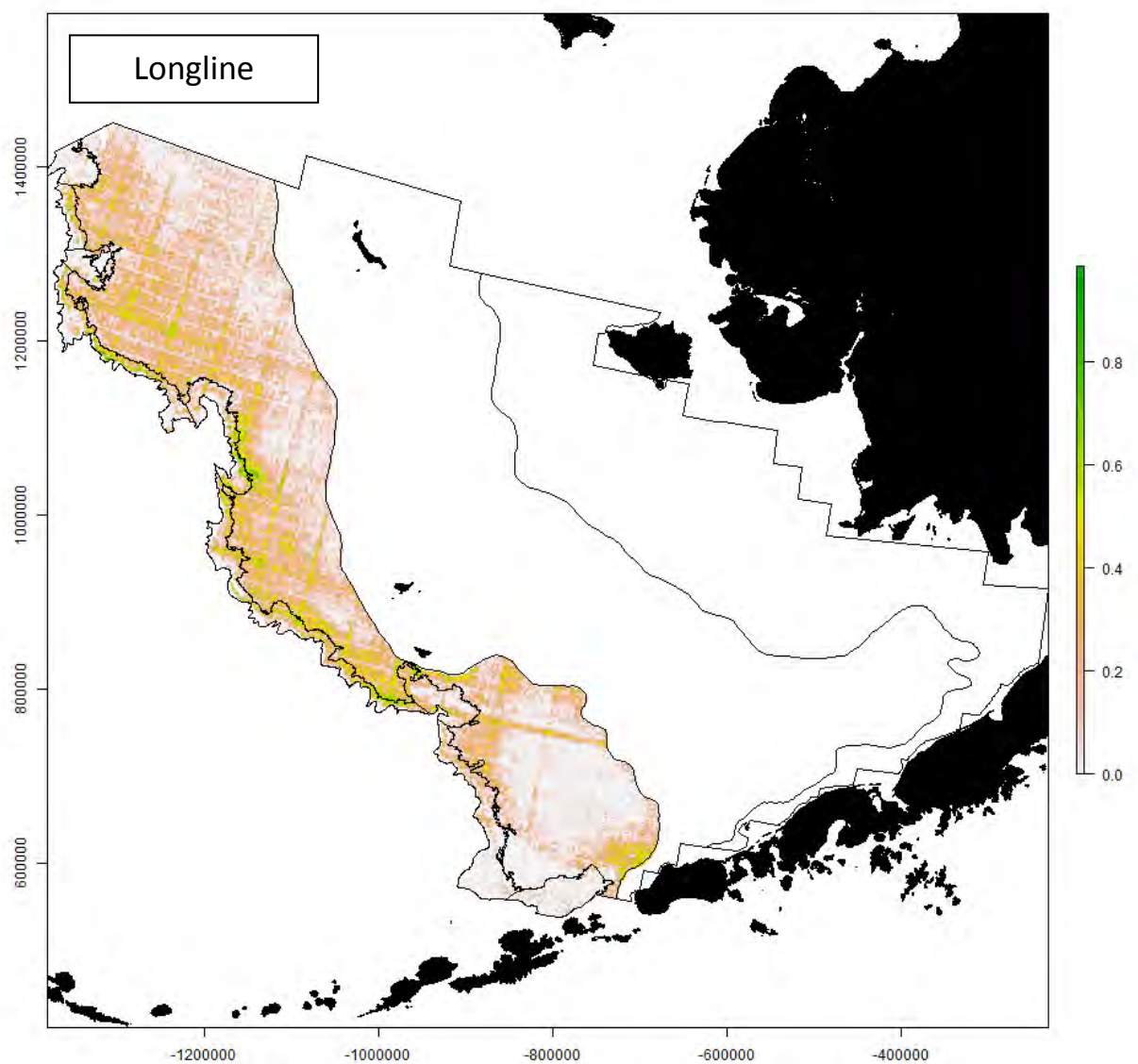
1286

1287



1288

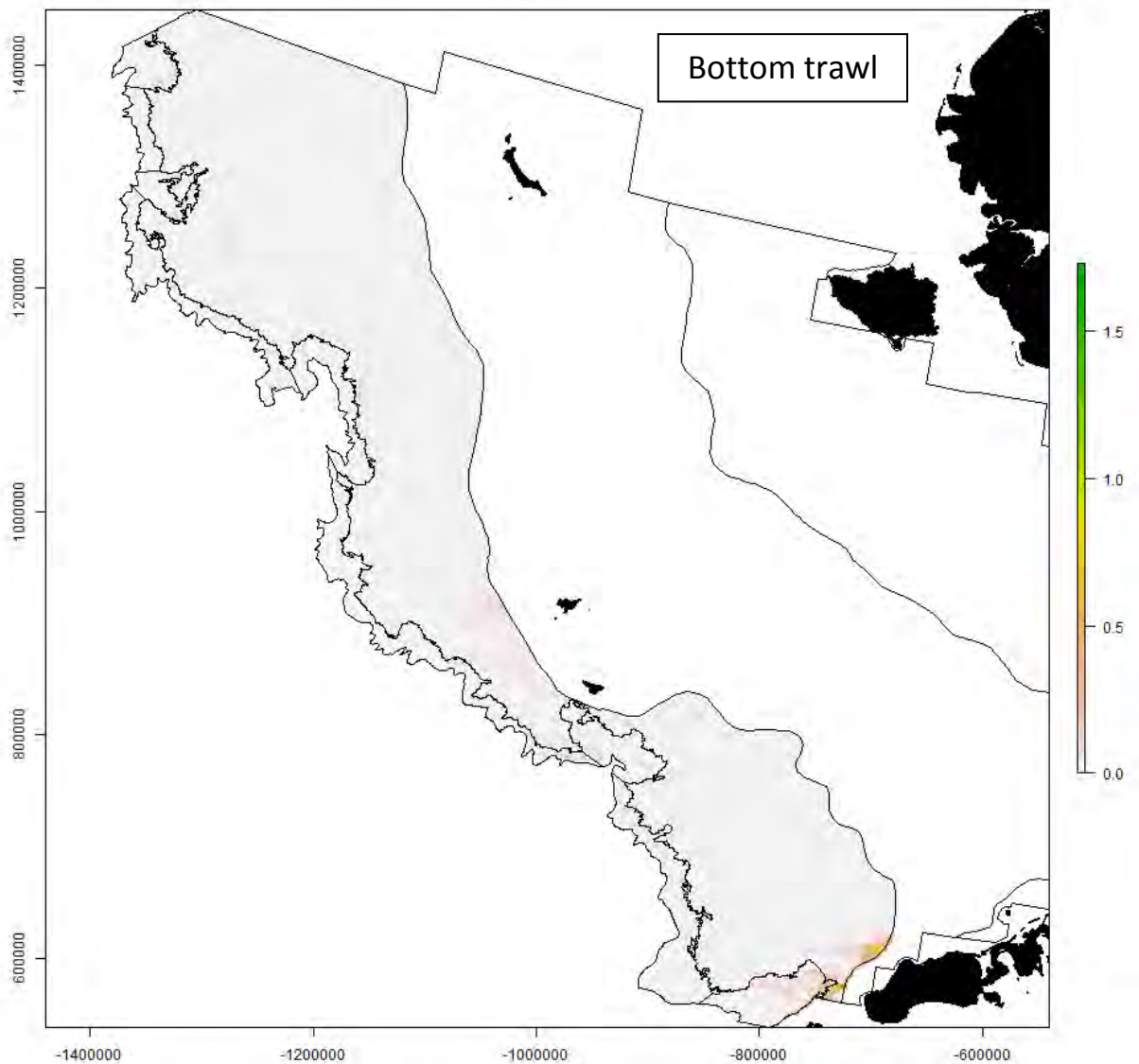
1289

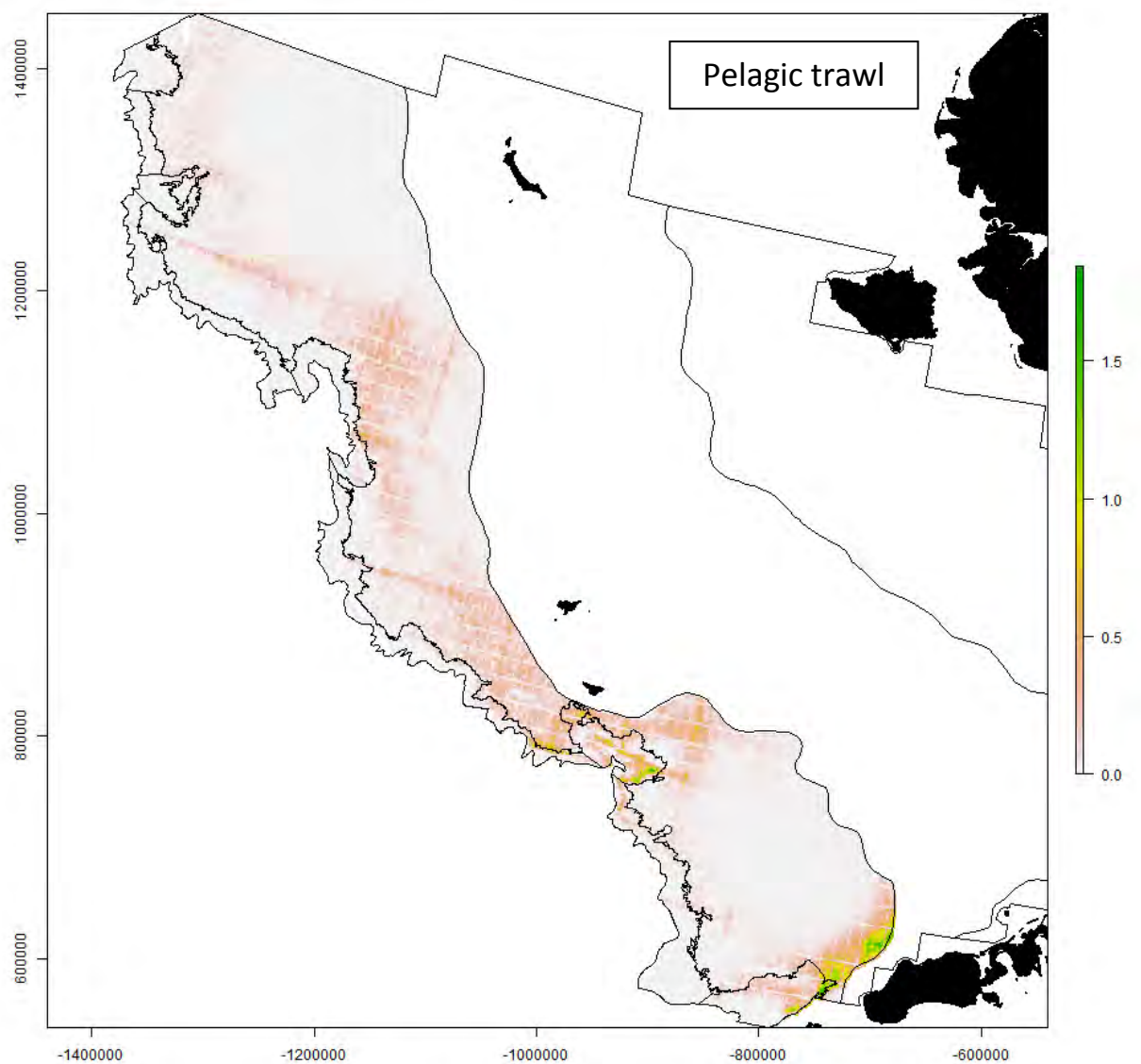


1290

1291

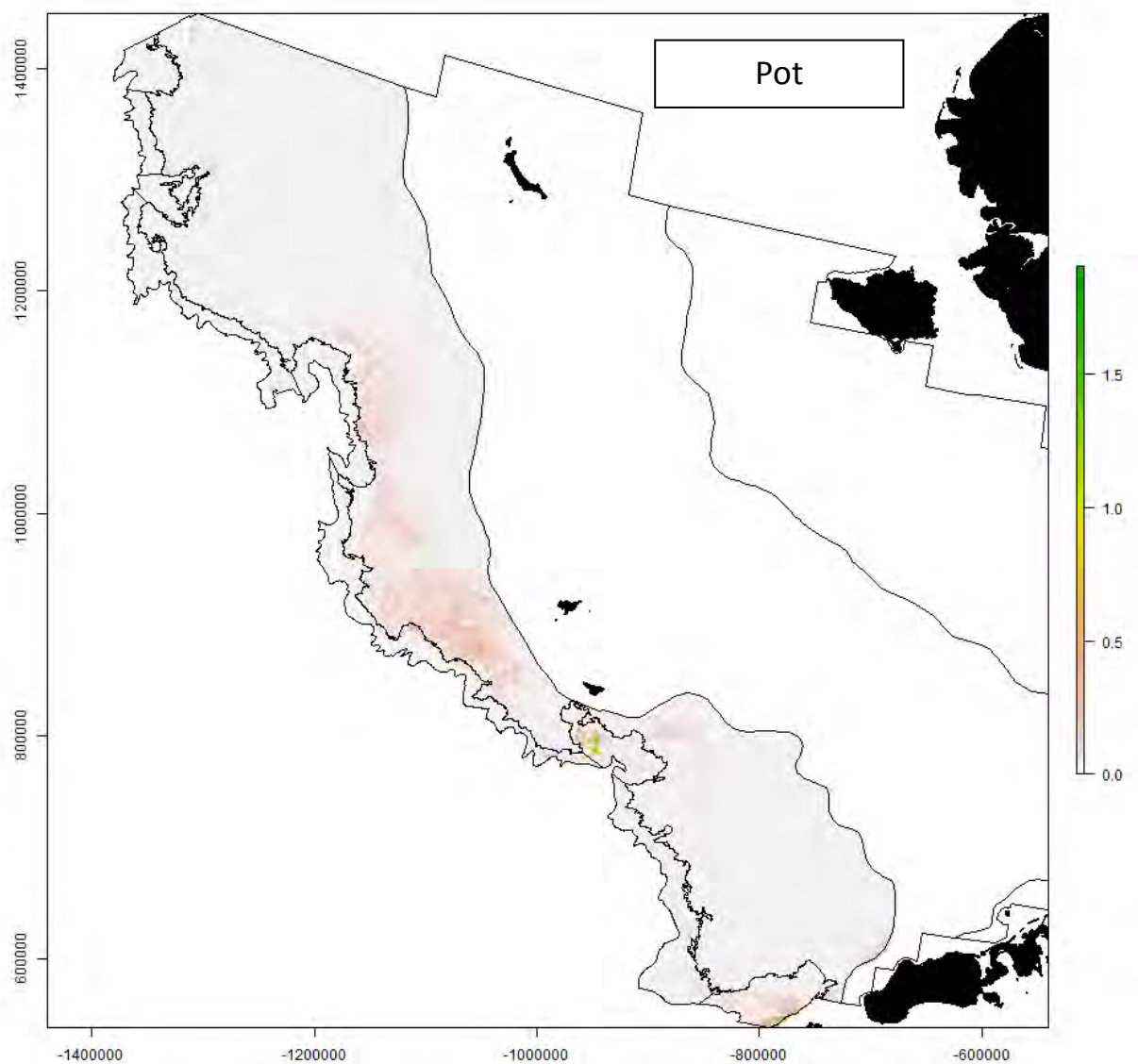
Figure 10. Overlap indices of fishing and vulnerable habitats by 1 x 1 km grid cell and by gear type including bottom trawl, pelagic trawl, pot and longline for the eastern Bering Sea slope and outer shelf. The overlap indices are log-transformed in the maps for display. The x-axis label is easting and the y-axis label is northing and the unit is meters (Alaska Albers Equal Area Conic projection with center latitude = 50° N and center longitude = 154° W).





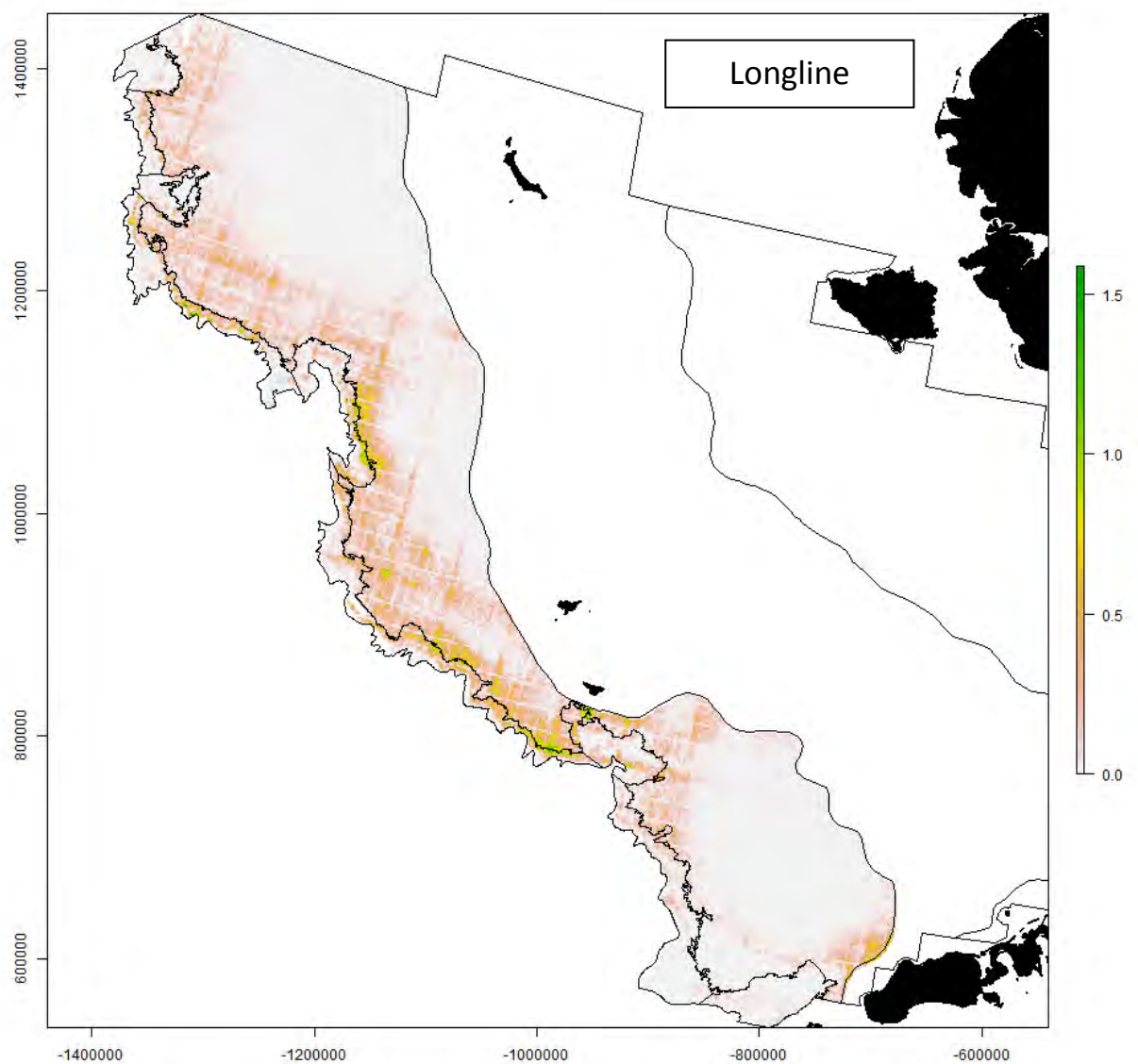
1299

1300



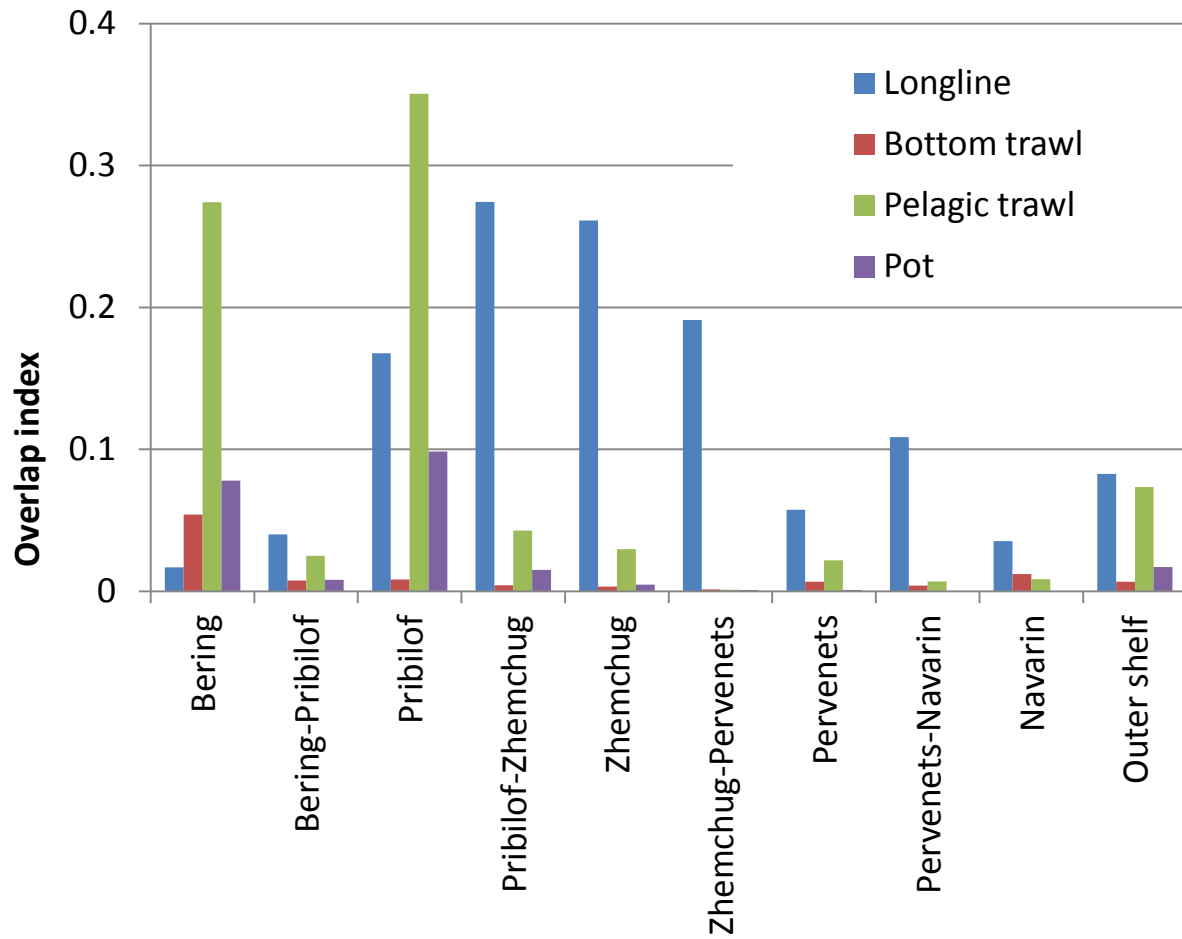
1301

1302



1303
1304

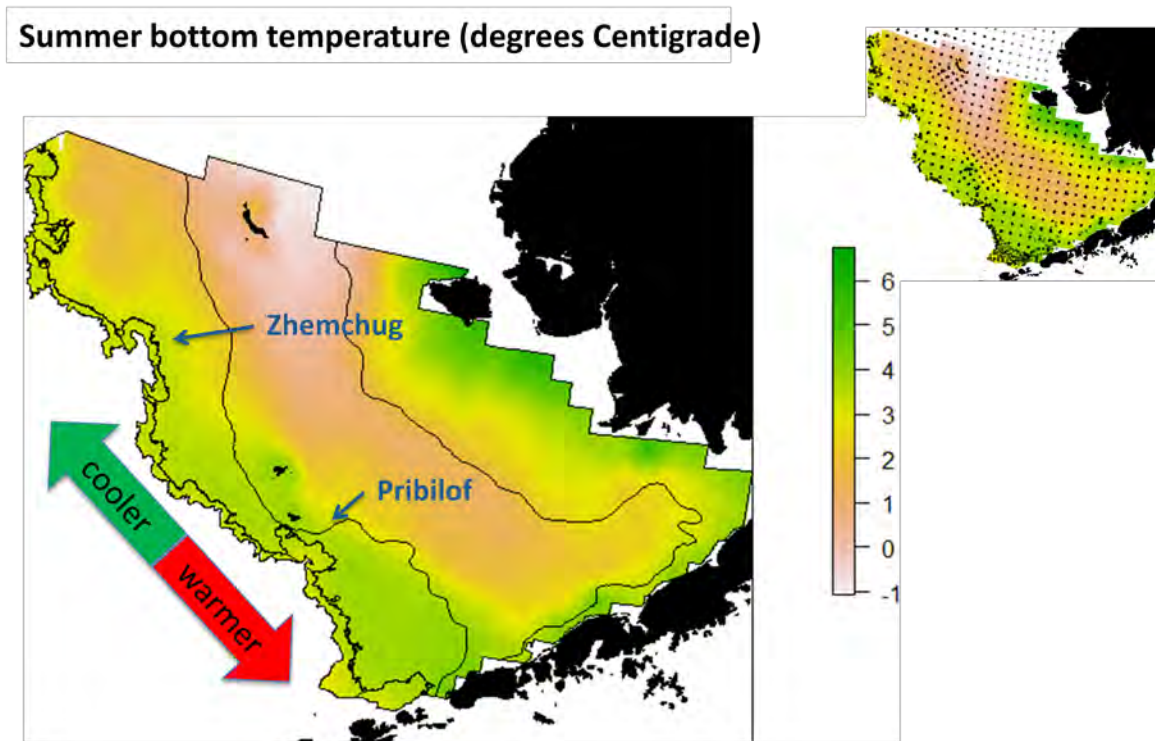
1305 Figure 11. Average overlap indices by area and gear type (bottom trawl, pelagic trawl, pot,
1306 longline) for the eastern Bering Sea slope and outer shelf.



1307

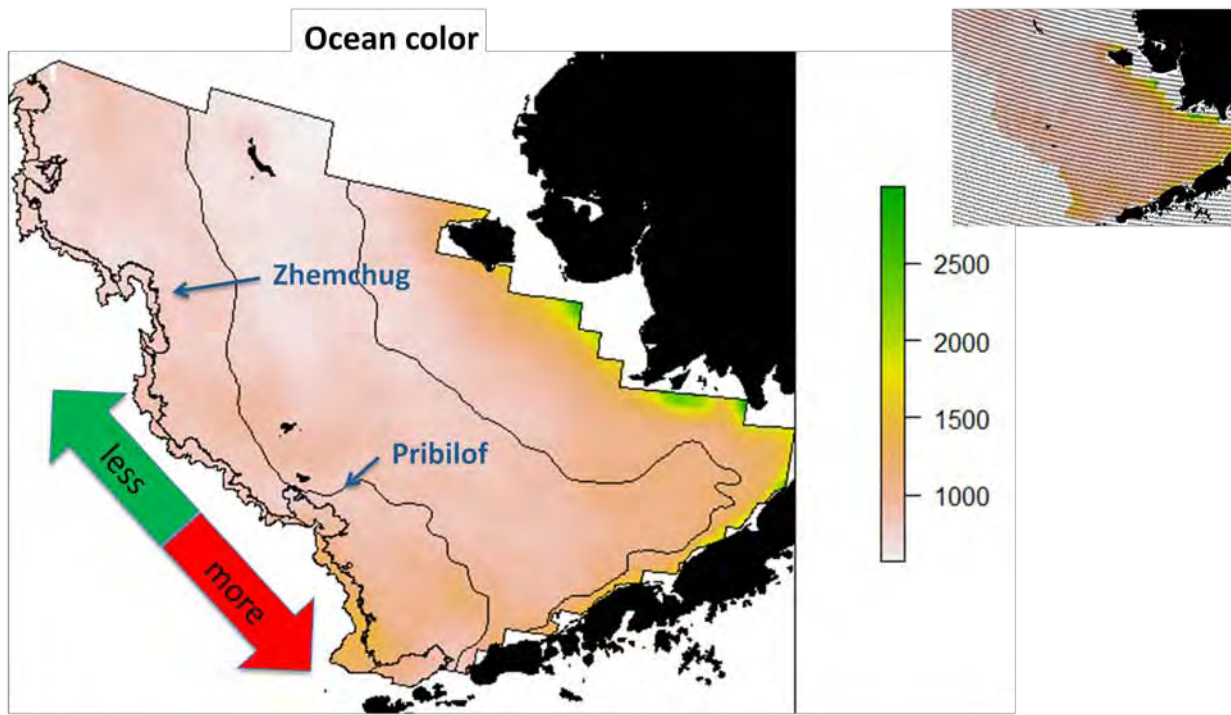
1308

1309 S1. Long-term average of summer bottom temperature in the eastern Bering Sea. The upper right
1310 panel shows sample locations (black dots). Source: NOAA Alaska Fisheries Science Center
1311 bottom trawl surveys, 1996-2012, n = 7,177.



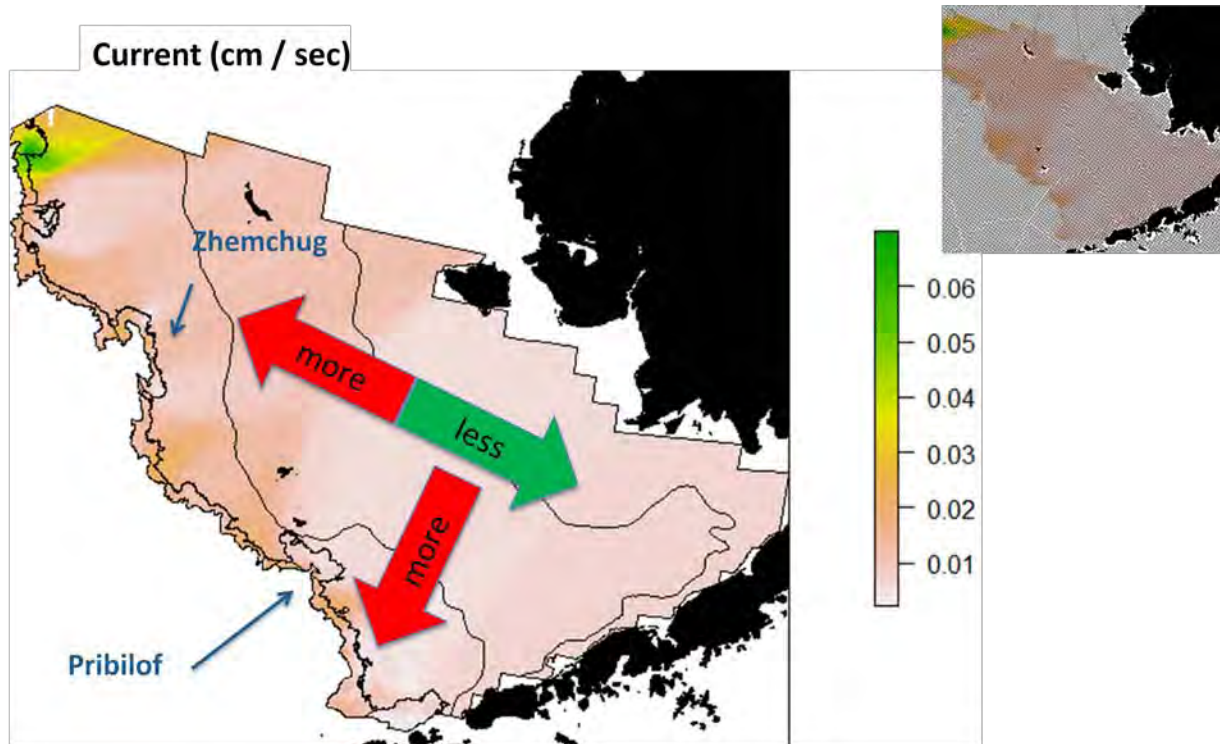
1312

1313 S2. Long-term average of summer ocean color in the eastern Bering Sea. The upper right panel
1314 shows sample locations (black dots). Source: Oregon State University's Ocean Productivity
1315 website (Behrenfeld and Falkowski 1997), n = 58,070, May-September 2003-2011.



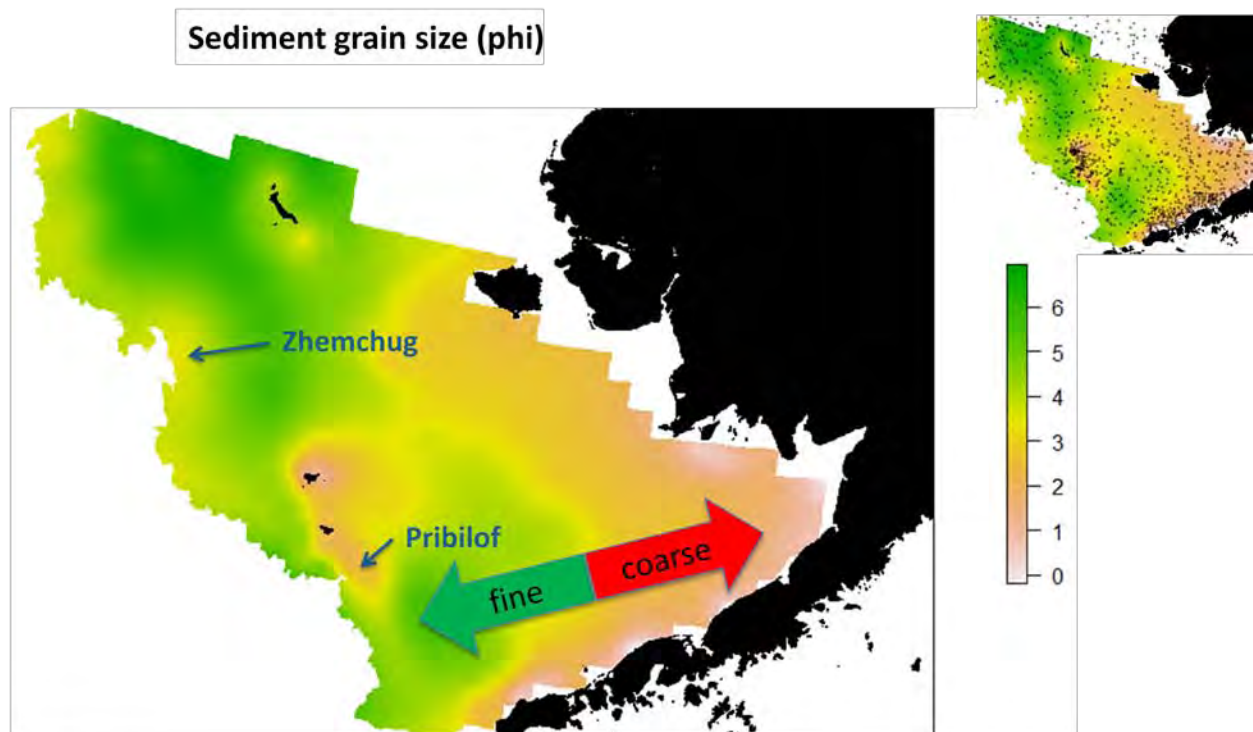
1316

1317 S3. Long-term average of ocean current in the eastern Bering Sea. The upper right panel shows
1318 model grid (black dots). Source: ROMS model output (A. Hermann, NOAA's Pacific Marine
1319 Environmental Laboratory, pers. comm., October 2012), $n = 109,194$, gridded average from
1320 1975-2010.



1321

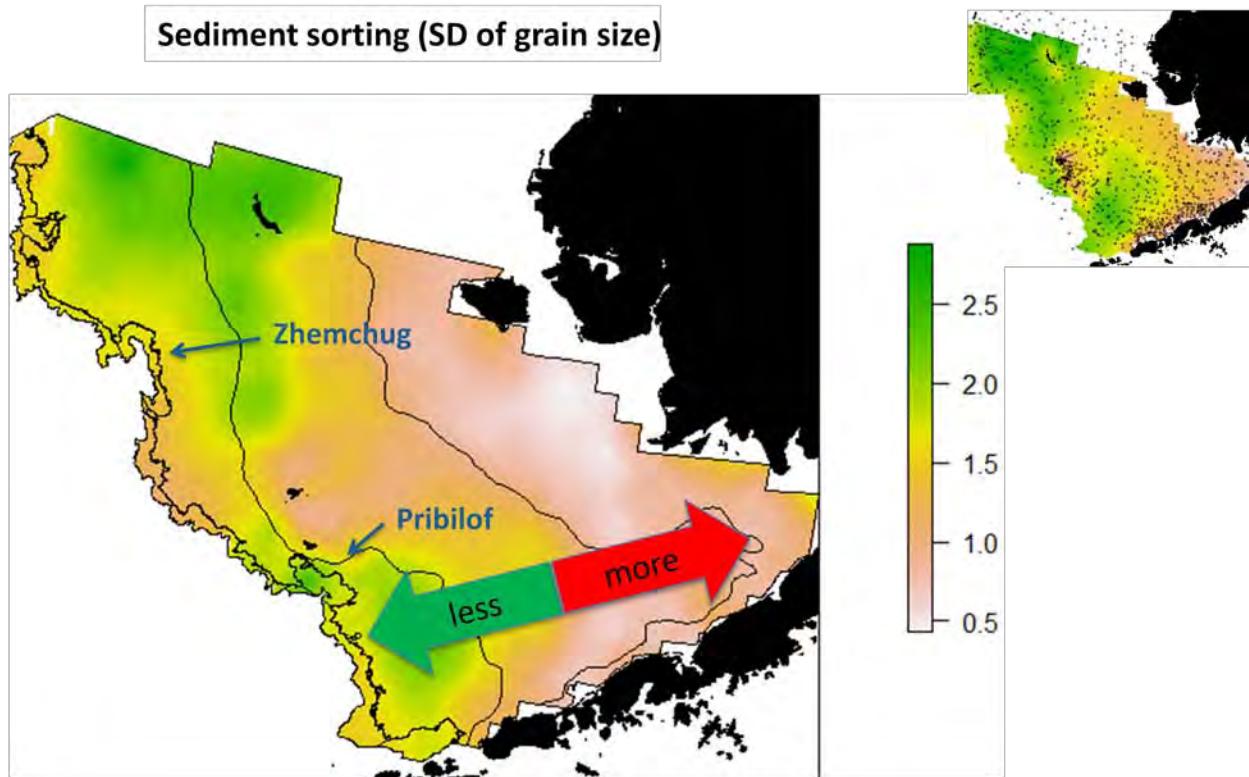
1322 S4. Predicted sediment grain size in the eastern Bering Sea. The upper right panel shows sample
1323 locations (black dots). Source: Eastern Bering Sea Sediment (EBSSed) database (Smith and
1324 McConnaughey 1999), $n = 1,201$.



1325

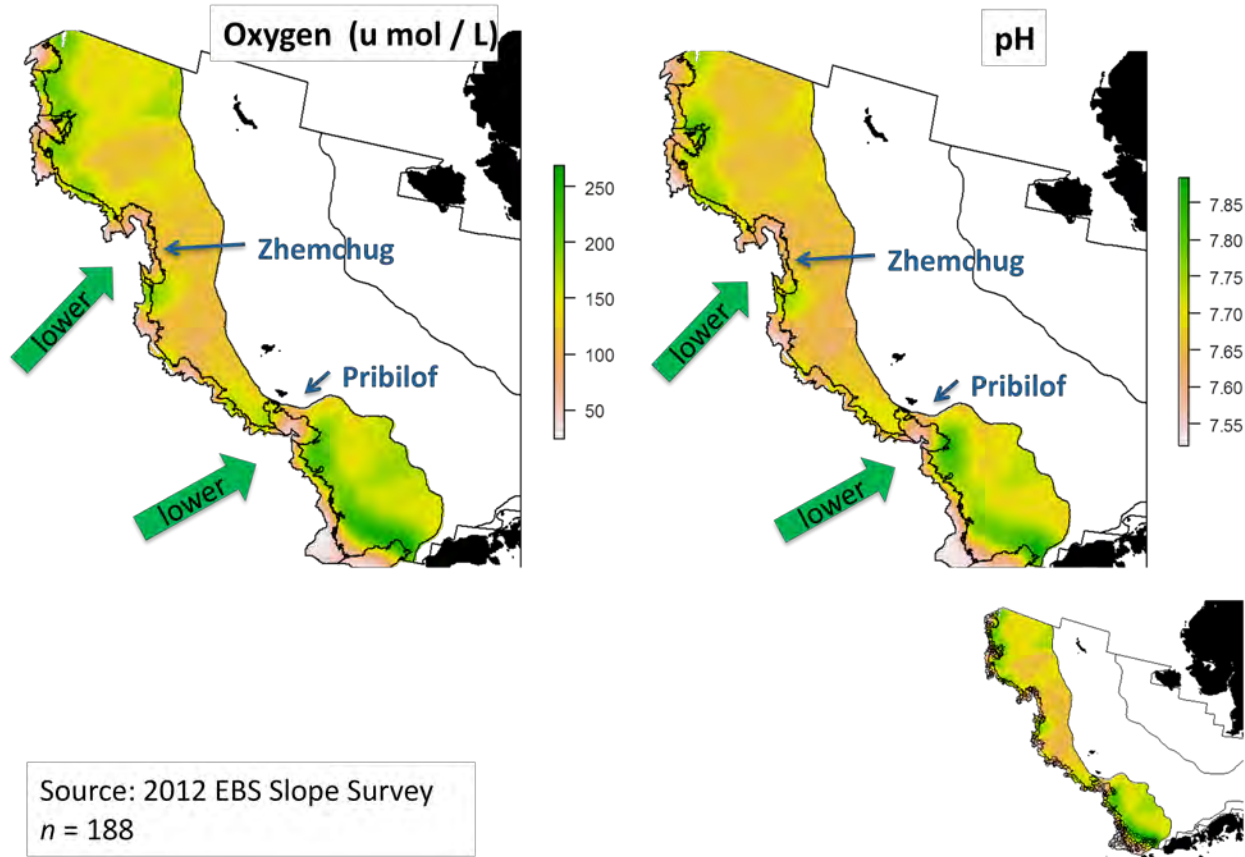
1326

1327 S5. Predicted sediment sorting in the eastern Bering Sea. The upper right panel shows sample
1328 locations (black dots). Source: Eastern Bering Sea Sediment (EBSSed) database (Smith and
1329 McConnaughey 1999), n = 1,201.



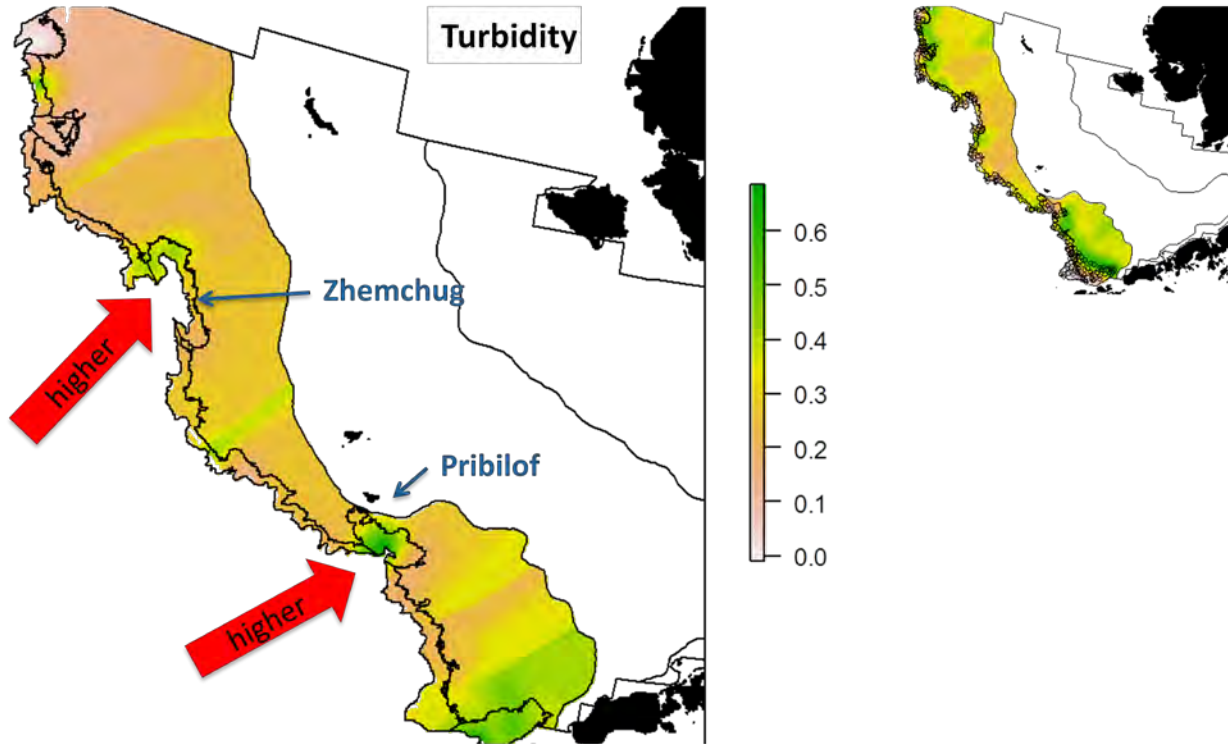
1330
1331

1332 S6. Summer 2012 bottom oxygen and pH in the eastern Bering Sea. The lower right panel shows
1333 sample locations (black dots). The values were extrapolated onto the outer shelf even though
1334 samples were collected only on the slope (sample locations are the open circles shown in the
1335 lower right map). Source: Eastern Bering Sea slope survey, n = 188.



1336

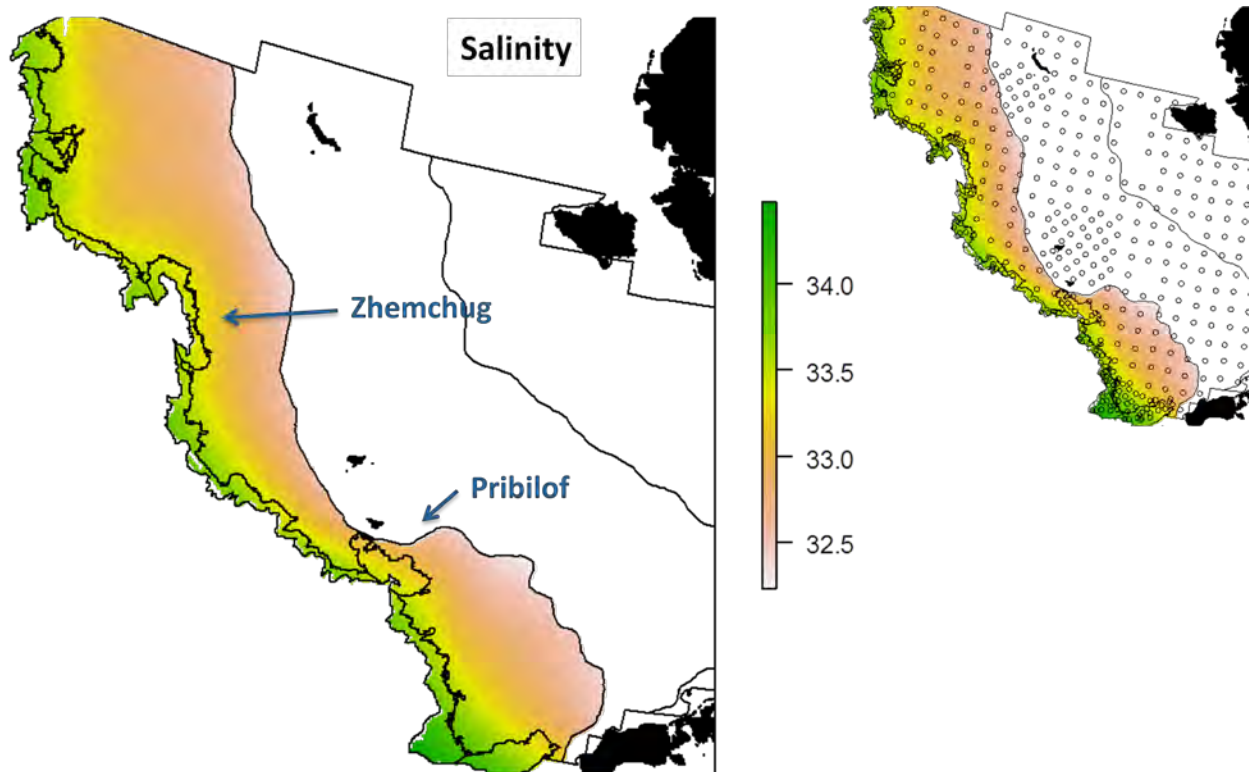
1337 S7. Summer 2012 turbidity in the eastern Bering Sea. The upper right panel shows sample
1338 locations (black dots). The values were extrapolated onto the outer shelf even though samples
1339 were collected only on the slope (sample locations are the open circles shown in the righthand
1340 map). Source: Eastern Bering Sea slope survey, n = 188.



1341

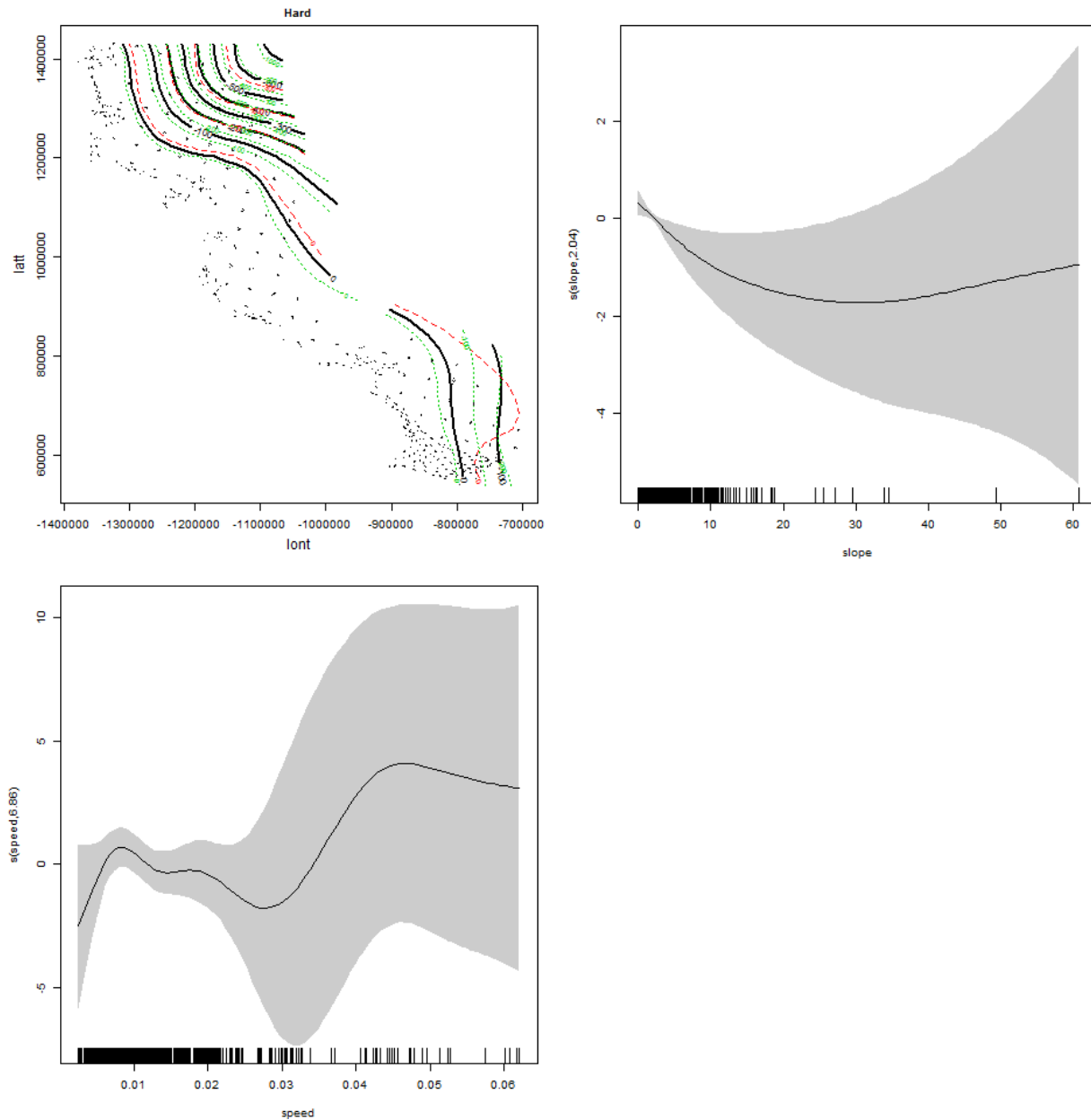
1342

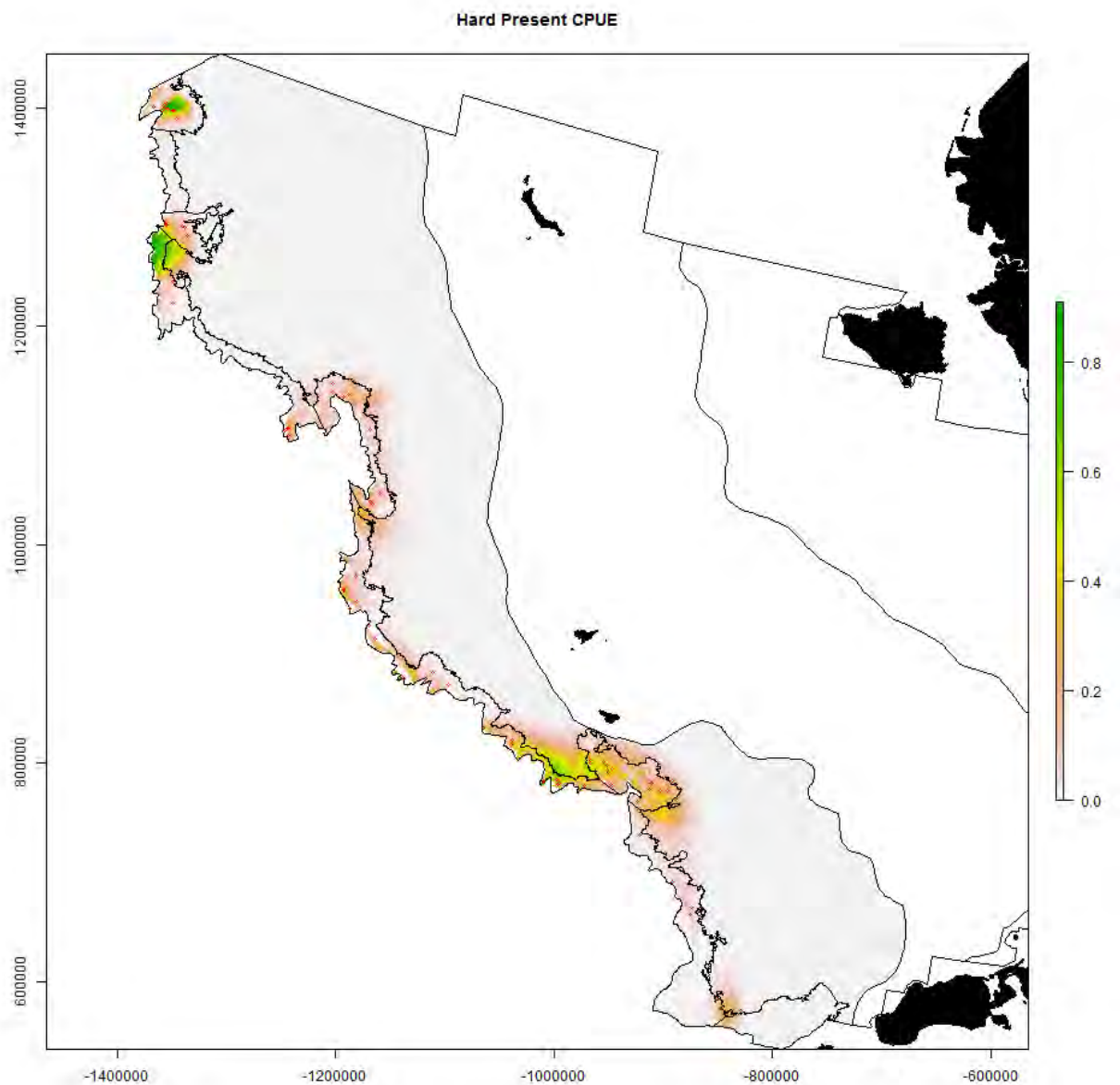
1343 S8. Summer 2012 salinity in the eastern Bering Sea. The upper right panel shows sample
1344 locations (black dots). Source: Eastern Bering Sea shelf and slope surveys, n = 512.



1345
1346

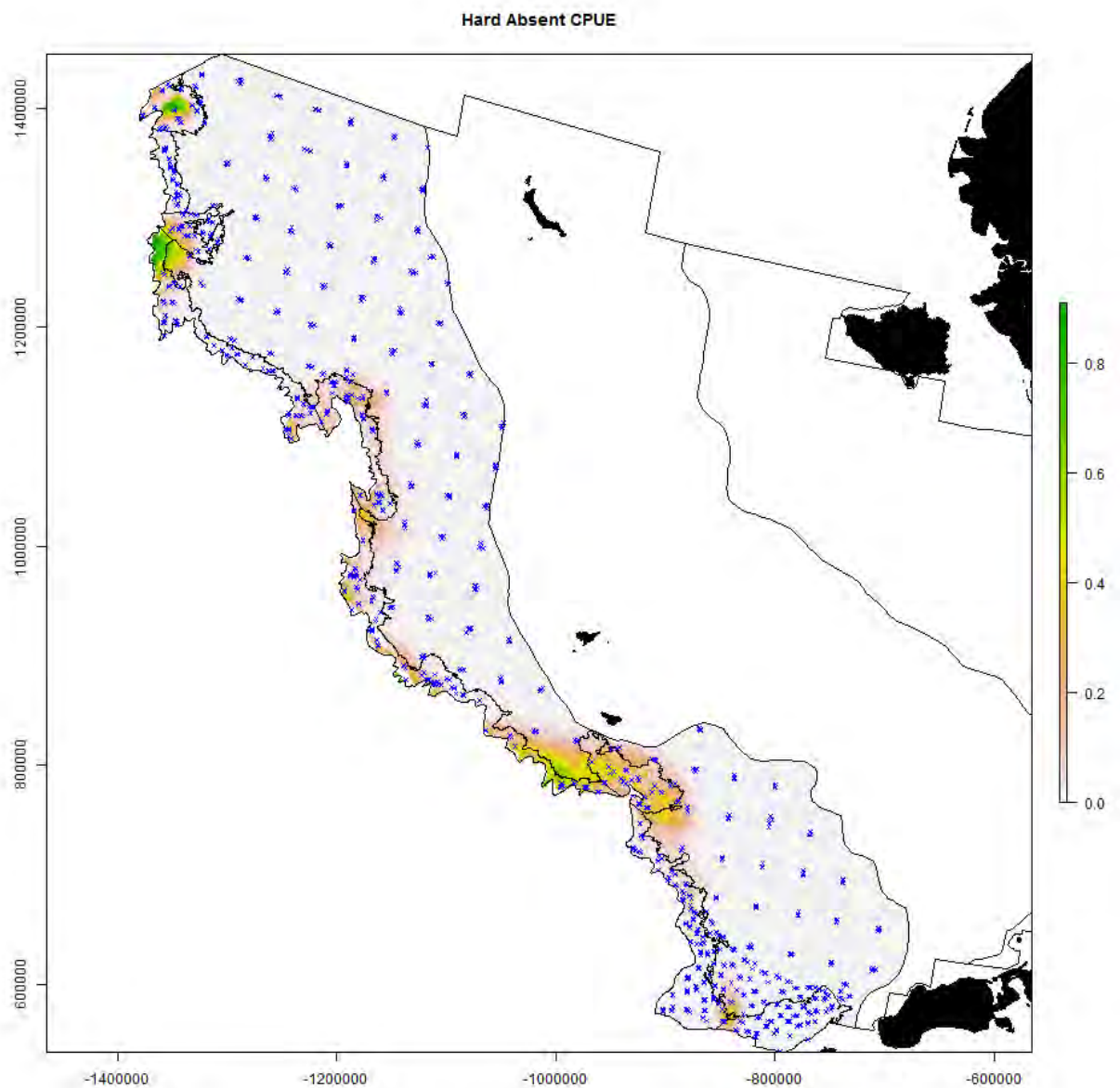
1347 S9. Generalized additive modeling results for coral. In the spatial plots, the x-axis label is easting
1348 and the y-axis label is northing and the unit is meters (Alaska Albers Equal Area Conic
1349 projection with center latitude = 50° N and center longitude = 154° W).





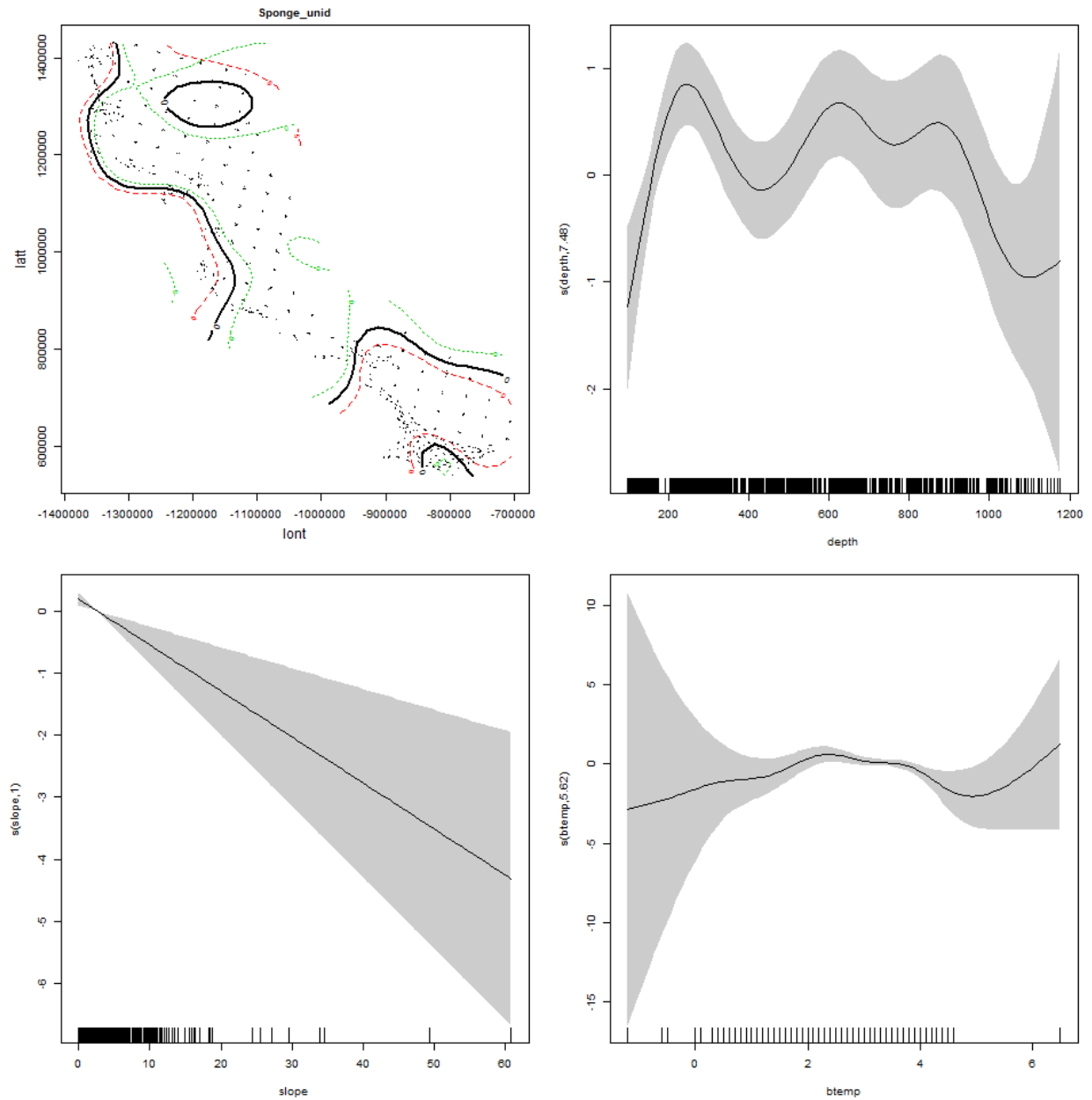
1352

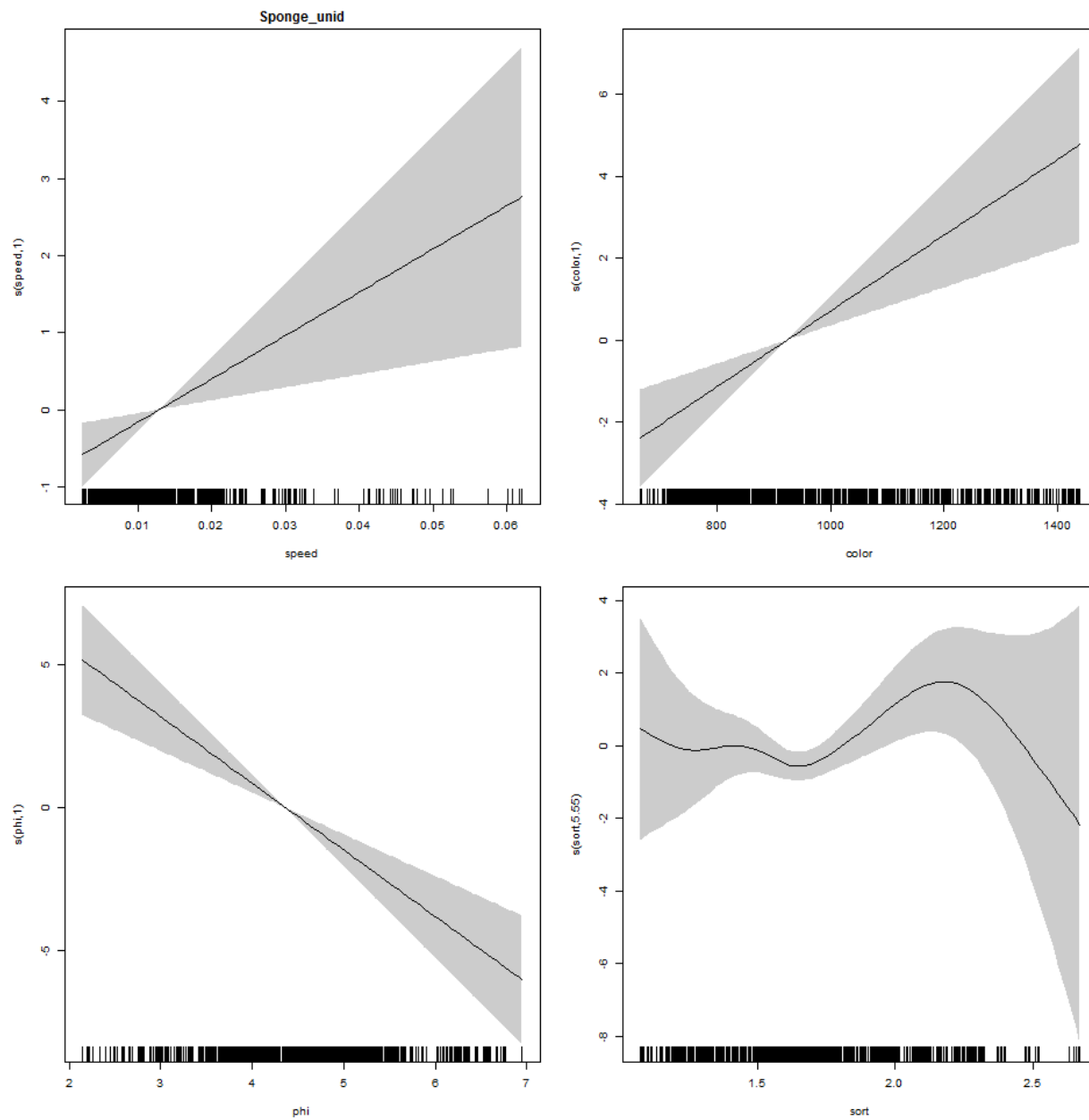
1353



1354
1355

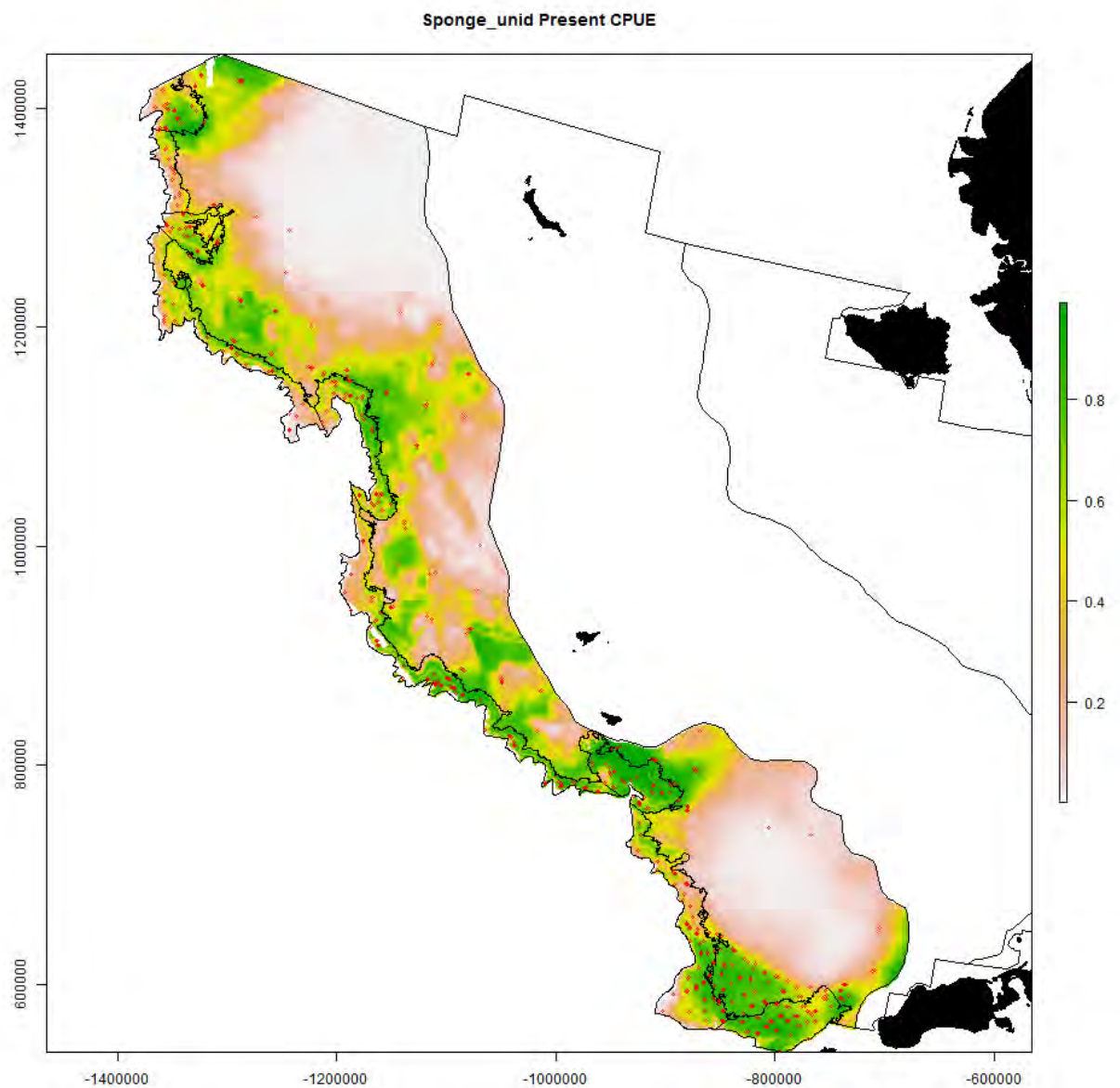
1356 S10. Generalized additive modeling results for sponge. In the spatial plots, the x-axis label is
 1357 easting and the y-axis label is northing and the unit is meters (Alaska Albers Equal Area Conic
 1358 projection with center latitude = 50° N and center longitude = 154° W).





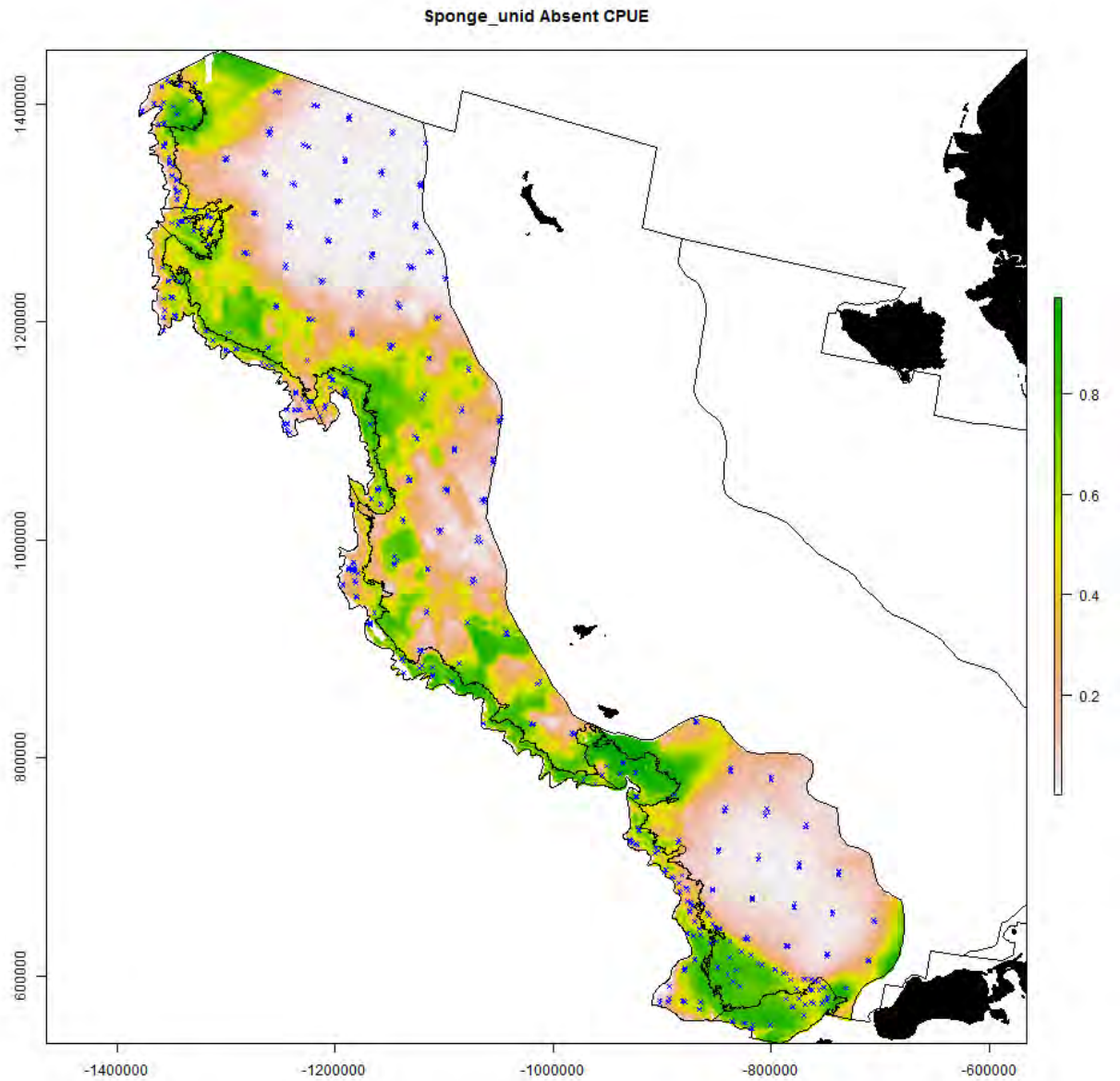
1361

1362



1363

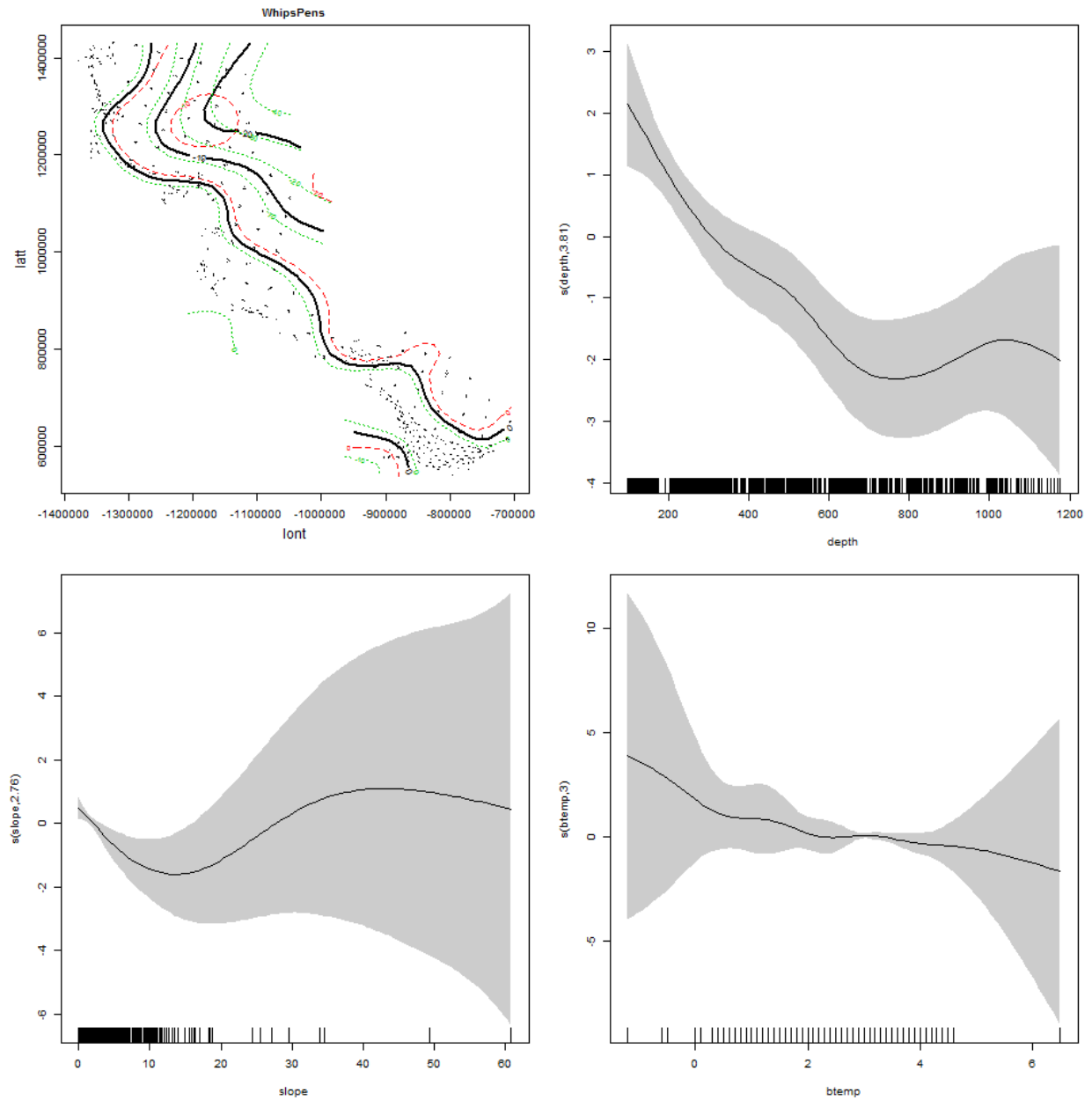
1364

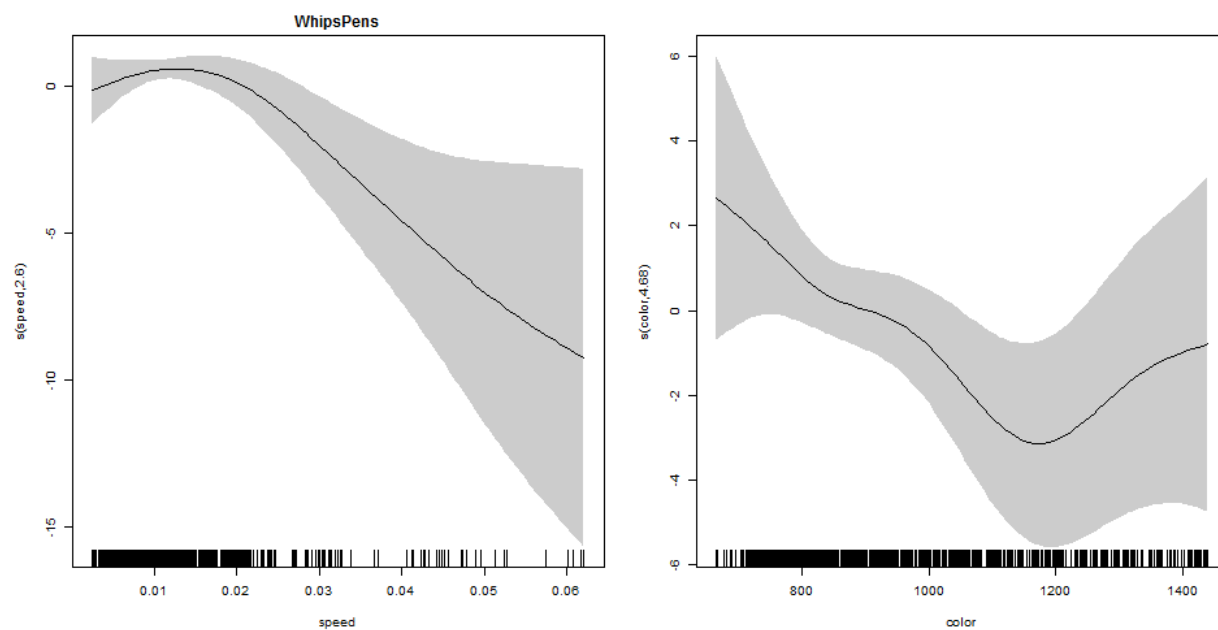


1365

1366

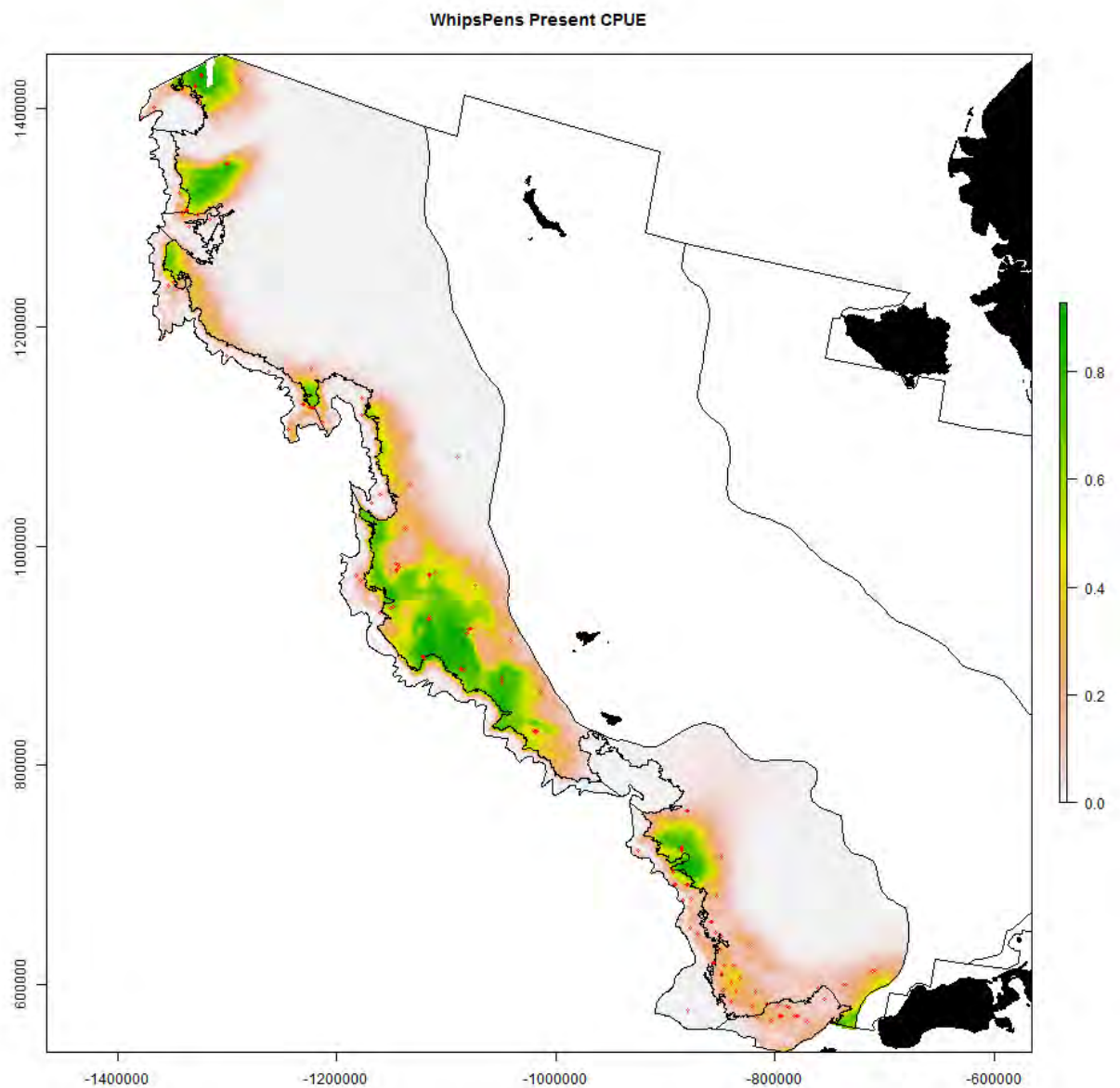
1367 S11. Generalized additive modeling results for sea whip. In the spatial plots, the x-axis label is
 1368 easting and the y-axis label is northing and the unit is meters (Alaska Albers Equal Area Conic
 1369 projection with center latitude = 50° N and center longitude = 154° W).





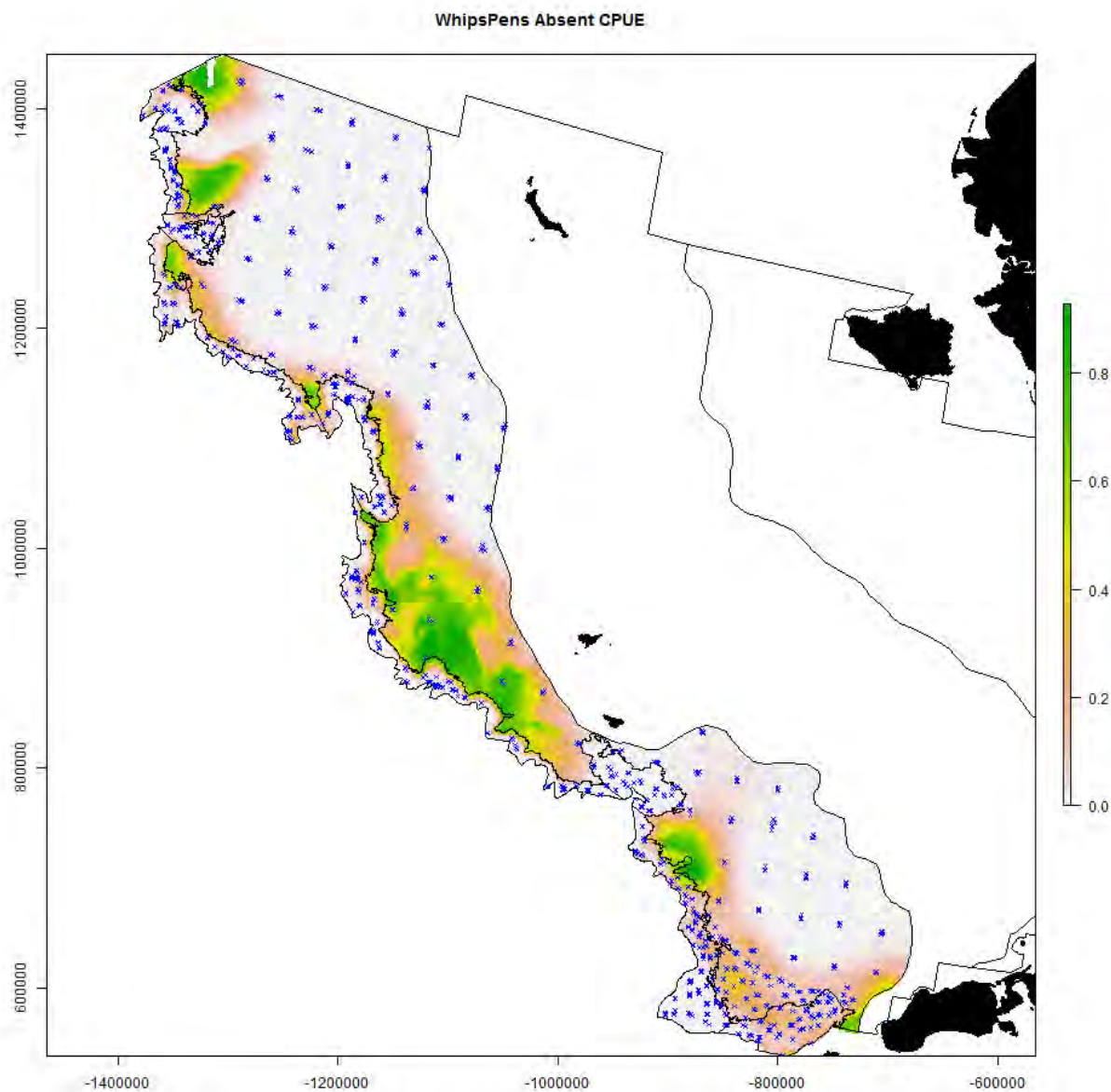
1372

1373



1374

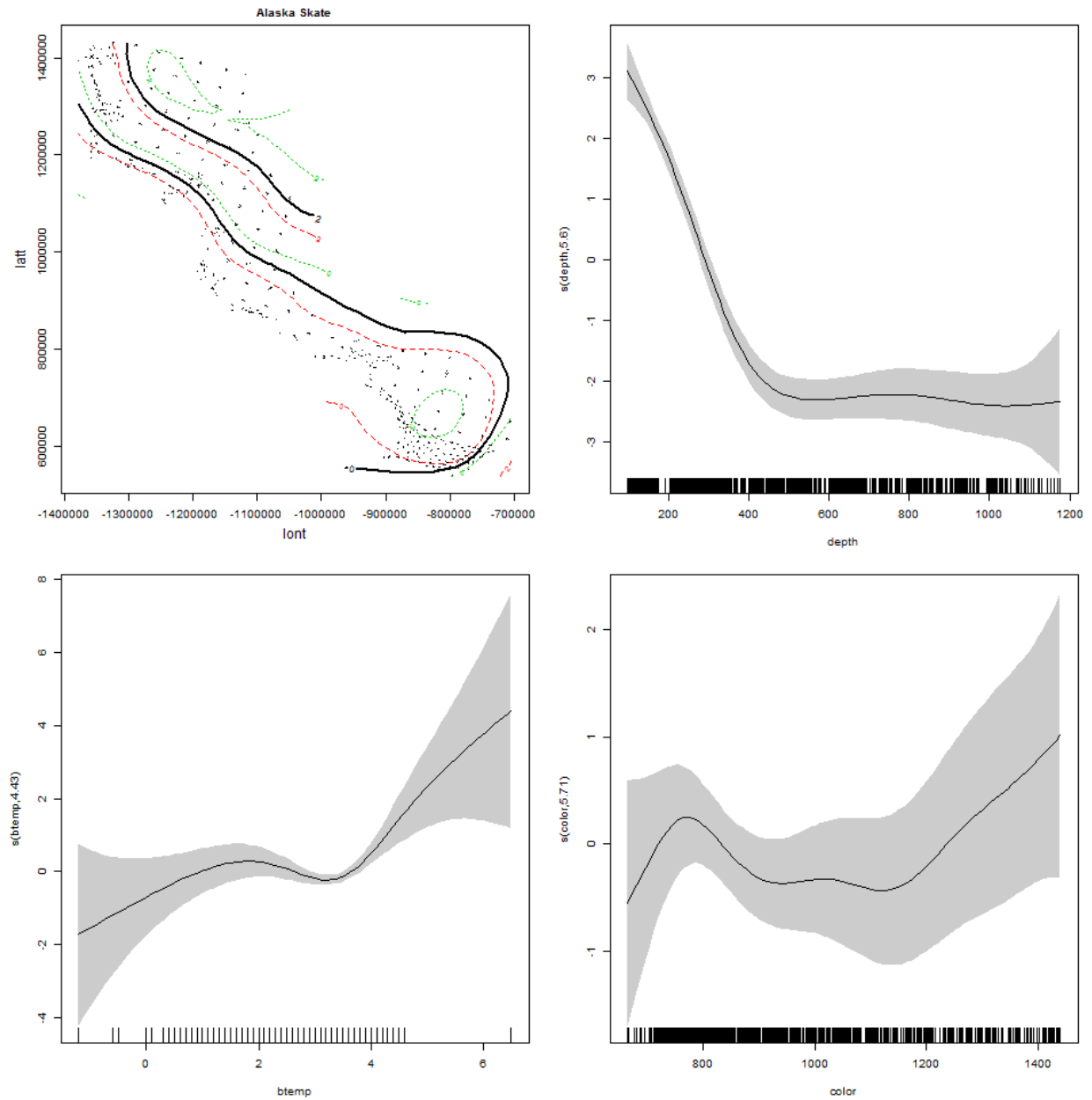
1375

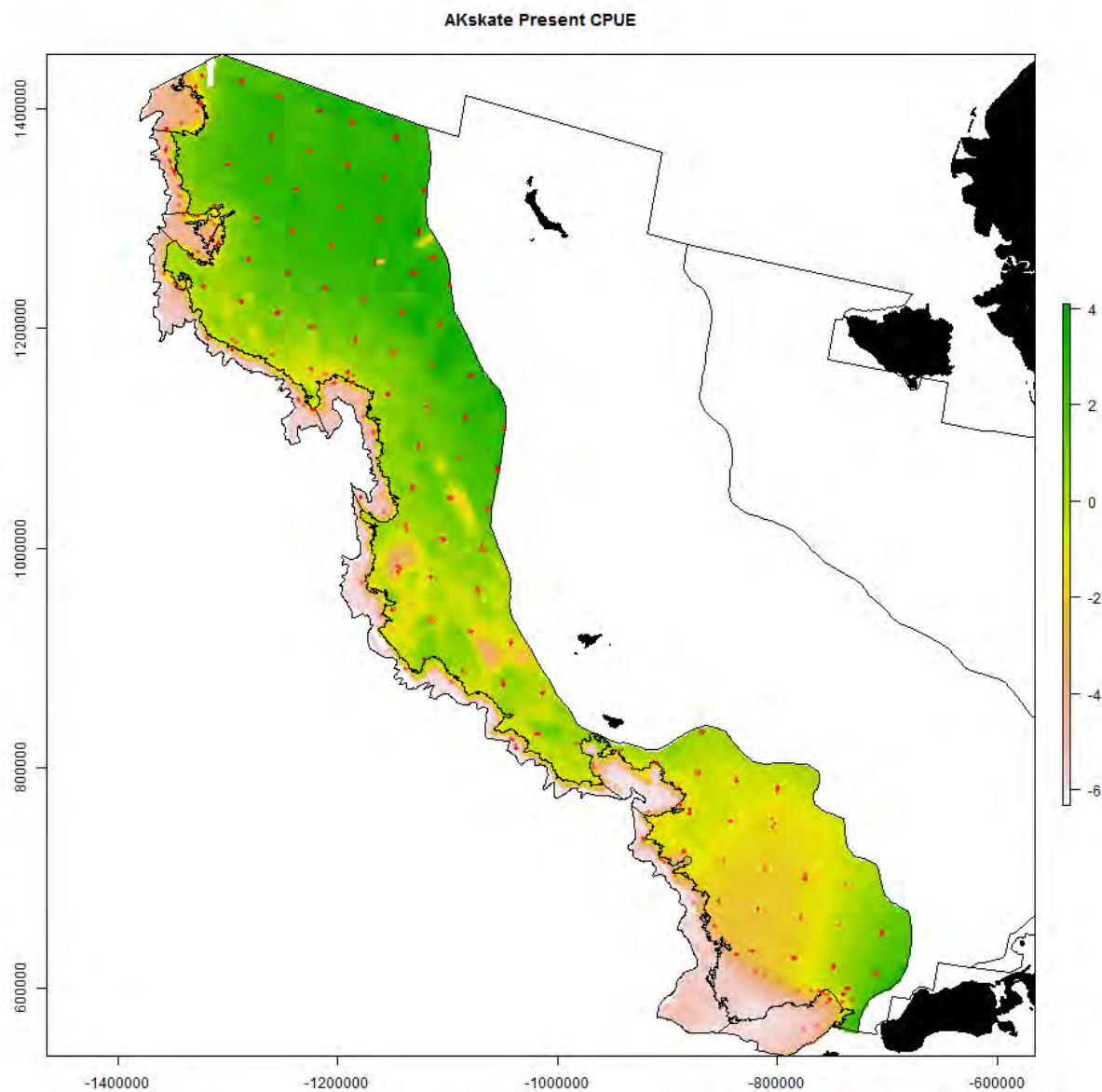


1376

1377

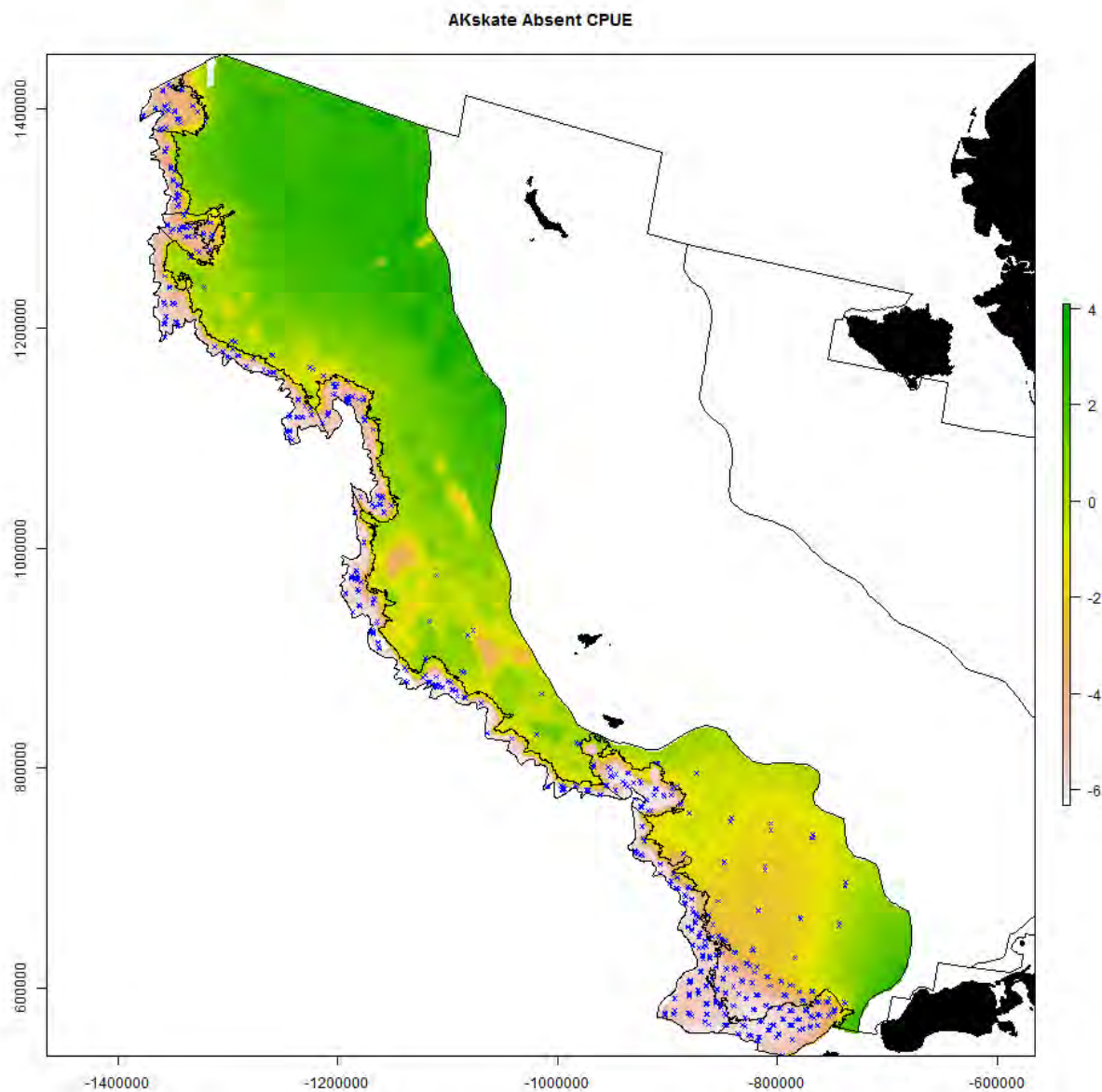
1378 S12. Generalized additive modeling results for Alaska skate. In the spatial plots, the x-axis label
 1379 is easting and the y-axis label is northing and the unit is meters (Alaska Albers Equal Area Conic
 1380 projection with center latitude = 50° N and center longitude = 154° W).





1383

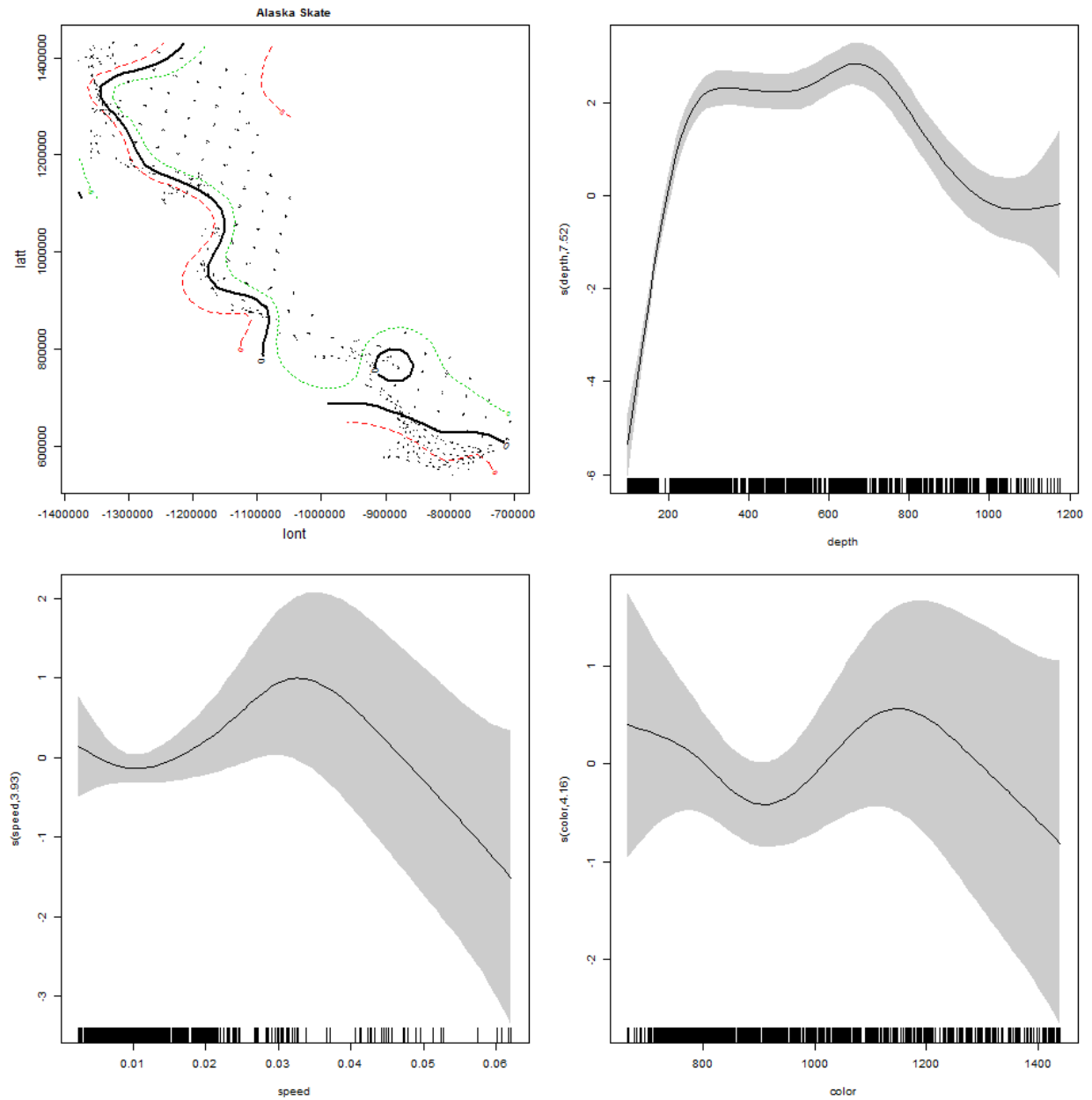
1384



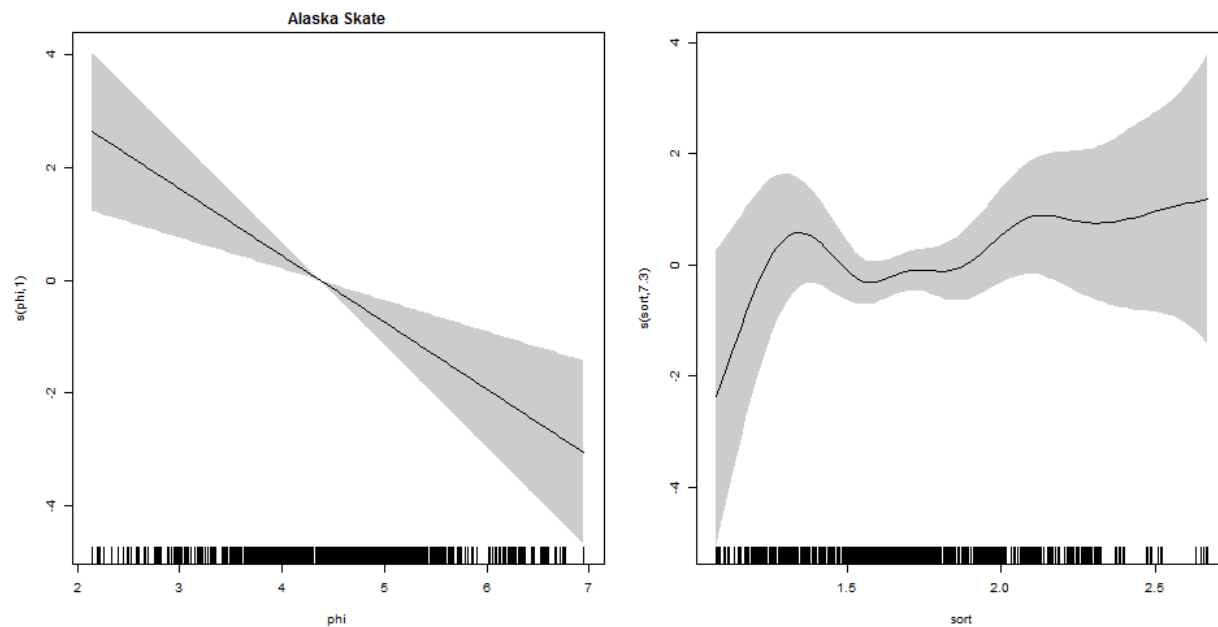
1385

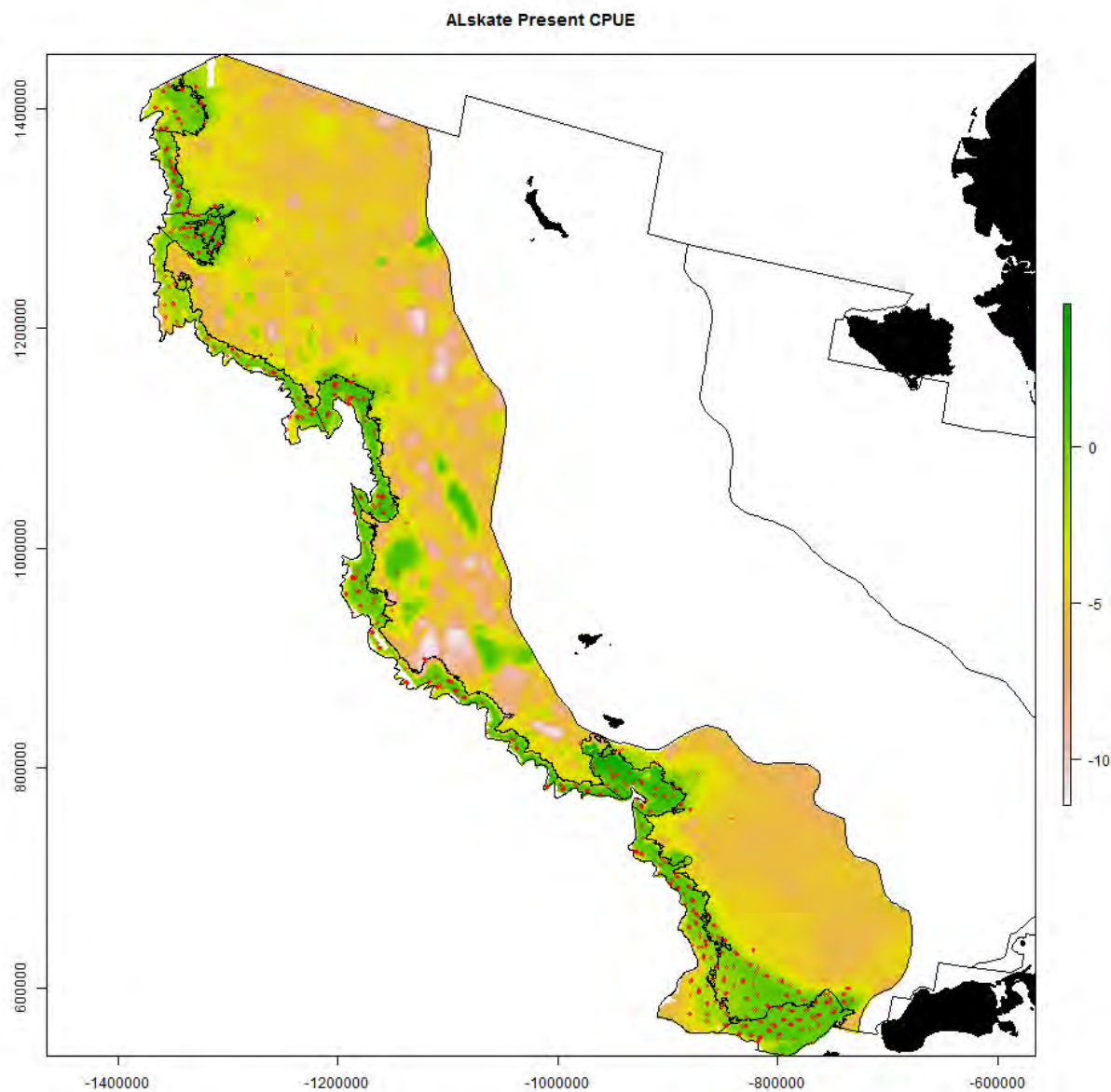
1386

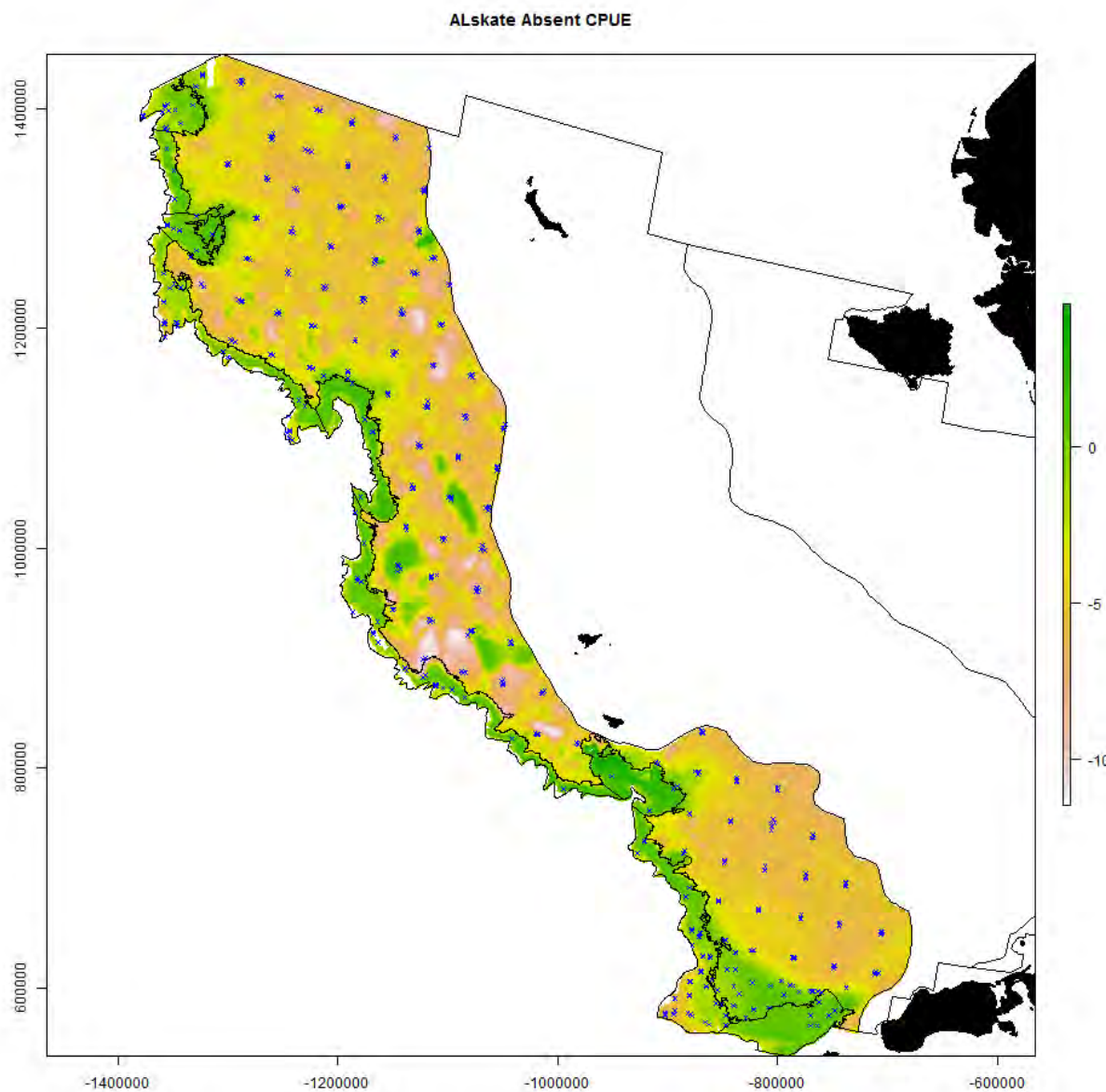
1387 S13. Generalized additive modeling results for Aleutian skate. In the spatial plots, the x-axis
 1388 label is easting and the y-axis label is northing and the unit is meters (Alaska Albers Equal Area
 1389 Conic projection with center latitude = 50° N and center longitude = 154° W).



1390



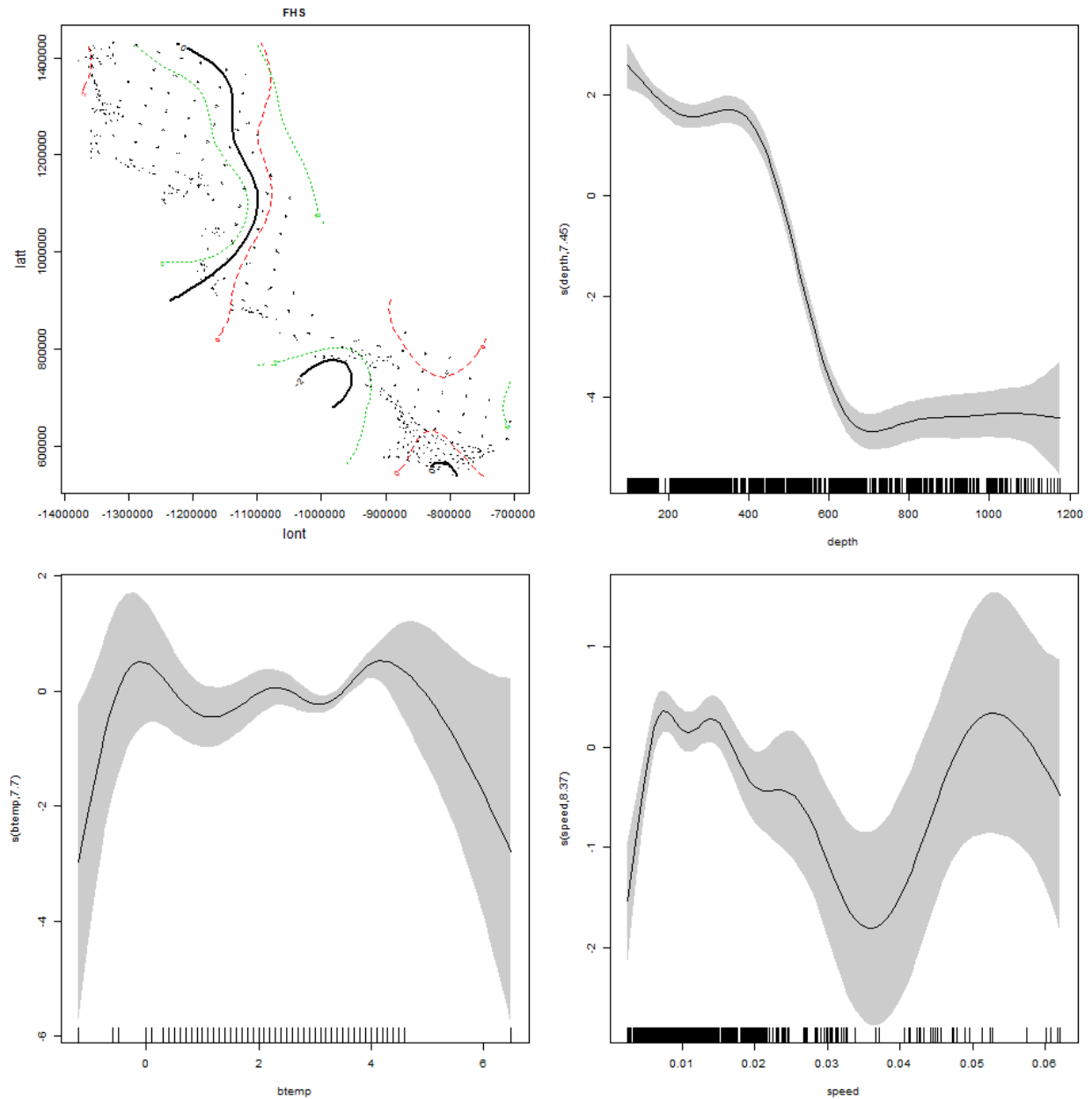




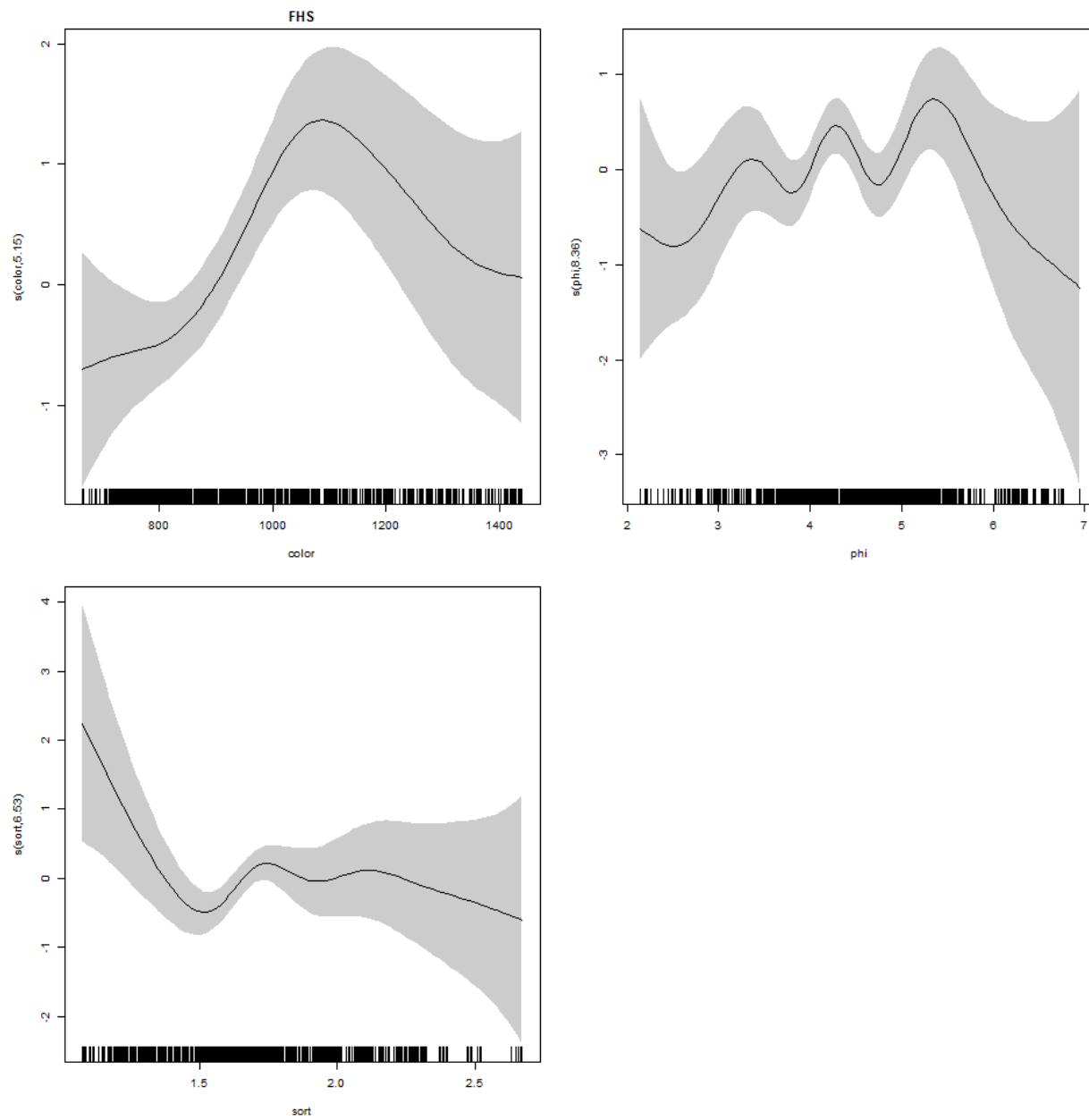
1393

1394

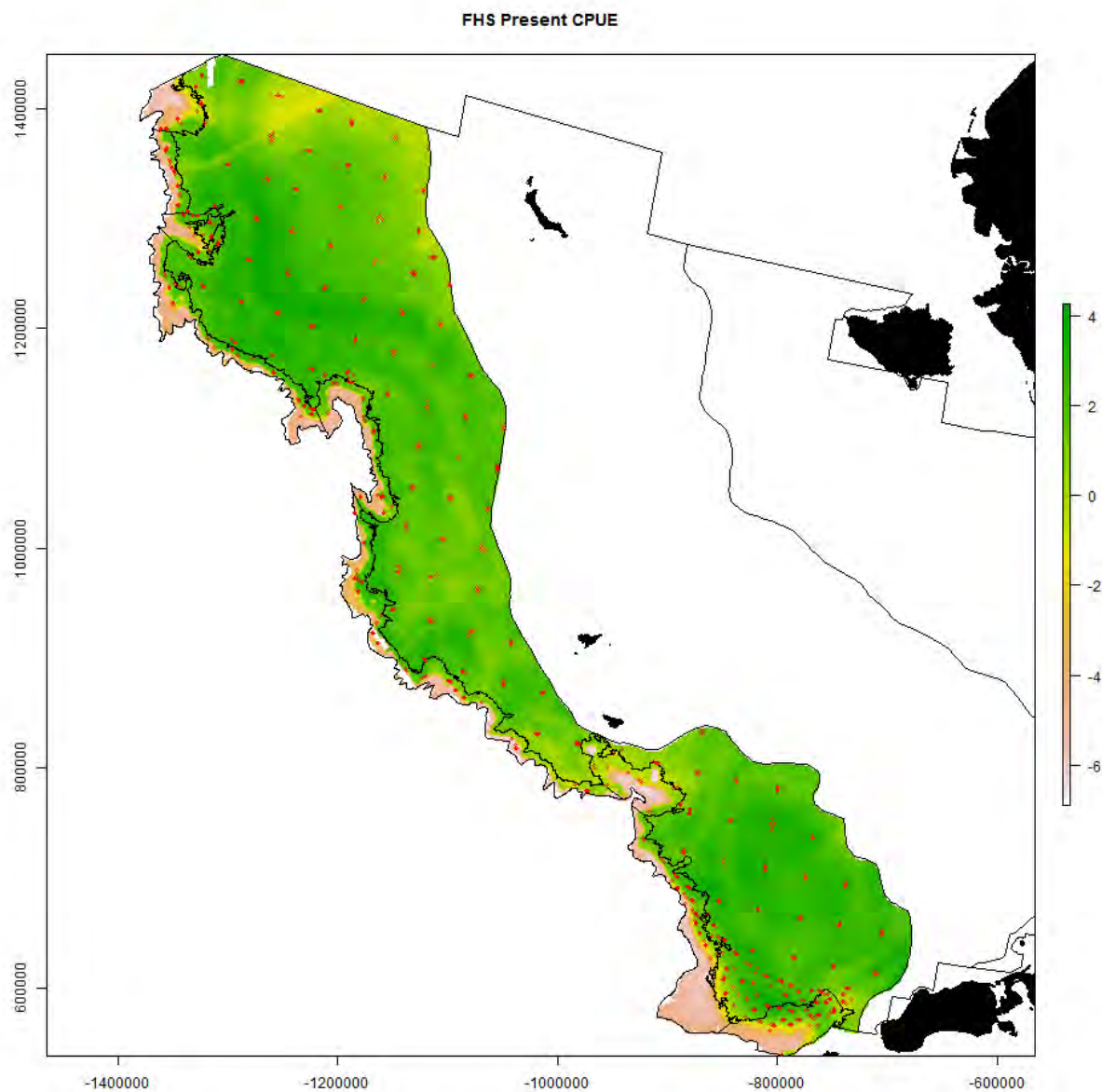
1395 S14. Generalized additive modeling results for flathead sole. In the spatial plots, the x-axis label
 1396 is easting and the y-axis label is northing and the unit is meters (Alaska Albers Equal Area Conic
 1397 projection with center latitude = 50° N and center longitude = 154° W).



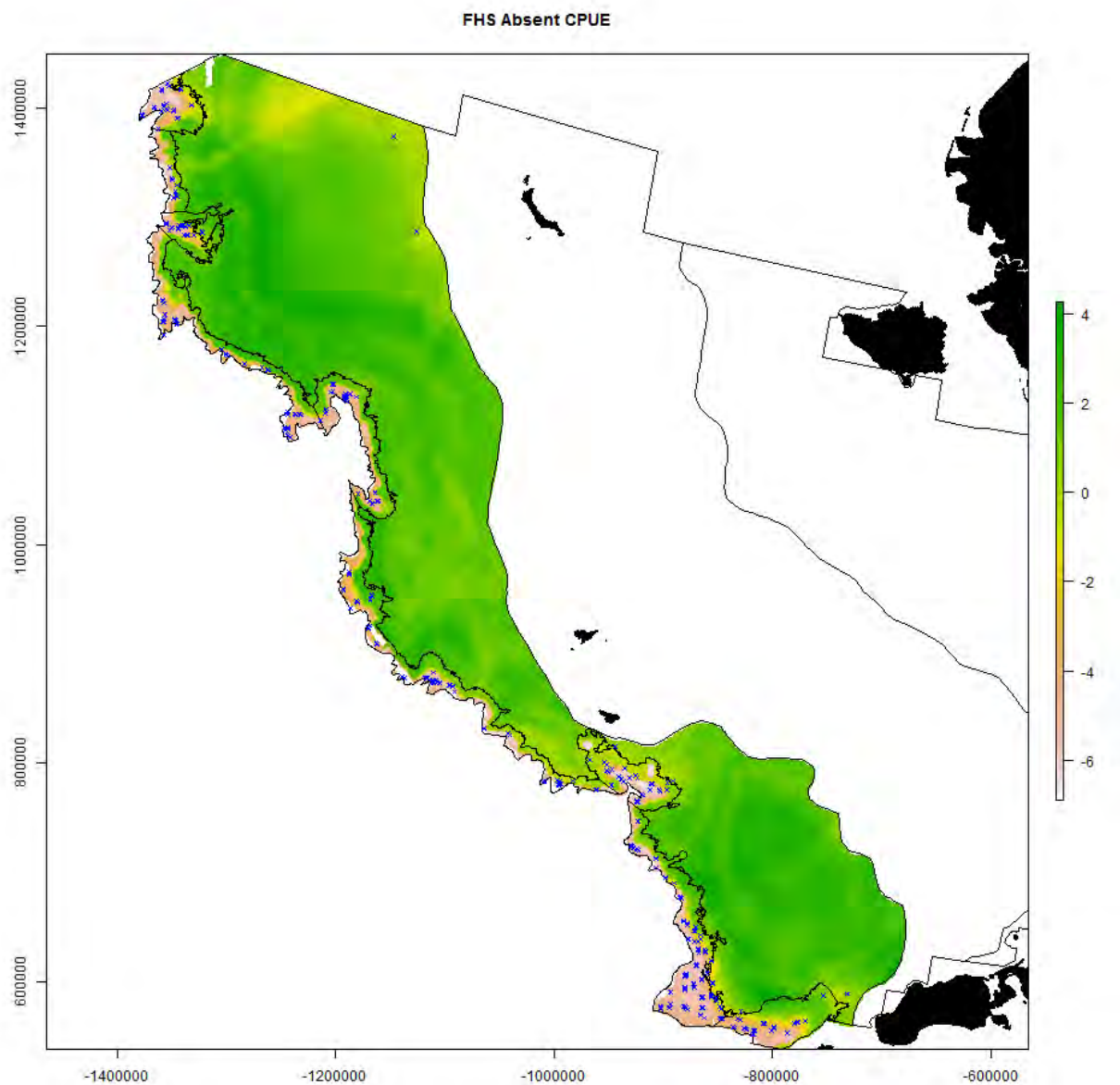
1398



1399



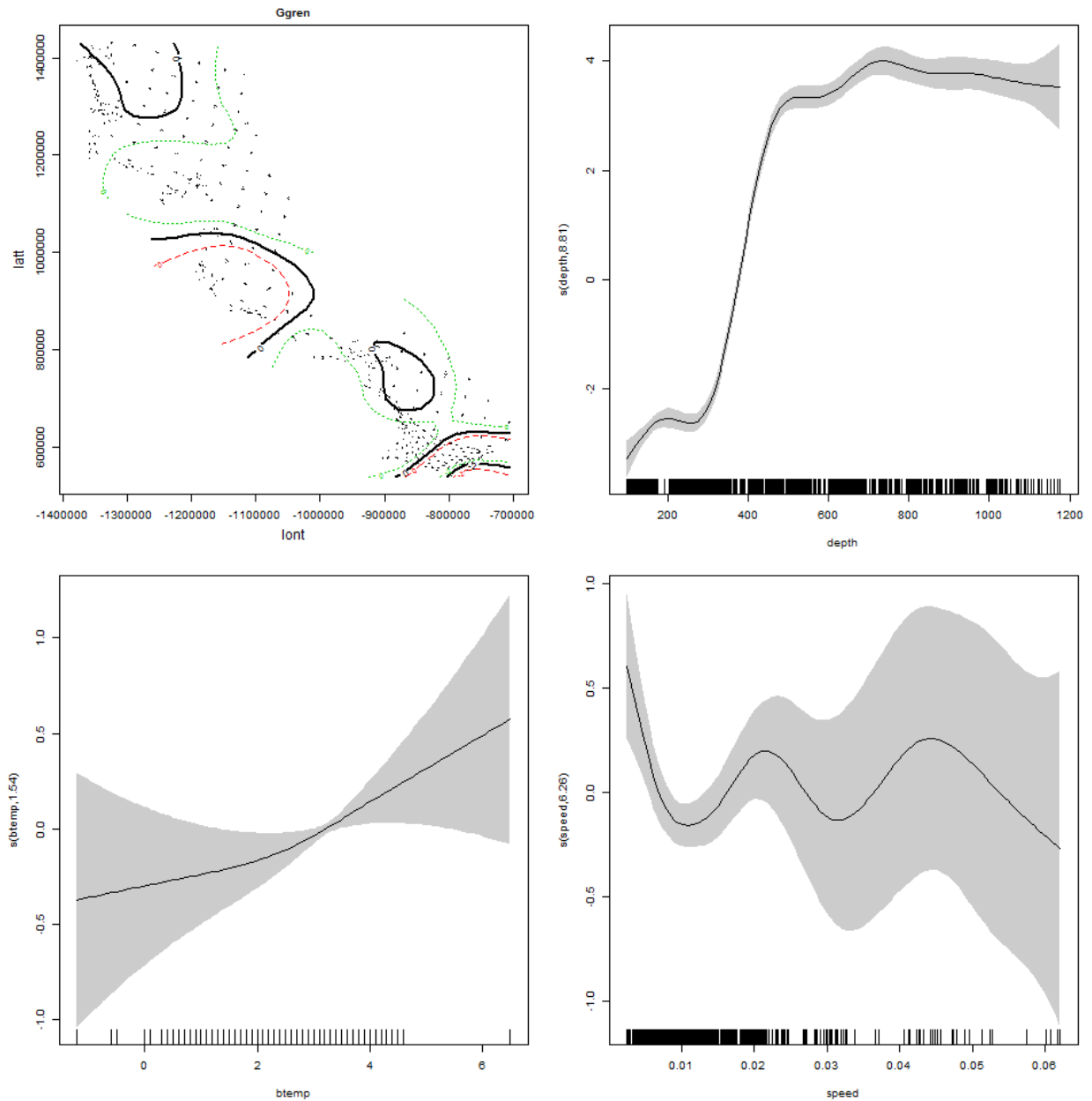
1400



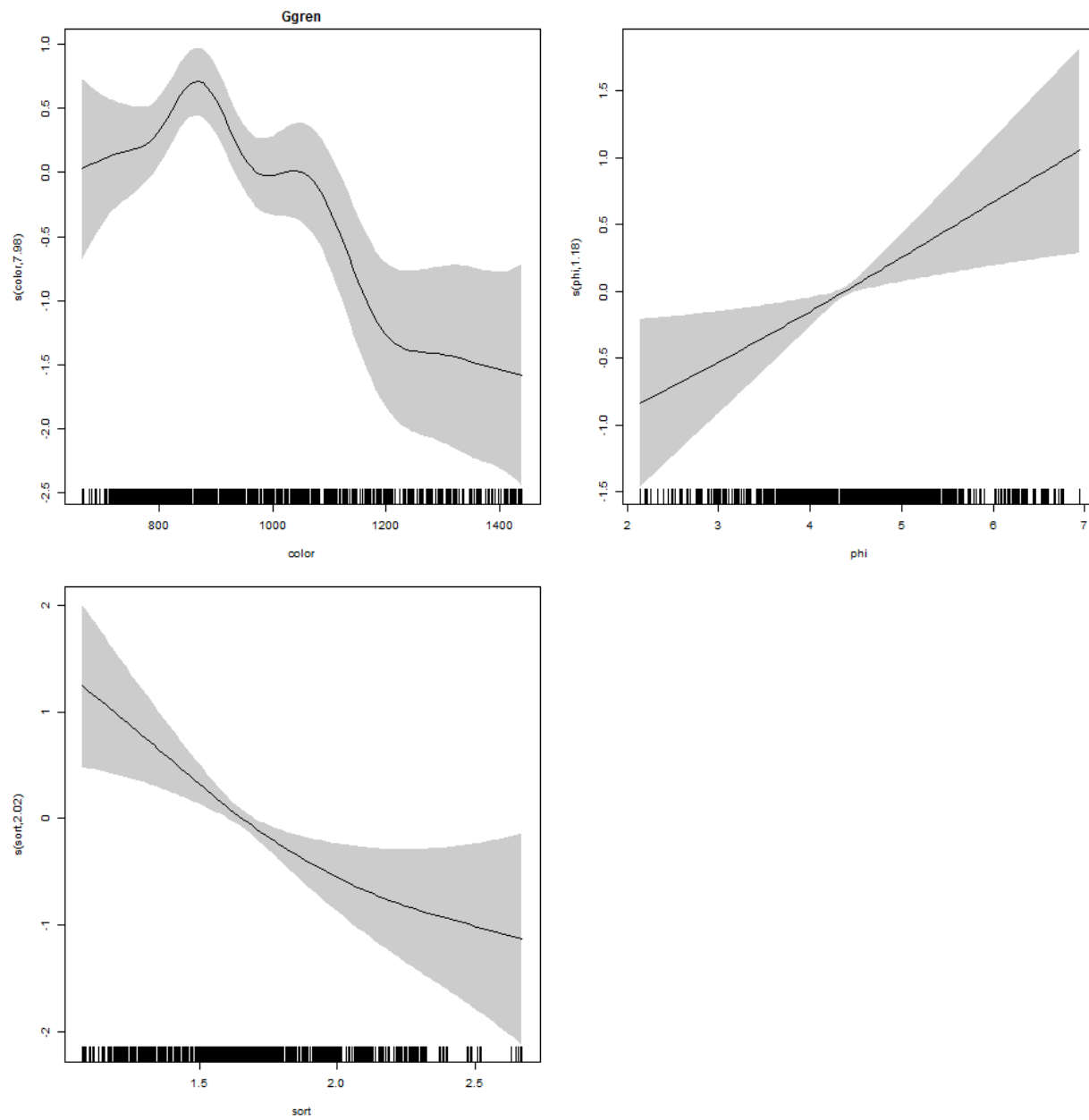
1401

1402

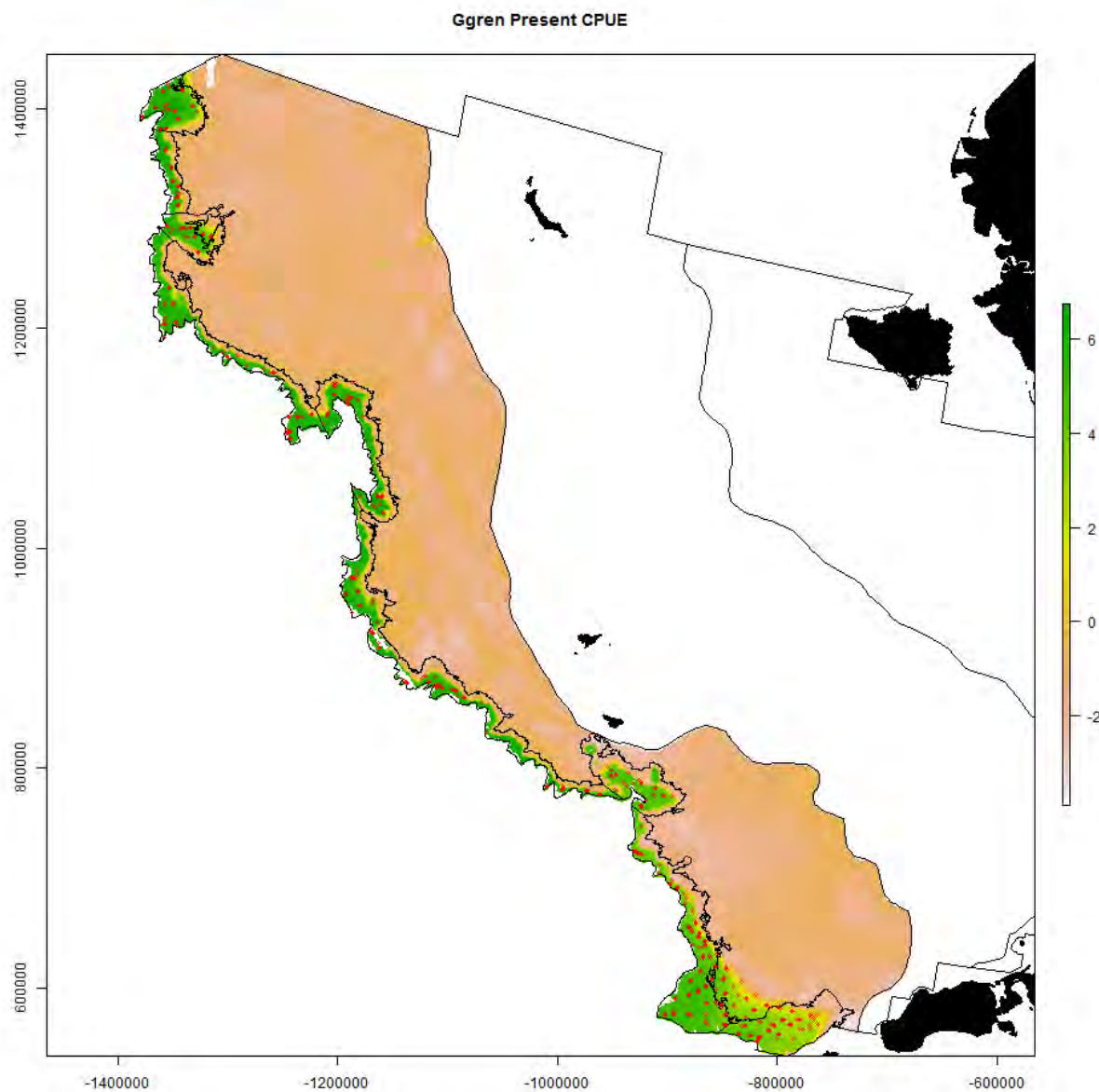
1403 S15. Generalized additive modeling results for giant grenadier. In the spatial plots, the x-axis
 1404 label is easting and the y-axis label is northing and the unit is meters (Alaska Albers Equal Area
 1405 Conic projection with center latitude = 50° N and center longitude = 154° W).



1406

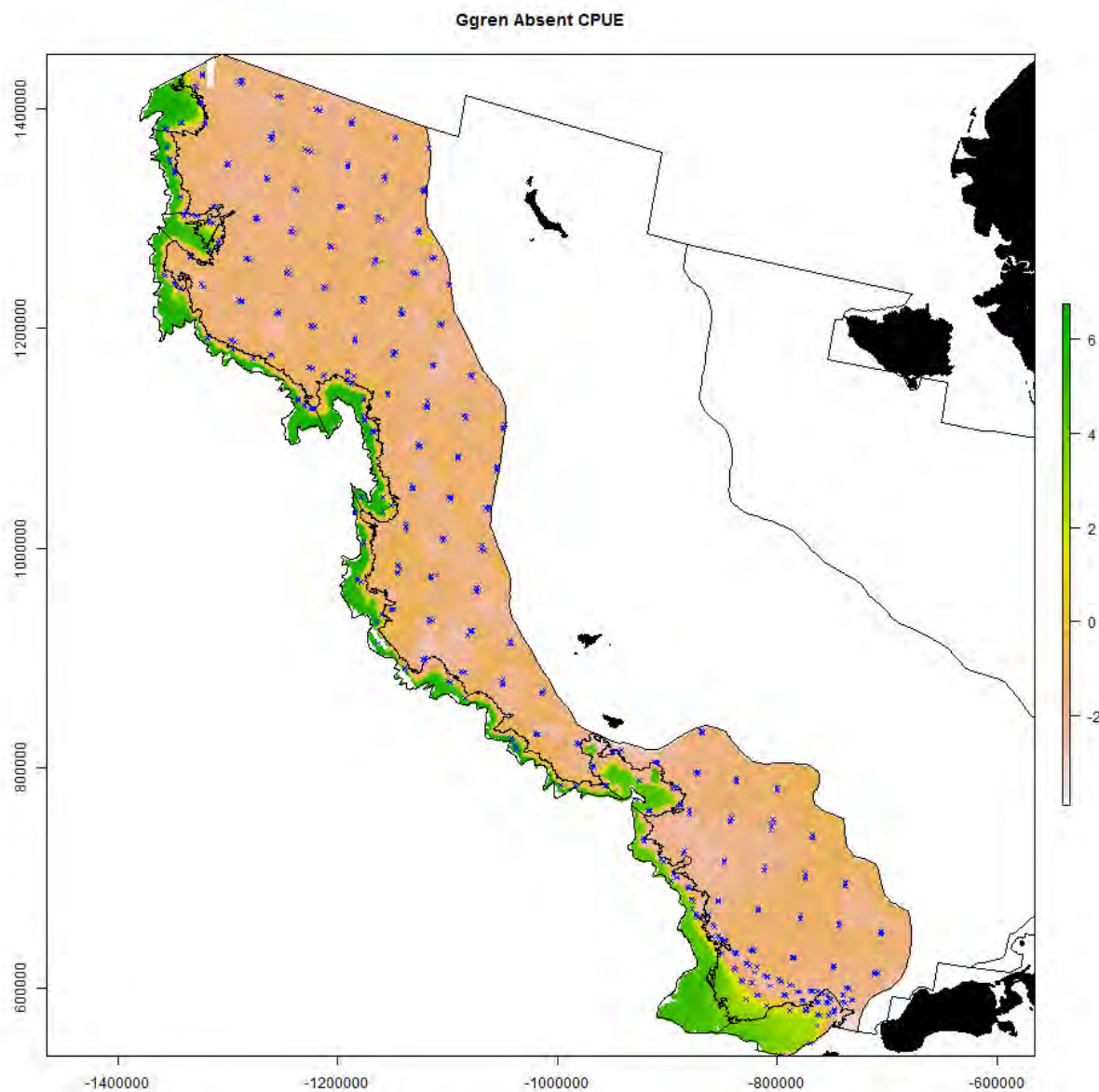


1407



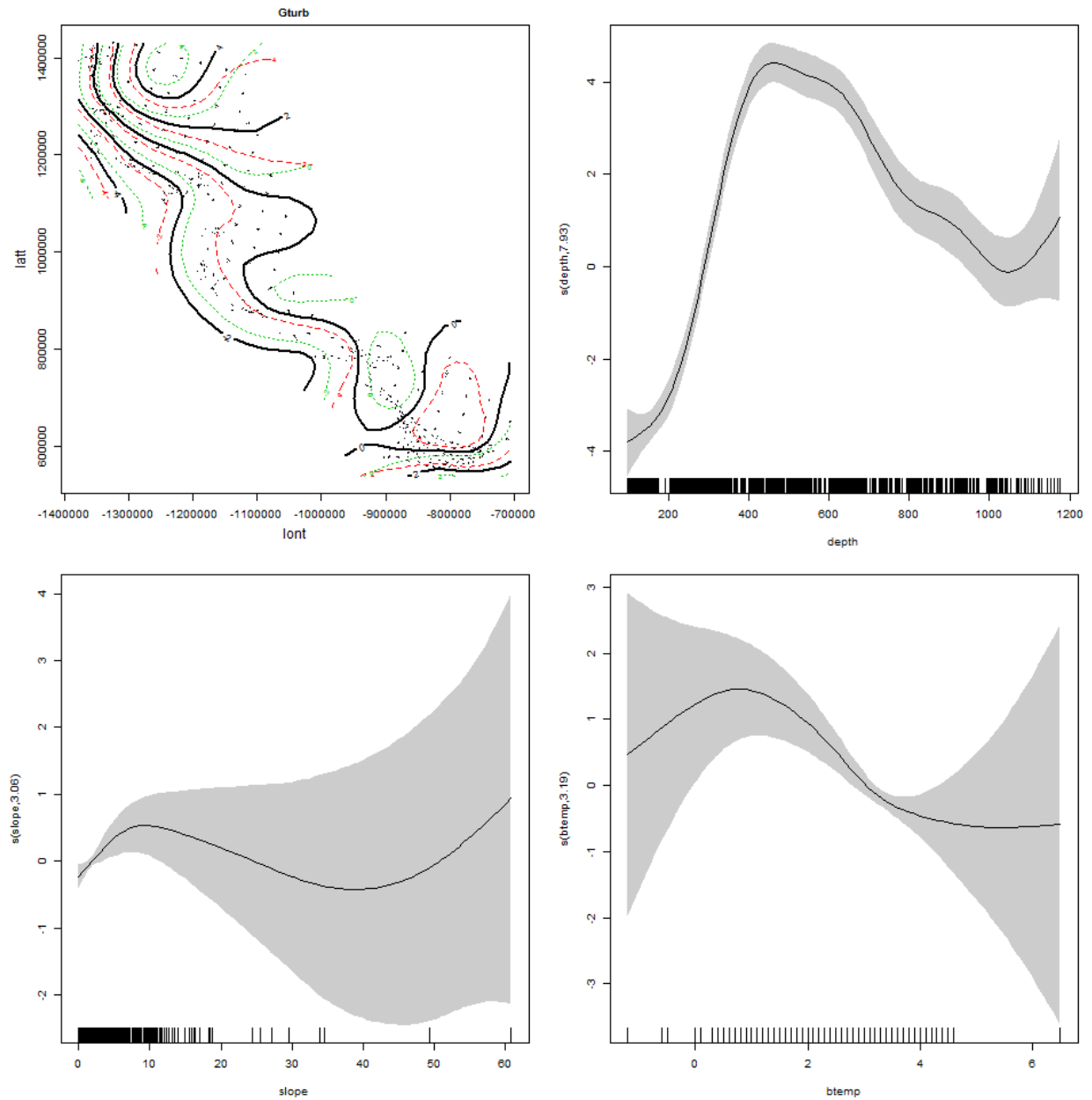
1408

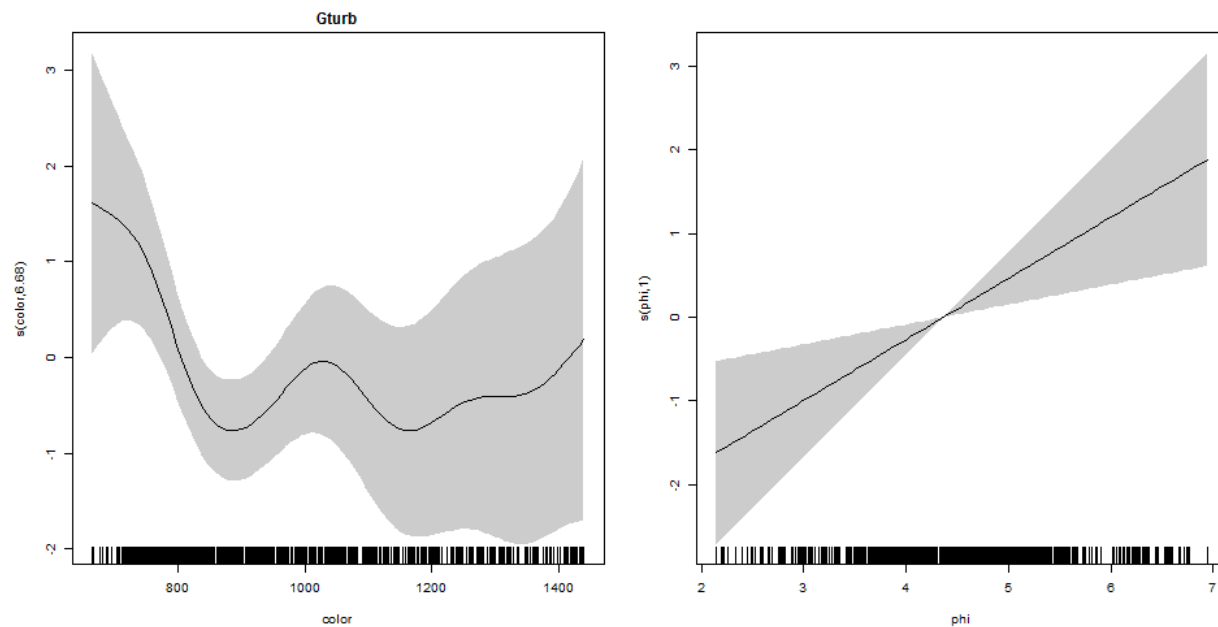
1409



1410
1411

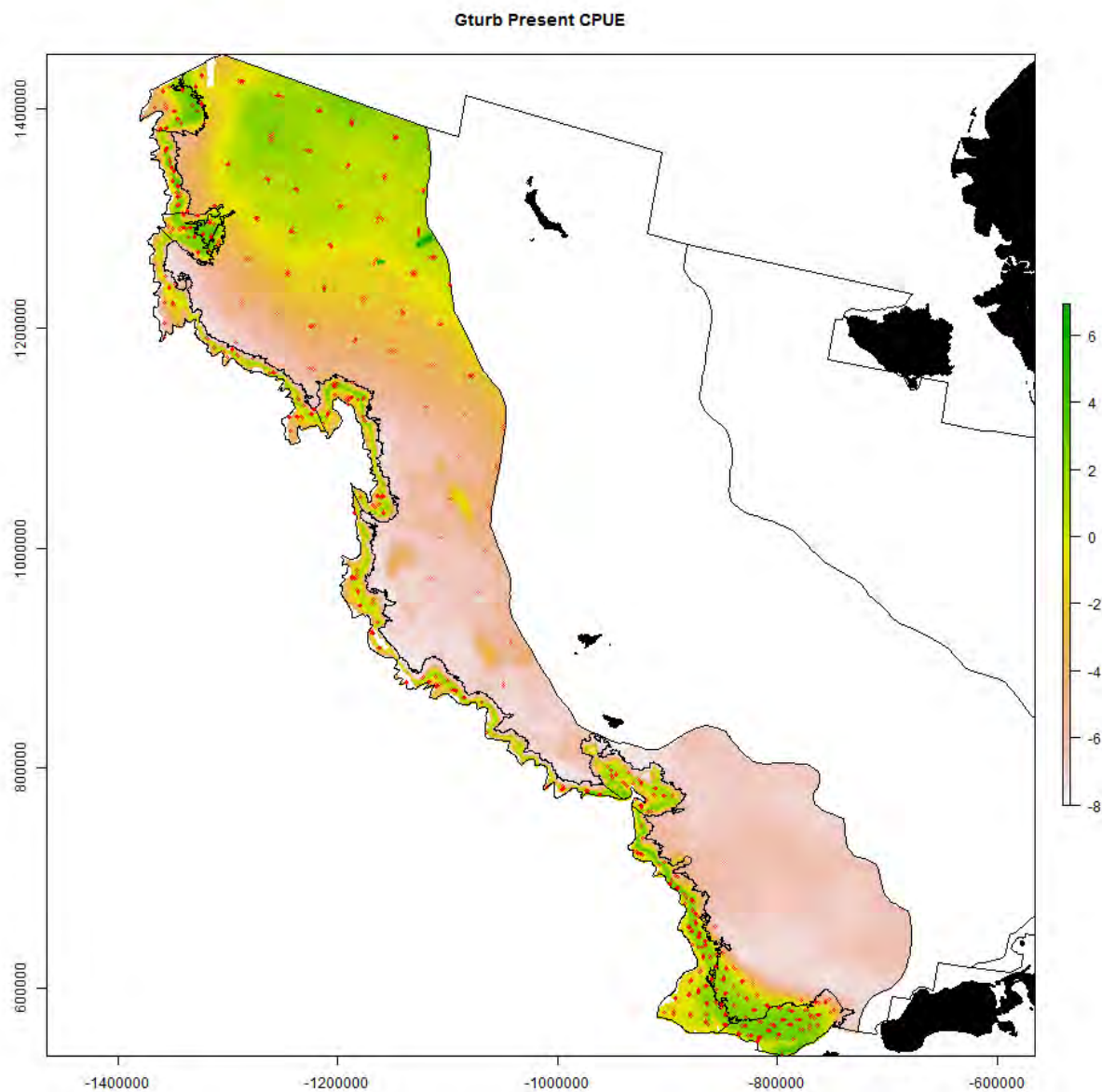
1412 S16. Generalized additive modeling results for Greenland turbot. In the spatial plots, the x-axis
 1413 label is easting and the y-axis label is northing and the unit is meters (Alaska Albers Equal Area
 1414 Conic projection with center latitude = 50° N and center longitude = 154° W).





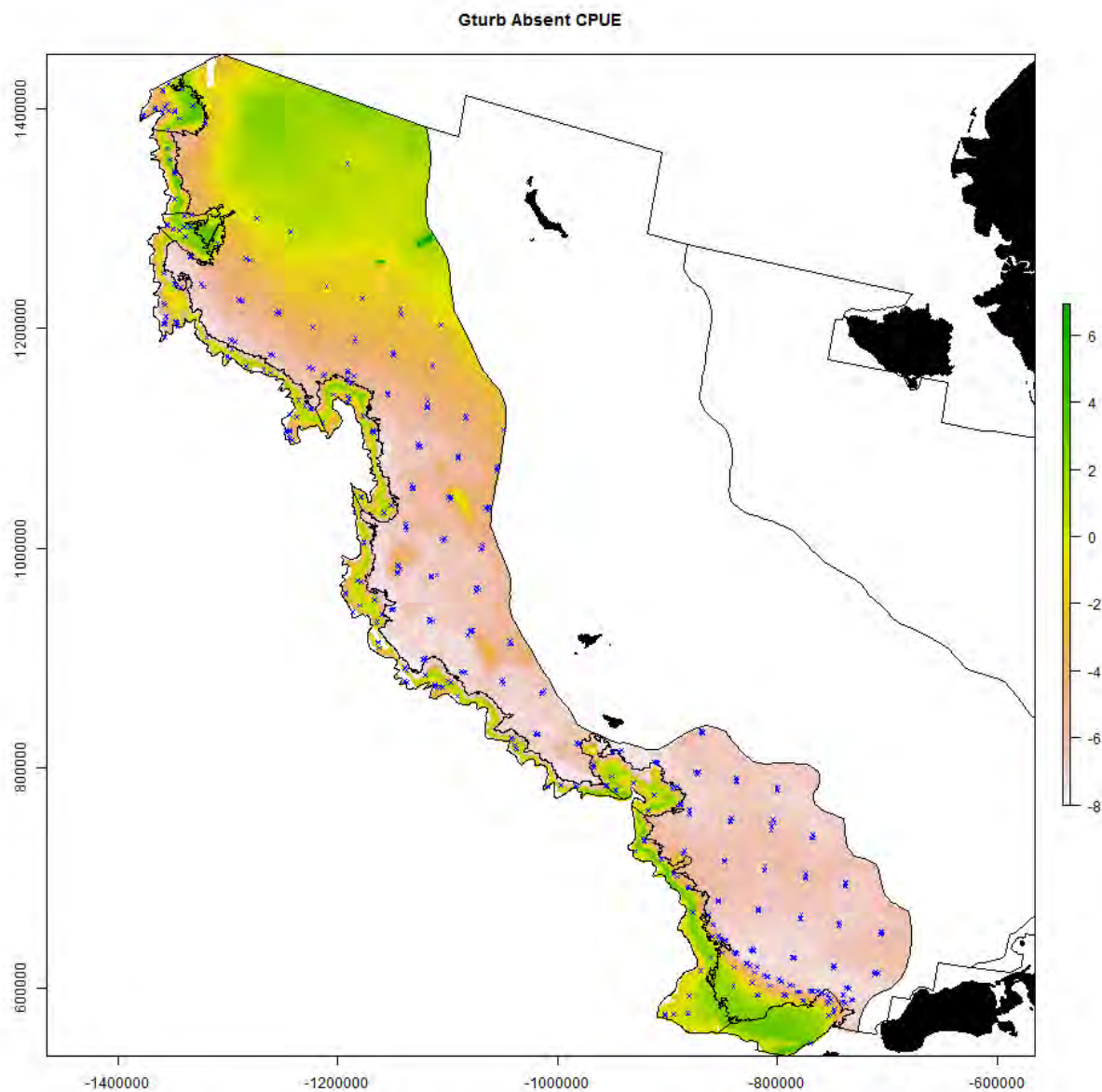
1417

1418



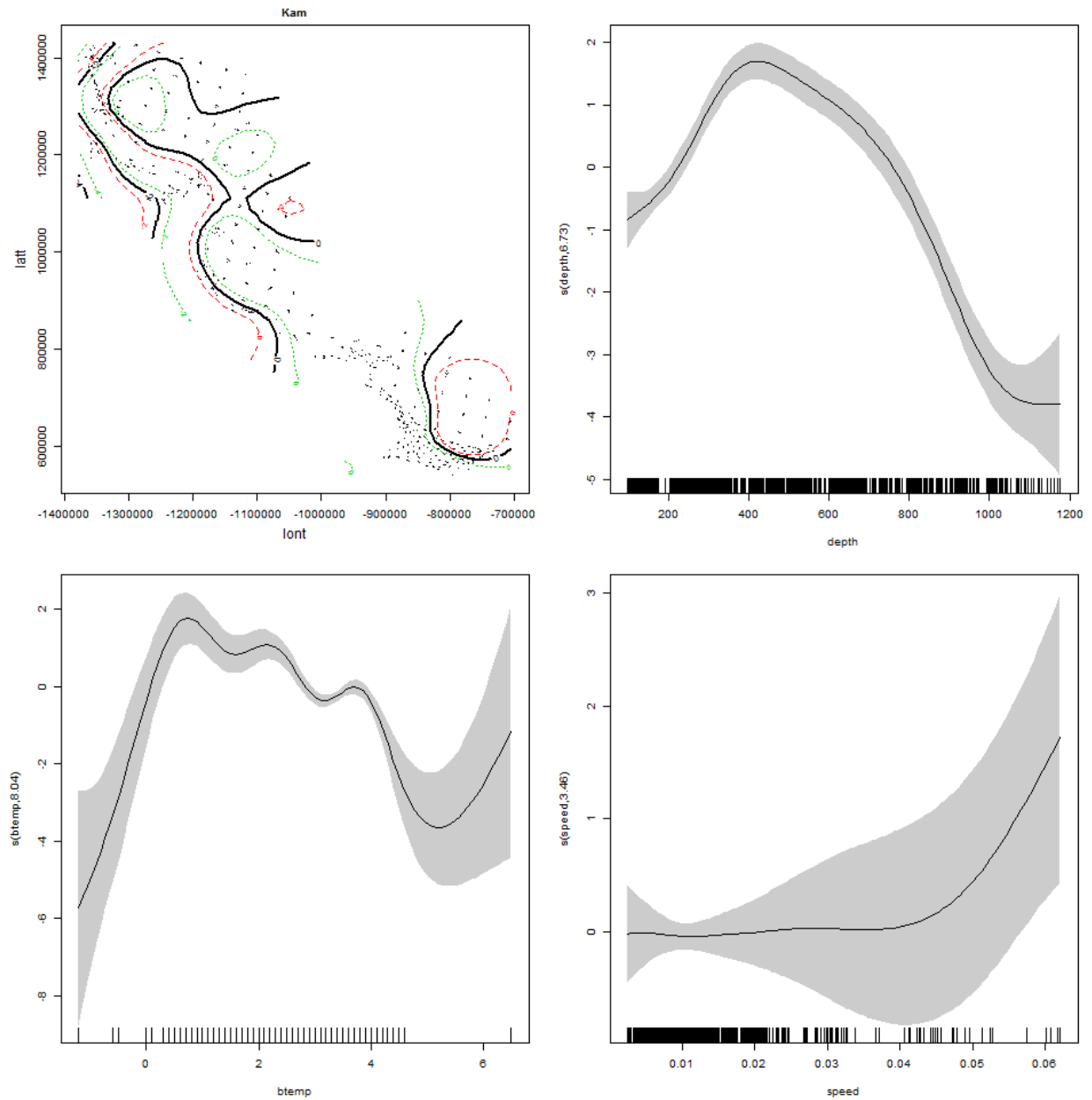
1419

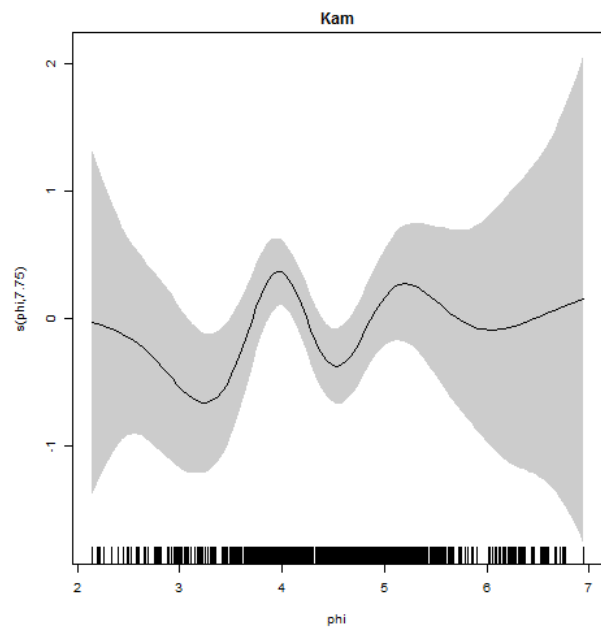
1420



1421
1422

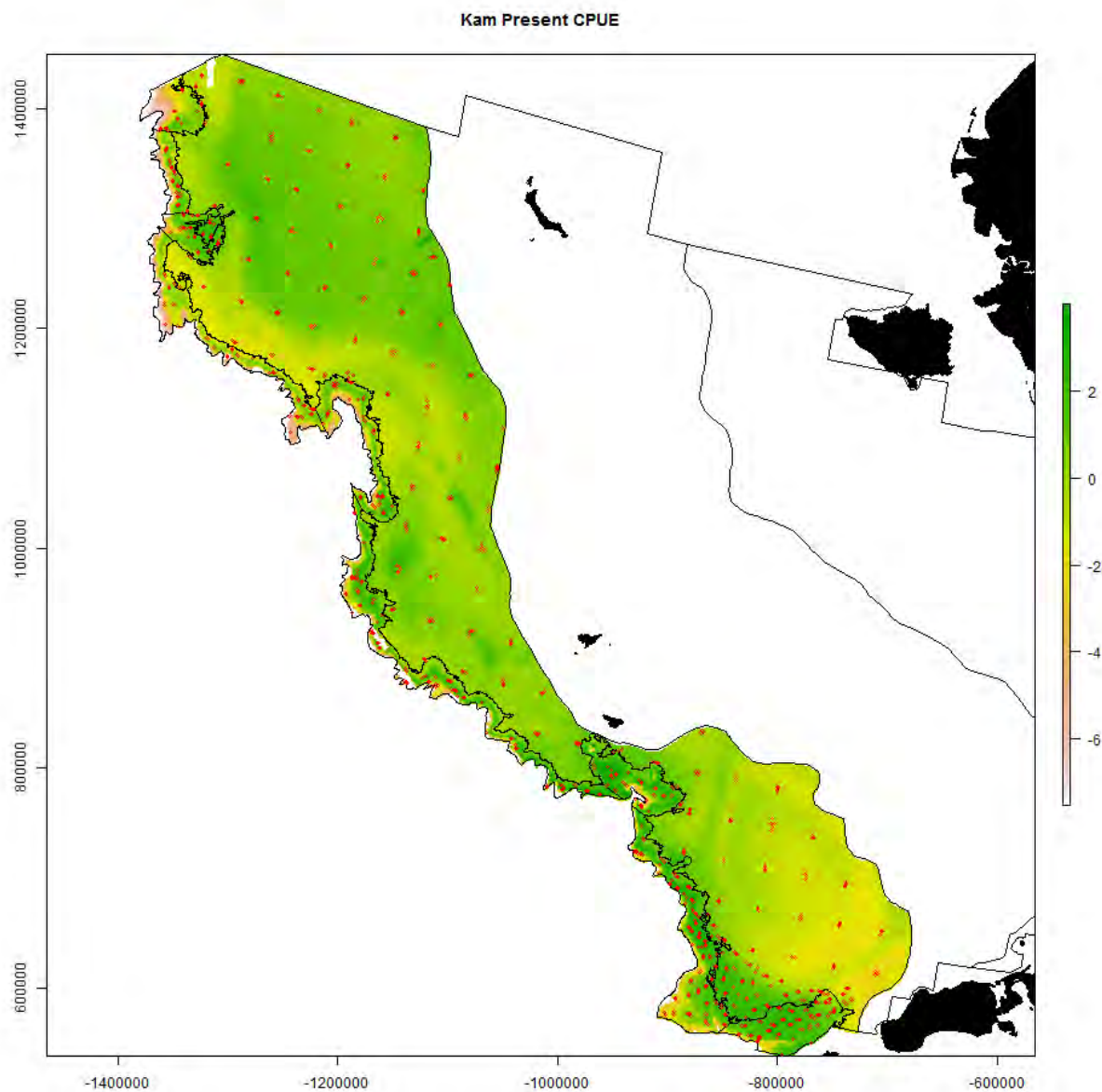
1423 S17. Generalized additive modeling results for Kamchatka flounder. In the spatial plots, the x-
 1424 axis label is easting and the y-axis label is northing and the unit is meters (Alaska Albers Equal
 1425 Area Conic projection with center latitude = 50° N and center longitude = 154° W).





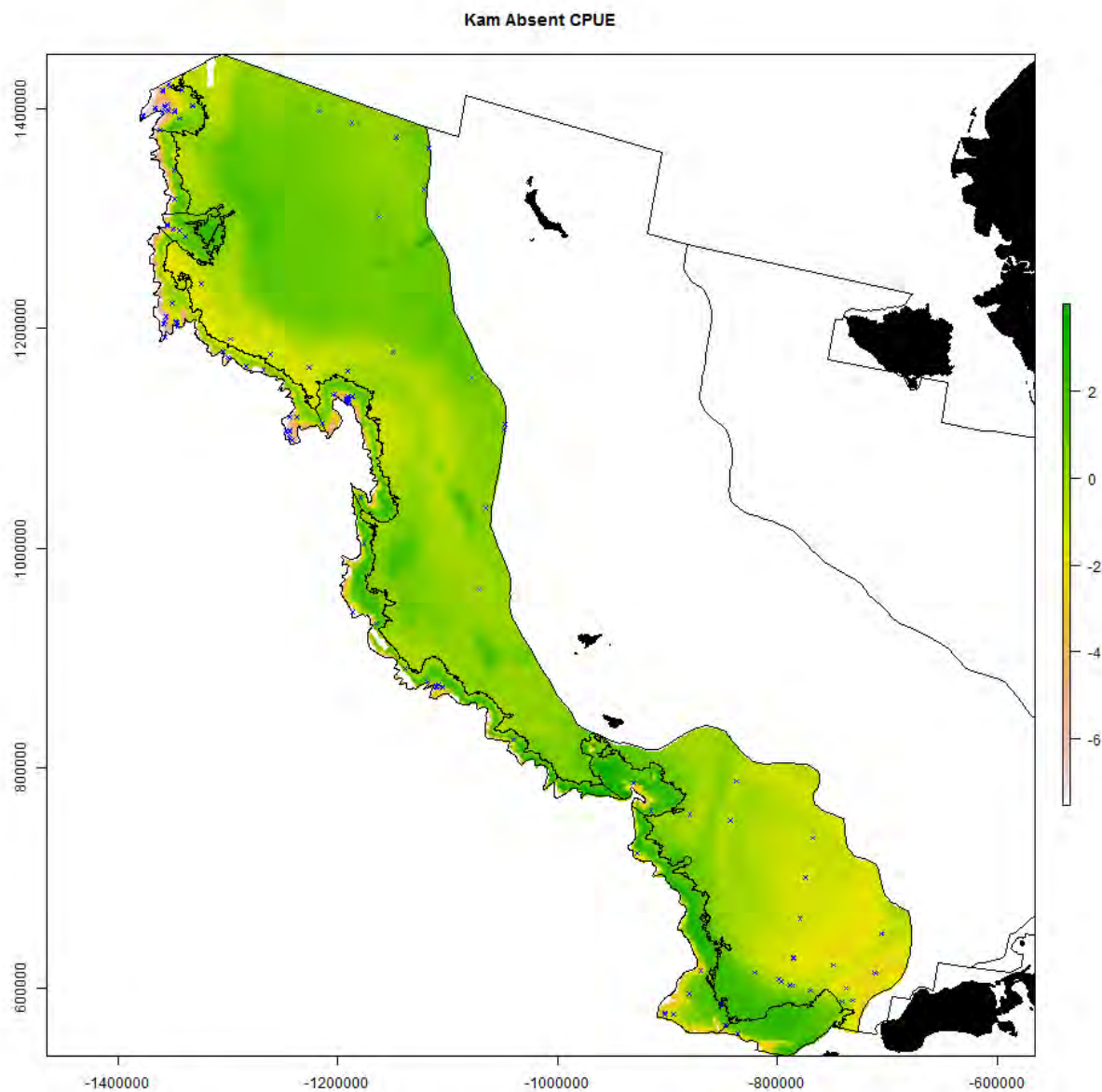
1428

1429



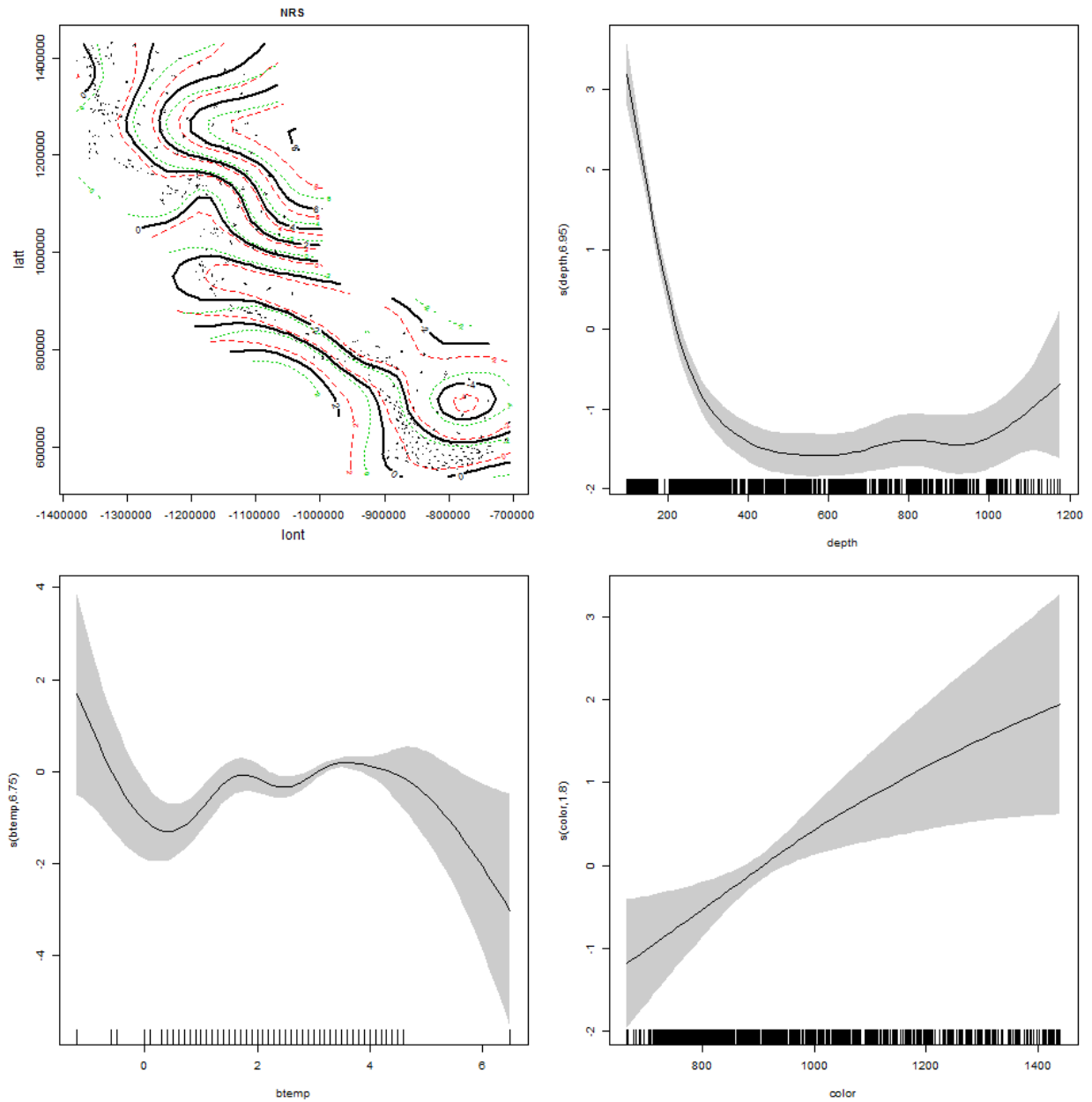
1430

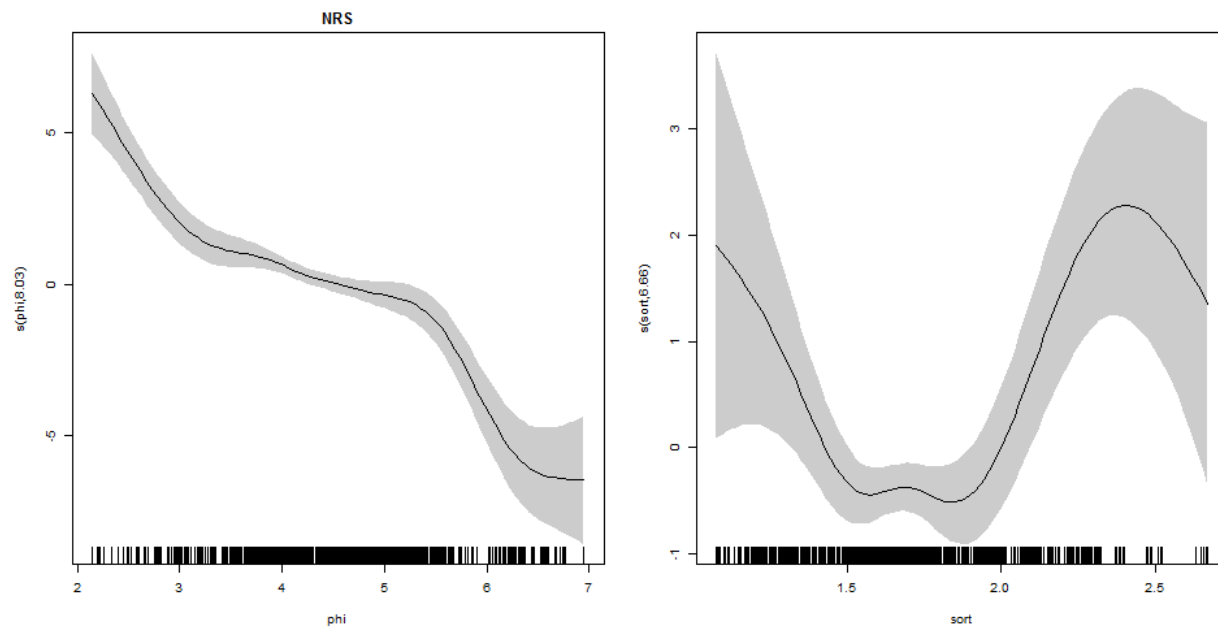
1431



1432
1433

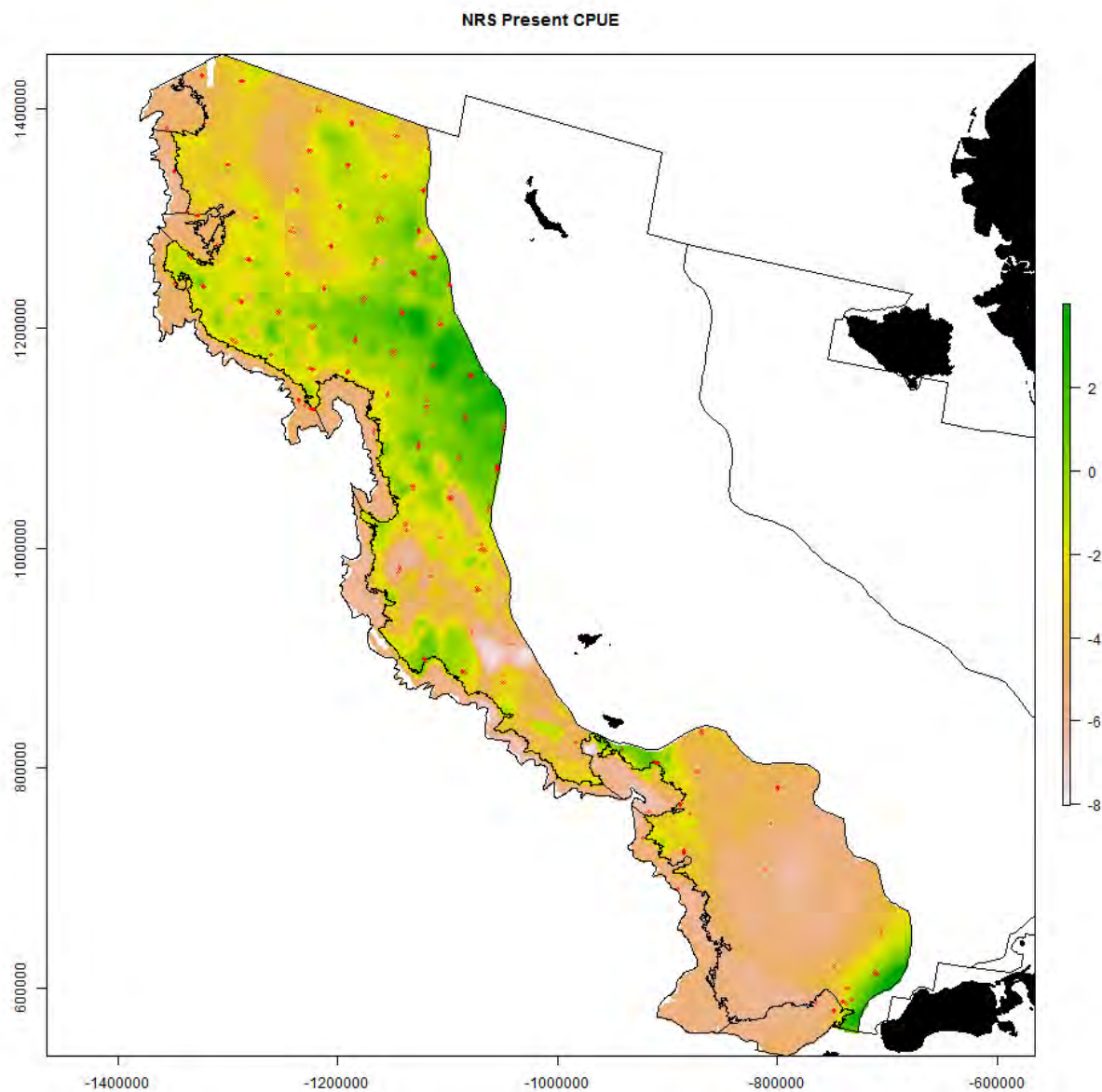
1434 S18. Generalized additive modeling results for northern rock sole. In the spatial plots, the x-axis
1435 label is easting and the y-axis label is northing and the unit is meters (Alaska Albers Equal Area
1436 Conic projection with center latitude = 50° N and center longitude = 154° W).





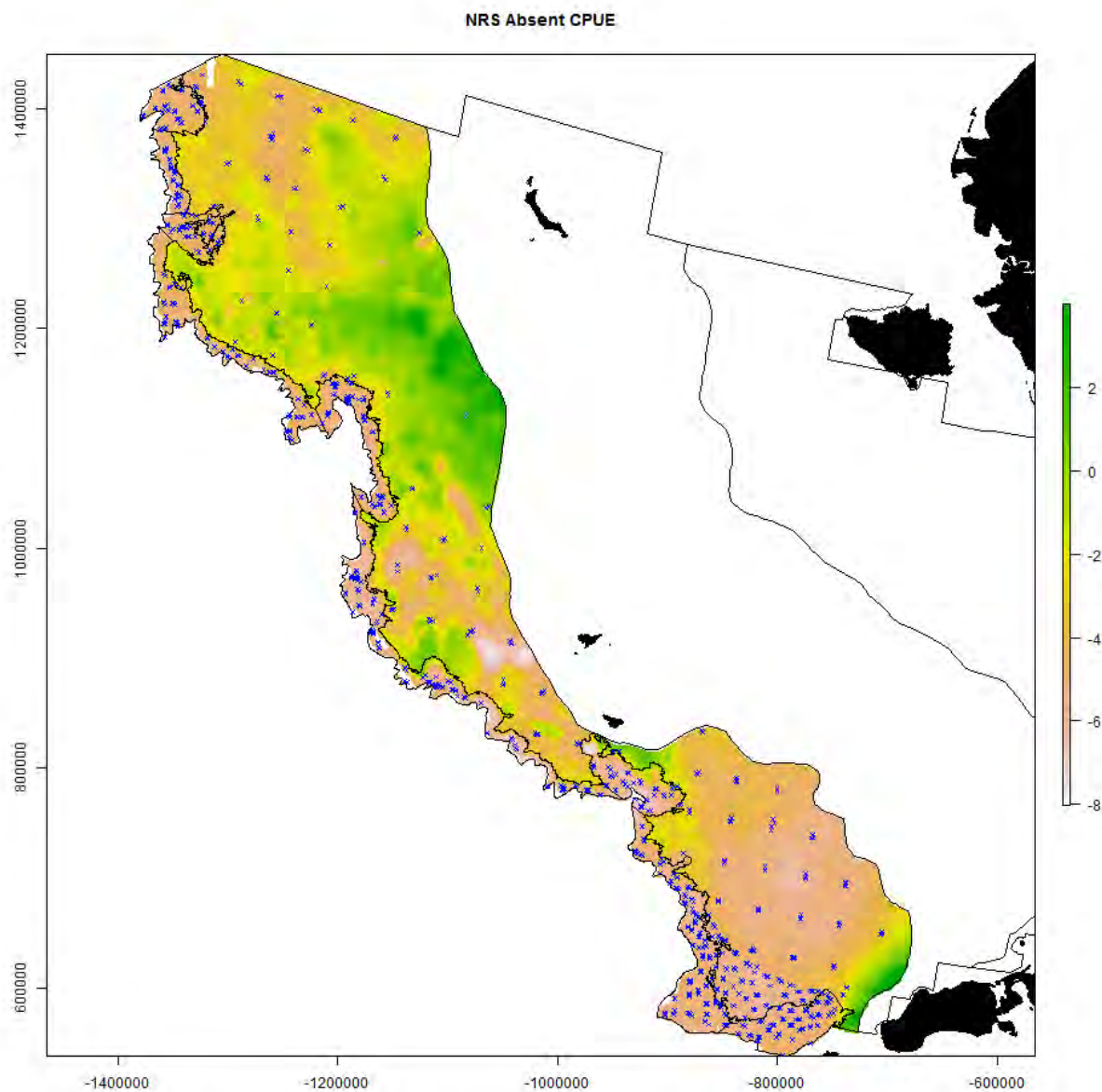
1439

1440



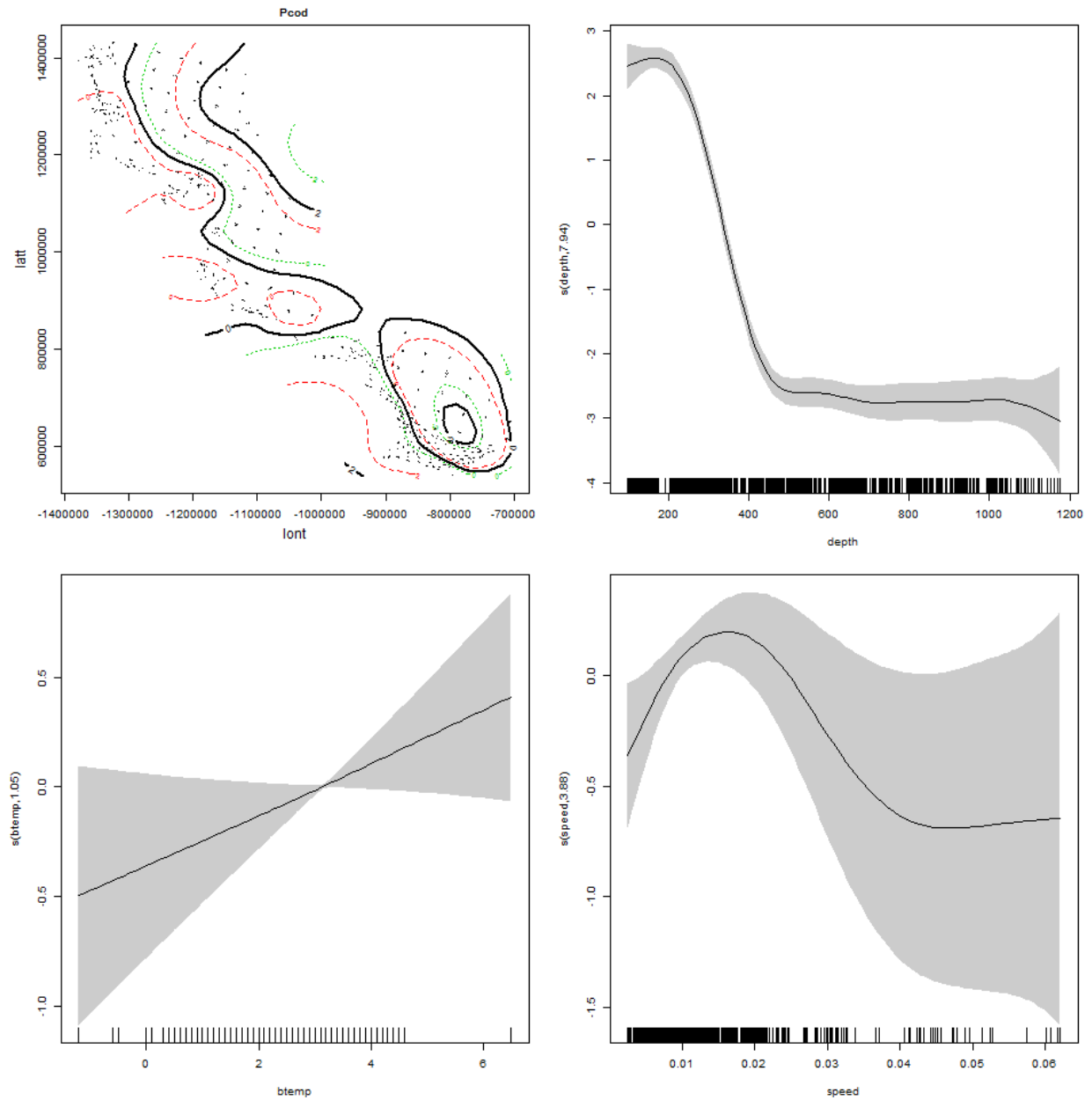
1441

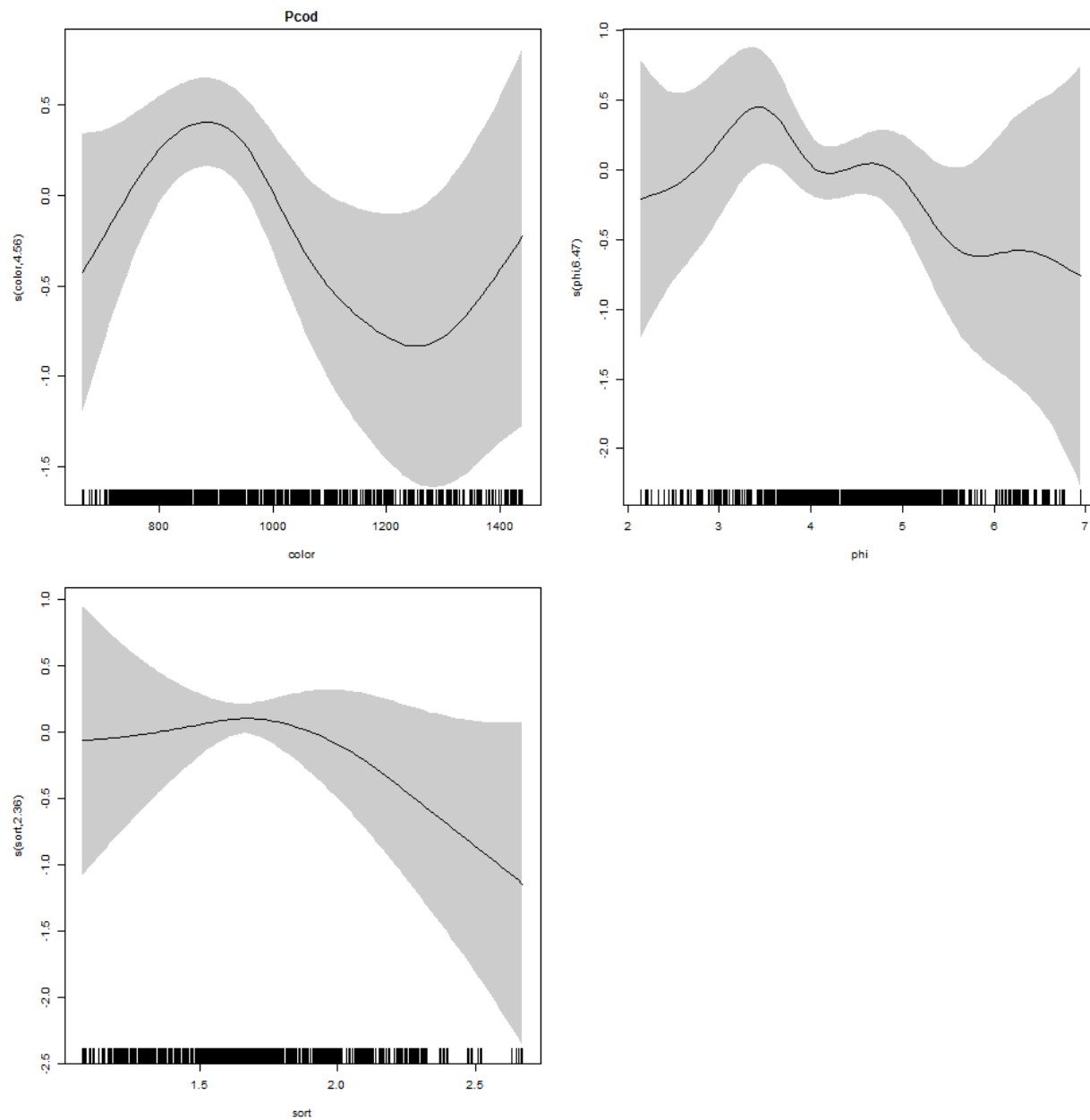
1442



1443
1444

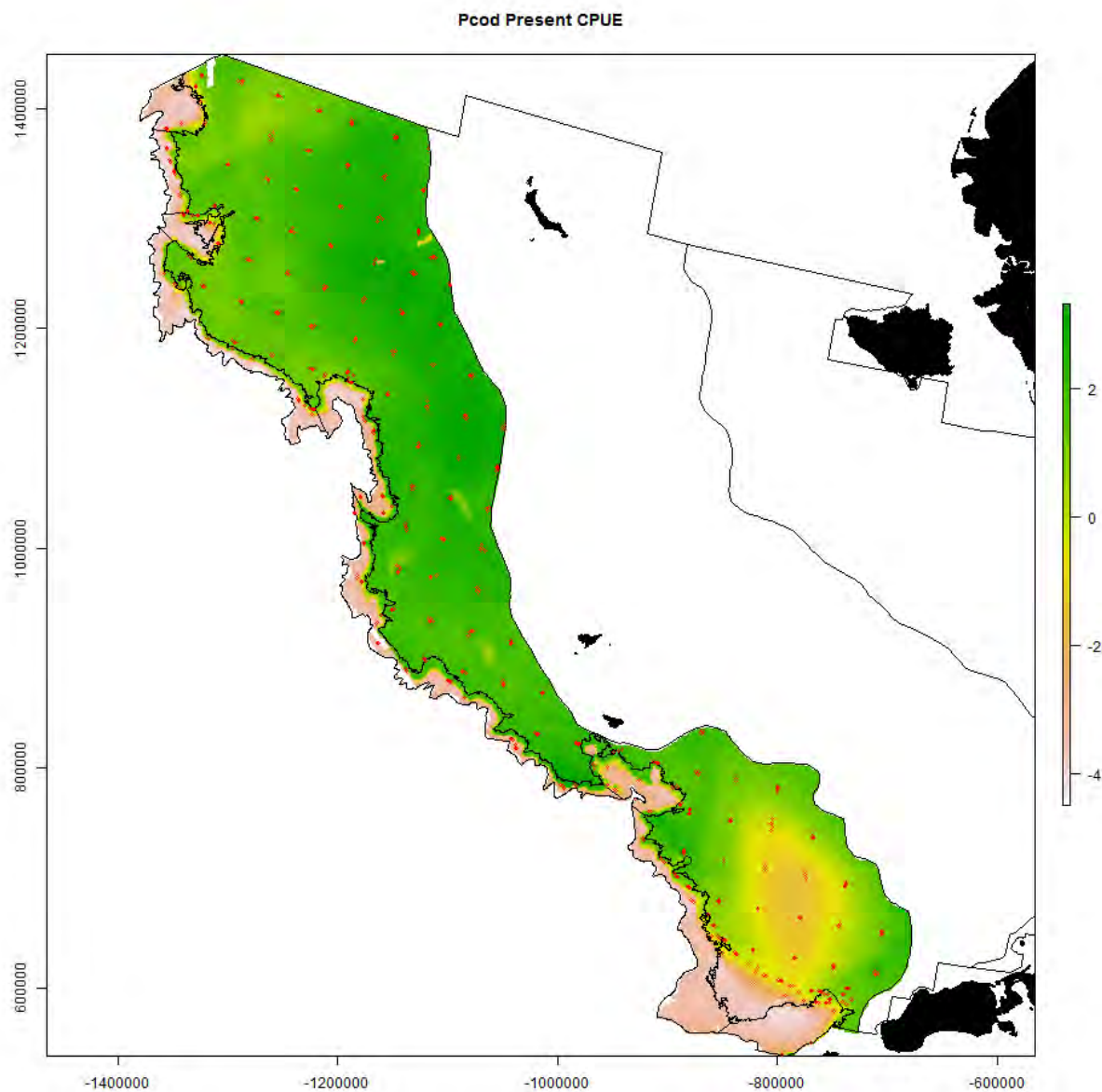
1445 S19. Generalized additive modeling results for Pacific cod. In the spatial plots, the x-axis label is
 1446 easting and the y-axis label is northing and the unit is meters (Alaska Albers Equal Area Conic
 1447 projection with center latitude = 50° N and center longitude = 154° W).





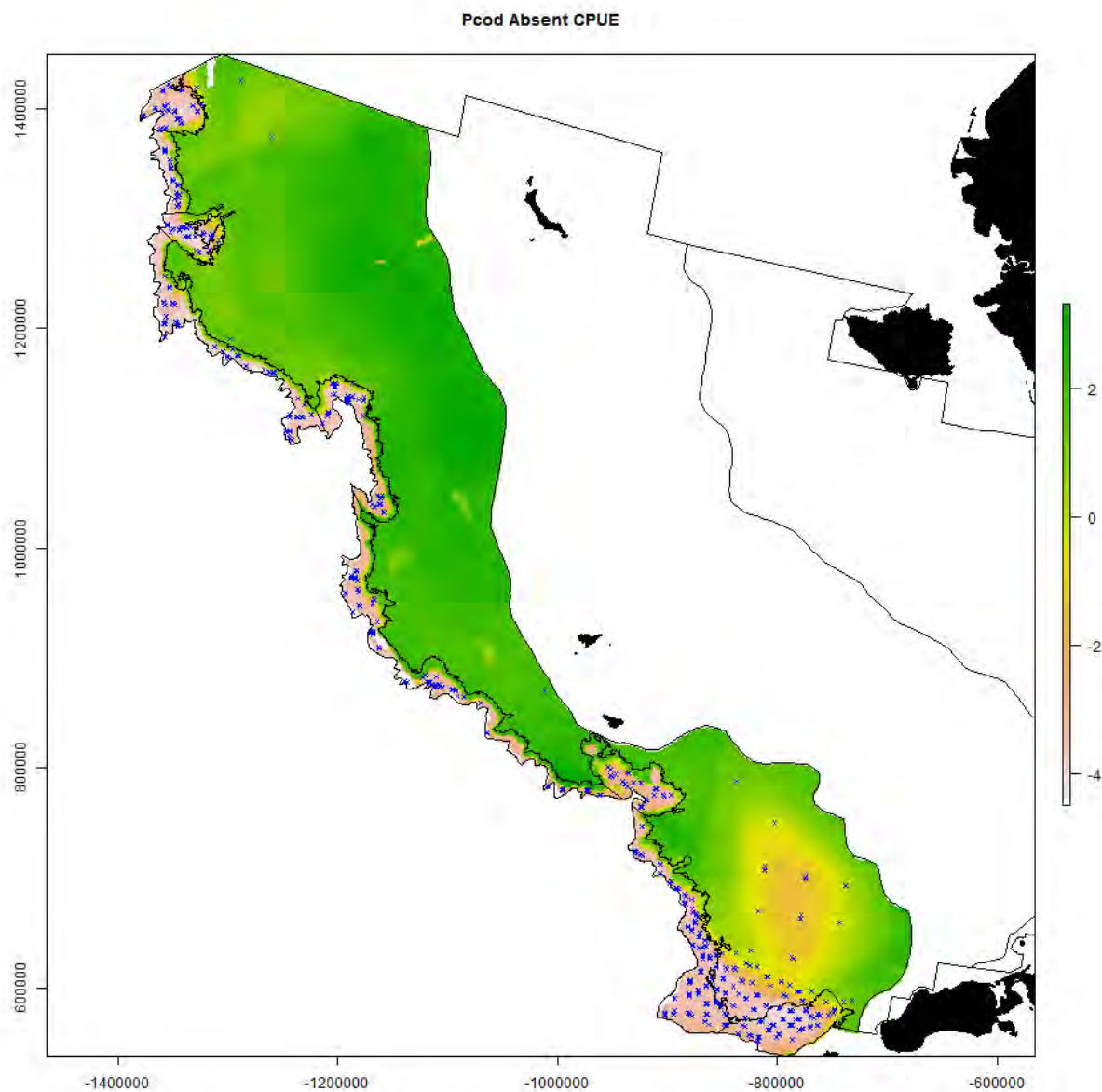
1450

1451



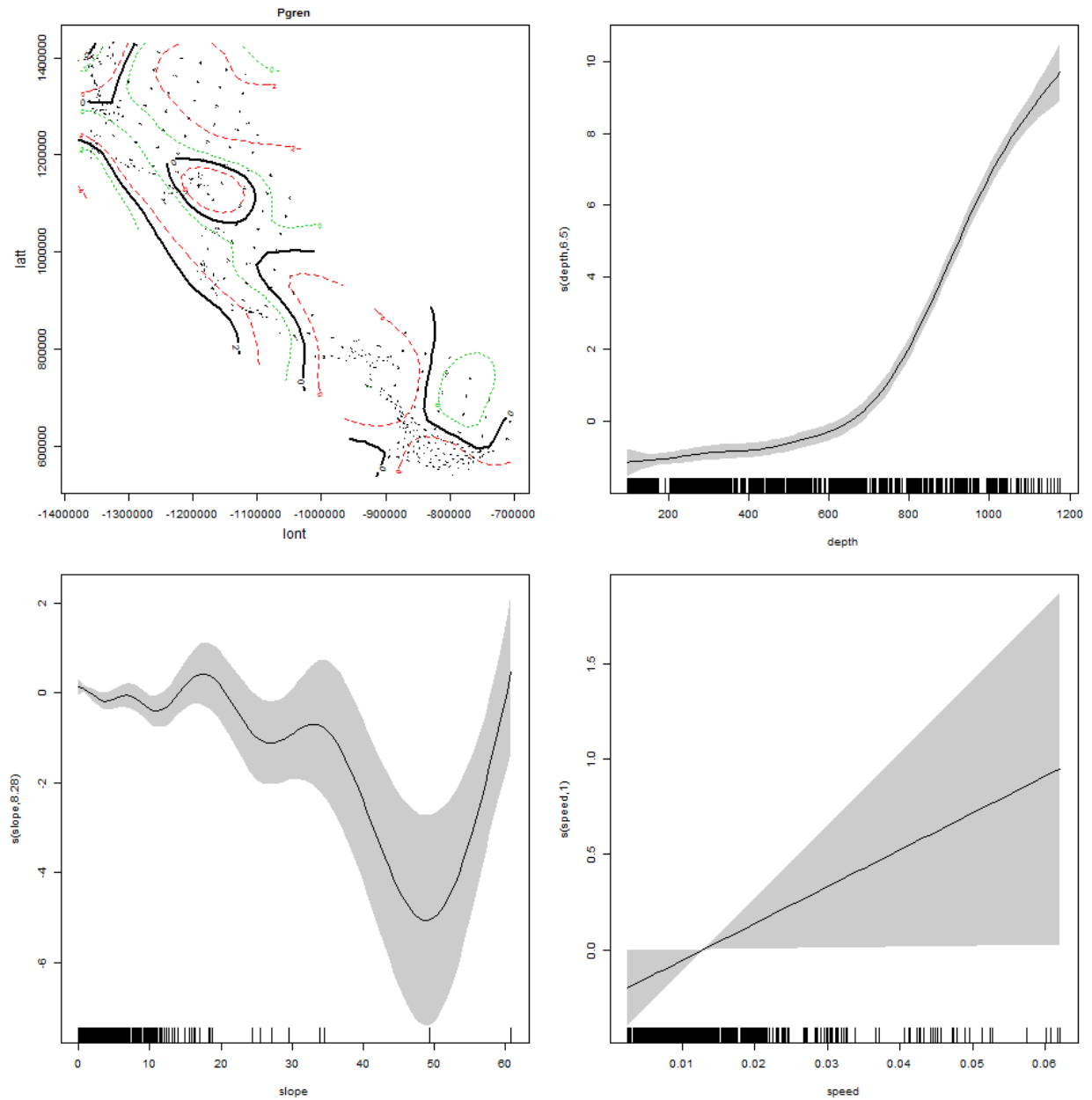
1452

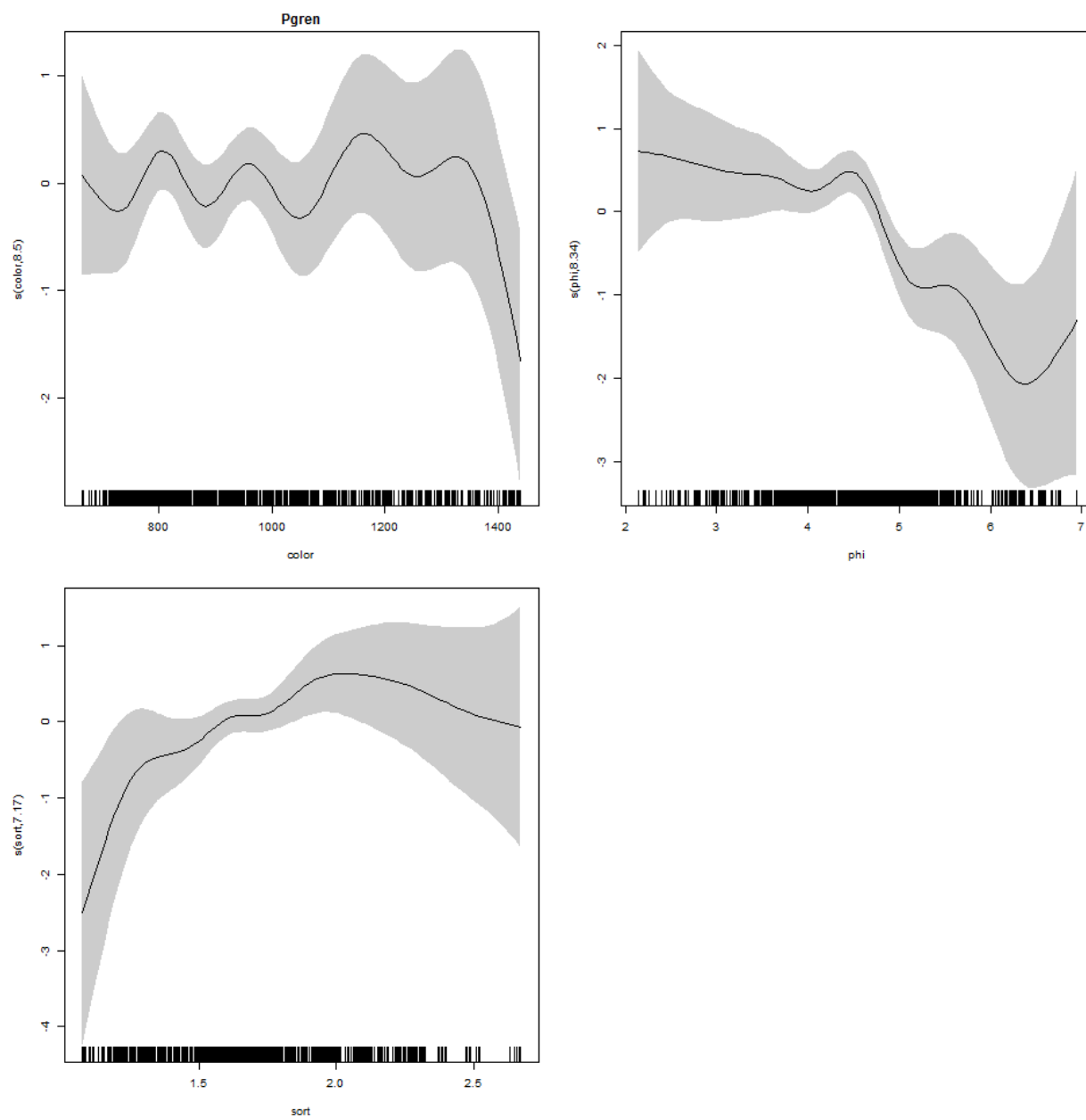
1453



1454
1455

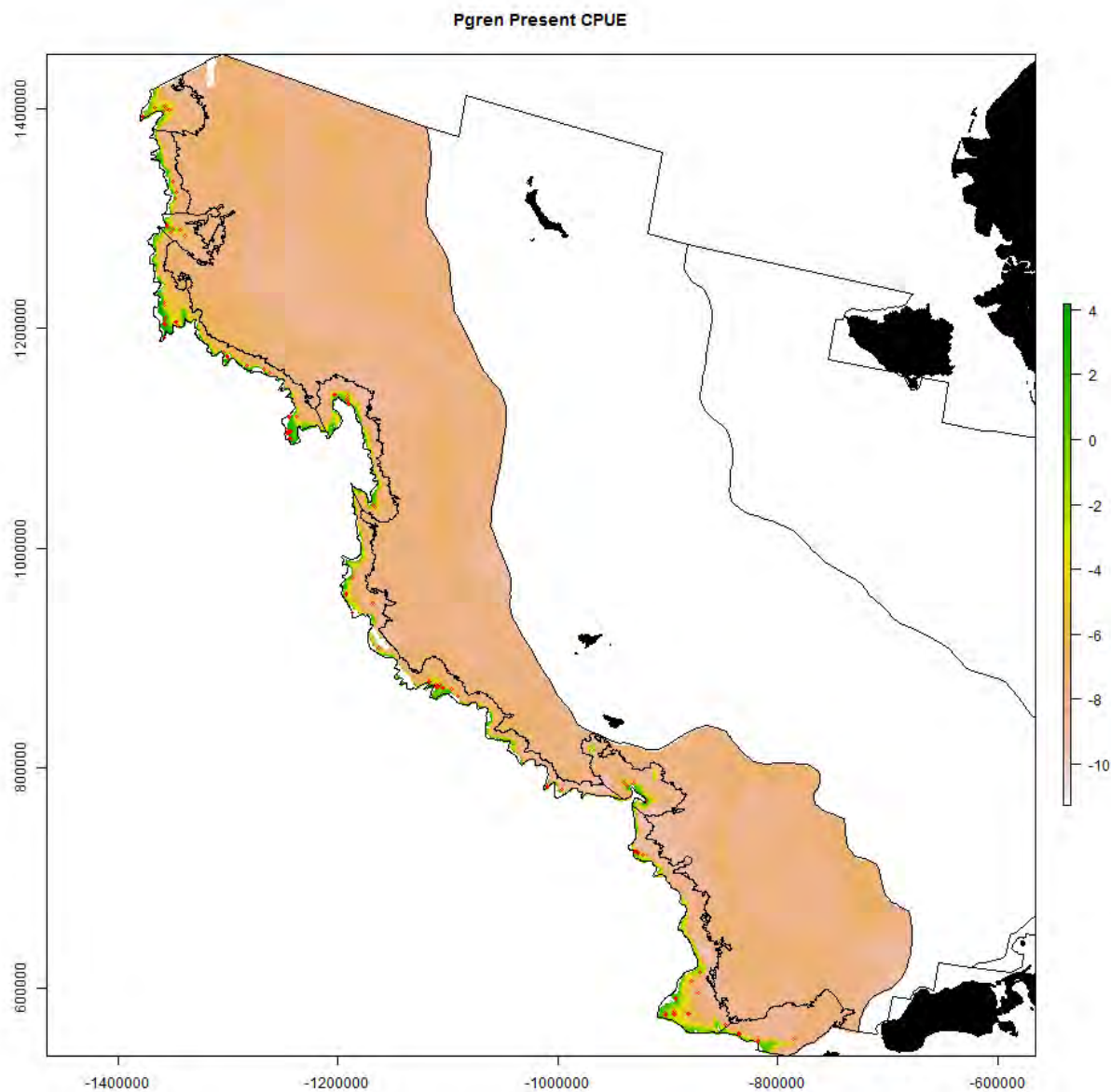
1456 S20. Generalized additive modeling results for Pacific grenadier. In the spatial plots, the x-axis label is easting and the y-axis label is northing and the unit is meters (Alaska Albers Equal Area
 1457 label is easting and the y-axis label is northing and the unit is meters (Alaska Albers Equal Area
 1458 Conic projection with center latitude = 50° N and center longitude = 154° W).





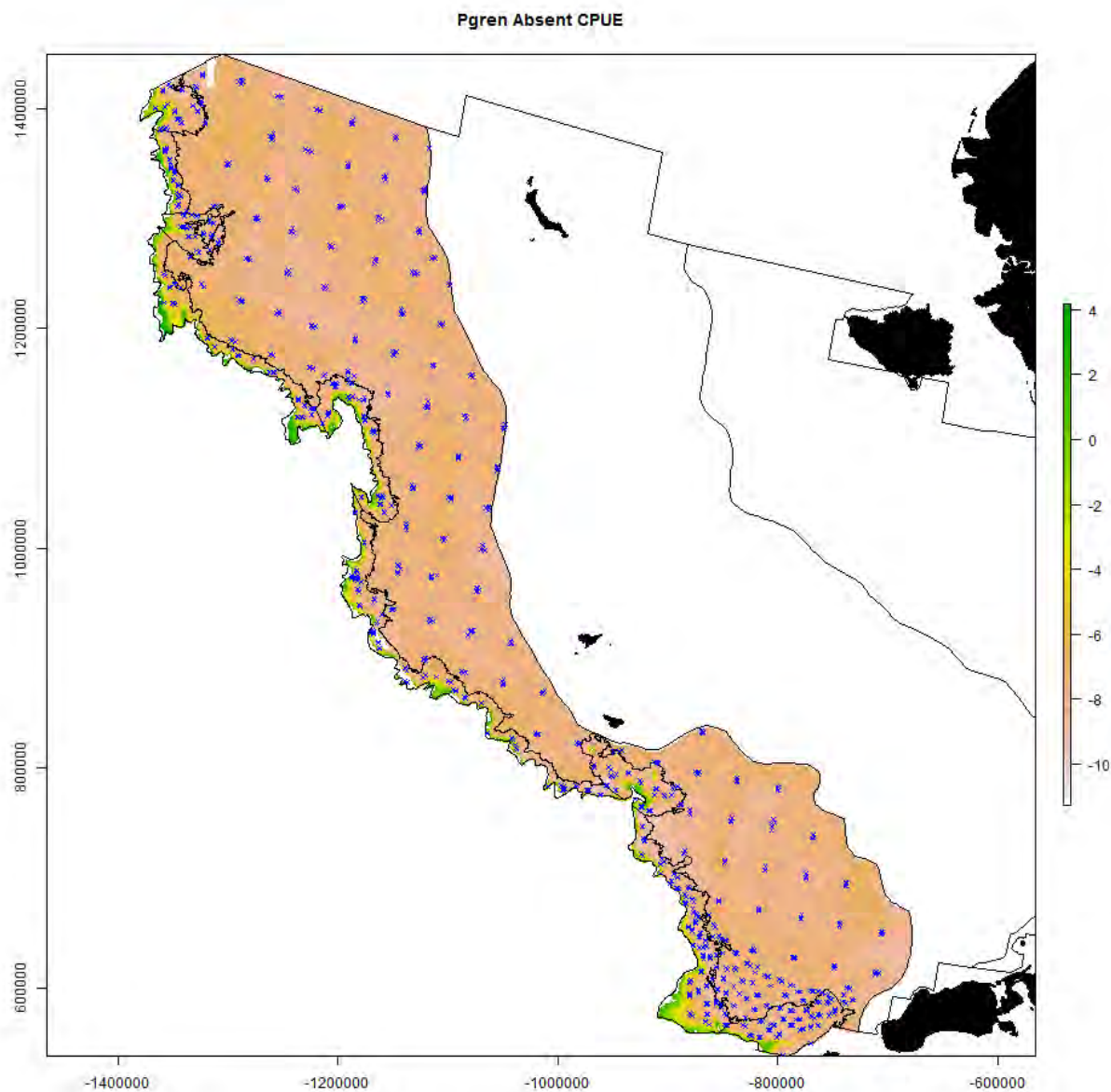
1461

1462



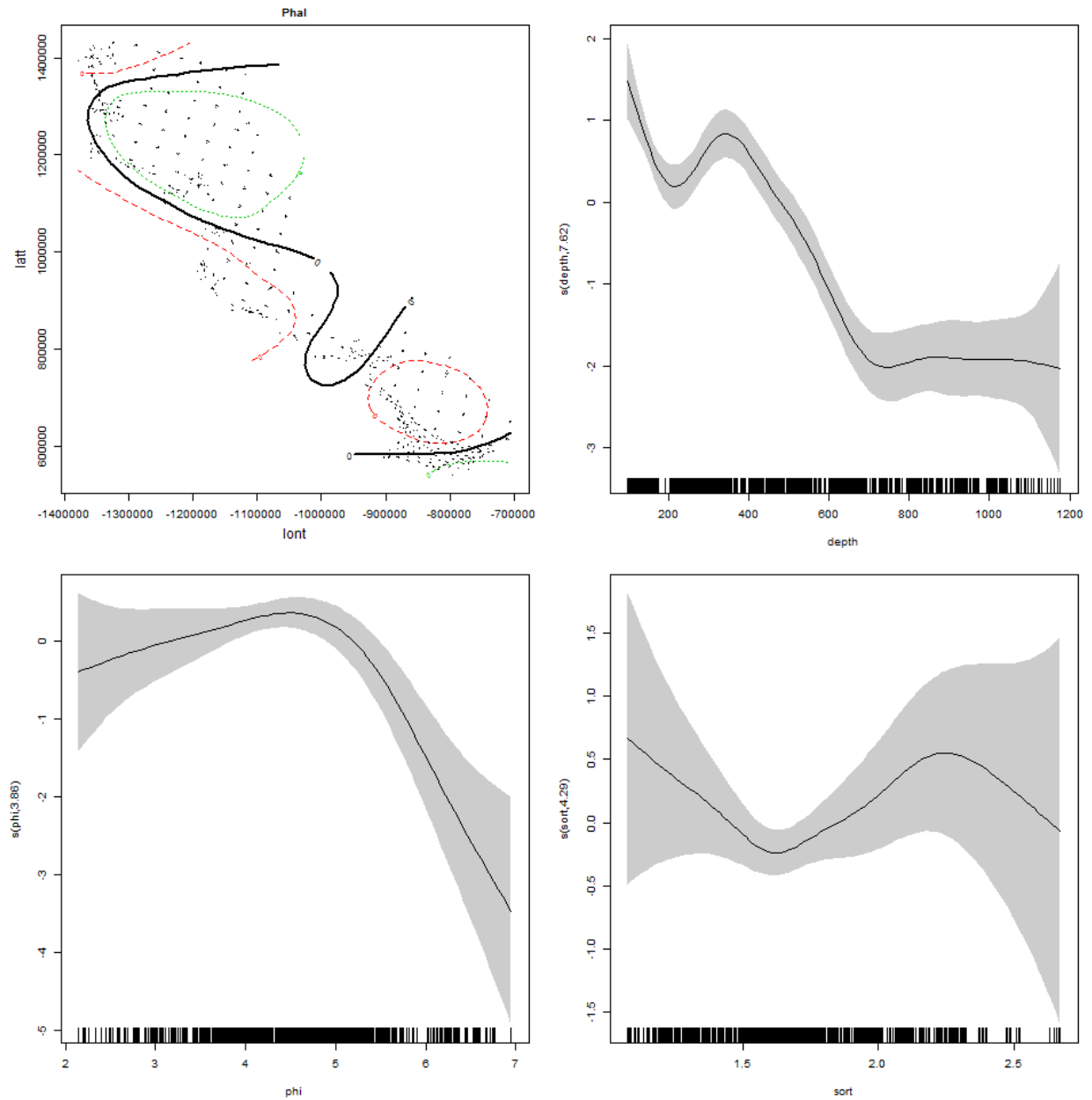
1463

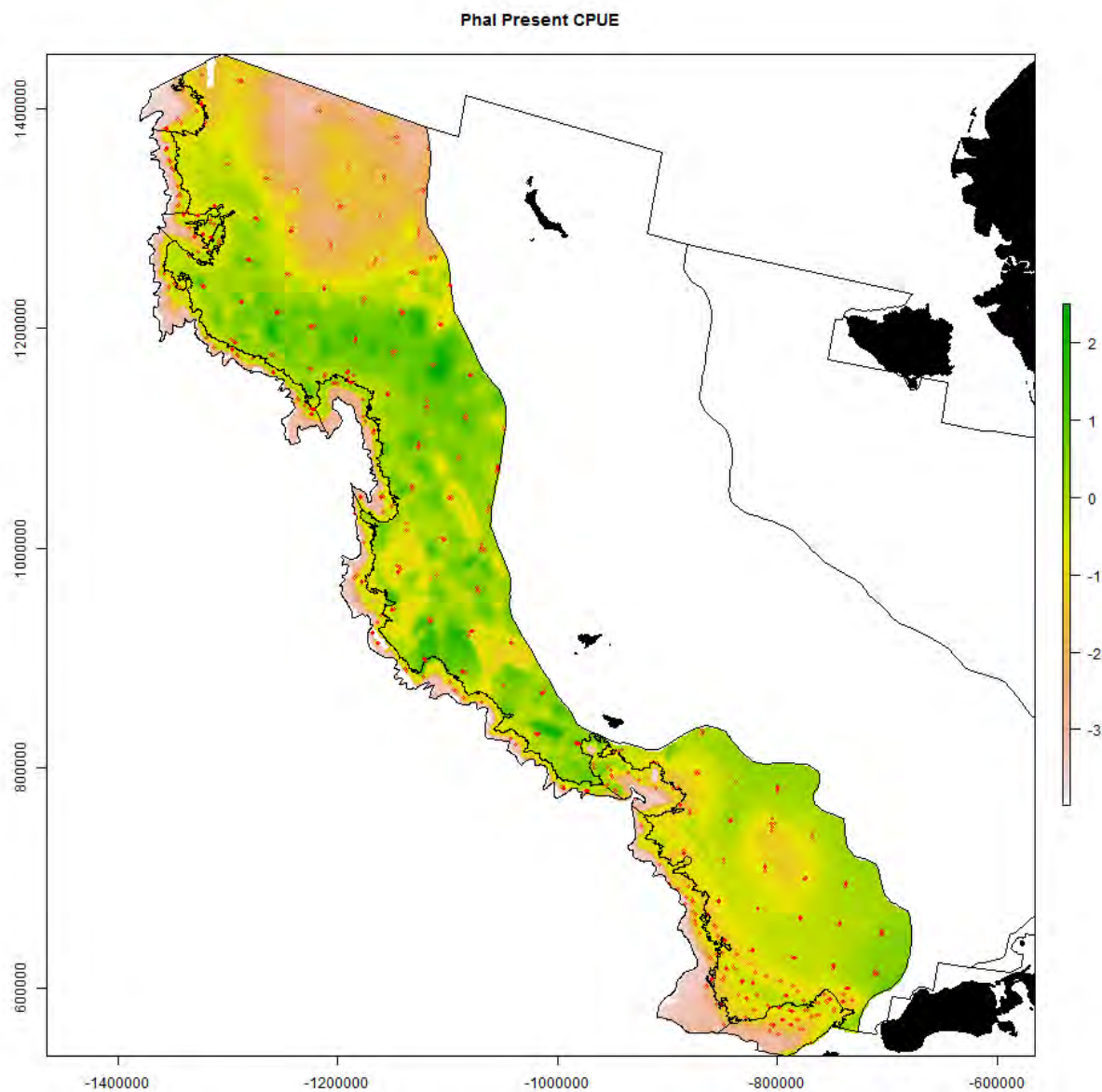
1464



1465
1466

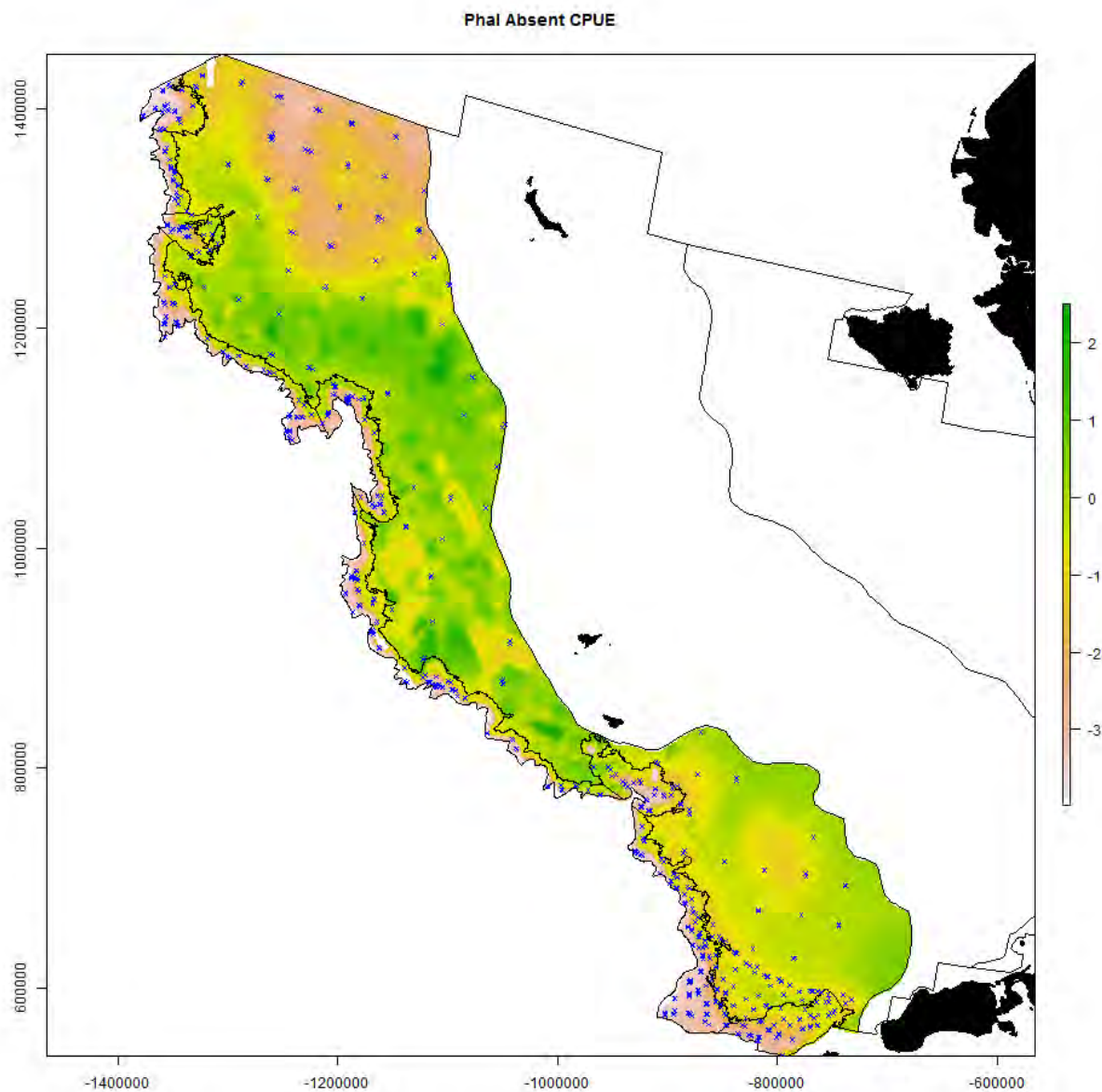
1467 S21. Generalized additive modeling results for Pacific halibut. In the spatial plots, the x-axis
 1468 label is easting and the y-axis label is northing and the unit is meters (Alaska Albers Equal Area
 1469 Conic projection with center latitude = 50° N and center longitude = 154° W).





1472

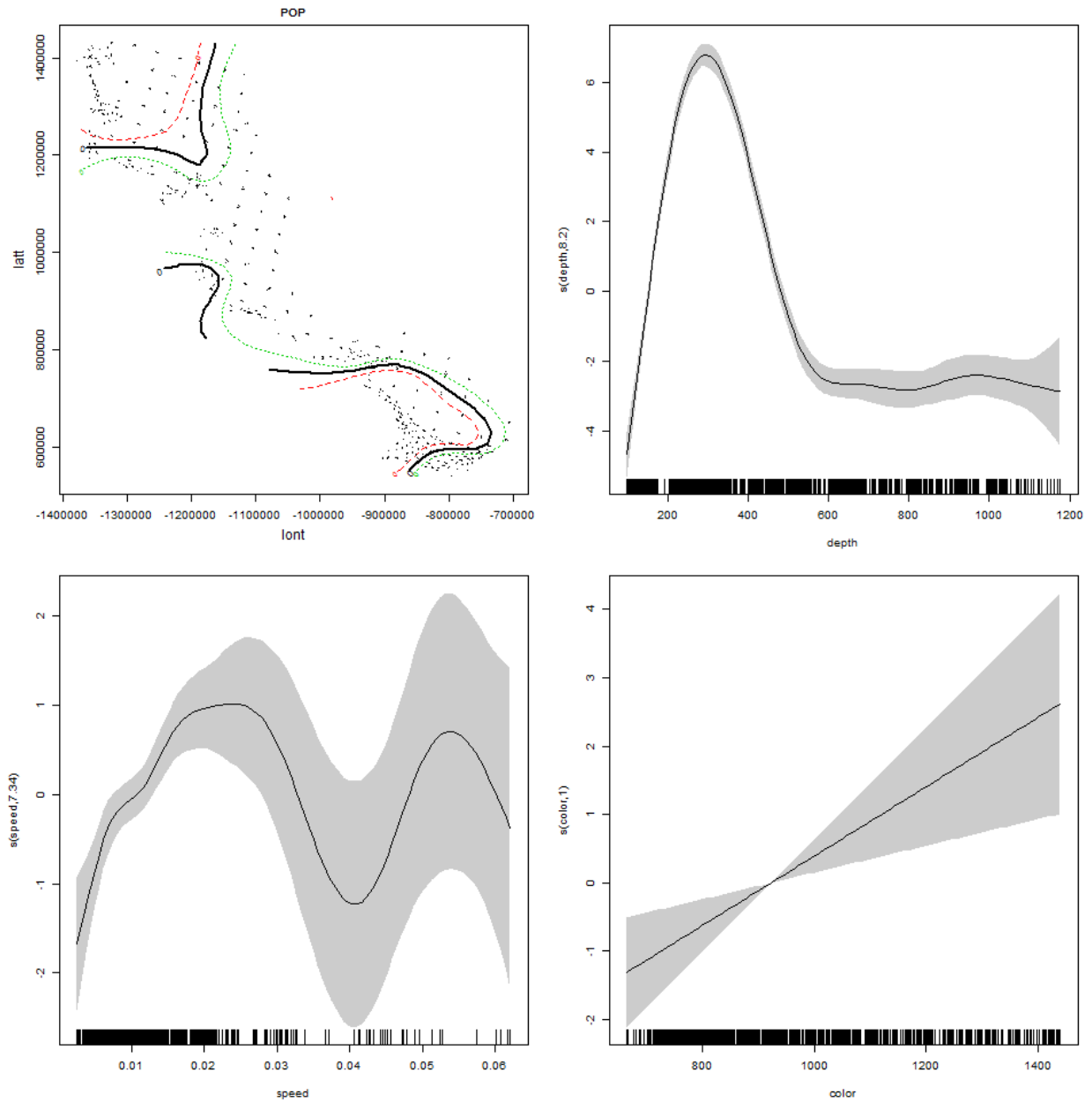
1473

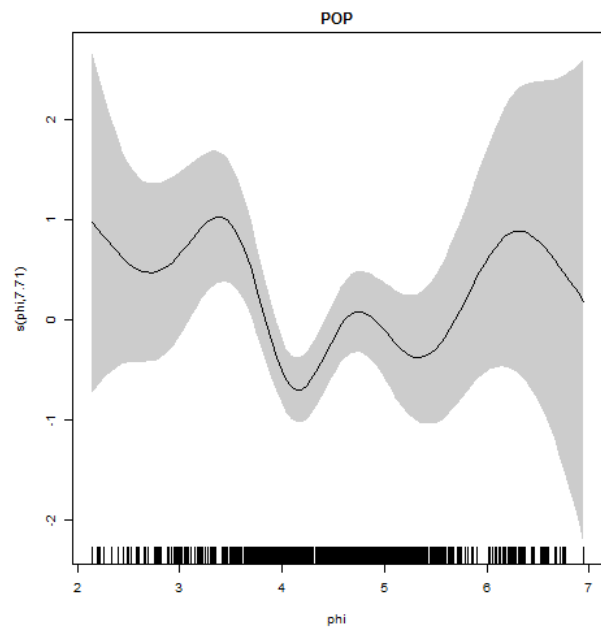


1474

1475

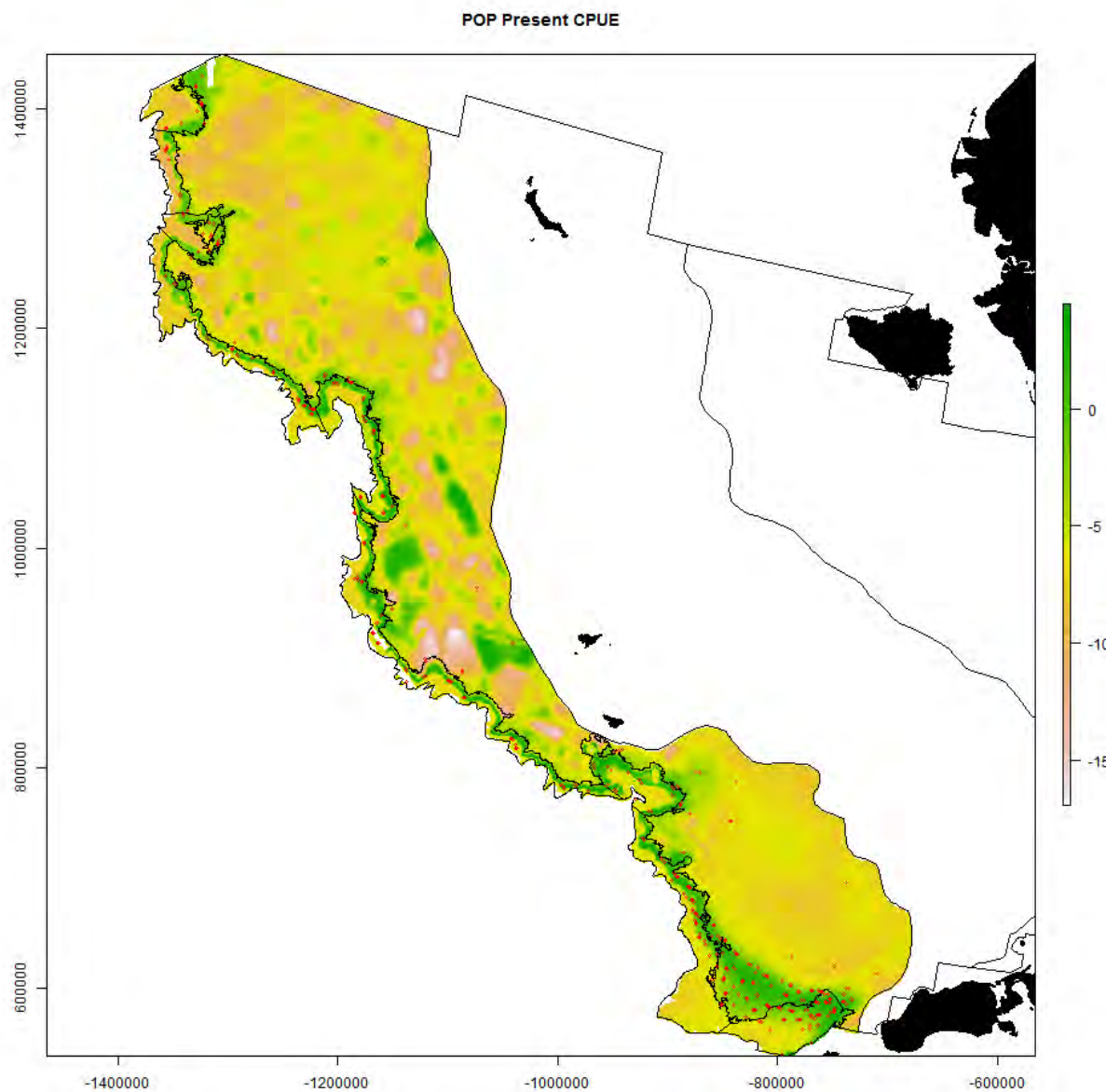
1476 S22. Generalized additive modeling results for Pacific Ocean perch. In the spatial plots, the x-
 1477 axis label is easting and the y-axis label is northing and the unit is meters (Alaska Albers Equal
 1478 Area Conic projection with center latitude = 50° N and center longitude = 154° W).





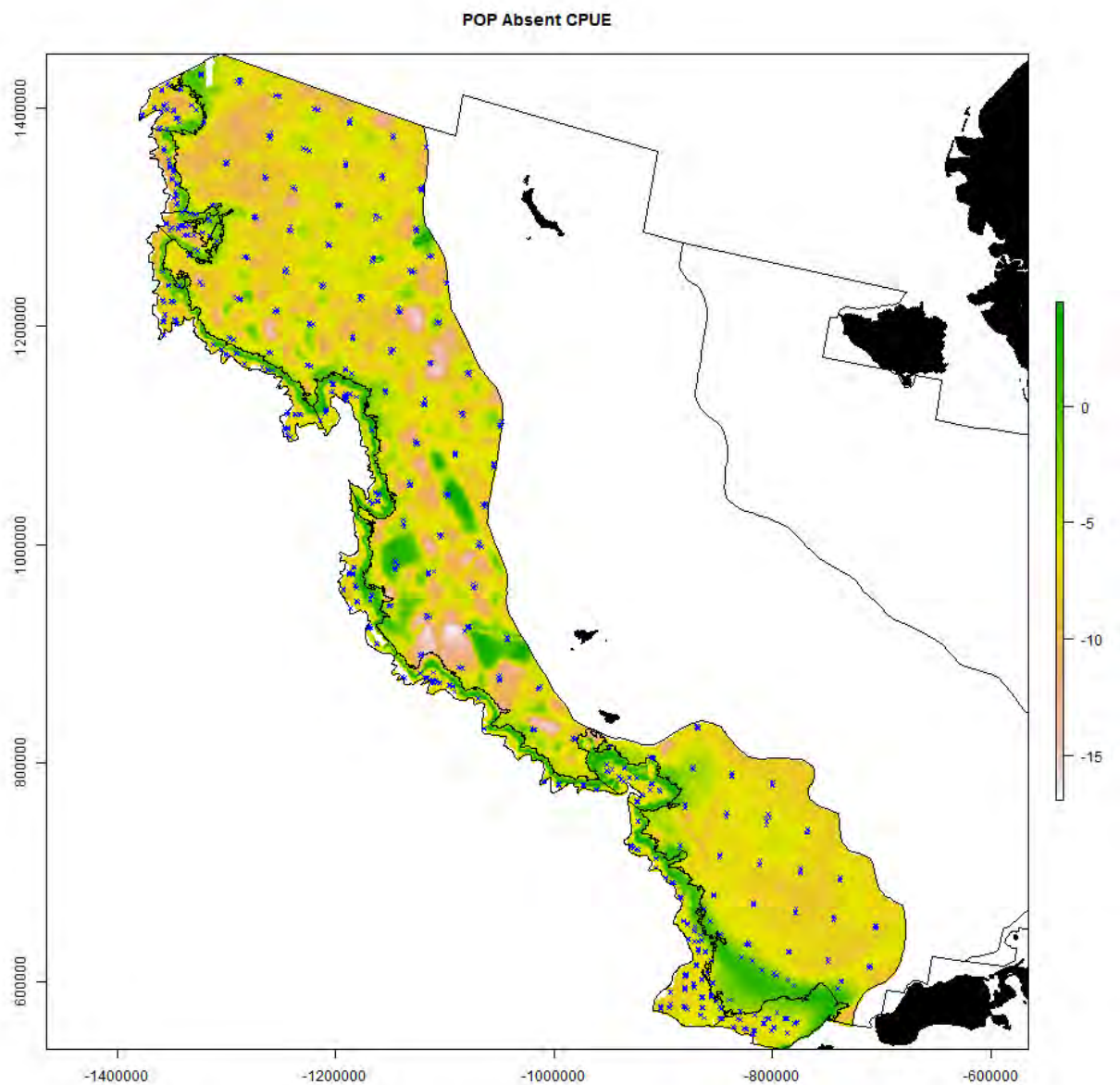
1481

1482



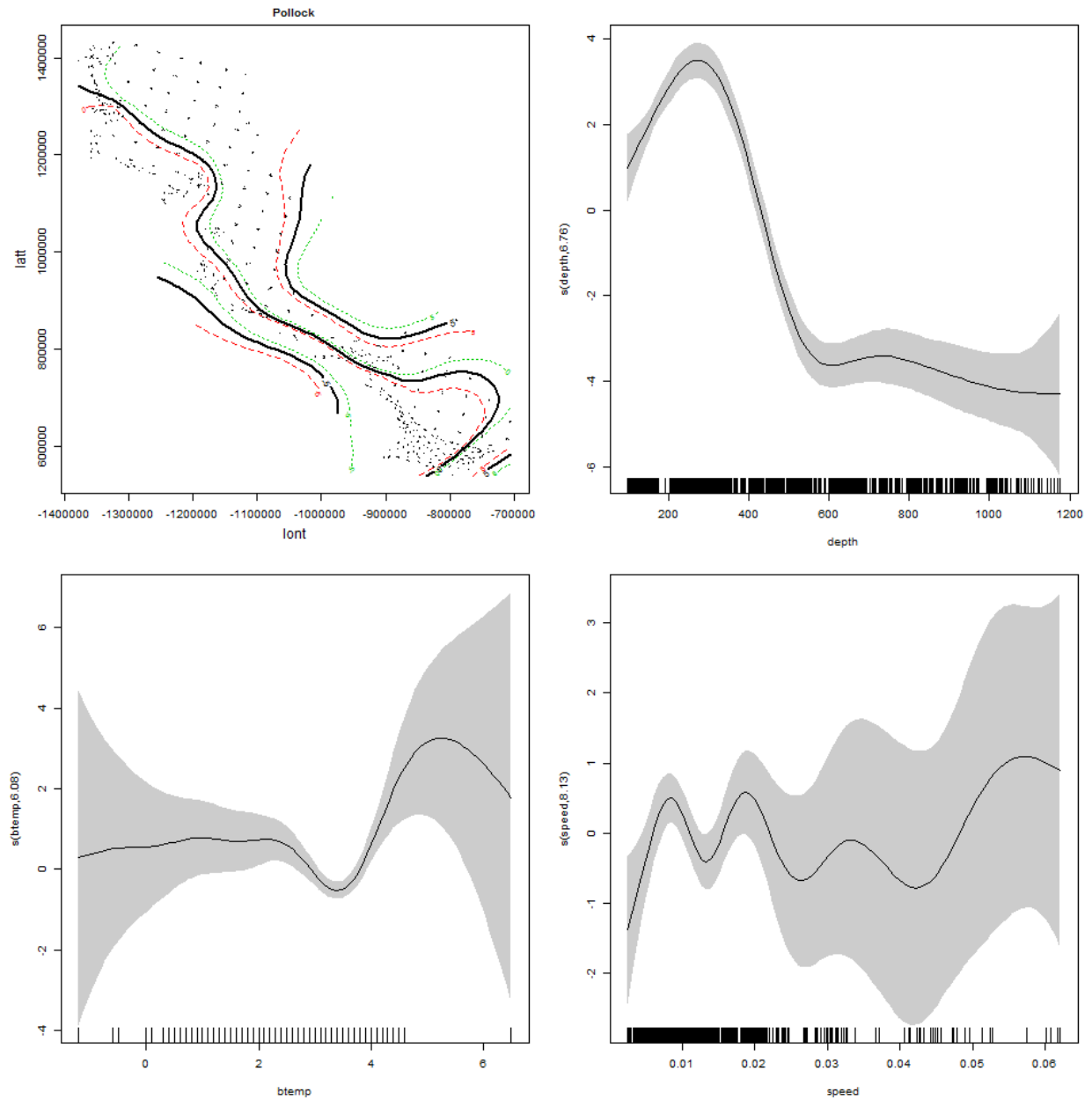
1483

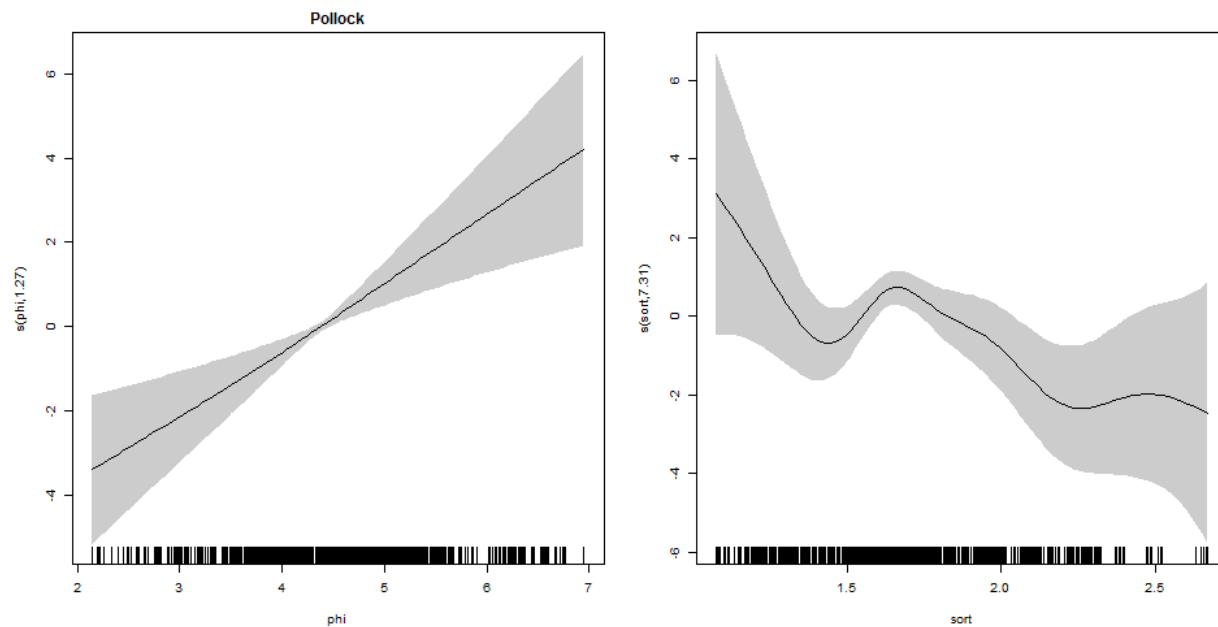
1484



1485
1486

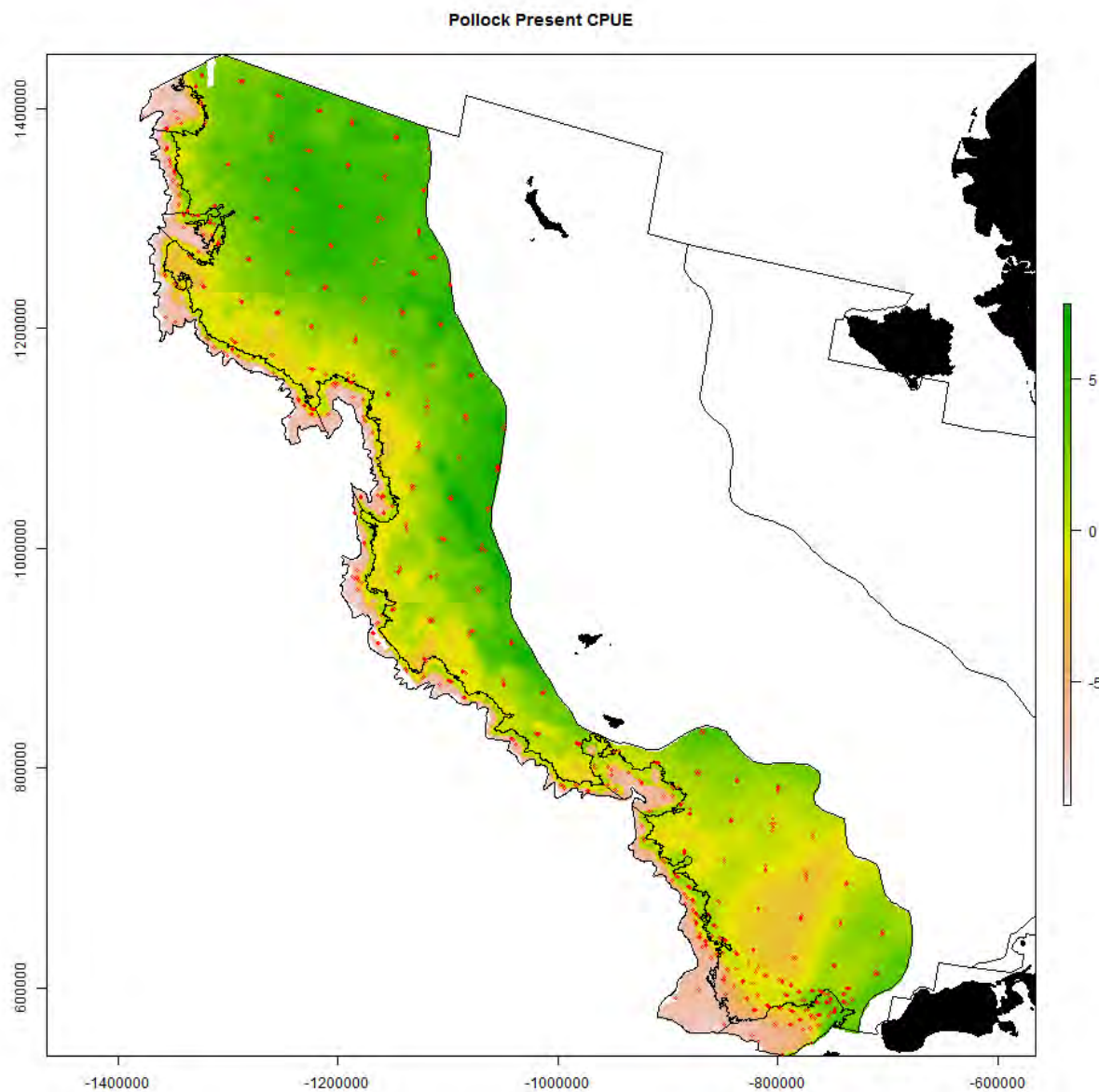
1487 S23. Generalized additive modeling results for walleye pollock. In the spatial plots, the x-axis
 1488 label is easting and the y-axis label is northing and the unit is meters (Alaska Albers Equal Area
 1489 Conic projection with center latitude = 50° N and center longitude = 154° W).





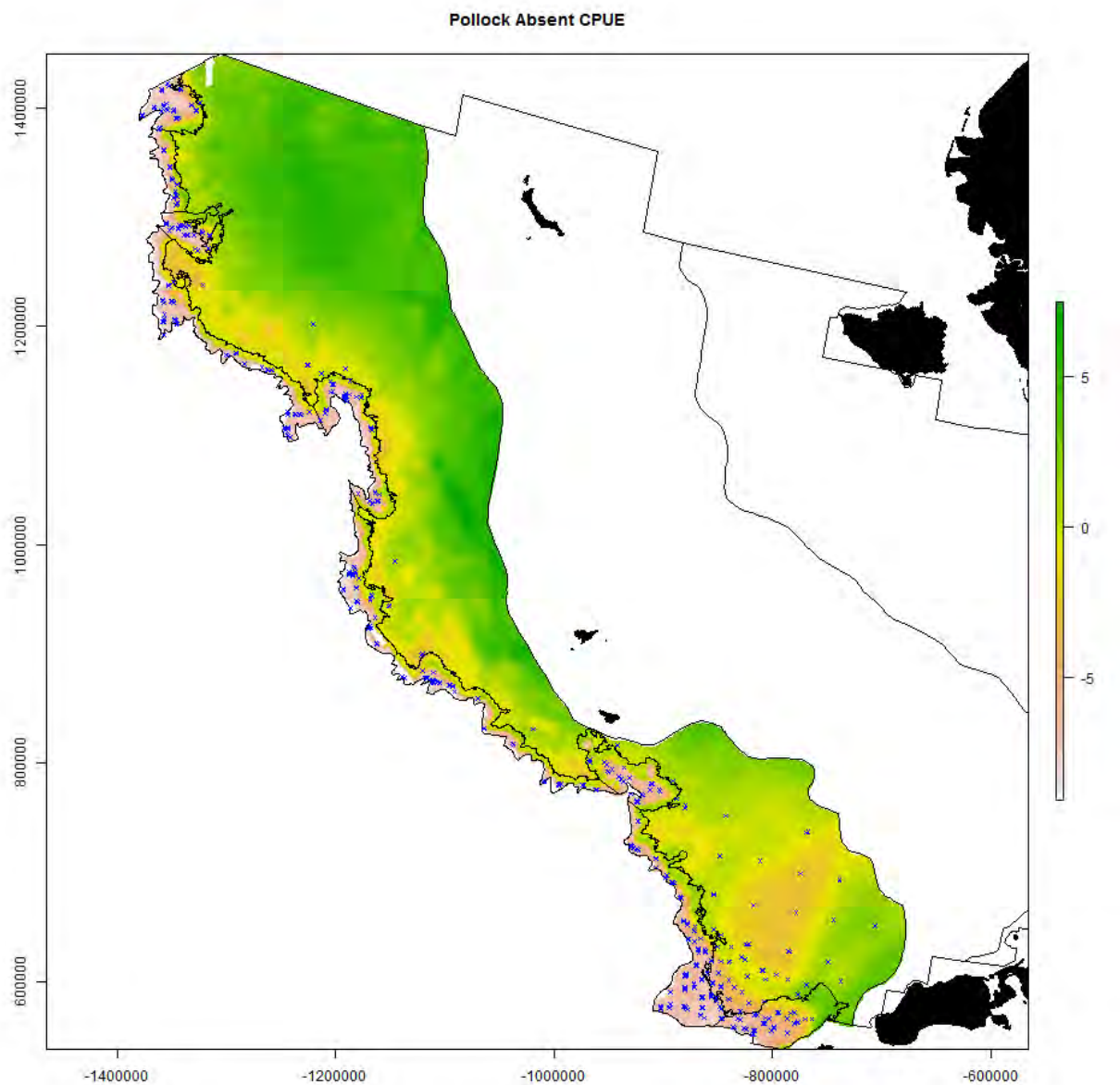
1492

1493



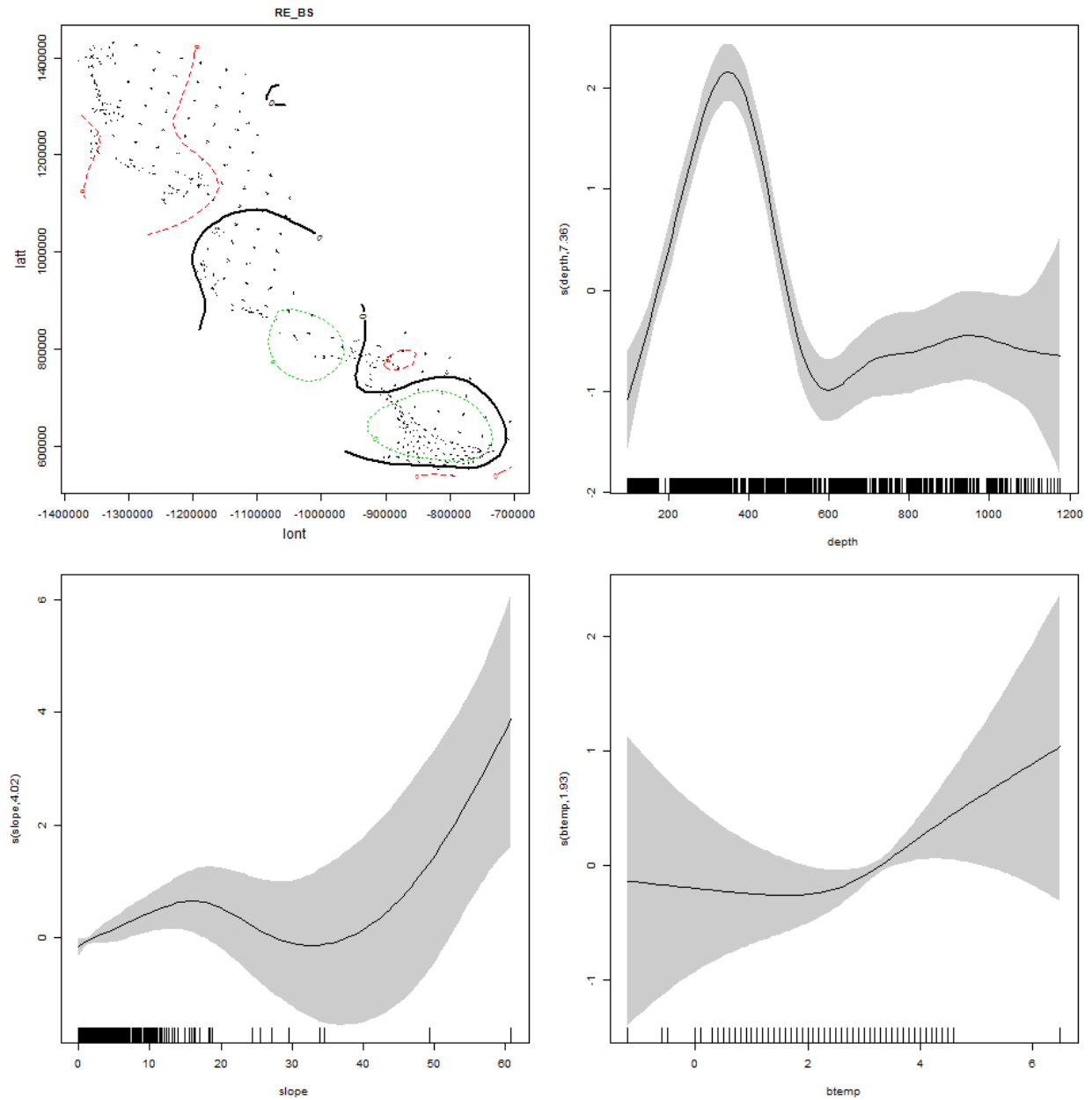
1494

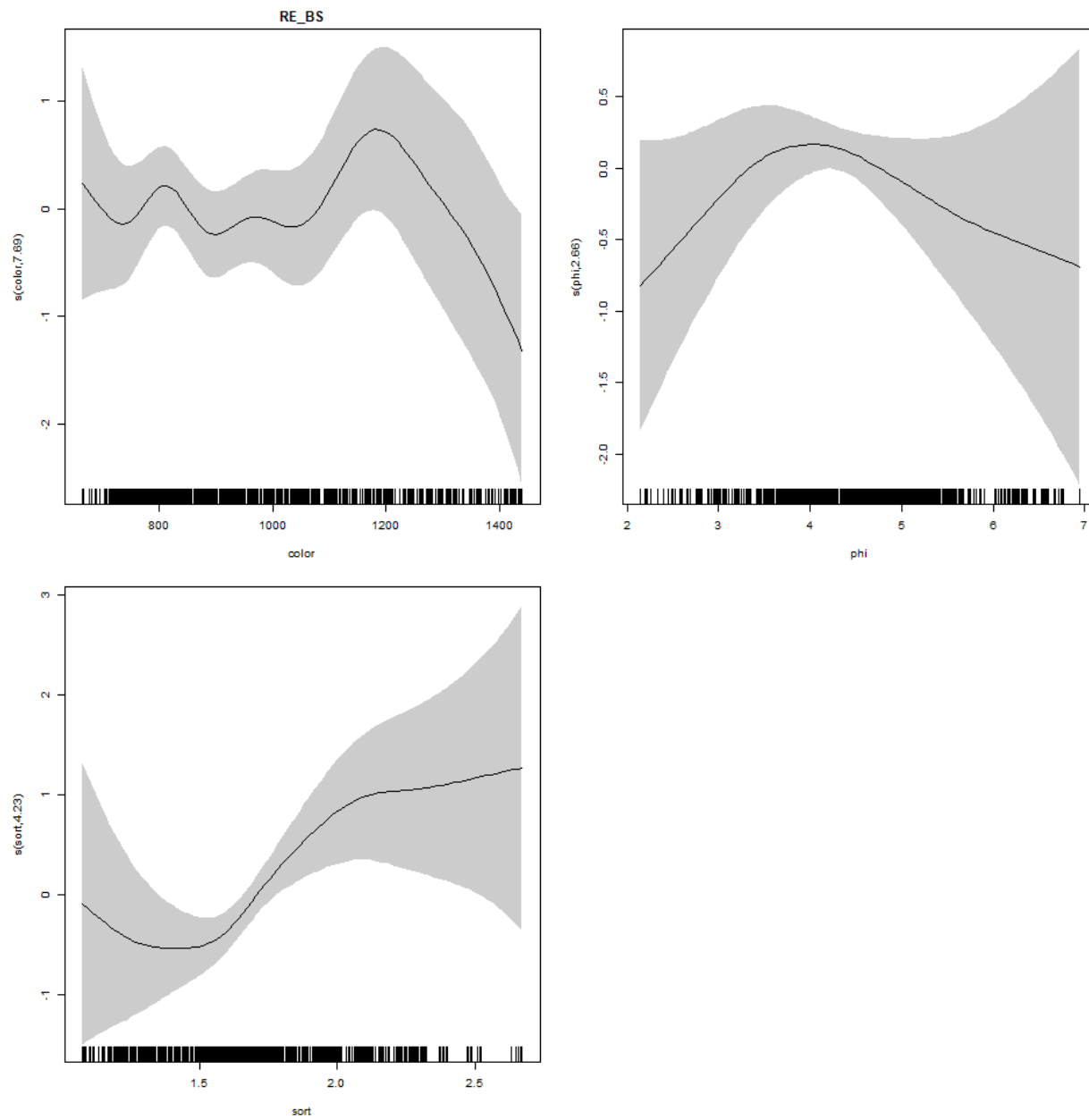
1495



1496
1497

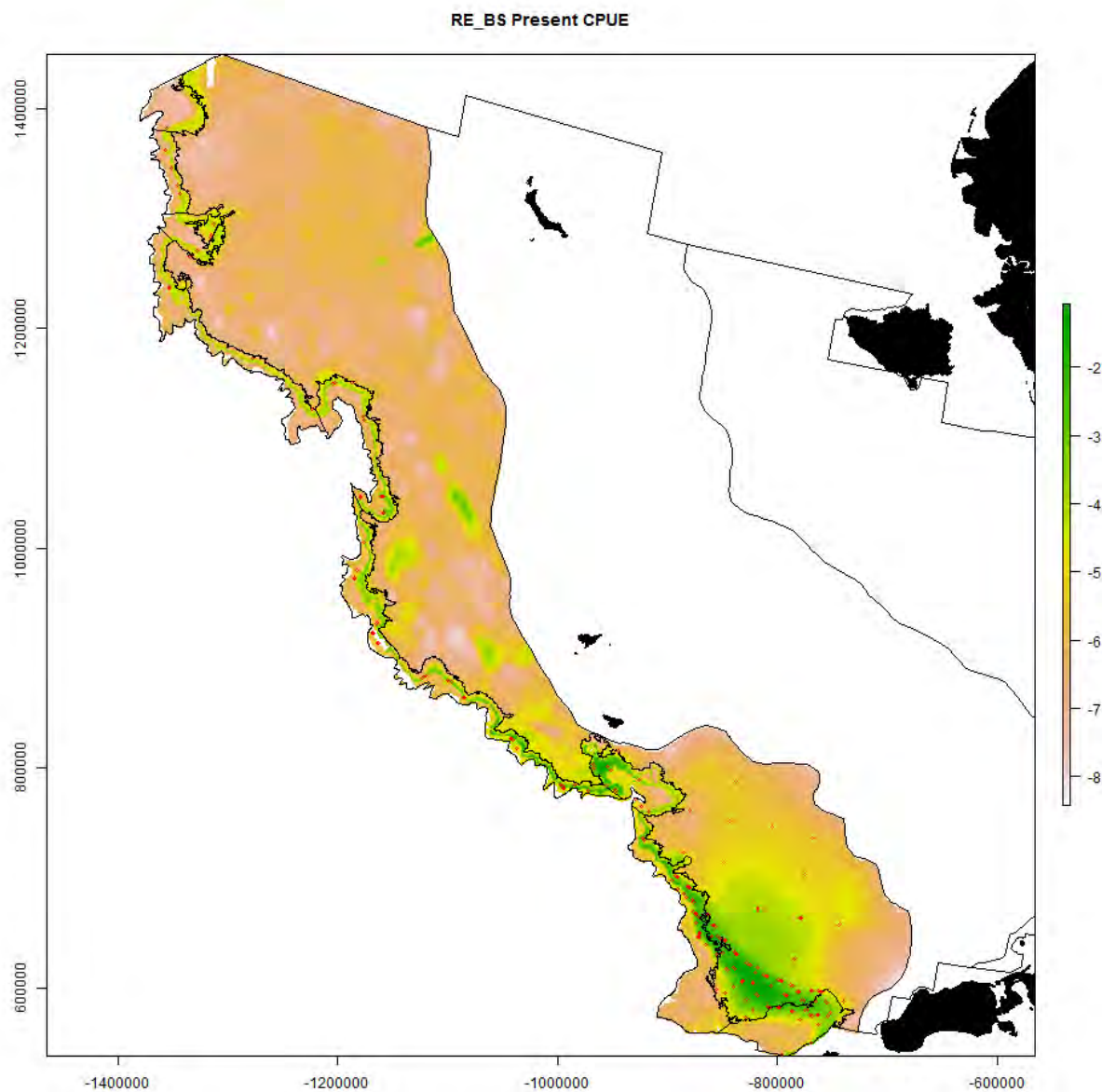
1498 S24. Generalized additive modeling results for rougheye/blackspotted rockfish. In the spatial
 1499 plots, the x-axis label is easting and the y-axis label is northing and the unit is meters (Alaska
 1500 Albers Equal Area Conic projection with center latitude = 50° N and center longitude = 154° W).





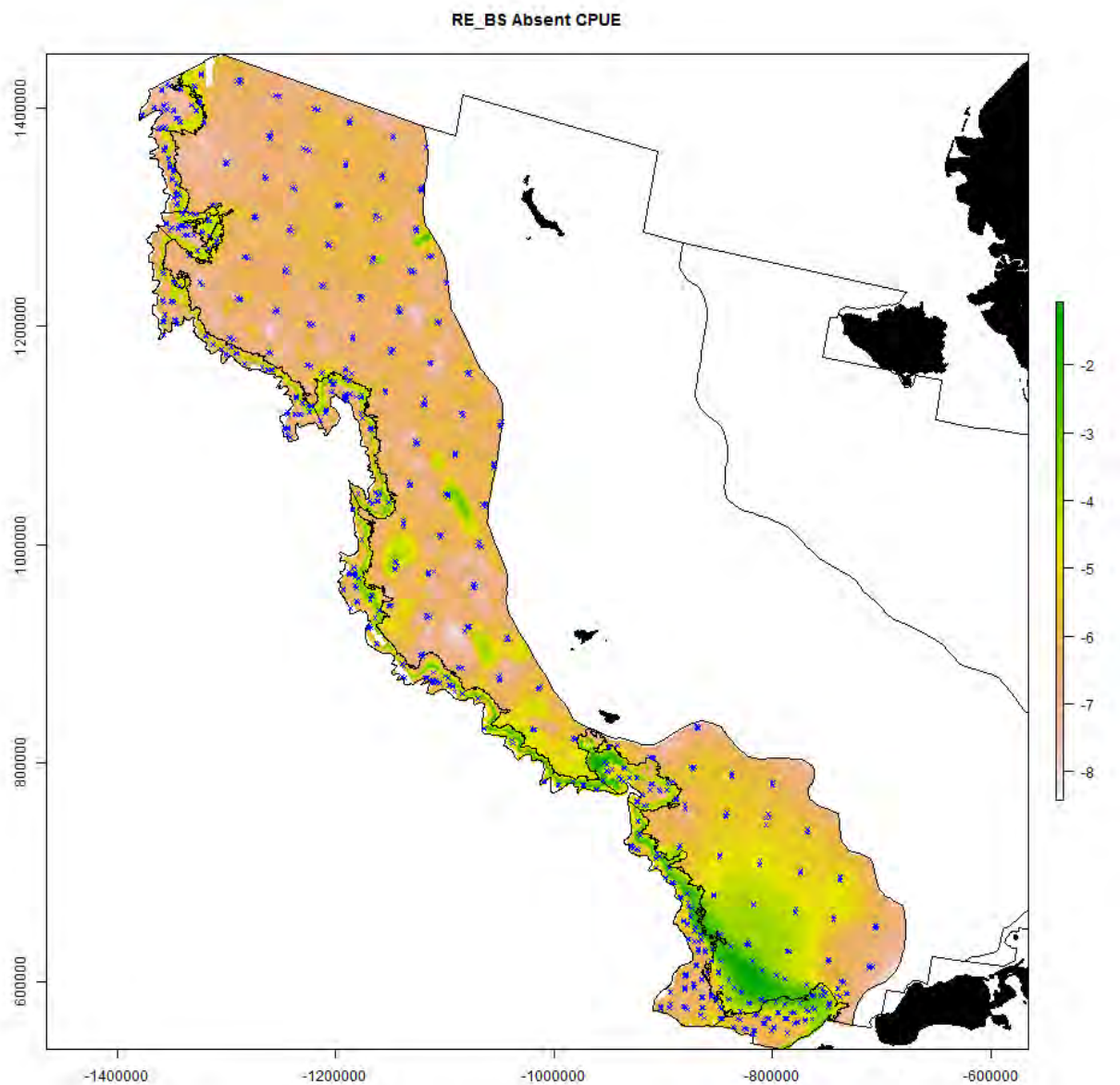
1503

1504



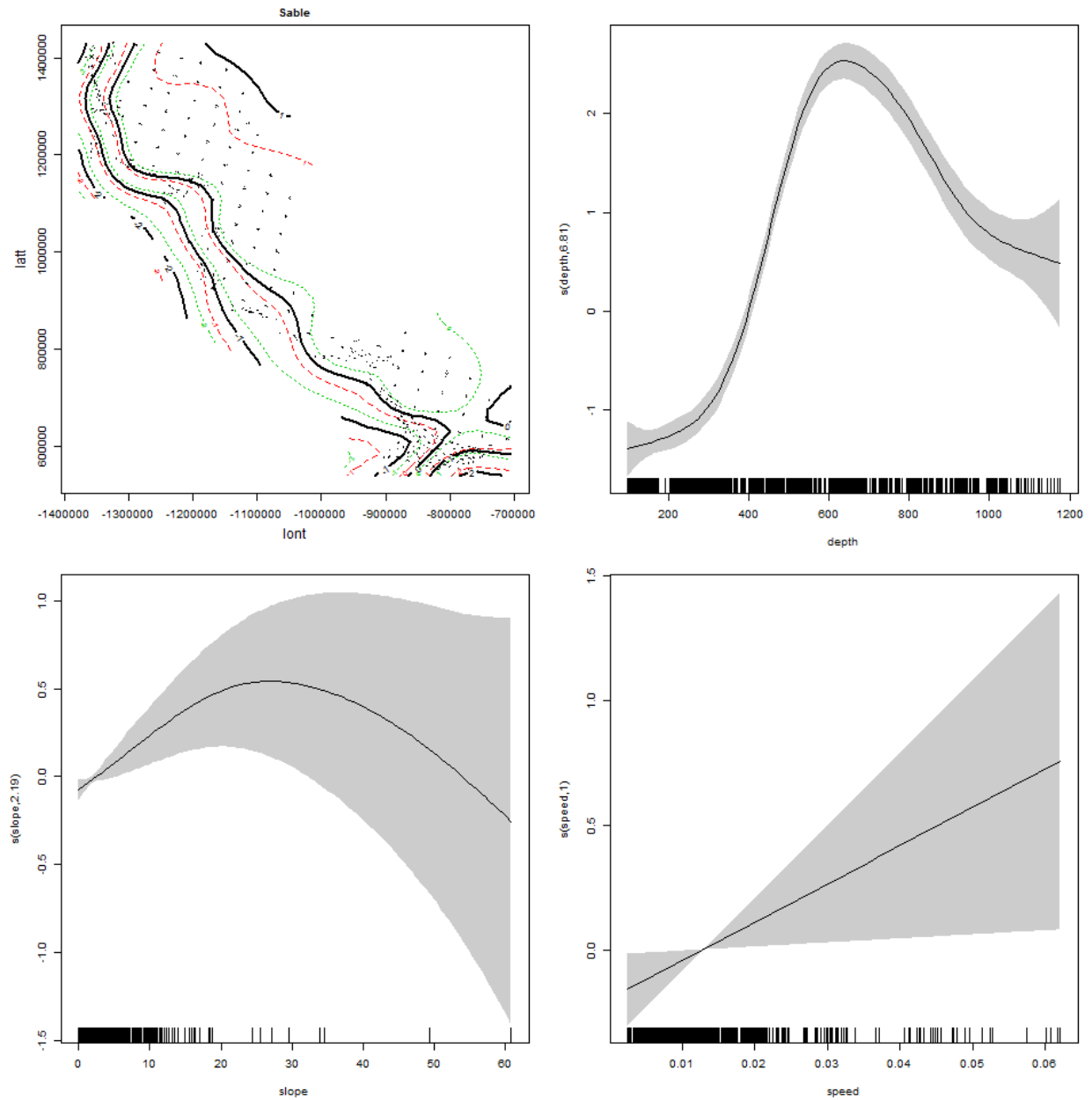
1505

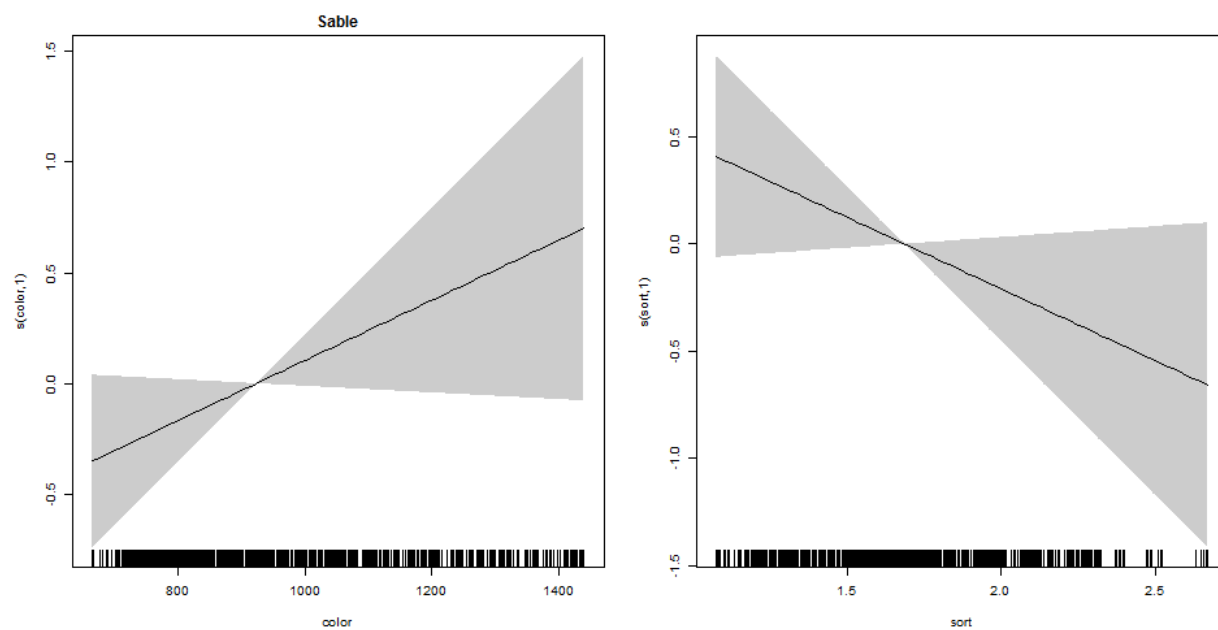
1506



1507
1508

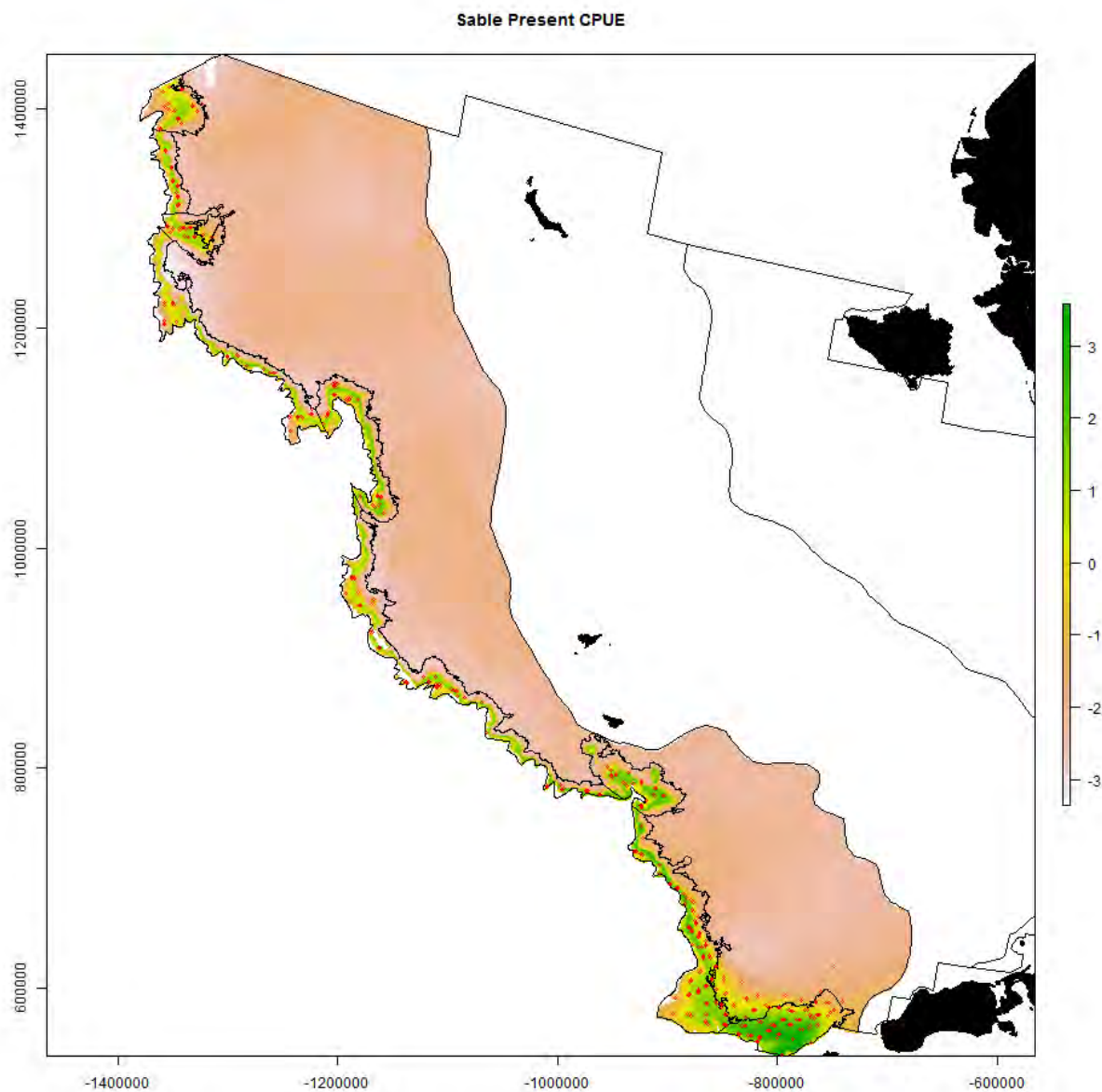
1509 S25. Generalized additive modeling results for sablefish. In the spatial plots, the x-axis label is easting and the y-axis label is northing and the unit is meters (Alaska Albers Equal Area Conic
 1510 easting and the y-axis label is northing and the unit is meters (Alaska Albers Equal Area Conic
 1511 projection with center latitude = 50° N and center longitude = 154° W).





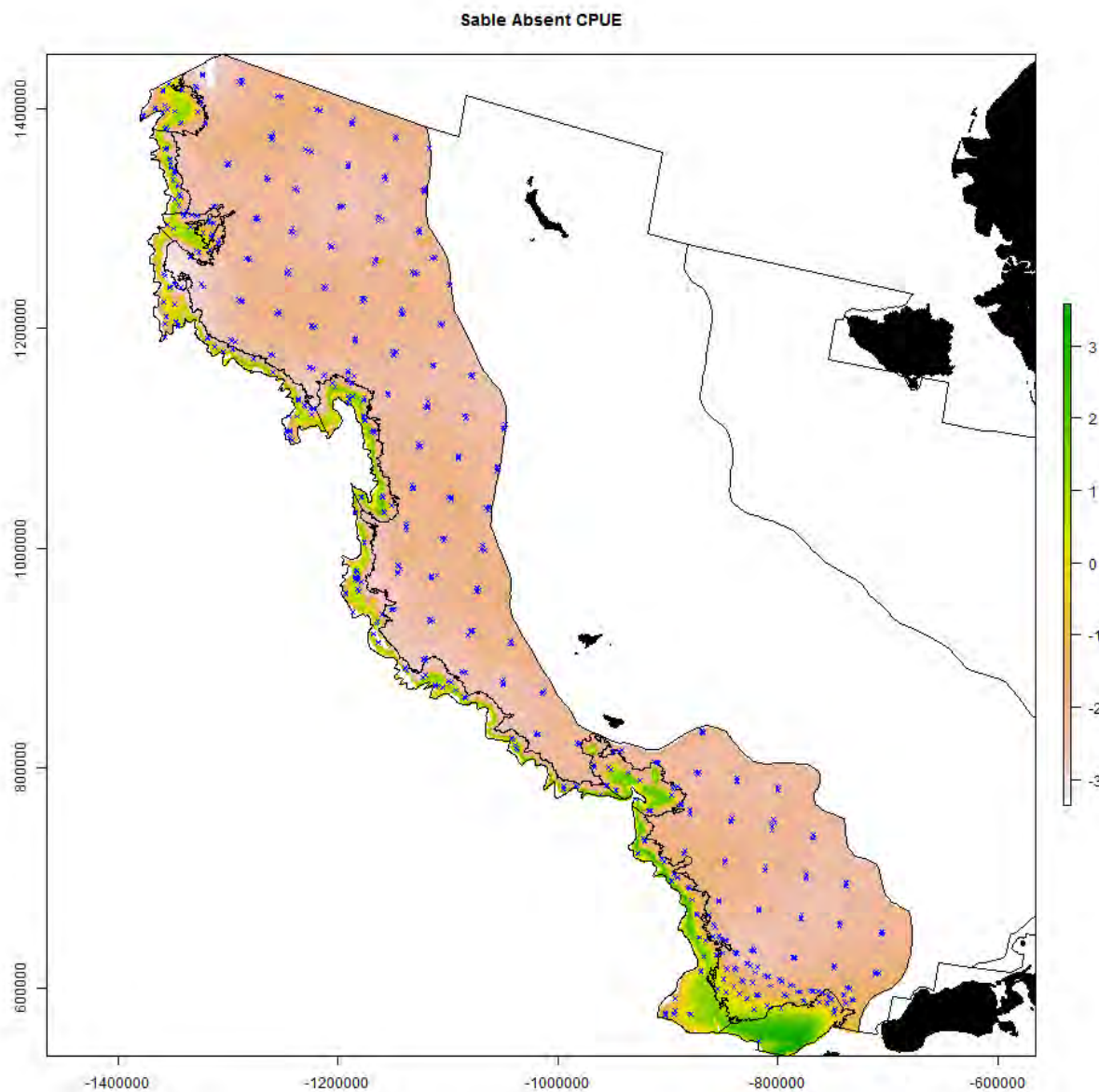
1514

1515



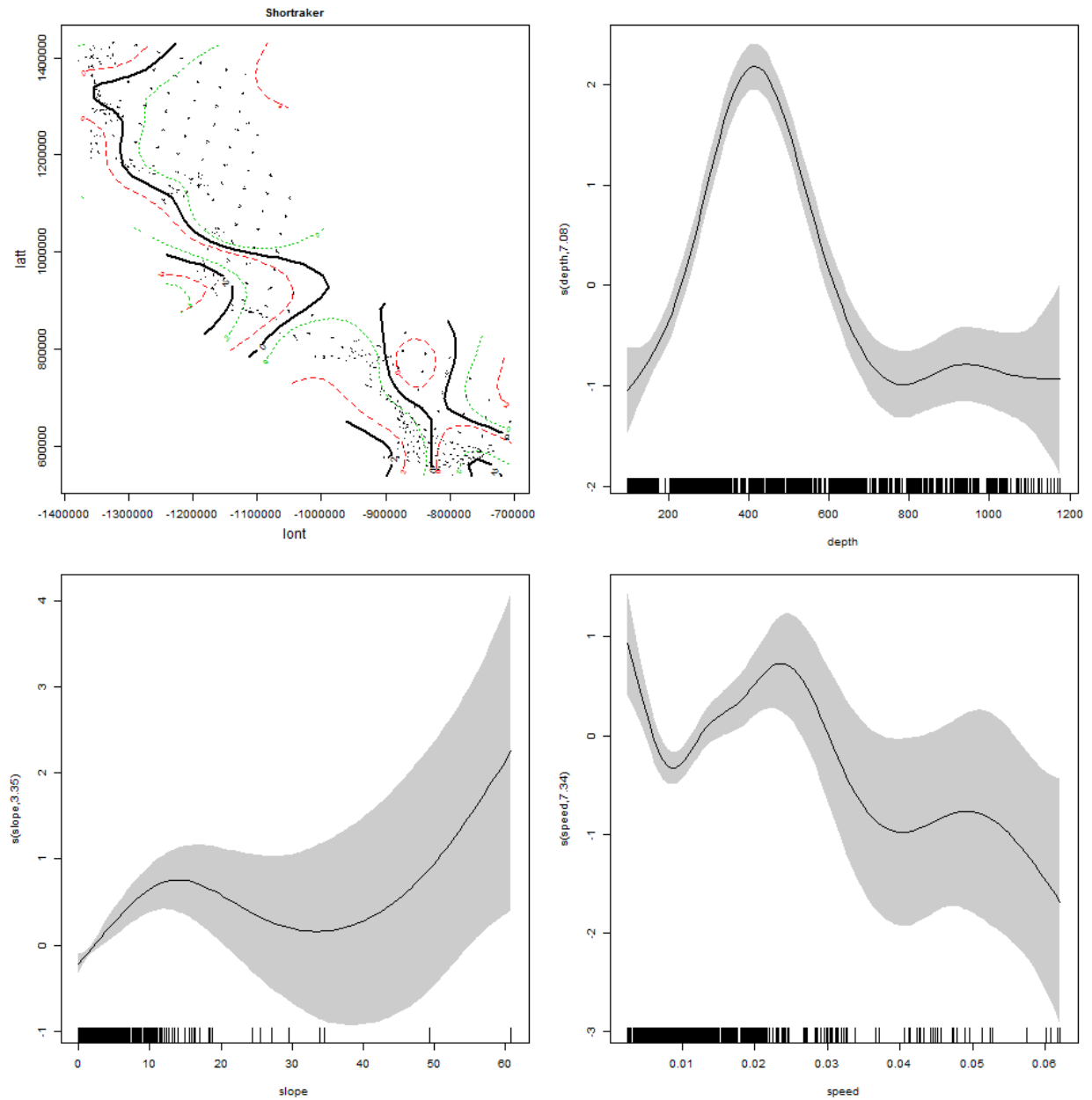
1516

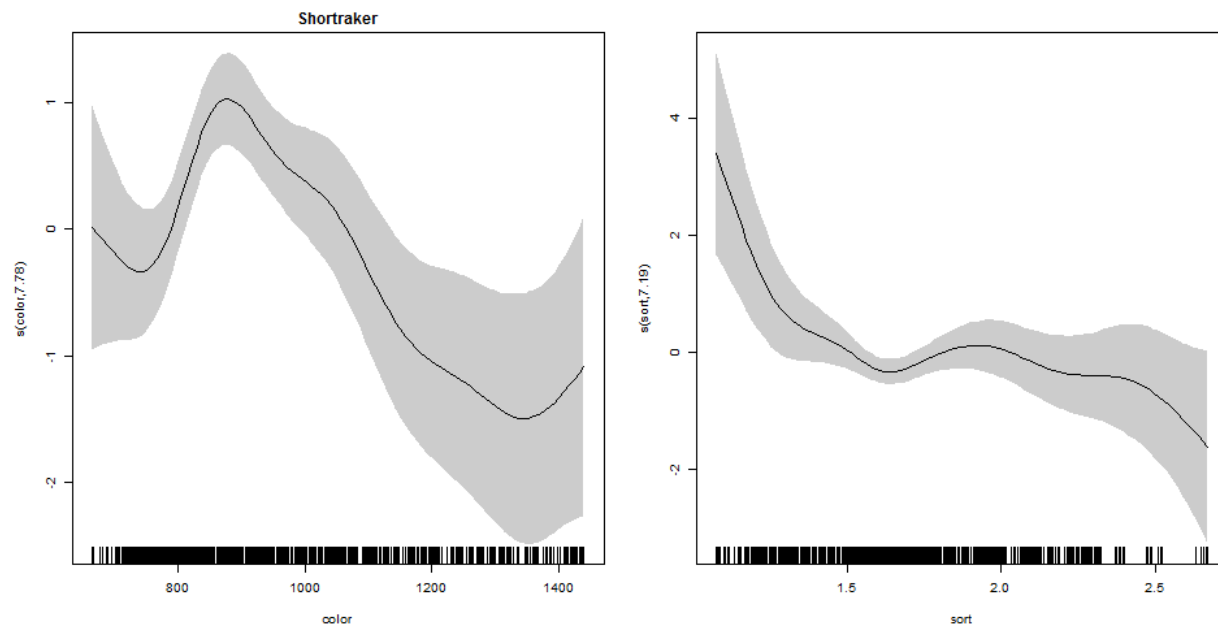
1517



1518
1519

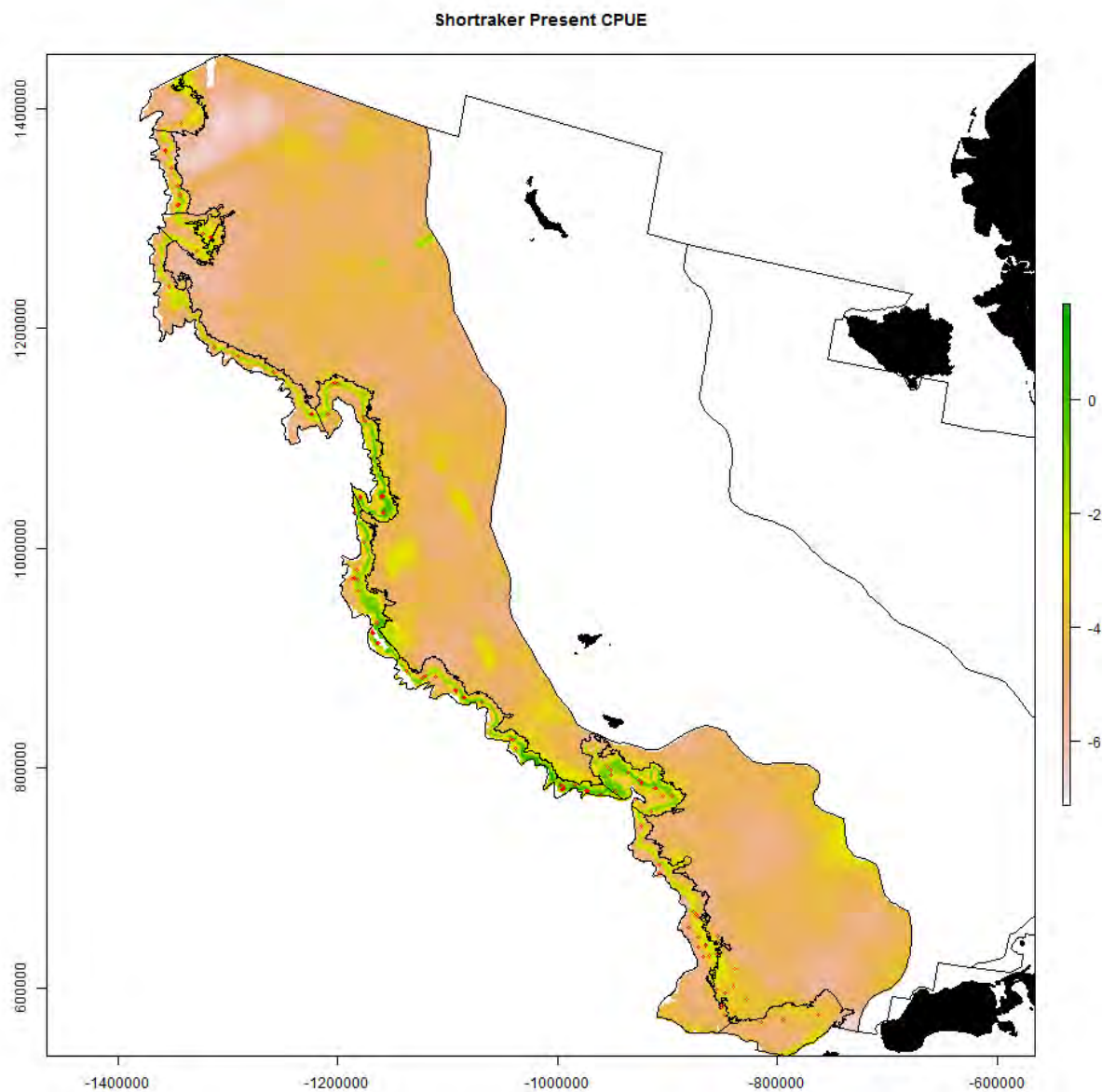
1520 S26. Generalized additive modeling results for shortraker rockfish. In the spatial plots, the x-axis
 1521 label is easting and the y-axis label is northing and the unit is meters (Alaska Albers Equal Area
 1522 Conic projection with center latitude = 50° N and center longitude = 154° W).





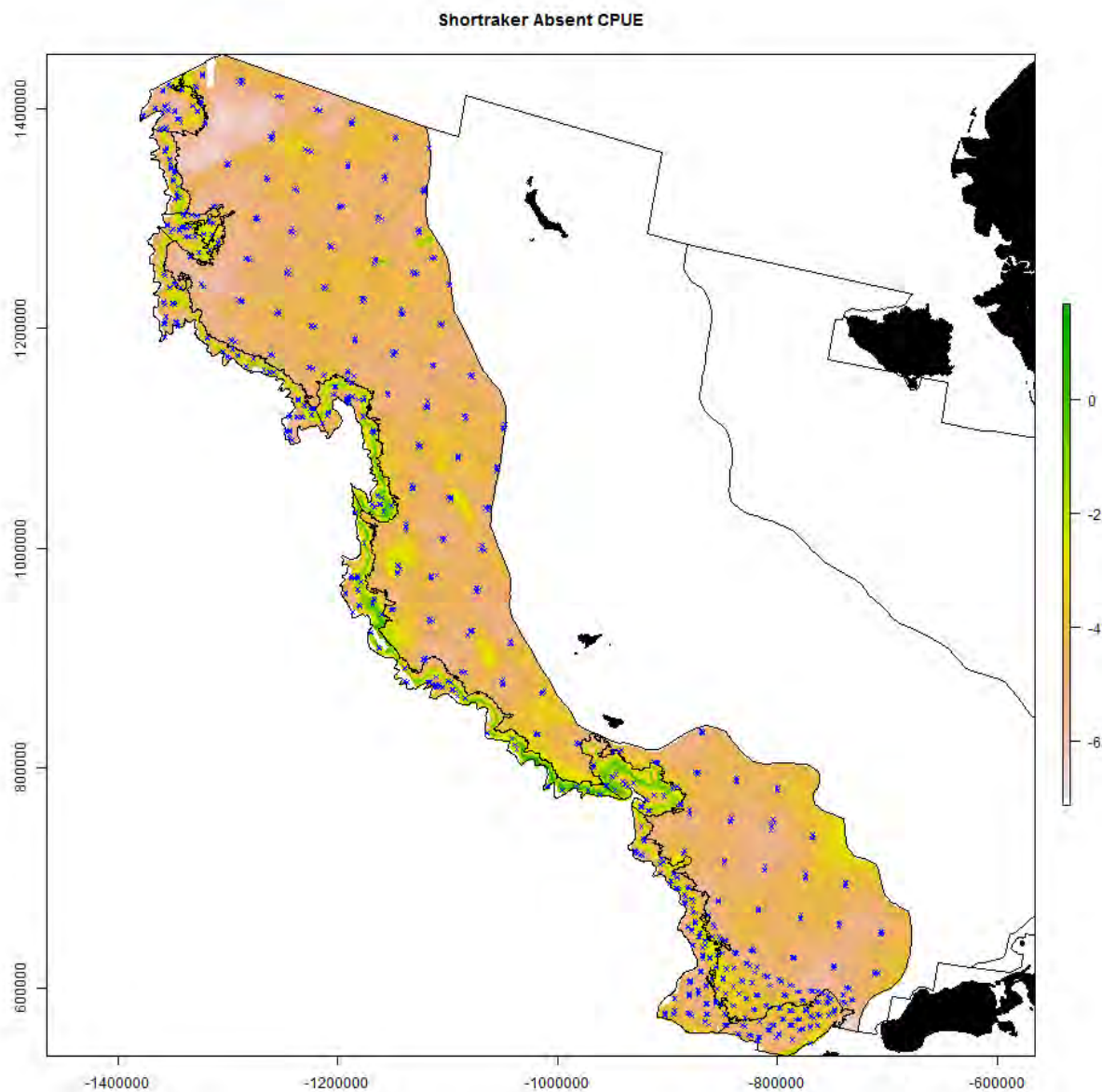
1525

1526



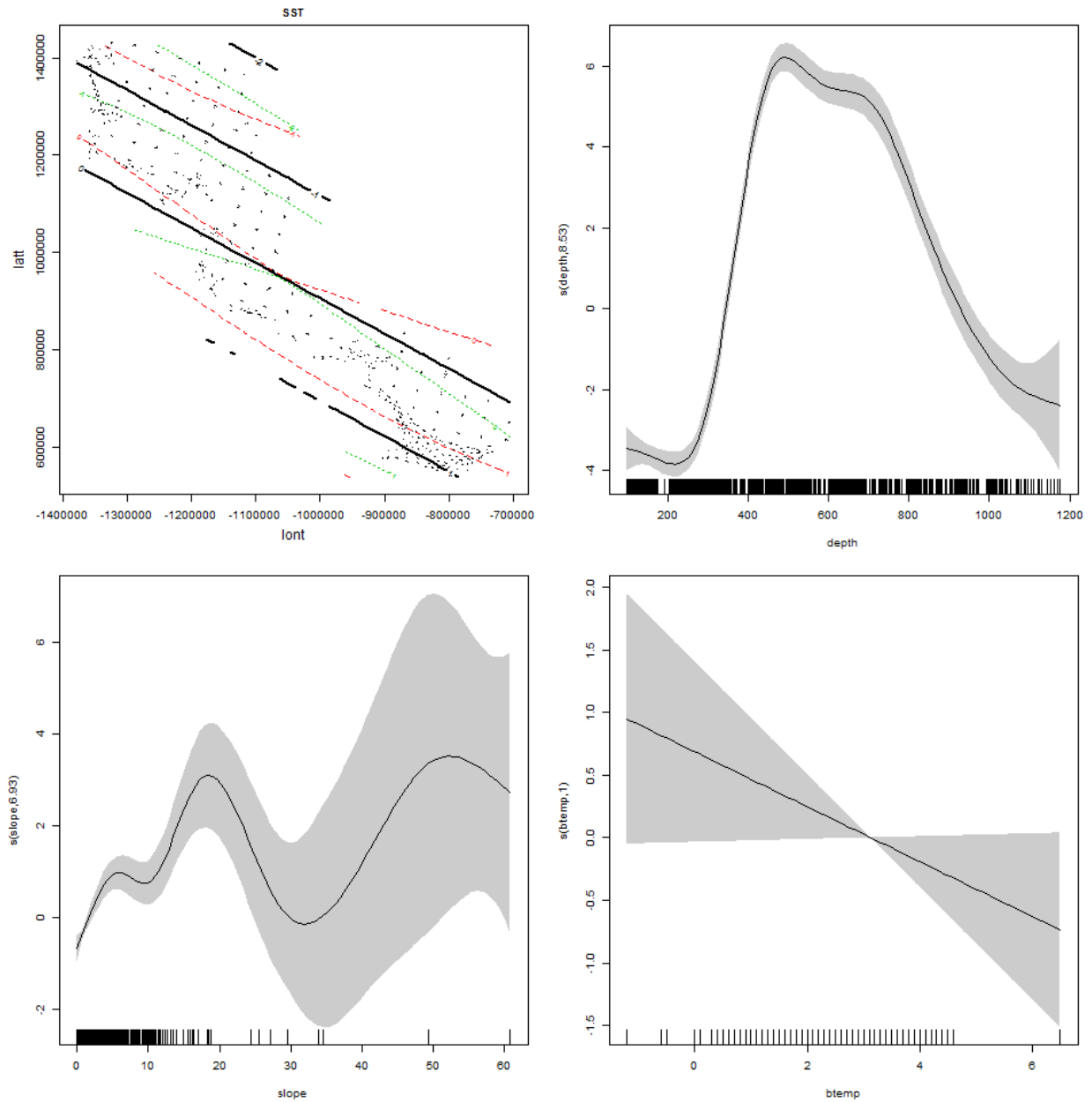
1527

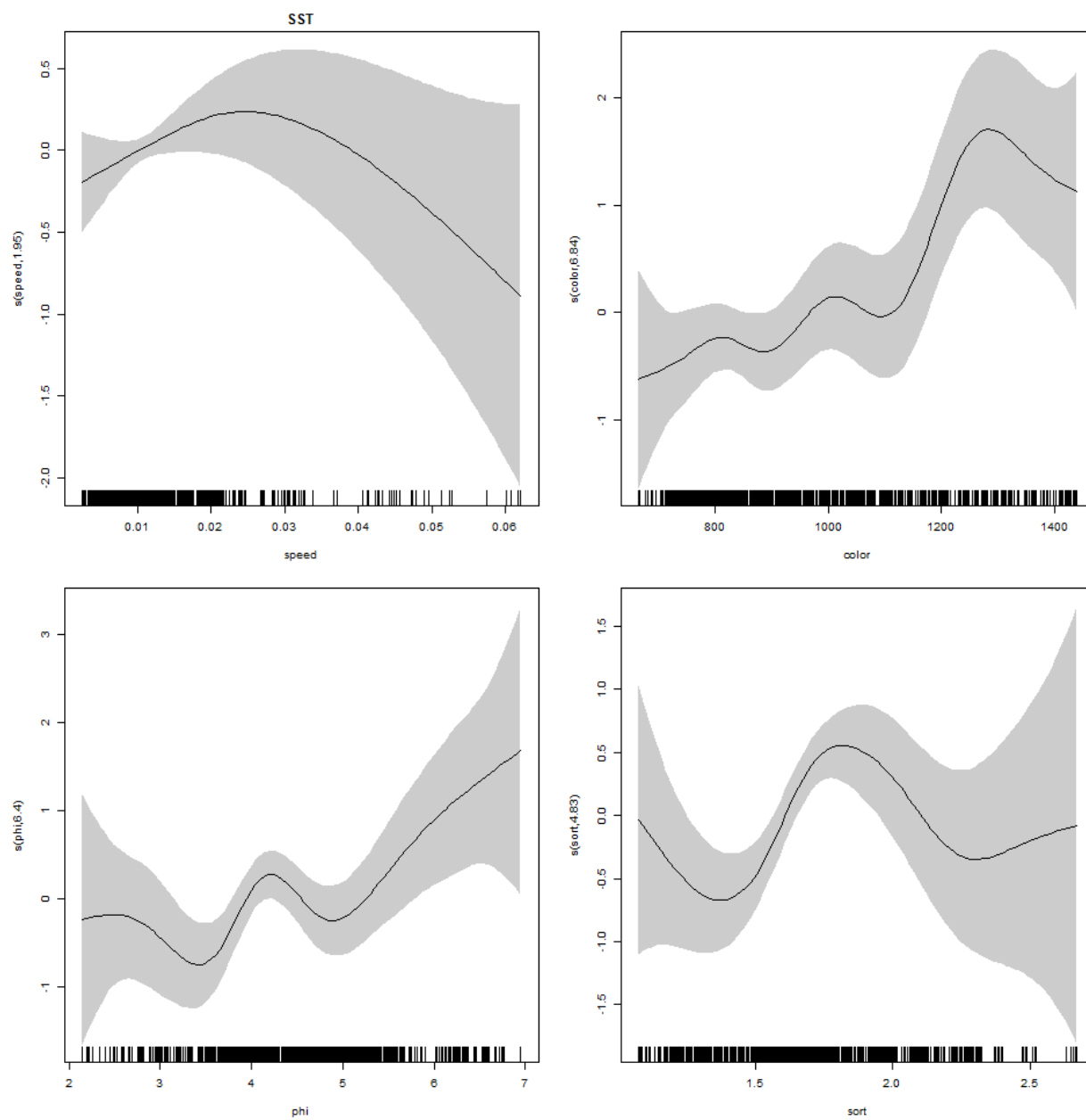
1528



1529
1530

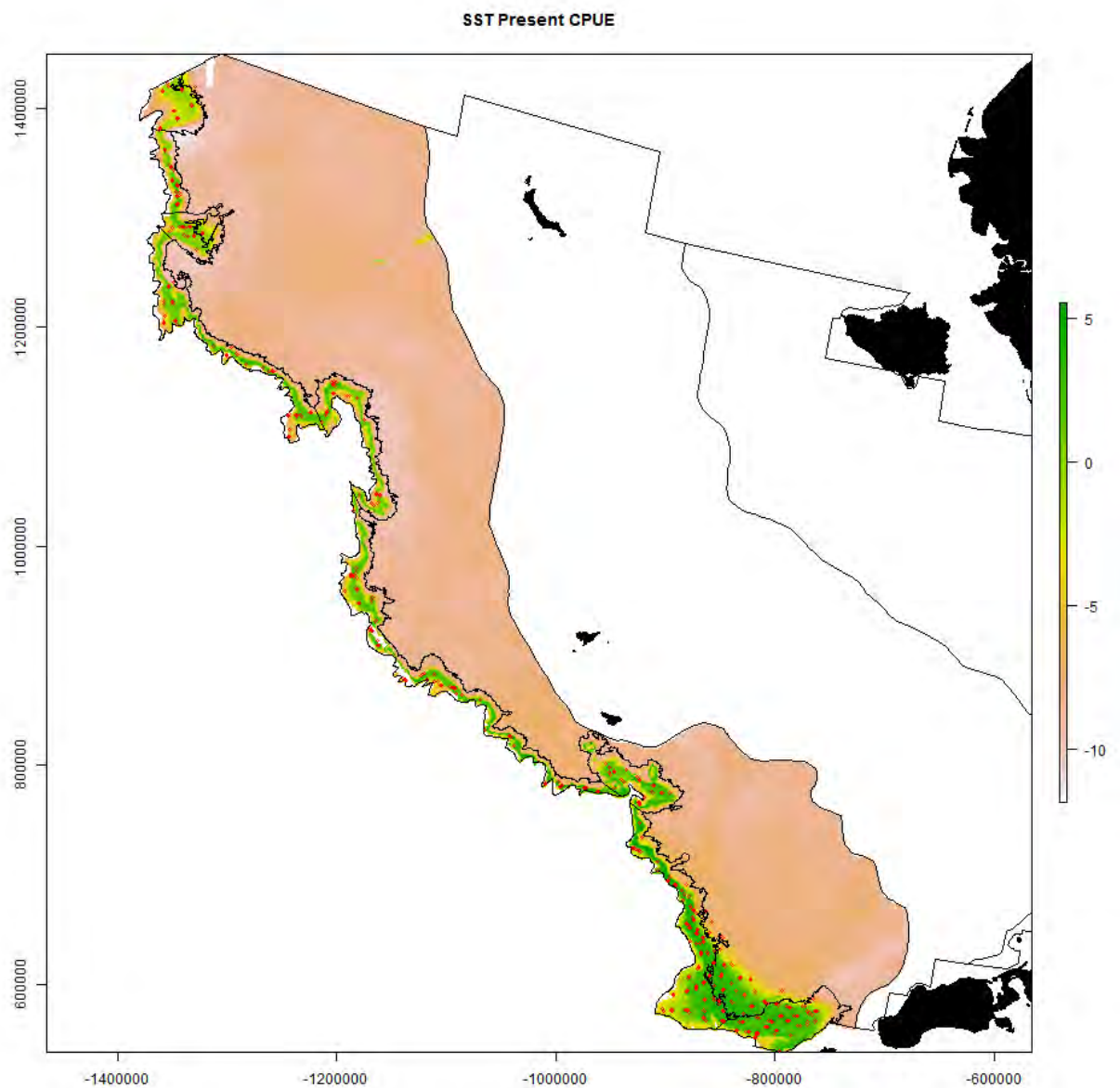
1531 S27. Generalized additive modeling results for shortspine thornyhead. In the spatial plots, the x-
 1532 axis label is easting and the y-axis label is northing and the unit is meters (Alaska Albers Equal
 1533 Area Conic projection with center latitude = 50° N and center longitude = 154° W).





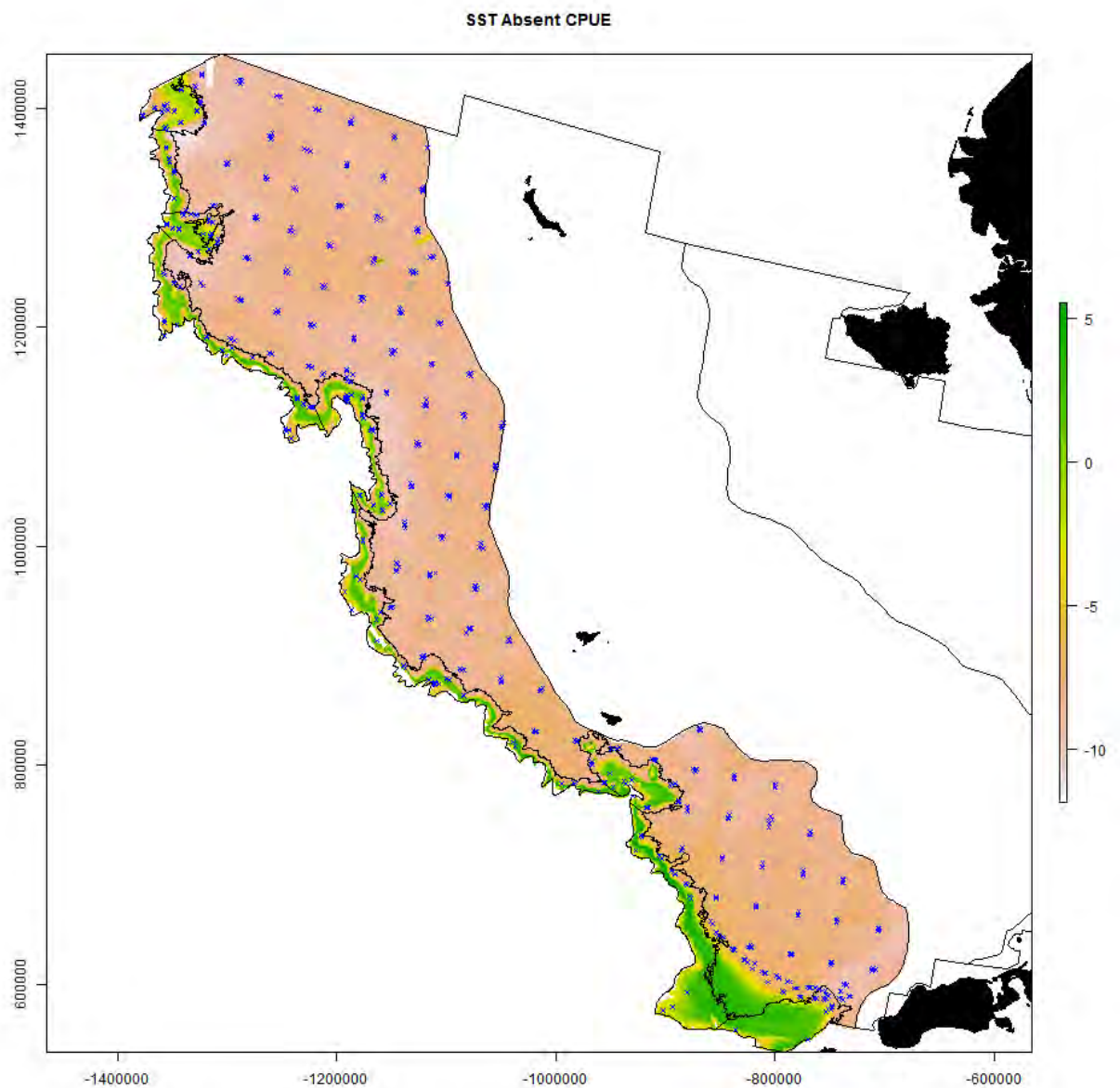
1536

1537



1538

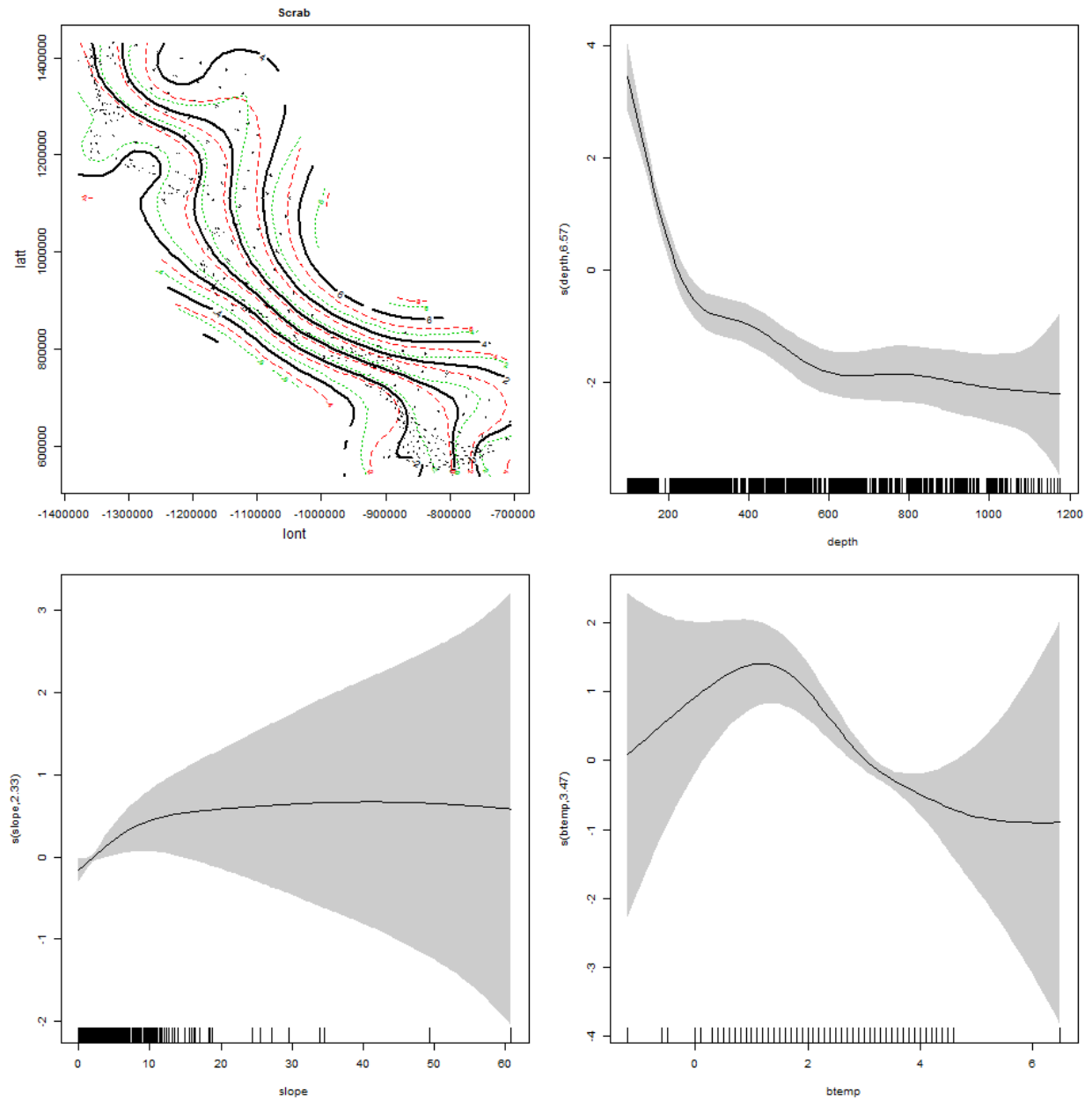
1539

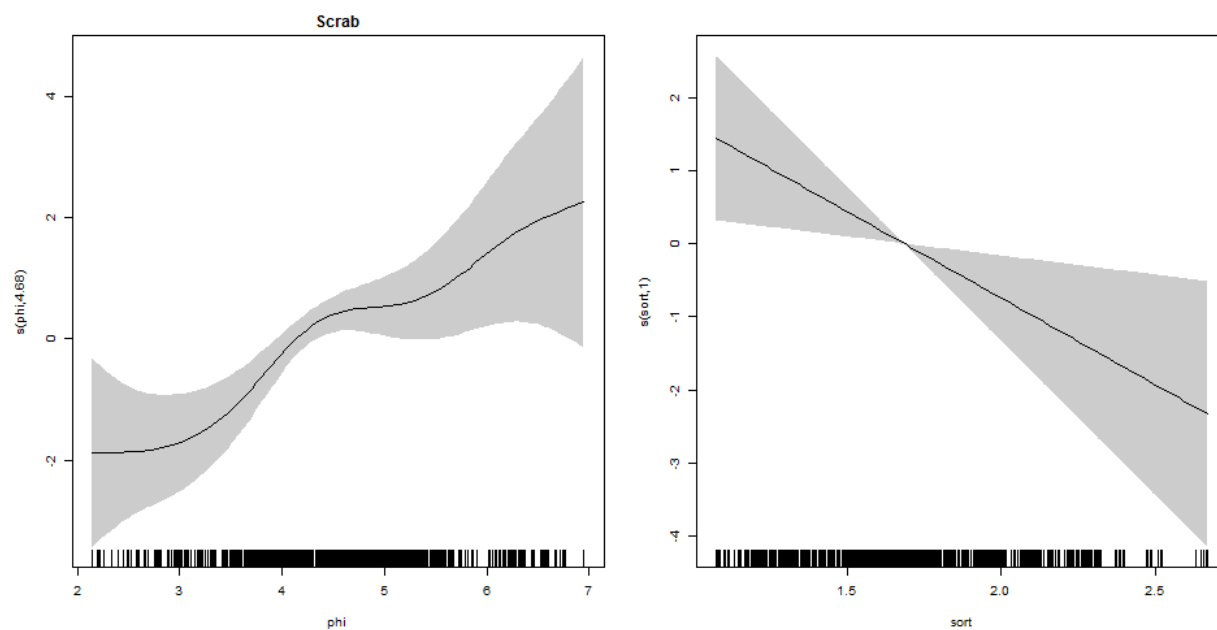


1540

1541

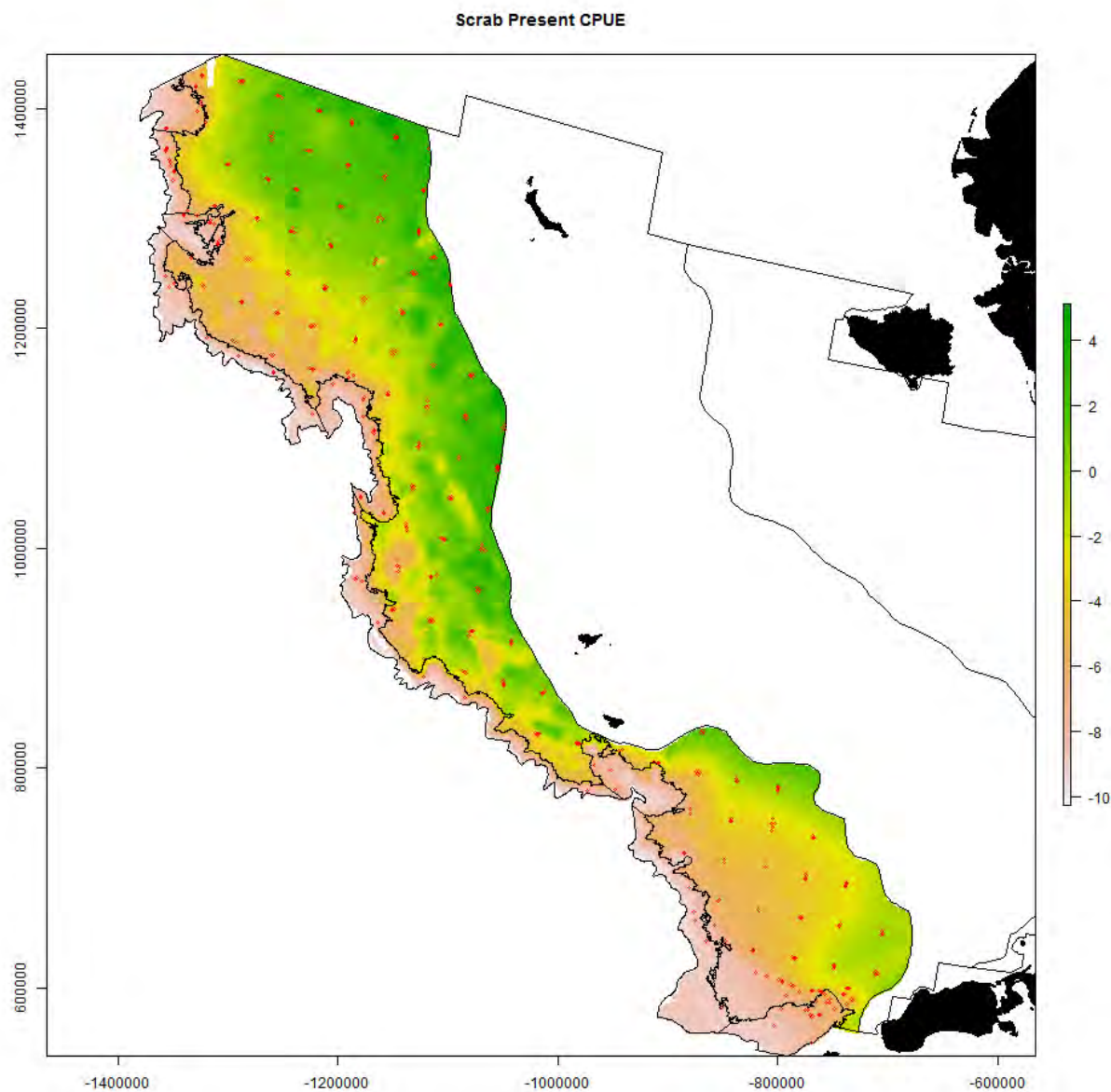
1542 S28. Generalized additive modeling results for snow crab. In the spatial plots, the x-axis label is
 1543 easting and the y-axis label is northing and the unit is meters (Alaska Albers Equal Area Conic
 1544 projection with center latitude = 50° N and center longitude = 154° W).





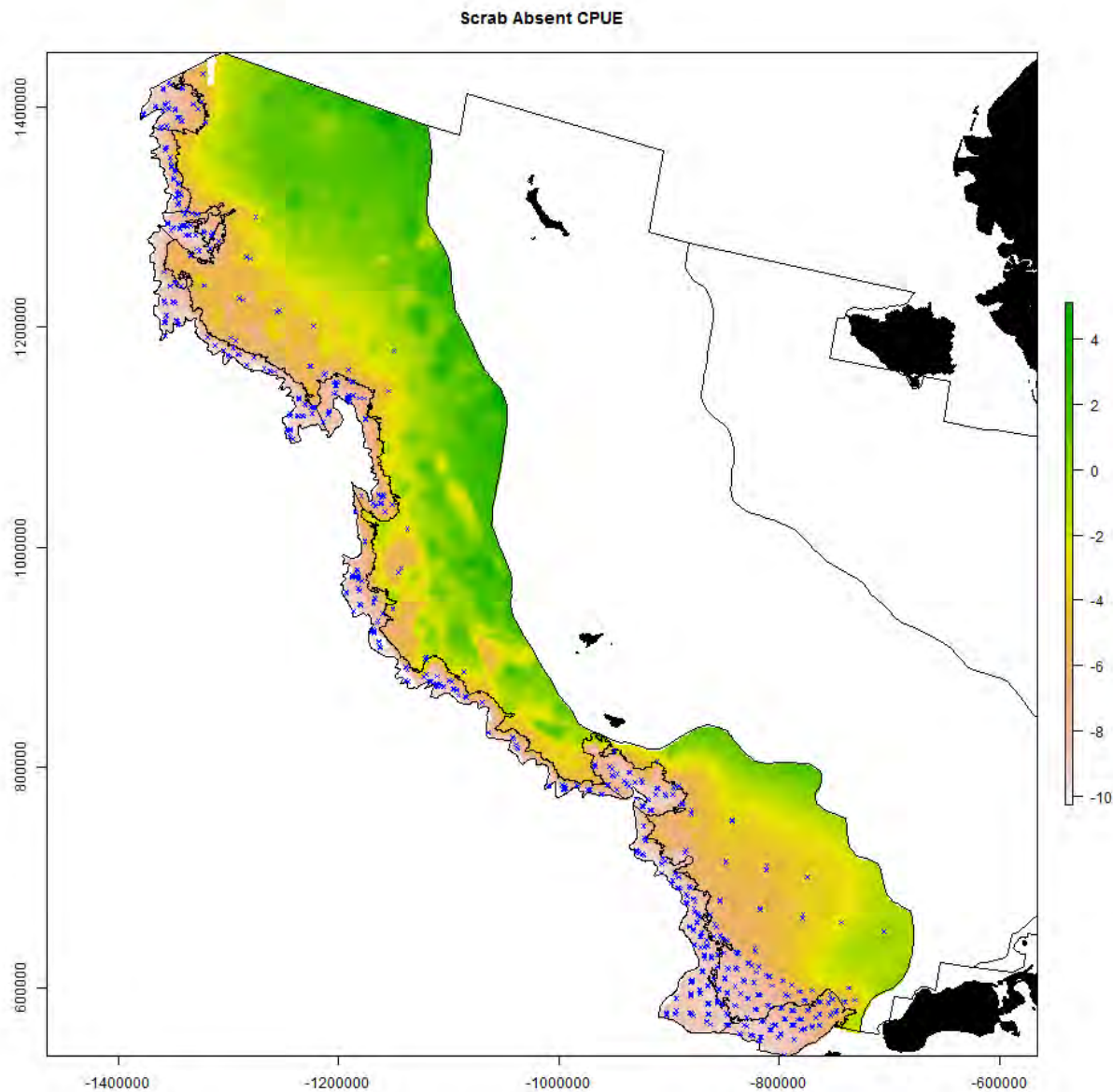
1547

1548



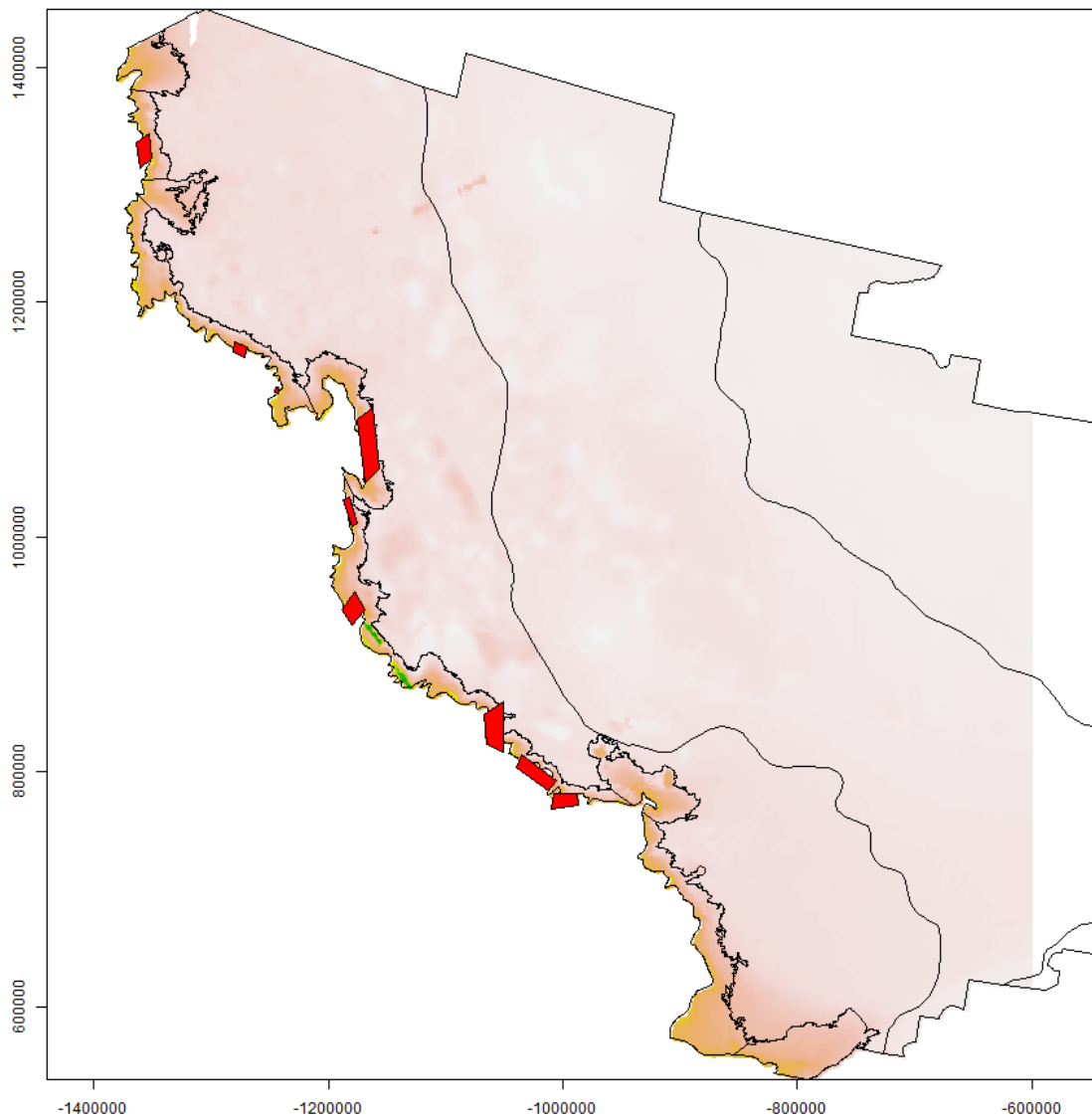
1549

1550



1551
1552

1553 S29. Areas identified as “untrawlable” during trawl surveys of the Bering Sea slope (red
1554 polygons). In the spatial plots, the x-axis label is easting and the y-axis label is northing and the
1555 unit is meters (Alaska Albers Equal Area Conic projection with center latitude = 50° N and
1556 center longitude = 154° W).



1557

1558